Calmodulins and their confederates drive defense and touch responses in *Arabidopsis thaliana*

By

Cullen Stewart Vens

A dissertation submitted in partial fulfillment of

the requirements for the degree of

Doctor of Philosophy

(Botany)

at the

University of Wisconsin - Madison

2019

Date of final oral examination: March 28, 2019

This dissertation is approved by the following members of the Final Oral Committee:

Simon G. Gilroy, Professor, Botany
Edgar P. Spalding, Professor, Botany
Hiroshi A. Maeda, Associate Professor, Botany
Sebastian Y. Bednarek, Professor, Biochemistry

This dissertation is dedicated to my daughters Kennedy and Allison.
You are the tears in my eyes and the beats in my heart.

Acknowledgements

It's very nice to find people who will support you – especially emotionally – during times of intense activity, difficult decision-making, or utter tragedy. I have made and lost friends and family-members since beginning the work that culminates with this PhD. None of this would have been worth doing without them. They kept me going, pursuing knowledge and my goals, all the while keeping me grounded and grateful for the opportunities I have had.

The Department of Botany has been a welcoming place for me and my family. I have always felt encouraged to involve my children and my partner in the extracurricular activities engaged in by the members of the botany community. Also, the invitations by my graduate student peers and faculty mentors to gather together outside of regular work hours were important to my sense of community. For example, FAC is a wonderful place to get to know graduate students in a non-academic setting, while also being a safe space for lamenting the troubles we all face, collectively and alone.

My mentor and advisor, Simon Gilroy, widely regarded as a wizard of plant physiology, afforded me countless occasions to discover truth and question canon because of his experience and openness to free scientific exploration. Being able to pop into his office or invite myself to a video chat with him meant fewer hours of mentally wrestling with myself over my own trivial preoccupations. I am grateful for his eminence and omnipresence.

My other mentor and former advisor, Donna Fernandez, has been a true pleasure to know and was wonderful to work for. I will always appreciate her candor, thoughtful evaluations, and willingness to listen. I cannot recommend her as a mentor and advisor highly enough.

My peer mentor, of sorts, Richard Isam Hilleary, is an intensely patient human. His unjustly onerous devotion to honesty in academic research combined with his equally burdensome

understanding of the immense pressure the current system of academic research puts on one's ability to remain honest and honor-bound are something worth aspiring to. I have learned, from him, to take pride in questioning everything and believing nothing lest we all be made fools by the lax conduct of others.

As a relatively new – as of this writing – member of the lab, my friend Dr. Arthur Poitout has been a welcome addition to the beautiful chaos of the Gilroy family unit. He has thrown himself, headlong, into a fraught situation and made it all work. From him, I have learned to keep going, no matter how difficult (hilariously or otherwise) the situation might be. He works hard, finds new ways of doing things and makes the effort worth it.

I must express my appreciation for several others I have worked with or learned a great deal from. First, Dr. Nathan Miller, I thank for his consistent, gradual attempts at eroding the philosophical foundations of my worldview. While at times exhausting, they are undeniably beneficial and appreciated. He is a kind person, wonderful father, and great friend. Next, Dr. Makoto Yanagisawa has always been insightful, brutally honest, and pleasant to be around. He is a great person, especially when you want to commiserate or celebrate any accomplishment. His infectious laugh and delightful peculiarities make me proud to call him my friend. Ryan Swanson always reminds me to keep pushing but never forget to slow-down and enjoy life. Dr. Julio Paez-Valencia is a great person, better friend, and welcome company on any adventure. Dr. Richard Barker is a lovely man with the grandest of plans. Thankfully, he always has an army of undergraduate students to hurl like pawns into them. Dr. Arko Bakshi is a thorough and deliberative scientist with whirling fists-of-fury. Dr. Sarah Swanson keeps me on my toes. Future doctors, Sarah (Johnny) Johns and Ariel Sorg, have been fantastic additions to the Gilroy family unit. Johnny's kindness and Ariel's wit have made the last several months much more enjoyable.

Last, not in my heart but on the page, I thank my entire family for being the absolute best family I could ever hope for. My parents, Stacey and Todd and Lisa, have always been there for me and I hope that my efforts in completing this PhD make them proud. My brother, Ian, and my sister, Franny, are brilliant, creative, and beautiful souls. My sister, Mia, has returned to the stars, where she is, no doubt, regaling the gods with the stories of her life, the white-hot flame they snuffed-out far too early. My grandmother, Peggy, has encouraged me in everything I've done, picked me up after every mistake, and has made me a far better person. My partner, Ashley, is the trees and the sun and the air I breathe. She strengthens me in every way and works harder than anyone I know to make this terrifying world a better place to live. And my daughters, the sparks that keep me going, are the most special little turkeys, have the biggest hearts, make every day lovely, and make this life the best life.

I know I should express, more often, the manner in which each of the people listed above have made their big impacts on my life. For failing in that, I truly apologize. I should also take this opportunity to make sure that everyone knows that I have learned, through repeated trials, that no career is the last career you could ever have, the end of a relationship is not love lost forever, and no tragedy is impossible to overcome. In much the same way, giving up or staying in a situation that makes you deeply unhappy or resigning yourself to the results of a bad decision may be easier than the pain that comes with confronting those situations, but refusing to fight and failing to advocate for yourself can feel far worse than that momentary pain. In this way, everyone needs at least a little help sometimes and I am deeply grateful to those who have helped me get through tough times in my life, over the years. If you're reading this, I will try my hardest to always be there for you, too.

Preface:

Why Science Fiction Should be Important to Scientists

As scientists, my colleagues and I spend an enormous proportion of our lives attempting to derive the *why* and *how* from observations and experimentation. This reflection on the nature of events or activities that are – by their very nature – in the past, is a fundamental aspect of the commitment scientists make to their craft. Indeed, one could be forgiven for, wrongly, thinking that scientists focus only on the past (or present) construction of the world and the universe. What's worse, we frequently find ourselves caught up in the tiny little details, such as: this transcription factor binds to this promoter element, which then releases this gene from repression by this transcriptional repressor, this gene then produces this protein, which is allosterically inhibited by this ligand, *et cetera*, *et cetera*.

We crave scientific fact. We hold the pursuit of scientific fact up above nearly everything. This pursuit of scientific fact is even romanticized by those within, and without, the academy. Hence, there is certainly a tendency, by scientists and non-scientists alike, to idealize the lives of scientists, the work they do, and the meaningfulness of the results they publish. What is surprising, then, is how rarely the idealist nature of scientists translates into scientists who indulge in – or rarer still, produce – thought-provoking futurist or premonitory works of science fiction.

Science fiction is found in all styles of media: books, graphic novels, television, movies, radio programs, podcasts, and more. The subjects are wide-ranging, as well. Super heroes, some endowed with their abilities by laboratory accidents, line the pages of graphic novels and splash across every kind of screen. You don't have to look hard to find dystopian tales of a world overrun by technology or stories of alternate realities hiding behind doors and within wardrobes. And it is no shock to find that space exploration is obviously a well-represented topic.

It was there, being carried to the far-off reaches of space that I was first captivated by science and its place in our universe. Science fiction, in the form of weekly episodes of *Star Trek: The Next Generation*, *Red Dwarf*, and *Doctor Who* and in monthly comic book installments of *X-Men*, *Batman*, and *Sandman*, brought (in ways that were sometimes more fiction than science) the distant stars and planets, and the beings inhabiting them, into my mind and my living room. Unfortunately – though there are certainly exceptions – the people who created, produced, wrote, illustrated, directed, voiced, penciled, and acted in these series were not, generally, scientists. In fact, the vast majority of people creating science fiction have no scientific training, whatsoever. And, though many of the works they produce are fine products, it's hard to become rapt in a tale of a possible future if it is based upon flawed scientific foundations.

So, it is my sincere hope that more scientists, those who are deeply concerned with the operation of the universe, regardless of scale, will take up the mantle and help new generations of science fiction lovers, in the words of the great Jean-Luc Picard (timelessly portrayed by Sir Patrick Stewart, OBE): *seek out new life and new civilizations; boldly go where no one has gone before*. Simply, it is because of this imperative from my favorite fictional starship captain that I chose to heed the call of scientific exploration and work toward a better understanding of the real universe, the one that *we all* live in. Therefore, it is my wish that more scientists will find the consideration of the 'could-be' as thrilling and intriguing as the pursuit of what is.

TABLE OF CONTENTS

CONTRIBUTIONS OF OTHERS TO THIS WORK

Professor Simon Gilroy (Chair) – provided real (e.g. research funding, reagents, lab space, consumables, etc.) and other resources during the planning and execution of this research, including, but not limited to, thoughtful discussion of best practices and results, insights on data analysis, and a significant contribution to writing the chapters.

Professor Edgar Spalding (Vice-Chair) – contributed to thoughtful discussion of methods and results.

Cullen S. Vens (Author) – designed and performed the majority of the experiments contained herein, analyzed the majority of the results, and wrote the majority of the content.

Gabrielle Li (Research Intern) – performed a portion of the quantitative transcriptional analyses, genotyping, double mutant development, and general plant growth.

Savana Lipps (Research Intern) – performed a portion of the pathogenesis assays, microscopy, development of calcium sensor lines, and general plant growth.

Professor Abraham Koo (Collaborator - University of Missouri) – provided the resources for, and the time and support for the student to perform, the salicylic acid measurements.

Rebekah Holtsclaw (Collaborator - University of Missouri) – performed the salicylic acid measurements and provided insight into their interpretation.

Caleb Fitzgerald (Engineering Intern) – developed, constructed, and programmed the Automated Botanical Contact Device (ABCD).

Dr. Nathan Miller (Scientist) – contributed to thoughtful discussion of methods and results and developed the image-analysis pipeline for implementation of the ABCD.

Jerry Miao (Engineering Intern) – developed the software for operating the automated imaging components of the ABCD.

John Lombardino (Research Intern) – contributed to thoughtful discussion of methods and results and maintained a portion of the plants grown on the ABCD.

Dr. Richard Hilleary (Peer Mentor) – provided research insights and contributed to thoughtful discussion of methods and results.

Dr. Arthur Poitout (Peer Mentor) – provided research insights and contributed to thoughtful discussion of methods and results.

Dr. Arkadipta Bakshi (Post-Doctoral Researcher) – wrote a portion of Chapter 1.

LIST OF ABBREVIATIONS

Ca^{2+} – calcium ion
CaBP – Ca^{2+}-binding protein
CaM – calmodulin
CAMTA – CaM-binding transcription activator (SR)
CBP – CaM-binding protein
CBP60 – CaM-binding protein 60 family
CCaMK – CaM-dependent protein kinase
CPK – Ca^{2+}-dependent protein kinase
CML – calmodulin-like protein
CRK – CPK-related protein kinase
EF-hand – motif from E and F α-helices in Ca^{2+}-binding carp parvalbumin
ETI – effector-triggered immunity
FLS2 – flagellin-sensitive 2
HR – hypersensitive response
ICS1 – isochorismate synthase 1
LRR-RLK – leucine-rich repeat receptor like kinase
MAMP – microbe-associated molecular pattern
MAPK – mitogen-activated protein kinase
PRR – pattern-recognition receptor
PTI – pattern-triggered immunity
RBOH – respiratory burst oxidase homolog
ROS – reactive oxygen species
SA – salicylic acid
SAA – systemic acquired acclimation
SAR – systemic acquired resistance

Chapter 1:

Reading Signatures: Calmodulin and Calmodulin-like Proteins in *Arabidopsis thaliana*

This chapter has been formatted for submission to the *Journal of Experimental Botany*.

I would like to acknowledge the following people for contributing to the writing of this chapter: Dr. Arkadipta Bakshi and Simon Gilroy.

Arkadipta Bakshi, Simon Gilroy and I wrote all parts of the manuscript.

Abstract: Changes in cytosolic Ca^{2+} levels occur in plants in response to an almost bewildering array of stimuli. This Ca^{2+} signal is thought to act as a regulator of downstream cellular processes, with information about each different stimulus proposed to be encoded in the spatial and temporal dynamics of the elicited Ca^{2+} changes, the so-called Ca^{2+} signatures. Responses to the Ca^{2+} changes are mediated through a diverse array of Ca^{2+}-binding proteins (CaBPs). Calmodulins (CaMs) represent a major and highly conserved family of these Ca^{2+}-responsive proteins found in all eukaryotes and are central to the molecular control of many of these Ca^{2+}-regulated processes. In plants, the CaM-related Ca^{2+} sensor toolkit is greatly extended by a family of Calmodulin-like (CML) proteins. Through their diversity of structure and function, the CaM/CML family is capable of being tuned to respond to specific Ca^{2+} dynamics and trigger a huge range of selective downstream events. Ca^{2+}-binding kinetics, e.g., on- and off-rates, tune individual CaMs and CMLs to multiple Ca^{2+} signatures, potentially enabling them to coordinately generate appropriate downstream responses. This network of interactions between diverse stimuli, distinct Ca^{2+} signatures, numerous CaBPs and multiple downstream responses is the cell's "decoding cloud." Thus, CaM and CaM-related proteins provide a key element in a fine-tuned molecular network needed to interpret the information in stimulus-specific Ca^{2+} signatures.

Ca^{2+} Signaling through Ca^{2+} Signatures

The phosphate-based energy metabolism used by all life immediately imposed chemical constraints on the composition of the cytoplasm. For example, acommodating the millimolar levels of cytoplasmic phosphate required to sustain ATP-powered biology forced the earliest cells to maintain a cytosolic calcium concentration ($[Ca^{2+}]_{cyt}$) at orders of magnitude lower than the $[Ca^{2+}]$ of their aquatic environment. Higher Ca^{2+} levels would lead to cytotoxic calcium phosphate formation and precipitation within the cells (Hetherington and Brownlee, 2004). Thus, in all modern-day organisms, basal $[Ca^{2+}]_{cyt}$ levels are closely regulated at ~10^{-7} M by the combined action of Ca^{2+} influx through channels and efflux through pumps and co-transporters (Hetherington and Brownlee, 2004). This low resting $[Ca^{2+}]_{cyt}$ in turn set the scene for the operation of a ubiquitous signaling system based on Ca^{2+} fluxes. The low $[Ca^{2+}]_{cyt}$ means that: (1) only a relatively small absolute number of Ca^{2+} ions need to enter the cell to yield a large increase in cytosolic concentration that can then act as a signal, (2) the large $[Ca^{2+}]$ gradient from outside to inside also means that opening only a few channels is sufficient to support the required influx, (3) the efficient Ca^{2+} homeostasis system can then rapidly return the system to the resting Ca^{2+} levels before the elevated calcium's cytotoxic effects become evident and (4) as a relatively small number of ions are moving, the system does not have to expend large amounts of energy in moving Ca^{2+} ions across membranes in order to maintain cellular homeostasis. The evolution of these dynamically modulated influx and efflux mechanisms led to the processes we now recognize as Ca^{2+} signaling, a regulatory system conserved amongst prokaryotic and eukaryotic lineages (Plattner and Verkhratsky, 2015).

When a stimulus triggers an increase in $[Ca^{2+}]_{cyt}$, information about the signal is thought to be encoded in the spatio-temporal characteristics of the $[Ca^{2+}]_{cyt}$ changes, the so-called Ca^{2+}-

signature of the stimulus. Features such as the amplitude, duration, rise time, kinetics of resetting to basal levels and frequency of repetition of the Ca^{2+} change are all likely to play into the specifics of the signature. In addition, subcellular locales may show very distinct Ca^{2+} changes, e.g., nuclear and cytosolic Ca^{2+} fluxes can be uncoupled and this uncoupling results in the generation of separate Ca^{2+} signals under distinct conditions (Charpentier *et al.*, 2016). Thus, Ca^{2+} signatures offer enormous potential to encode specific signaling information within the plant, even down to the subcellular level. Not surprisingly then, changes in $[Ca^{2+}]$ are known to play an important regulatory role in plant cells during a wide array of growth and developmental processes and in response to diverse environmental stimuli ranging from extreme temperatures, flooding, drought, high salinity, wounding, pathogen attack and light stress (Reddy, 2001; Rudd and Franklin-Tong, 2001; Sanders *et al.*, 2002; White and Broadley, 2003). Indeed, no other cellular messenger has been demonstrated to respond to more stimuli than Ca^{2+} (Rudd and Franklin-Tong, 2001; Hetherington and Brownlee, 2004), often leading to the question, is there any specificity in such a ubiquitous signal? It has even been suggested that there is in fact no specific information in the Ca^{2+} change other than 'something has changed' (Scrase-Field and Knight, 2003). In this scenario other signaling molecules carry information about the nature of the change. The reader is directed to several excellent recent reviews on the generation and shaping of the Ca^{2+} signatures and the evidence that in plants it does or does not carry information (Snedden and Fromm, 2001; Kim *et al.*, 2009; Yuan *et al.*, 2017). Rather, we will tackle the other side of this information processing question: how could the plant decode the intricacies of the Ca^{2+} signature into specific cellular outputs in response to various cellular stimuli? We will therefore focus on the finely tuned network of Ca^{2+} sensing and response proteins (Ca^{2+}-binding proteins, CaBPs) with the potential to extract

specific information from what at first sight might appear as a generic stimulus-induced increase in $[Ca^{2+}]_{cyt}$.

Ca^{2+}-Binding Proteins in Plants

Although numerous CaBPs have evolved to interact with cellular Ca^{2+} (Day *et al.*, 2002), not all CaBPs act as signaling molecules. Thus, CaBPs come in a range of classes including: (1) proteins whose structure or catalytic activity requires Ca^{2+} as a cofactor (such as the amylase enzyme) but that are not directly regulated by changes in $[Ca^{2+}]_{cyt}$; (2) Ca^{2+}-buffers that function to maintain the steady-state $[Ca^{2+}]$ of a particular cellular compartment but that lack enzymatic activity or further protein- or nucleic acid-binding capacity (such as calreticulin in the plant ER lumen); (3) Ca^{2+} transporters that move calcium ions across membranes and so help maintain Ca^{2+} homeostasis and shape any Ca^{2+} signature (such as the numerous Ca^{2+} channels, pumps and co-transporters found in plant cell membranes), and (4) Ca^{2+}-sensors (Gifford *et al.*, 2007) where the binding of Ca^{2+} either directly modulates the CaBP's own intrinsic enzymatic activity (e.g., a directly Ca^{2+}-regulated protein kinase such as the CPKs) or causes a conformational change whereby the CaBPs can go on to regulate other cellular targets (e.g., calmodulin or calcineurin B, see below) (Dodd *et al.*, 2010). The proteins in this latter class are diverse in the nature, but many share a relatively few, well-conserved Ca^{2+} binding domains. The following sections will therefore introduce examples of the major families of Ca^{2+}-binding domains found in plant Ca^{2+}-sensors and begin to dissect how their nature helps explain some of the ability of the plant's molecular decoding network to extract information from the dynamics of Ca^{2+} signatures.

Ca^{2+}-Binding Motifs are More Common than You Might Guess

There are some physical constraints on the amino acids lining the protein "pocket" that can bind the calcium ion, with Ca^{2+}-binding requiring coordination with several (typically 4-8) amino-acid residues. The pattern of coordination frequently includes amino acid backbone or side-chain carbonyl oxygen atoms and bridged H_2O molecules (Kretsinger, 1976; Zhou *et al.*, 2013). Therefore, although evolution has equipped cells with multiple classes of Ca^{2+}-binding motifs, these structural constraints have led to some conserved and relatively ubiquitous themes such as: the alpha-helix based EF-hand, the beta-sheet based C2 domain and the alpha/beta-based alpha/beta fold found in e.g., Phospholipase C (Bindreither and Lackner, 2009).

The EF-hand motif was named for the Ca^{2+}-binding structures found in the E and F helices of carp muscle parvalbumin and their symbolic similarity to a hand with the thumb up and forefinger pointed outward (**Figure 1.1**) (Kretsinger and Nockolds, 1973). The Ca^{2+}-binding loop

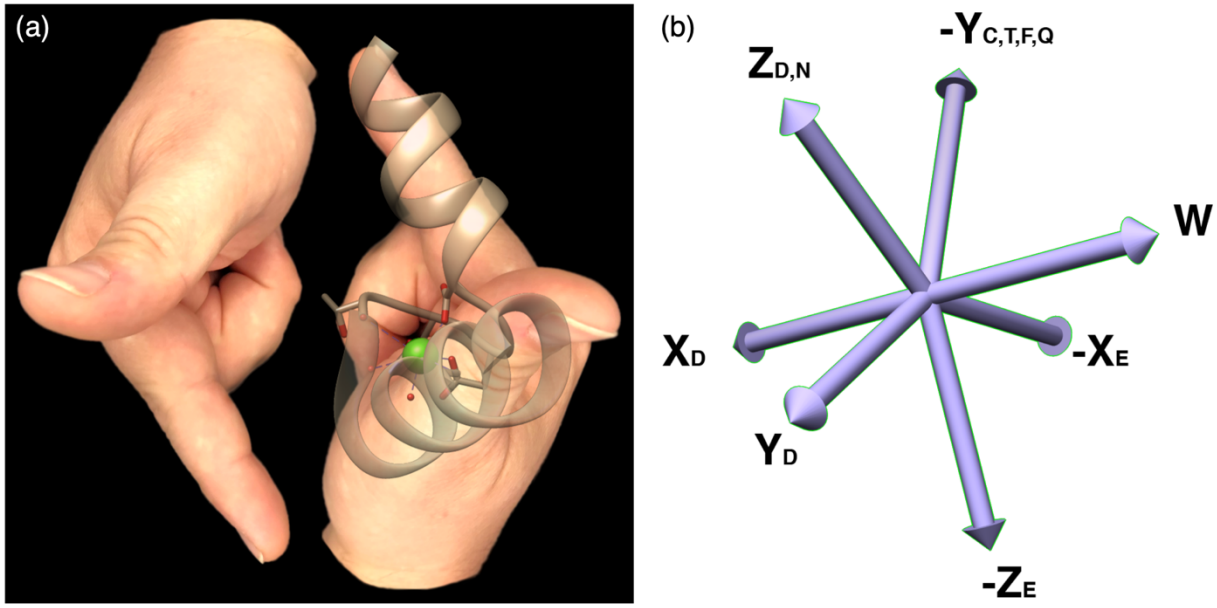

FIGURE 1.1 Visualizing EF-Hands. (a) A classic figure from Kretsinger and Nockolds, 1973, recapitulated: this pair symbolizes the EF-Hand motifs found in some Ca^{2+}-binding proteins. Helix E runs from the tip to the base of the forefinger. The bent middle finger corresponds to the E-to-F Ca^{2+}-binding loop. Helix F runs from the tip of the middle finger to the tip of the thumb. The outward-tilted thumb corresponds to the bend due to the kink in helix F at the N-terminal leucine residue. **(b)** Idealized representation of the pentagonal bipyramidal coordination of Ca^{2+} (at the model's vertex) by EF-hand residues.
3D models: Chimera v.1.13.1 (Yang *et al.*, 2012).

of the EF-hand is pentagonal bipyramidal in conformation, containing six Ca^{2+}-coordinating residues (X,*,Y,*,Z,*,-Y,*,-X,*,*,-Z, where the asterisks represent non-binding residues) that support the molecular interactions that form a Ca^{2+} coordination pocket (Nakayama *et al.*, 2000). EF-hands are frequently found together within the same protein and this paired conformation promotes more stable binding of Ca^{2+} (Kawasaki *et al.*, 1998). This motif is found, for example, in the most abundant and highly-conserved family of CaBP regulators, the calmodulins (CaMs), where 2 pairs of EF-hands define a Ca^{2+}-dependent switch that acts on this protein's conformation to reveal or hide an internal protein-protein interaction domain (Halling *et al.*, 2016; La Verde *et al.*, 2018). It is important to note here, that not all EF-hand domains are capable of binding Ca^{2+}. Mutations in the E-to-F loop residues or three-dimensional arrangement of the two helices leads to the disruption of required coordinating residues that either alter the strength of Ca^{2+} binding or abolish this activity completely. For example, mutations in the second EF hand domain of the salt tolerance gene *SOS3* (for *salt overly sensitive 3*) causes *Arabidopsis* plants to become hypersensitive to Na^{+}-induced growth inhibition. The mutation in the *sos3* mutant disables the calcium binding of the second EF hand (Liu and Zhu, 1998). Natural divergence in Ca^{2+} binding capacity likely facilitates adaptive divergence in function (La Verde *et al.*, 2018) and means that caution must be applied when assigning an uncharacterized protein to a Ca^{2+}-based signaling cassette simply on the basis of it possessing a predicted EF-hand.

While CaBPs containing EF-hand motifs are arguably the best known, other Ca^{2+}-binding domains exist in eukaryotic proteins. For instance, C2 domains, named for the second regulatory domain of mammalian Ca^{2+}-dependent protein kinases C (Cho and Stahelin, 2006) are also found in many plant Ca^{2+}-regulatory proteins. Most C2 domains exhibit Ca^{2+}-dependent phospholipid membrane binding activity and so are often important components of membrane-interacting, Ca^{2+}-

related signaling proteins (Nalefski and Falke, 1996; Yamazaki *et al.*, 2010). As with EF hand-containing proteins, proteins can contain multiple tandem C2 domains. For example, *Arabidopsis* has 16 transmembrane proteins that are predicted to have multiple C2 domains (the MCTPs) (Liu *et al.*, 2018). However, not all C2 domains have retained their Ca^{2+}-binding abilities, e.g., *Rattus norvegicus* (rat) synaptotagmin 4 has a degenerate C2 domain that binds phospholipids but not Ca^{2+} (Dai *et al.*, 2004). Conversely, the MCTPs bind Ca^{2+} but have lost the phospholipid binding capabilities in their C2 domains (Shin *et al.*, 2005). However, the MCTPs are still membrane associated proteins as transmembrane domains elsewhere in their structures appear to now provide the membrane association function for these proteins.

EF-hand and C2 domains that have retained their bona-fide Ca^{2+} binding activities show further diversity in the significant variation in their affinity for Ca^{2+} (Linse *et al.*, 1987; Snijder *et al.*, 2001; Erickson *et al.*, 2005; Apiyo *et al.*, 2005; Gifford *et al.*, 2013; Astegno *et al.*, 2016). For instance, the C2 domain in rat synaptotagmin 1 has a K_d^{Ca} of 2.8 nM (Yao *et al.*, 2011) whereas the C2 domain in rat otoferlin has a K_d^{Ca} of 348-456 μM (Meese *et al.*, 2017), representing a 10^5-fold range of C2 domain Ca^{2+}-binding affinity within proteins from the same organism. Likewise, in plants, the EF-hand Ca^{2+}-binding affinity of different CaM-like proteins (CMLs) has been demonstrated to cover the nM to μM ranges, again suggesting divergent EF hand structures with Ca^{2+} affinities that can span many orders of magnitude (Dobney *et al.*, 2009; Gifford *et al.*, 2013; Bender *et al.*, 2014; Astegno *et al.*, 2017; Ogunrinde *et al.*, 2017). Diversity in Ca^{2+} binding affinity builds in a feature necessary to decode different Ca^{2+} signatures, i.e., the lower the affinity, the higher the magnitude of the Ca^{2+} signal required to trigger binding and activation of the CaBP. Thus, specific CaBPs can be tailored to respond to a specific threshold amplitude of Ca^{2+} signature. Coupled with other biochemical differences in CaBP Ca^{2+} binding domain parameters, such as on-

and off-rates of Ca^{2+} or the kinetics of interactions of the Ca^{2+}-activated protein with its downstream partners, could all theoretically tailor the activation of a CaBP and its target pathway(s) to both a specific magnitude and duration of Ca^{2+} change. Indeed, there is now accumulating experimental evidence for the action of such biochemical fine-tuning of response to signature.

Thus, in animal cells, the combination of affinity and on- and off-rates have been shown to be able to tune CaM Kinase II activity to a specific frequency of Ca^{2+} spiking within the cell (De Koninck and Schulman, 1998). Similarly, in plants, the Ca^{2+}/CaM-dependent protein kinase (CCaMK) has been shown to be biochemically tuned to respond to the nuclear Ca^{2+} transients that are triggered by nod factor signaling. Nod factors are key signals in the pathway leading to the induction of symbiotic nitrogen-fixing root nodules in legumes. In this system, Ca^{2+} acts in both an inhibitory and stimulatory manner on CCaMK, dependent on the Ca^{2+} binding domain in operation within this protein (Miller *et al.*, 2013). This ability arises from CCaMK having both EF hands and a CaM-binding domain. Modeling of the effects of the relative Ca^{2+} affinities and binding kinetics at each of these sites suggests Ca^{2+} binding to the EF hands stimulates CCaMK autophosphorylation, locking the kinase in an inactive mode at basal Ca^{2+} levels. However, as Ca^{2+} increases during the nuclear Ca^{2+} spiking triggered by nod factor signaling, Ca^{2+}/CaM binds and overrides the EF hand effect, activating the kinase, with the rate of activation being coupled to the spiking rate. Consistent with these ideas, when the affinity for CaM of CCaMK is enhanced (by mutation within the CaM-binding site), and kinase activity is constitutively promoted, the system is no longer able to decode the Ca^{2+} signal to appropriate (nodulation) output (Jauregui *et al.*, 2017). Intriguingly, there is a further element of information decoding reported in this system. The plant response of root nodule induction is tuned to a specific accumulated number of Ca^{2+}

transients (~36 in *Medicago truncatula*) (Miwa *et al.*, 2006), suggesting the decoding machinery is capable of both decoding the Ca^{2+} transient and 'counting' the number of activations that fall within this signature envelope. The machinery behind the counting process remains undefined but may operate via the accumulation of some biochemical output such as the buildup of phosphorylated CCaMK target protein(s).

These examples provide evidence that the biochemistry of Ca^{2+} binding domains should be capable of tailoring outputs to specific Ca^{2+} signal input characteristics. However, as noted previously, Ca^{2+} changes are seen in response to myriad stimuli. As a result, plants are required to produce a suite of diverse CaBPs that operate a network of decoding systems with a wide range of different responses to these varied Ca^{2+} signature inputs. In the next section we will explore just how extensive this plant CaBP network is likely to be.

Prevalence and Diversity of Plant Ca^{2+}-binding Proteins

Ca^{2+} changes are thought to modulate the activity of a wide range of CaBPs. These include proteins in the CaM and CML family but also proteins as diverse as Calcineurin-B-like proteins (that often act through a paired CIPK protein kinase), Ca^{2+}-dependent protein kinases (CPKs), CCaMKs, calcium-regulated phosphatases, NADPH oxidases (e.g. respiratory burst oxidase homolog D - RBOHD) (Miller *et al.*, 2009) and a host of other binding proteins that directly interact with Ca^{2+}.

Original estimates made in 2002 of the number of EF hand containing proteins in the *Arabidopsis* genome was ~250 (Day *et al.*, 2002). Reanalysis of the current genome annotations for CaBPs using UniProtKb (Bateman *et al.*, 2017) and InterProScan (Finn *et al.*, 2017) coupled with critical curation (Poux *et al.*, 2016) are shown in **Figure 1.2**.

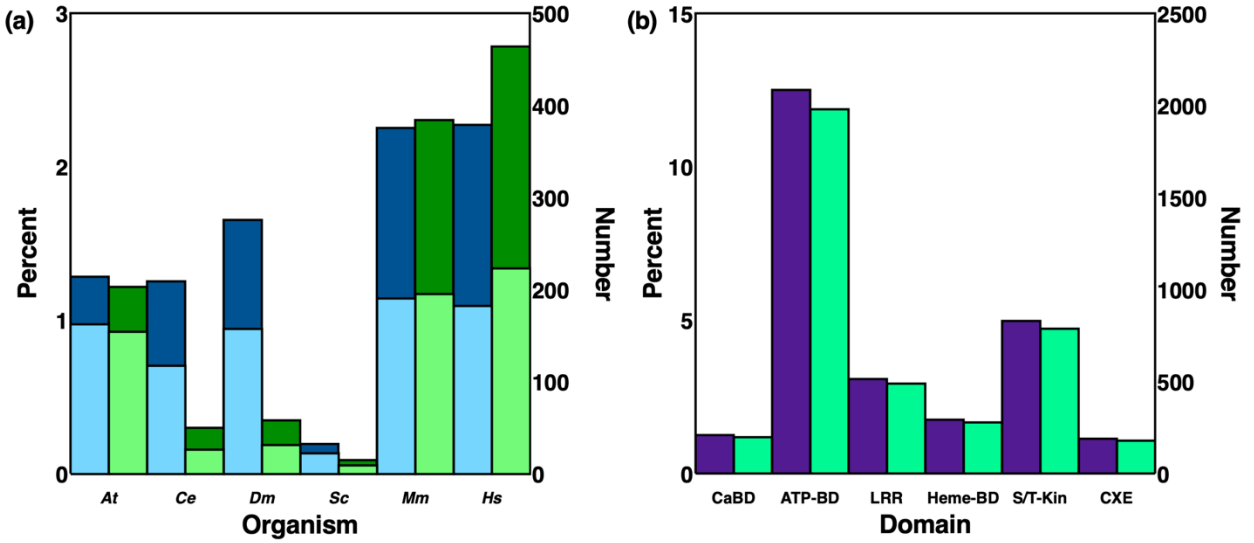

FIGURE 1.2 Comparing CaBD and EF-Hand Genome Enrichment (a) A comparison of the number of CaBPs (dark green), EF-hand proteins (light green), and their percentage of the total number of proteins (dark and light blue, respectively) in each species. *At*, *Arabidopsis thaliana*; *Ce*, *Caenorhabditis elegans*; *Dm*, *Drosophila melanogaster*; *Sc*, *Saccharomyces cerevisiae*; *Mm*, *Mus musculus*; *Hs*, *Homo sapiens*. **(b)** The number of *Arabidopsis* proteins containing Ca^{2+}-binding, ATP-binding, leucine rich repeat (LRR), heme-binding, serine/threonine kinase, or carboxylesterase domains (green) and their percentage of the total number of proteins (purple). Proteins in **(a)** and **(b)** were annotated by Swiss-Prot from 'records with information extracted from literature and curator-evaluated computational analysis'. Data compiled from UniProtKB (https://www.uniprot.org) and InterProScan (http://www.ebi.ac.uk/interpro).

This analysis reveals that *Arabidopsis* likely invests ~1.5% of its genome in CaBPs, with the majority being EF-hand domain containing proteins. Indeed, there is an apparent expansion of the proportion of the EF-hand family within *Arabidopsis* CaBPs vs. the other organisms analyzed. Thus, EF-hand proteins were found to constitute 62.88% of CaBPs in *Arabidopsis* but only 35.55% of CaBPs in *Homo sapiens* and 36.32% of CaBPs in *Mus musculus*. The disparity in relative levels may be due to the different metabolic and rapid Ca^{2+} buffering requirements of animals versus plants, or effects of recent gene duplications in the plant lineage (Hepler, 2005; Panchy *et al.*, 2016; Wagner *et al.*, 2016).

Therefore, plants appear to have dedicated a significant proportion of their genomes to proteins with readily identifiable Ca^{2+}-regulation-related domains. While these putative Ca^{2+} dependent regulators are nowhere near as prevalent as the generic major classes of metabolic enzymes, such as the ATP-binding protein family (**Figure 1.2b**), they are present at approximately 25% of the prevalence of the most ubiquitous cellular regulatory elements, such as the protein

kinase superfamily, and on a par with other major regulatory groups of plant proteins such as the LRRs (**Figure 1.2b**). This extensive investment in CaBPs is consistent with the requirements to decode diverse Ca^{2+} signatures, but how strong is the evidence that these proteins do indeed play widespread roles in signal-response networks in plants? To explore this question, we will ask how well we understand the role(s) of one of the major families making up this CaBP network, the CaM/CML proteins, in plant response signaling.

CaM/CML Proteins

Calmodulin is a CaBP that has been reported in all eukaryotes studied. The *Arabidopsis* genome contains 7 *CaM* and 50 *CML* genes. The seven *CaM* genes encode 4 isoforms: *CaM1*/*CaM4* (both encode an identical protein), *CaM2*/*CaM3*/*CaM5* (all 3 encode an identical protein), *CaM6*, and *CaM7*. The reason behind why there are multiple genes encoding the same proteins has yet to be extensively explored. However, it seems likely that this would offer the plant a great deal of flexibility in fine-tuning expression and dosage to environmental or developmental signals.

The CaMs bind four Ca^{2+} ions and, in response, undergo a conformational change that exposes up to two hydrophobic domains capable of binding and regulating a diverse set of proteins (Zeng *et al.*, 2015). Protein-protein interaction studies using *Arabidopsis* protein microarrays has identified an array of potential targets of CaM/CML family members, which include transcription factors, intracellular and receptor protein kinases, F-box proteins, RNA-binding proteins, cell-cycle-specific proteins, Ca^{2+}-binding EF hand proteins, and diverse proteins of unknown functions (Popescu *et al.*, 2007). All *Arabidopsis* CaM isoforms exhibit >85% amino acid identity with *Homo sapiens* Calmodulin 1 (**Figure 1.3**), in part reflecting the small size of the protein coupled

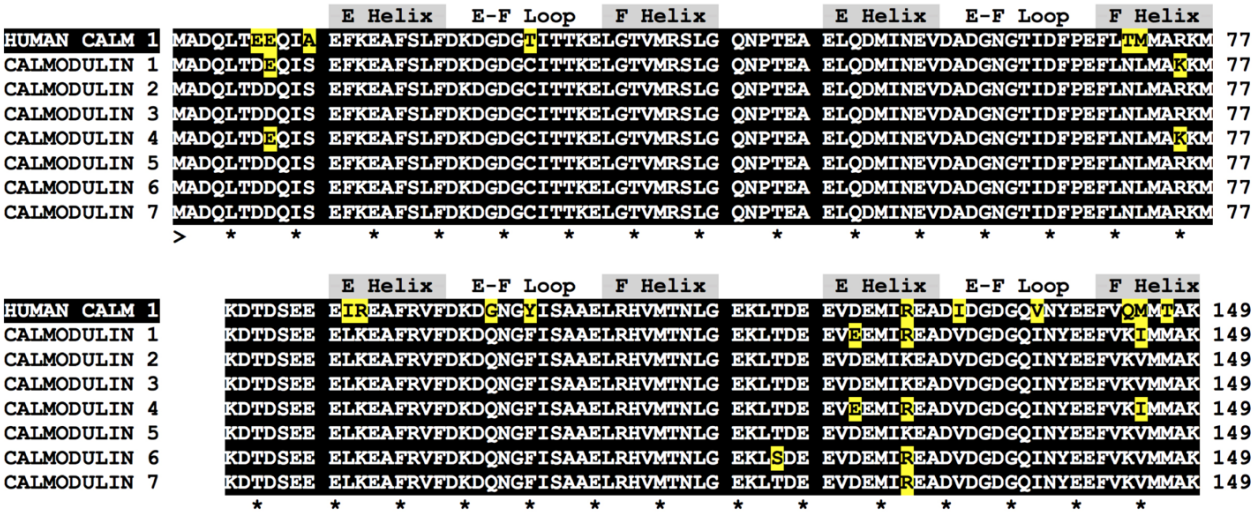

FIGURE 1.3 Alignment of CALM1 from *Homo sapiens* with Arabidopsis CaM1-7. The protein alignment shows that 14 of 149 amino acids (9.39%) in CALM1 differ from CaM2/3/5 and CaM6. Only 12 of 149 (8.05%) differ between CALM1 and CaM1/4 and 13 of 149 (8.72%) differ between CALM1 and CaM7. Alterations in the E and F helices are not thought to directly alter Ca^{2+}-binding, but may have implications for allosteric regulation of other processes. This alignment shows that *CaM1* and *CaM4* encode identical proteins, as do *CaM2*, *CaM3*, and *CaM5*. Further, *CaM6* and *CaM7* differ by one serine to threonine substitution at residue 118. Differences between CaM2/3/5 and the others (including CALM1) are highlighted in yellow. Methionine is marked with (**>**). Every fifth residue is marked with an asterisk (*).

to the tight functional constraints on the structure of the EF hand domains that make up a significant proportion of the CaM sequence. Indeed, all four *Arabidopsis* CaM isoforms are almost identical in sequence at the level of their EF-hand containing loop regions (**Figure 1.3**).

CaMs are usually thought of as allosteric regulators of protein function, interacting with target enzymes to modulate their activity. However, *Arabidopsis* CaM7 has been shown to directly interact with Z/G-box DNA, possibly due to the arginine at position 127 in its fourth E-helix, allowing it to directly act as a transcription factor (**Figures 1.3, 1.4**) (Kumar *et al.*, 2016) and to interact with the transcriptional machinery. For example, CaM7 physically interacts with the HY5 transcription factor to regulate photomorphogenesis (Abbas *et al.*, 2014). CaM2/3/5 is identical in amino acid sequence to CaM7 but substitutes a lysine at position 127 and does not have this DNA binding capacity. An arginine at amino acid 127 is also seen in CaMs 1, 4 and 6, but there are other amino acid changes in these isoforms relative to CaM7 and the activity of these other CaMs in transcriptional regulation remains to be fully explored.

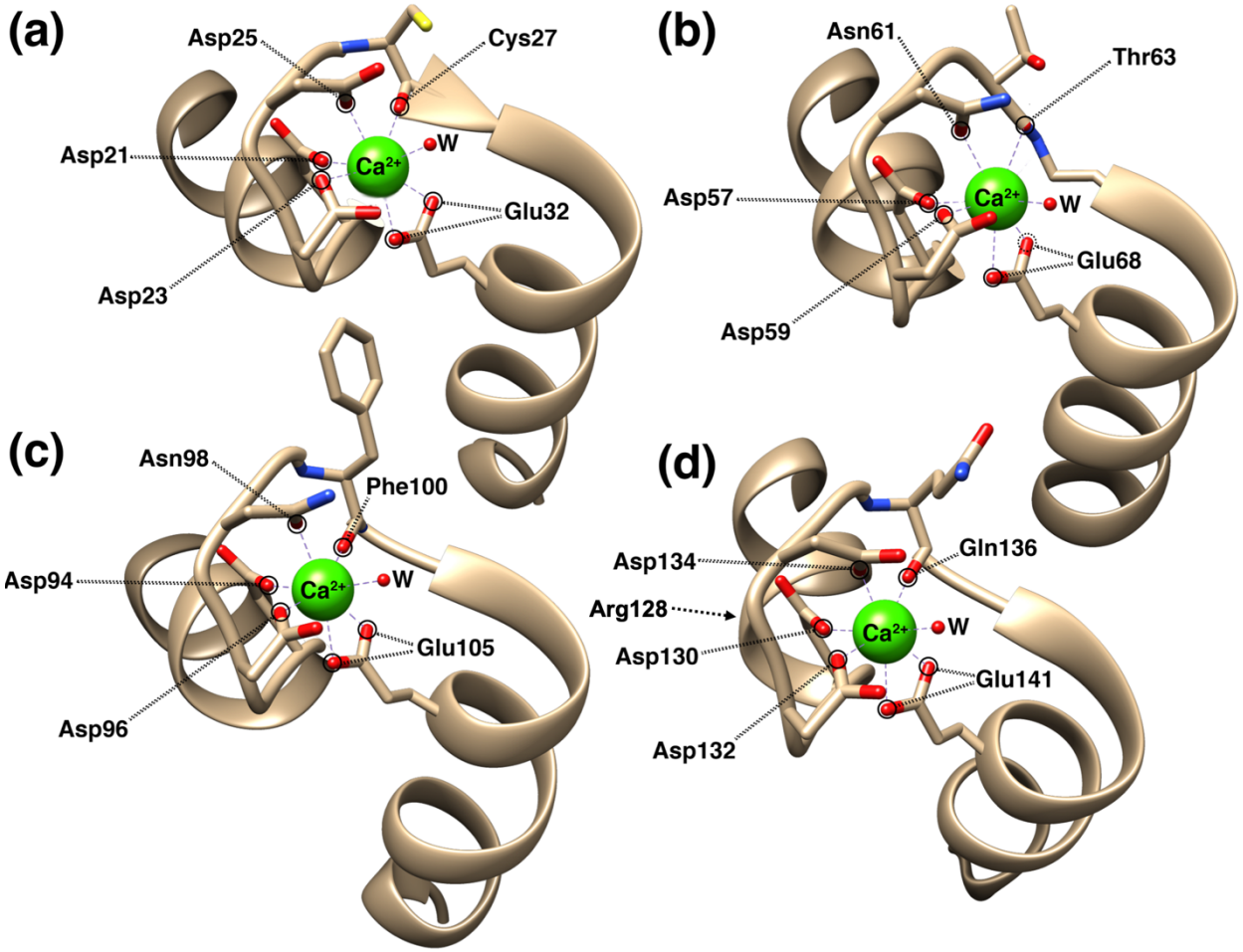

FIGURE 1.4 The Ca^{2+}-binding EF-hands of *Arabidopsis* CaM7 (a) depicts the helix – Ca^{2+}-binding loop – helix structure of the first EF-hand with the critical conserved Ca^{2+}-coordinating residues noted ; **(b—d)** depict the other 3 EF-hand motifs. "W" is water (H_2O). Residue Arg128 in **(d)** is thought to be responsible for the DNA-binding activity of CaM7 relative to, e.g., CaM2 (having Lys128, instead). 3D models: Chimera v.1.13.1 (Yang *et al.*, 2012).

In contrast to the almost identical sequence of the CaMs in *Arabidopsis*, CMLs share <50% amino acid sequence identity with *Arabidopsis* CaM2 or *H. sapiens* calmodulin 1 (CALM1; humans have 3 calmodulin genes that encode almost identical protein isoforms). To be considered a CML, a proteins must also: contain EF hands; have no other obviously identifiable functional domains (such as a protein kinase or NADPH oxidase domains); and still share at least 16% amino acid identity with CALM1 (McCormack and Braam, 2003). CML proteins contain a range from 1-6 Ca^{2+}-binding EF hands: CML1 contains 1 EF hand; CML28, CML29, and CML47-50 contain 2 EF hands; CML13, CML14, and CML42-46 contain 3 EF hands; CML2-11, CML15-27,

CML30-39, and CML41 contain 4 EF hands; and CML12 contains 6 EF hands, although the precise residues in the EF hands vary. Clearly, differences in the numbers of EF hands and of the amino acid residues in these domains have implications for the Ca^{2+}-binding affinity of the CaMs and CMLs. As noted, divergence in Ca^{2+}-binding affinity likely leads to subfunctionalization (McCormack *et al.*, 2005), as CaM/CML family members that more readily bind Ca^{2+} could respond to more minute increases in $[Ca^{2+}]_{cyt}$ than those members that only bind Ca^{2+} at higher concentrations.

Thus, the 50 CMLs comprise a hugely diverse family. Considering that even within the highly conserved *Arabidopsis* CaM family, CaM isoforms are able to be targeted to the regulation of very different cellular outputs, (such as CaM7's direct transcriptional regulation), the diversity of the CMLs implies their involvement in a wide range of networks coupling Ca^{2+}-signature to varied cellular outputs. The CMLs are also found in a range of different subcellular compartments including the extracellular matrix and in some cases are known to relocate between these compartments in response to different stimuli (Zielinski, 1998; Snedden and Fromm, 2001; Bouché *et al.*, 2005; Aldon and Galaud, 2006; Bender and Snedden, 2013). As such, the CaM/CML superfamily should, in theory, be able to link a huge range of Ca^{2+} signal dynamics to an equally wide array of physiological outputs through their binding to, and activation/inactivation of, a diverse group of downstream target proteins (Whalley and Knight, 2013). Therefore, the CaMs and CMLs offer a potential network capable of extracting the stimulus-specific information in the fine scale dynamics of apparently generic stimulus-evoked changes in cytoplasmic Ca^{2+}. In the following sections we will explore some examples that suggest that this potential for CaM/CML-linked flexibility in decoding Ca^{2+} signaling is in fact realized within the plant but that also highlight some of the important gaps in our understanding of this regulatory network.

The Families of CaBPs Decoding Ca^{2+} Signatures in Plants

In plants, the paradigm is therefore that CaM and CML proteins decode and transmit information from Ca^{2+} signatures to modulate target protein activities (Sanders *et al.*, 1999; Dodd *et al.*, 2010), i.e., individual Ca^{2+}-free CaMs (apoCaMs) (Jurado *et al.*, 1999) and CMLs bind cytosolic Ca^{2+} only after an increase above basal $[Ca^{2+}]_{cyt}$ levels that relate to a Ca^{2+} signature (Perochon *et al.*, 2011). However, before describing the evidence supporting this model for decoding Ca^{2+} signatures through CaM and CML action, we should note there that there is a distinct possibility that these proteins also have Ca^{2+}-independent activities (Akyol *et al.*, 2004; Rainaldi *et al.*, 2007). For example, there are reports indicating calcium-independent responses mediated via CaM in animals, such as regulation of the intracellular movement of brush border myosins along actin filaments (Houdusse *et al.*, 1996) and maintenance of apoCaM levels by binding to neuromodulins in neurons (Kumar *et al.*, 2013). However, the major action of the CaMs and CMLs in plants is likely to be in Ca^{2+}-dependent signaling where CAM action leads to modulation of targets in response to specific Ca^{2+} signatures. The following section therefore briefly surveys the diversity of plant responses linked to CaM and CML action. This is a vast area of research and so we have selected a few instructive case studies. We apologize to the many researchers whose work we have had to omit solely due to space constraints.

CaMs, CMLs and Plant Abiotic Stress Responses

Overview and Description of the Role of Stress-Related GABA Signals

Abiotic stresses such as flooding, drought, salinity, extreme temperatures, ultraviolet radiation, and other adverse environmental conditions are the primary threats behind limiting crop productivity worldwide (Virdi *et al.*, 2015). In recent times, preventing these crop losses and

fulfilling the demands of agricultural production to feed the world have gained unprecedented importance. Ca^{2+} signaling plays a key role in mediating these abiotic stress responses in different plant species and there should be no surprise to find that CaM and CML family members have been implicated in the regulation of many target proteins involved in the associated signal transduction pathways.

γ-aminobutyric acid (GABA) is a well-characterized ubiquitous, non-protein amino acid, perhaps best known as a major inhibitory neurotransmitter in the central nervous system of animals (Mody *et al.*, 1994)**.** However, this molecule also plays important stress signaling roles in plants**.** GABA is produced from L-glutamate by the action of glutamate decarboxylase (GAD). Phylogenetic studies have shown that the general structure of GAD is well conserved from bacteria to plants and animals (Ueno, 2000). In plants, GAD activity has been found to be modulated by Ca^{2+}/CaM in response to various abiotic stresses such as salt, osmotic, heat, cold, anoxia and reactive oxygen species related damage, leading to increased levels of GABA synthesis (Bouché and Fromm, 2004). All of these stimuli have been characterized as triggering a diverse array of Ca^{2+} signatures (Tuteja and Mahajan, 2007; Boudsocq and Sheen, 2009). Analysis of transgenic lines expressing either truncated versions of GAD lacking the CaM-binding domain or that overexpress CaM, indicate that CaM is indeed a key regulator of GABA synthesis in plants *in vivo* (Baum *et al.*, 1996). Different GAD isoforms are expressed in both a tissue- and stress- dependent manner in various plant species such as rice, petunia, tomato and soybean (Baum *et al.*, 1996). Although the diverse roles of GABA in plants are still being uncovered, the activation of GAD activity by Ca^{2+}/CaM-binding appears to be important for the growth and development of plants in response to various abiotic stimuli. GABA may even be involved in systemic stress responses, with local wounding in one leaf causing GABA accumulation in unwounded tissues (Scholz *et al.*,

2017). However, it is important to note that in this latter case, the authors argue that the regulatory signal may not be Ca^{2+}. GAD is activated by many different stimuli and defining which CaM, or potentially CML, isoforms are the key regulators of GAD activity under these diverse stress environments and what features of these diverse Ca^{2+} signatures are used to commonly activate this enzyme, remain key questions to be addressed.

Light Quality and Flowering

Two closely-related *Arabidopsis* CMLs, CML23 and CML24, with non-identical but overlapping functions, are involved in the regulation of leaf to flower transition in response to seasonal day length in plants (Tsai *et al.*, 2007). Altered flowering responses to photoperiod were observed in *Arabidopsis* transgenic plants with either single *cml24* loss-of-function mutants or double *cml23 cml24* loss-of-function mutants, all grown under long-day conditions (16h light/8h dark). The *cml24-4* mutant exhibits late flowering and generates a greater number of rosette leaves. On the contrary, the *cml24-2* mutant flowers early and produces fewer leaves prior to flowering, compared to wild type (Col-0). In addition, altered expression of genes involved in flowering time regulation such as *flowering locus T* (*FT*), *constans* (*CO*), and *suppressor of overexpression of constans 1* (*SOC1*) correlated with early flowering in *cml24-2* and late flowering in *cml24-4* and *cml23 cml24* double mutants (Tsai *et al.*, 2007). Directed yeast two-hybrid screening revealed that CML24 interacts with a member of the AtG4-regulated autophagy protein family, AtG4b. Altered responses to autophagy progression (altered formation of autophagic bodies and sensitivity to prolonged darkness) were recorded in transgenic plants with missense mutations in the *CML24* gene (Tsai *et al.*, 2013).

CML24 (initially identified as a touch-inducible gene, *TOUCH2*/*TCH2*), has also been found to be highly responsive to diverse environmental stress stimuli such as darkness, extreme temperatures, mechanical perception, oxidative damage, and hormone signals (Delk *et al.*, 2005). Phenotypic results of *CML24*-underexpressing lines indicated the roles of CML24 in ion homeostasis, ABA-mediated inhibition of seed germination, and long-day induction of transition to flowering (Delk *et al.*, 2005). This involvement of CML24 in so many processes suggests the likely multifaceted nature of the CaM/CML network, a theme that will develop in later sections.

Salt/Osmotic Stress

CaMs and CMLs also appear important for responses to salt- and osmotic-related stress conditions, stimuli closely linked to triggering rapid changes in Ca^{2+} (Donaldson *et al.*, 2004; Mahajan *et al.*, 2008; Park *et al.*, 2016). For example, the CaM-binding transcription factor (MYB2) controls the expression of salt- and dehydration- responsive genes in *Arabidopsis* (Yoo *et al.*, 2005). *In vitro*- and *in vivo*- studies have demonstrated that the DNA binding ability of MYB2 is differentially regulated by two closely related soybean CaM isoforms (*Gm*CaM4 vs. *Gm*CaM1), resulting in altered salt tolerance in plants (Yoo *et al.*, 2005).

Other CaM-binding proteins have been implicated in both positive and negative regulation of stress responses (Delk *et al.*, 2005). For instance, *Arabidopsis* CaM-binding protein 25 (CaMBP25), functions as a negative regulator of osmotic and salt stress tolerance in plants with a likely nuclear site of action (Perruc *et al.*, 2004). Molecular analyses indicate that *CaMBP25* is differentially expressed in plant tissues through ethylene- and ABA- independent pathways, induced by various environmental stresses. Similarly, the CMLs have also been linked to salt stress signaling. For example, CML9 plays a key role in mediating salt tolerance by negatively regulating

ABA-mediated signaling pathways. Transgenic *cml9* knock-out plants are also found to have impaired salt stress responses and hypersensitivity to ABA-mediated inhibition of seed germination (Perruc *et al.*, 2004; Magnan *et al.*, 2008). Thus, a theme is emerging of a Ca^{2+}/CaM-related signaling cassette, likely linked through ABA to salt stress responses. As might be predicted from our discussion of Ca^{2+} binding domain diversity and decoding Ca^{2+} signatures, this CaM-driven series of events is just one component of a multifaceted Ca^{2+}-dependent salt response network. Thus, in parallel, the *S*alt Overly *S*ensitive (SOS) signaling pathway decodes Ca^{2+} signals via the EF-hands of CBL4/CBL10/CIPK24 (Köster *et al.*, 2019). This network of response elements raises key questions about how these various elements are integrated. For example, does the structure of their EF hands tune CBL4 or CBL10 to the same elements of the salt Ca^{2+} signature as the CaM(s) regulating MYB2, CaMBP25 or CML9?

Drought and Flooding Stress

Previous studies using *Arabidopsis* protein microarrays had identified several targets of CaM/CML family members, such as transcription factors, intracellular and receptor protein kinases, F-box proteins, RNA-binding proteins, cell-cycle-specific proteins, Ca^{2+}-binding EF hand proteins, and proteins of unknown functions (Popescu *et al.*, 2007), which are found to be involved in drought and flooding stress responses (Azimzadeh *et al.*, 2008; Reddy *et al.*, 2011; Hu *et al.*, 2018; Rastogi *et al.*, 2019). One of the CaM-binding transcription factors identified, ABA-responsive element binding factor 2 (ABF2/AREB1), is well-conserved in land plants and has been found to be involved in drought stress tolerance (Yoshida *et al.*, 2010). Like ABF2, ABF4/AREB2 and ABF3 act as master transcriptional regulators of the ABA-responsive element (ABRE). This element occurs in the promoters of a host of different genes, such as those encoding for

phosphatases, kinases, other transcription factors and late embryogenesis abundant (LEA) proteins that are responsive to ABA, dehydration and salinity stresses (Yoshida *et al.*, 2010). Indeed, the ABRE has been shown to connect a promoter sequence to regulation by Ca^{2+} transients (Kaplan *et al.*, 2006).

In tomato, two of the AREB/ABF family members, *Sl*AREB1 and *Sl*AREB2 are induced by drought and salinity stresses in both leaf and root tissues. Transgenic tomato plants overexpressing *SlAREB1* and *SlAREB2* are found to have elevated tolerance to salt and water stress conditions by activating genes encoding for lipid transfer proteins (LTPs), oxidative damage-related proteins, LEA proteins and some pathogenesis-related proteins (Orellana *et al.*, 2010). These observations reinforce the likely close link between Ca^{2+} signature response networks, ABA related transcriptional cascades and stress responses (Zhu, 2002).

Another CaM-binding protein (CBP), CBP60g, has been found to act as a positive regulator of drought tolerance in *Arabidopsis*. Transgenic plants overexpressing the *CBP60g* gene showed hypersensitivity to ABA and elevated tolerance to drought stress, suggesting the role of CaM-binding CBP60g in ABA signaling pathways regulating early seedling growth and development (Wan *et al.*, 2012). Interestingly, CML37 and CML42 have contrasting roles in mediating drought stress responses in *Arabidopsis*, where CML37 acts as positive regulator and CML42 acts as a negative regulator of ABA accumulation induced by drought stress (Dobney *et al.*, 2009; Vadassery *et al.*, 2012; Scholz *et al.*, 2015). The CML37 and 42 effects are particularly interesting as they highlight that despite these both being CML family members and experiencing the same drought-stress-related Ca^{2+} signatures, the kinds of information they extract, and their effects on downstream response networks, are opposed. CML42 also acts as a positive regulator of UV-B tolerance, hinting at the likely role of individual CMLs in integrating multiple signaling pathways.

Thus, *cml42* loss-of-function plants were found to be compromised in their resistance to UV-B exposure, likely from a defect in the accumulation of protective secondary metabolites such as flavanol glucosides (Vadassery *et al.*, 2012). These kinds of observations highlight the complex interactions and balances that are expected to exist within the Ca^{2+} signature-decoding network.

Just as CaM/CML-mediated regulation of target proteins plays an important role in drought stress responses; similar patterns are expected for the opposite end of the water availability spectrum, i.e., Ca^{2+} signatures in response to flooding conditions. During flooding, plants encounter limited oxygen availability, leading to the switch from oxidative to fermentative carbohydrate metabolism pathways and also an elevation of $[Ca^{2+}]_{cyt}$ levels (Subbaiah and Sachs, 2003). In *Arabidopsis*, the hypoxia-induced CaM-binding transcription factor, AtMYB2 activates the expression of *ALCOHOL DEHYDROGENASE 1* (*ADH1*) by binding to the GT-motif (5'-TGGTTT-3') under low-oxygen conditions (Hoeren *et al.*, 1998). However, the biological and molecular roles of CaM/CMLs in response to flooding and low oxygen stress conditions are still relatively unknown.

Heat and Cold Stress

Fluctuations in temperature leading to extreme hot or cold environmental conditions affect plant growth and development. Under extreme temperature conditions, cellular Ca^{2+} levels are raised resulting in a host of responses from biochemical adaptations to the modulation of patterns of gene expression, including genes encoding for different CaM/CML interacting proteins. Previous studies have shown that *CaM* expression levels are up-regulated in response to heat stress in maize (*Zea mays*) seedlings and in wheat, suggesting the role of Ca^{2+}/CaM signaling under heat stress (Gong *et al.*, 1997; Liu *et al.*, 2003; Zhang *et al.*, 2009). Furthermore, in *Arabidopsis*,

CaM-binding protein kinase 3 (CBK3) was found to play an important role in the Ca^{2+}/CaM-mediated heat shock signal transduction pathway (Liu *et al.*, 2008). In response to heat shock, these CBPs are thought to aid plant survival by mediating the upregulation and accumulation of heat shock proteins (HSPs), molecular chaperones that allow cells to cope with events such as misfolding and aggregation of proteins that occur as temperature stress damages cellular structure and disrupts metabolic functions. Indeed, one of the first identified CBPs in plants, Ser/Thr phosphatase 7 (PP7) has been reported to be involved in thermotolerance in *Arabidopsis,* likely through these HSP-mediated events. Thus, transgenic plants with *AtPP7* either knocked out, or overexpressed, resulted in plants with impaired or increased thermotolerance respectively. Transcriptomic and proteomic analyses indicate the upregulation of both *AtHSP70* and *AtHSP101* gene and protein expression in the *PP7* overexpression lines after heat shock treatments (Liu *et al.*, 2007). Protein-protein interaction assays confirm the binding of PP7 with CaM3 and heat shock transcription factor 1 (HSF1), indicating the potential role of CaM interacting proteins in a regulatory complex facilitating activation of *HSP* genes under elevated temperatures.

Similarly, several studies have implicated the roles of Ca^{2+}/CaM-mediated signal transduction pathways in plant survival, in response to cold stress (Palta, 1996; Lee and Lee, 2003). Thus, a Ca^{2+}/CaM-regulated member of the receptor-like kinase family (CRLK1) plays a pivotal role in conferring cold tolerance in plants. The gene expression of this plasma-membrane localized protein is induced by cold and hydrogen peroxide treatments, suggesting a potential role for reactive oxygen species (ROS) in the regulation of this receptor. Additionally, transcriptomic analysis indicated that CRLK1 acts as a positive regulator of cold tolerance by stimulating the gene expression of cold-responsive genes such as *CBF1*, *KIN1*, *RD29a* and *COR15a* (Yang *et al.*, 2010*a*). Later findings using *in-vitro* and *in-vivo* techniques confirmed that CRLK1 interacts with

MEKK1, a member of the mitogen activated protein kinase (MAPK) kinase kinase family, suggesting the integration of Ca^{2+}/CaM-dependent events with the MAPK signaling network in cold signal transduction pathways in plants (Yang *et al.*, 2010*b*).

Recent findings have also established the role of CaM-binding transcription activators (CAMTAs) in CBF cold acclimation pathways in plants (Doherty *et al.*, 2009). This response pathway is characterized by the cold-induced upregulation of three *CBF* genes, *CBF1-3*. All of these genes have seven conserved DNA motifs (CM1-7). CAMTA3 binds to the CM2 motif found in CBF2, positively regulating *CBF2* gene expression, resulting in enhanced cold tolerance in *Arabidopsis* (Doherty *et al.*, 2009). CAMTA3 does not operate alone in these pathways, as CAMTAs 1, 2 and 5 (Doherty *et al.*, 2009; Kim *et al.*, 2013; Kidokoro *et al.*, 2017) are seen to operate in concert with CAMTA3 to modulate cold-related gene expression. Thus, again, the evidence suggests a key role for a complex network of CaMs and CMLs in stress response signaling, in this case, in response to extreme high or low temperatures, where Ca^{2+} signals are rapidly generated.

Mechanical Stimuli – Focus on Touch

Gentle wind, light rain, plant-on-plant contact, and other organism-on-plant contact represent the most prevalent forms of non-wounding touch (Cipollini Jr., 1997) and often precede more forceful interactions with environmental factors. Thus, responding to these stimuli in a way that can prevent damage provides an adaptive advantage. Such touch stimulation is highly-reproducible, non-lethal, and elicits both molecular and physiological responses that can be tracked and evaluated reliably, when measured within minutes of the initial stimulus (Johnson *et al.*, 1998; Chehab *et al.*, 2009, 2012; Martin *et al.*, 2010; Cazzonelli *et al.*, 2014; Lange and Lange, 2015).

Longer-term physiological and developmental changes in response to touch, i.e., thigmomorphogenesis (Jaffe, 1973; Chehab *et al.*, 2009), can take days to weeks to manifest (Chehab *et al.*, 2012), which may make them significantly more difficult to retrace to the originating stimulus. Thigmomorphogenesis can take the form of priming of molecular responses via chromatin modifications (Cazzonelli *et al.*, 2014), increasing transcription of touch- and defense-related genes, activation of MAP Kinases (Ichimura *et al.*, 2000), producing phytohormones (Chehab *et al.*, 2009), remodeling of cell walls to reinforce them against further perturbations (Verhertbruggen *et al.*, 2013), reducing overall growth, darkening of leaves, and delaying flowering time (Jaffe, 1973). These responses are connected to intra- and intercellular signaling processes that are potentially mediated by Ca^{2+} signals (Knight *et al.*, 1991; Martí *et al.*, 2013). Again, CML24 (TCH2), has been studied further for its role in both mechanical sensation within the roots (by affecting microtubule orientation) (Wang *et al.*, 2011) and the extension of pollen tubes (by affecting actin scaffolding organization) (Yang *et al.*, 2014). CML24's involvement in these behaviors further reinforces its activity as a central signaling hub in response to diverse sensory inputs.

Studies of the transcription of genes in response to touch have identified multiple classes of genes encoding proteins thought to be involved in the process (Braam and Davis, 1990; Lee *et al.*, 2005). For example, Braam and Davis (1990) screened a large cDNA library for transcriptional increases after spraying plants with gibberellins. Several genes, including *CAM2* (thereafter referred to as *TCH1*), *CML24* (*TCH2*), *CML12* (*TCH3*), and *XTH22* (*TCH4*) dramatically increased in transcription under this condition. Interestingly, the transcription of these genes was at a similarly high level within plants sprayed only by water in the negative control, indicating that the mechanical stress of spraying was the cause of *TCH1-4* induction, not the gibberellin treatment

itself. Because of this finding, these genes were studied at length for their roles in a wide array of mechanical responses, especially touch. These results are intriguing because they describe touch-responsive calcium-binding genes in plants and we know that Ca^{2+} is a second messenger responsible for encoding plant touch signals and precipitating touch responses (Knight, 1999; Knight and Knight, 2001; Whalley and Knight, 2013).

CaMs, CMLs and Plant Biotic Stress Responses

Pattern-Triggered Immunity Against Pathogens

Although the previous examples have used a select set of abiotic stress responses to reveal the roles for CaM and CMLs, they are but the tip of the CaM/CML regulatory iceberg, with a host of other abiotic stresses having been linked to CaM/CML signaling (La Verde *et al.*, 2018). In addition, biotic responses, such as to pathogen defense, provide a similarly wide-ranging set of examples regarding how these systems operate to decode incoming signals. The complexity of the plant system for dissecting out Ca^{2+} signatures is mirrored by the complexity of the plant system for perceiving and initiating a signal in response to microbes (e.g. pathogenic bacteria). The perception of some molecule attached to, or left-behind by, their pathogen attacker, requires monitoring proteins at the cell-surface known as pattern-recognition receptors (PRRs). Initiating a signal, i.e., communicating the detection of the molecule, requires rapid accumulation of messenger ions (e.g. Ca^{2+}) or molecules (e.g. ROS) in the cytosol or apoplast and transmission of the information encoded in the signaling ions or molecules to another biochemical signaling system. Upon detection of a broad spectrum of bacterial elicitors, called microbe-associated molecular patterns (MAMPs), e.g. flagellin epitopes, lipopolysaccharides, peptidoglycan, fungal chitin, elongation factor-Tu (EF-Tu), by PRRs (Aslam *et al.*, 2008), the initiation of a plant

immune response is referred to as pattern-triggered immunity (PTI) (Jones and Dangl, 2006). PTI constitutes a primary level of innate immunity and is effective against a large number of pathogens (Newman *et al.*, 2013).

The plant pathogen *Pseudomonas syringae* pv. *tomato* DC3000 (*Pto* DC3000) moves using its flagella. The flagellum is assembled with the protein flagellin and within that flagellin protein is a 22-amino acid peptide (flg22), a classic MAMP, which is the minimal epitope required to trigger plant immune responses through PTI (Jones and Dangl, 2006; Suarez-Rodriguez *et al.*, 2007; Ishiga *et al.*, 2011; Danna *et al.*, 2011; Ranf *et al.*, 2011; Veluchamy *et al.*, 2014). It is possible that small amounts of flg22 are either shed naturally or are lost as they stick to PRRs, such as flagellin-sensing 2 (FLS2), as *Pto* DC3000 passes over the surface of a plant. Flg22 therefore acts as an indicator of bacterial (i.e. pathogen) presence and detection by FLS2 elicits a rapid influx of Ca^{2+} into the cytosol (Chinchilla *et al.*, 2006). As part of this signaling system, botrytis-induced kinase 1 (BIK1) - a membrane-associated, soluble cytosolic protein - forms heteromers with both FLS2 and BRI1-associated kinase 1 (BAK1) in a flg22-independent manner. When FLS2 binds flg22, BAK1 rapidly forms a complex with FLS2, resulting in trans-phosphorylation of FLS2, BAK1, and BIK1 (Chinchilla *et al.*, 2007; Heese *et al.*, 2007; Lu *et al.*, 2010; Schulze *et al.*, 2010; Zhang *et al.*, 2010; Schwessinger *et al.*, 2011). A functional flg22-FLS2-BAK1-BIK1 complex leads to BIK1 dissociation and induction of plant immune responses (Zhang *et al.*, 2010). Notably, while the absence of BAK1 and/or BIK1 does not prevent flg22 binding to FLS2 (Chinchilla *et al.*, 2007; Lu *et al.*, 2010), it does prevent downstream responses via inactivation of the complex.

In a manner that has yet to be elucidated, the formation of the flg22-dependent complex described above initiates a MAPK signaling cascade whereby a MAPK kinase kinase (MAPKKK)

phosphorylates a MAPK kinase (MAPKK), which then phosphorylates a MAPK. The response to chitin elicitation – which may be homologous to flg22-dependent signaling – in *Arabidopsis* has been reported to involve phosphorylation of AvrPphB susceptible 1-like 27 (PBL27) by chitin binding to the extracellular lysin motif (LysM) receptor-like kinase, chitin elicitor receptor kinase 1 (CERK1) (Yamada *et al.*, 2016). Upon chitin elicitation, PBL27 phosphorylates MAPKKK5, which phosphorylates MKK4 and MKK5. MKK4 and MKK5 have similarly been shown to redundantly phosphorylate MPK3 and MPK6 in response to flg22 elicitation (Asai *et al.*, 2002) and may provide a link between signaling in response to detection of chitin and flg22. Although various studies have explored flg22 elicitation and MAPK signaling, we don't have a clear indication of what sort of interaction mediates the connection between the two.

Downstream of MAPK signaling, Ca^{2+}/CaM-dependent regulation of a network of genes (many of them described as having roles in stress responses described above) translates pathogen-related Ca^{2+} signatures into distinct expression patterns. For example, a number of CBPs that are pathogen-inducible have been identified, including members of the CBP60 family (Wang *et al.*, 2009). One such member, CBP60g, when activated by CaM binding, positively regulates the expression of isochorismate synthase 1 (*ICS1*), a central enzyme in the production of salicylic acid (SA). Thus, CPB60g is thought to act in plant defense responses by triggering SA-regulated events in a Ca^{2+}/CaM-dependent manner (Truman *et al.*, 2013). Similarly, CAMTAs, such as CAMTA3 – also referred to as signal-responsive 1 (SR1) in the defense literature – also act in defense signaling. Interestingly, these CaM-bound CAMTAs can be made to swap interaction partners (i.e. CAMTA-regulated genes) in response to Ca^{2+} signature changes (Liu *et al.*, 2015) strongly implying that particular Ca^{2+} signatures are able to impose specificity on regulatory outputs.

Effector-Triggered Immunity Against Pathogens

Plant pathogens, like *Pto* DC3000, produce several MAMPs that elicit immune responses in plants. They also produce many virulence factors, called effectors, in charge of quelling plant defenses by interfering with the signaling cascades initiated by PTI (Bigeard *et al.*, 2015). *Pto* DC3000, a pathogen that is evolutionarily adapted to bypass the PTI system, injects effectors into plant host cells, via its type III secretion system (TTSS), that override the innate signaling mechanisms. This ability of pathogens to avoid PTI responses via production and secretion of effectors is called effector-triggered susceptibility (ETS) (Sanabria *et al.*, 2008). Strong selective pressure exists in favor of plants that can perceive effectors as signals of pathogen infection. If any one of these effectors is recognized by a nucleotide-binding leucine-rich repeat (NB-LRR) resistance (R) protein, the result is effector-triggered immunity (ETI). Strong selective pressure, therefore, also exists in favor of pathogens that produce effectors that plants cannot perceive. Here begins the evolutionary arms race. This battle between plant perception and pathogen interference, referred to as the "zigzag model" (Jones and Dangl, 2006), is an important layer of plant innate immunity.

Upon pathogen detection, plant cells prevent expansive colonization via the deposition of the β-1,3-glucan polymer, callose. While callose is ubiquitously present in many tissues, its deposition in times of pathogen stress is thought to be vital to stemming an infection. For example, to prevent further cellular intrusion by pathogens, cell wall fibers are reinforced via the formation of callose papillae at the site of infection, which form a structural barrier between the cell wall and plasma membrane (Voigt, 2014). Furthermore, plasmodesmata (PD) - mediating symplastic connections between cells - surrounding the site of bacterial, fungal, or viral infection, are constricted by PD-localized callose deposition to prevent further invasion or transmission of

compounds secreted by the infectious agent to neighboring, uninfected cells (Lee and Lu, 2011). Depositing callose at the PD to minimize transport of bacterial effectors and other signaling molecules may prevent local and distal inhibition of antimicrobial activity, in an SA-dependent manner (Wang *et al.*, 2013). Importantly, uninterrupted connections between leaf mesophyll cells and phloem companion cells can provide direct access to all plant tissues. Therefore, shutting down the symplastic and apoplastic connections between leaf and vascular tissues would be necessary. Thus, while callose is clearly important to inhibiting local infections, it may also be critical to preventing systemic disease progression.

Further downstream from pathogen detection, the hypersensitive response (HR) – a mechanism that results from ETI – is characterized by widespread cell death in an attempt to stem infection at its source (Dangl *et al.*, 1996; Jones and Dangl, 2006). For example, FLS2 mediates the detection of flg22 (and other MAMPs) by initiating a signaling cascade responsible for induction of plant immune responses (Nürnberger and Kemmerling, 2006; Suarez-Rodriguez *et al.*, 2007; Danna *et al.*, 2011; Ranf *et al.*, 2011; Newman *et al.*, 2013; Rosli *et al.*, 2013; Clarke *et al.*, 2013; Sun *et al.*, 2013; Veluchamy *et al.*, 2014). In response to these signals, secondary metabolites such as salicylic acid and antimicrobial phytoalexins (Bednarek and Osbourn, 2009) responsible for creating an inhospitable environment for the infecting organism, are produced in the local tissues. Detection of pathogen effectors by R proteins initiates ETI. Various signals are then transmitted to distal tissues, informing them of the presence of the infection, initiating systemic acquired resistance (SAR). Finally, necrotic lesions due to the hypersensitive response form at the site of infection, destroying the tissue and, potentially, cutting-off the pest from further infecting surrounding tissues. This is just one of numerous examples of a full-scale immune response coordinated by the multi-layered pathogen recognition and response system.

CaMs and CMLs in Plant Immunity

Mounting a comprehensive response to pathogen infection requires numerous proteins to function as relays, through which one kind of signal is translated into another. The plant pathogen response model is complex, as it involves multiple signaling pathways involving kinase phosphorylation (Suarez-Rodriguez *et al.*, 2007; Zhou *et al.*, 2014), transcriptional regulation, hormone production (e.g. brassinosteroids, ethylene, jasmonic acid, salicylic acid) (Thomma *et al.*, 1998), Ca^{2+} fluxes, and ROS generation (Miller *et al.*, 2009). For example, CaM2 is intimately linked to the regulation of *PR1* via its relationship with a member of the TGACG-binding transcription factor family. CaM2 has been demonstrated to bind to TGA3 (Fang *et al.*, 2017) that binds the type-B response regulator, ARR2. nonexpressor of pathogenesis related genes 1 (NPR1) then binds ARR2-TGA3 to induce SA- and cytokinin-dependent *PR1* expression (Choi *et al.*, 2010).

Another member of the CaM/CML family, CML24 (TCH2), has been shown to also play a key role in the response to pathogens. A *TCH2* mutant, *cml24-4*, is unable to generate nitric oxide (NO) in response to pathogen attack, and cannot, therefore, initiate HR in response to *Pto* DC3000 infection (Ma *et al.*, 2008), leaving it susceptible. Similarly, in wild type *Arabidopsis*, application of a cation channel blocker (e.g. La^{3+}) or a Ca^{2+} chelator (e.g. BAPTA) (Boudsocq *et al.*, 2010) prevents *Pto* DC3000-induced ROS (e.g. NO and H_2O_2) generation, potentially connecting Ca^{2+} influxes and the activity of CaBPs, like CML24, to signaling during pathogen responses. Another CaM/CML family member, *CML9*, has demonstrated rapid transcriptional induction in response to *Pto* DC3000 infection and is involved in PTI through a flagellin-dependent signaling pathway (Leba *et al.*, 2012). Furthermore, because of its rapid response to abscisic acid and other abiotic

stressors (Magnan *et al.*, 2008; Kudla *et al.*, 2010; Bender *et al.*, 2013) CML9 appears to be a node of convergence for signals in response to diverse stimuli, much like CML24.

Concluding Remarks

Ca^{2+} Signatures and the Multi-Decoding "Cloud"

Instead of thinking of Ca^{2+} signatures as isolated pieces of unique information each programming the plant to produce a particular output, it may be more realistic to think of each signature as part of a composite signal spectrum (**Figure 1.5A**), contributing to the overall output of a multi-decoding cloud system. Earlier, we have mentioned how CBP60g operates in both drought (abiotic) and pathogen (biotic) signal decoding systems (Wan *et al.*, 2012). Similarly, CAMTA3 played a role in cold stress and pathogen responses in plants (Doherty *et al.*, 2009). However, the more we reveal the roles of these CBPs, the more it becomes clear that CAMTA3 is also involved in wound response signaling (Qiu *et al.*, 2012), the general stress response (GSR) pathway (again along with CAMTA2 and 4) (Benn *et al.*, 2014) and in senescence (Nie *et al.*, 2012). Similarly, PP7 not only acts in heat stress response (Liu *et al.*, 2007) but also seems to play a role in cryptochrome-related growth of the hypocotyl and cotyledons in *Arabidopsis* (Moller *et al.*, 2003). The list continues; CML42 is not only involved in drought stress responses (Vadassery *et al.*, 2012) but also in the regulation of trichome branching (Dobney *et al.*, 2009). In addition to the roles in touch- and pathogen- responses described above, other studies suggest the functioning of CML24 in regulation of leaf-to-flower transitioning (Tsai *et al.*, 2007) and autophagy progression in plants (Tsai *et al.*, 2013).

The accumulating evidence suggests that it is likely that the cell-, tissue-, and organ-specific expression of members of the decoding cloud (e.g. CaBPs, like CaMs and CMLs)

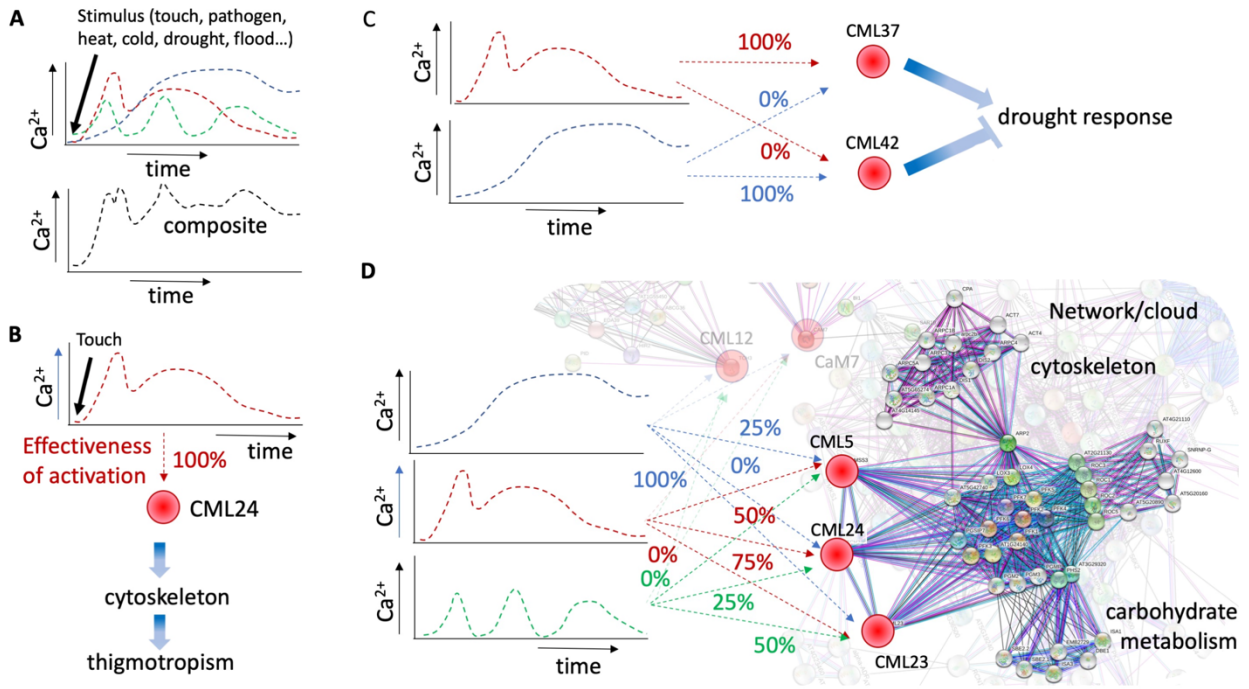

Figure 1.5. Hypothetical models of Ca^{2+} signature decoding. (A) Multiple stimuli arrive simultaneously triggering overlapping Ca^{2+} signatures but their composite may still carry specific elements of each, providing information to the decoding network. (B) Simple linear decoding. CML24 is activated by the appropriate touch-related Ca^{2+} signal to regulate cytoskeletal dynamics and so modulate thigmotropism (Wang *et al.*, 2011; Zha *et al.*, 2016). (C) Opposing Ca^{2+} signals feed into a CML decoding network that is tuned to interpret both the positive and negative regulatory information encoded in multiple Ca^{2+} signatures. Decoding is likely to be more complex than (B) and (C). (D) Ca^{2+} signature decoding elements are linked to each other and to a complex web of downstream systems. The precise outcome of decoding the signal inputs will depend on the fine-tuning of each CaM/CML response to specific elements of the Ca^{2+} signatures, the connections of each to the downstream network, interconnections between the CaMs/CMLs and how the levels and connectivity of all these elements change with time. A simplified genetic network built around CML24 and generated using STRING 11.0 is shown for illustrative purposes in (D) and greatly reduces the connectivity already known for this protein.

determines how the information from a specific Ca^{2+} signature within an individual cell leads to a specific output. For example, **Figure 1.5B** illustrates a simple linear decoding event, wherein a touch stimulus elicits a particular Ca^{2+} signature that is decoded by CML24 and translated into a specific downstream response in a particular subcellular location. However, the mounting evidence also suggests that there can be numerous CaMs and CMLs involved in many responses and the process of coordinating response events may be driven by the balance between positive and negative regulatory information encoded by multiple Ca^{2+} signatures (**Figure 1.5C**). In this example, again, 100% of the information from one Ca^{2+} signature contributes to the activity of a single CaM or CML, which may also not be an accurate depiction of the functionality of the

decoding machinery. Instead, **Figure 1.5D** is probably the most accurate illustration. Here, there are various CaMs and CMLs modulating multiple downstream processes in response to several Ca^{2+} signatures. These Ca^{2+} signatures impact the activity of the various CaMs and CMLs to differing degrees. Integrating the activity of multiple CaBPs using a suite of Ca^{2+} signatures greatly expands the stimulus-response repertoire of the cell, enabling tuning of the response at a finer scale.

As *CaBP* gene expression changes in response to stimuli and the CaBPs change in level and position within the cell, the topology of the cloud is constantly changing. In this way the plant would be able to constantly adjust its sensitivity and responses to stimuli as the world around it changes, integrating many stimuli that trigger Ca^{2+} changes into an output governed by the current shape of the CaBP decoding network. The challenge this signaling architecture raises for the researcher is it would no longer be as easy as to say "this gene is involved in this process" as, in the background is the specter that this gene is part of a decoding cloud that contributes to a host of parallel information decoding processes. The relative contribution to each process will change as the decoding landscape alters. Signaling is then inherently a network feature and fortunately the tools to support network mining of plant responses, such as KnetMiner (Hassani-Pak, 2017), STRING (Szklarczyk *et al.*, 2015), ThaleMine (Krishnakumar *et al.*, 2016), and ShinyGO (Ge and Jung, 2018), have come of age. At present these exploration environments are focused on protein and genetic interactions but the possibility of more extensive cell biological data being woven into these databases is on the horizon.

Connecting Pathogen- and Touch-Response Systems

Devising and constructing a whole signaling pathway *de novo* for every stimulus a plant encounters would be implausible. Thus, plants leverage the preexisting functions of pathways such as the MAP Kinase phosphorylation cascade to carry information from diverse sites of biotic and abiotic stimulus detection to cellular locations where adaptive responses are generated (Ichimura *et al.*, 2000; Morris, 2001; Tena *et al.*, 2001; Jonak *et al.*, 2002; Mishra *et al.*, 2006; Lian *et al.*, 2018). CaM2 and CML24 have both been shown to be involved in both pathogen- and touch-responses (among many others, see above). That two canonical touch-responsive proteins have been found to be intimately linked to pathogen-responses is intriguing. However, there may be many more touch-responsive proteins and those proteins may also be involved in the pathogen-response. Indeed, a genome-wide differential expression analysis of mechanically-stimulated leaves (via bending), reported in Lee *et al.* (2005), revealed that over 2.5% of genes present on Affymetrix *Arabidopsis* ATH1 Genome Arrays were upregulated at least 2-fold. CaM2, CML12, CML24, and XTH22 were the archetypal touch-induced genes identified by Braam and Davis (1990) and in this broad survey of the genome response to touch, of the 7 *CaMs*, 50 *CMLs*, and 33 *XTHs* encoded by the *Arabidopsis* genome, one *CaM*, 9 *CML*s, and one *XTH* gene increased in expression at least two-fold, 30 minutes after mechanical stress treatment. Therefore, there are many genes that are candidates for mediating crosstalk between touch- and pathogen-responses.

One piece of evidence that supports the idea that Ca^{2+}/CaM-mediated crosstalk between the pathogen and touch molecular response systems is occurring is that, although changing the stimulus precipitates a different response, many signaling components these systems use to trigger these responses are shared (e.g. MAPK phosphorylation cascades and Ca^{2+}/CaM-dependent gene expression). Thus, some CaMs and CMLs are upregulated in response to mechanical stimuli and

many of these CaMs and CMLs are also involved in numerous stimulus-responses (see above), such as in the pathogen-response systems. Ca^{2+} signals connect these CaMs and CMLs to multiple distinct sensory inputs. Connections such as these are just single strands in a complex interconnected web of regulation. That begs the questions: What kind of network integrates information encoded in Ca^{2+} signatures produced by the pathogen- and touch-response machinery? Which genes and proteins are involved in crosstalk between these two systems? How is this information delivered to the proper locations to elicit suitable responses? CaMs and CMLs, especially due to their involvement in the numerous processes described in this chapter, are obvious candidates for involvement in crosstalk between the two systems and, as such, merit systematic study.

Therefore, in **Chapter 2** I describe generating an interaction network of touch- and pathogen-responsive genes based on experimentally-determined relationships between them, using KnetMiner (Hassani-Pak, 2017). I also test whether the *CAMs* and *CMLs* predicted to be in this network should remain, based upon the molecular and physiological responses to touch and pathogen treatments on loss-of-function mutants in each gene.

In **Chapter 3**, I further test the involvement of two CaMs, CaM2 and CaM7, in the pathogen response, as, in **Chapter 2**, *cam2* and *cam7* both exhibit molecular and physiological responses to pathogens that are strikingly dissimilar to those exhibited by others in the network. Furthermore, I describe generating a *cam2 cam7* double mutant that exhibits some pathogen responses that deviate from those exhibited by the *cam2* and *cam7* single mutants.

Chapter 4 provides a summary of the conclusions drawn from the investigations carried out in **Chapter 2** and **Chapter 3**. It also recommends studies that could be performed to further elucidate the roles of CaMs and CMLs in touch- and pathogen-responses. Additionally, as this

work required the development of some key techniques (i.e. the creation of a touch robot to ensure reliable and repeatable application of touch stimuli), **Appendix I** describes the construction and implementation of the Automated Botanical Contact Device (ABCD). Finally, **Appendix II** serves to highlight an interesting finding: *cam2* and *cam7* mutants exhibit attenuated Ca^{2+} signals in response to flg22. Through the research described in this dissertation, I hope to add additional clarity to our understanding of the roles of CaMs and CMLs in mediating the responses to the stresses imposed upon plants.

Literature Cited

Abbas N, Maurya JP, Senapati D, Gangappa SN, Chattopadhyay S. 2014. Arabidopsis CAM7 and HY5 physically interact and directly bind to the HY5 promoter to regulate its expression and thereby promote photomorphogenesis. The Plant Cell **26**, 1036–52.

Akyol Z, Bartos JA, Merrill MA, Faga LA, Jaren OR, Shea MA, Hell JW. 2004. Apo-calmodulin binds with its C-terminal domain to the N-methyl-D-aspartate receptor NR1 C0 region. The Journal of biological chemistry **279**, 2166–75.

Aldon D, Galaud J. 2006. Plant Calmodulins and Calmodulin-Related Proteins. Plant Signaling & Behavior **1:3**, 96–104.

Apiyo D, Zhao L, Tsai M-D, Selby TL. 2005. X-ray Structure of the R69D Phosphatidylinositol-Specific Phospholipase C Enzyme: Insight into the Role of Calcium and Surrounding Amino Acids in Active Site Geometry and Catalysis. Biochemistry **44**, 9980–9989.

Asai T, Tena G, Plotnikova J, Willmann MR, Chiu W-L, Gomez-Gomez L, Boller T, Ausubel FM, Sheen J. 2002. MAP kinase signalling cascade in Arabidopsis innate immunity. Nature **415**, 977–983.

Aslam SN, Newman M-A, Erbs G, *et al.* 2008. Bacterial Polysaccharides Suppress Induced Innate Immunity by Calcium Chelation. Current Biology **18**, 1078–1083.

Astegno A, Bonza MC, Vallone R, La Verde V, D'Onofrio M, Luoni L, Molesini B, Dominici P. 2017. Arabidopsis calmodulin-like protein CML36 is a calcium (Ca2+) sensor that interacts with the plasma membrane Ca2+-ATPase isoform ACA8 and stimulates its activity. The Journal of biological chemistry **292**, 15049–15061.

Astegno A, La Verde V, Marino V, Dell'Orco D, Dominici P. 2016. Biochemical and biophysical characterization of a plant calmodulin: Role of the N- and C-lobes in calcium binding, conformational change, and target interaction. Biochimica et Biophysica Acta (BBA) - Proteins and Proteomics **1864**, 297–307.

Azimzadeh J, Nacry P, Christodoulidou A, Drevensek S, Camilleri C, Amiour N, Parcy F, Pastuglia M, Bouchez D. 2008. Arabidopsis TONNEAU1 proteins are essential for preprophase band formation and interact with centrin. The Plant Cell **20**, 2146–59.

Bateman A, Martin MJ, O'Donovan C, *et al.* 2017. UniProt: the universal protein knowledgebase. Nucleic Acids Research **45**, D158–D169.

Baum G, Lev-Yadun S, Fridmann Y, Arazi T, Katsnelson H, Zik M, Fromm H. 1996. Calmodulin binding to glutamate decarboxylase is required for regulation of glutamate and GABA metabolism and normal development in plants. The EMBO Journal **15**, 2988–96.

Bednarek P, Osbourn A. 2009. Plant-microbe interactions: chemical diversity in plant defense. Science **324**, 746–8.

Bender KW, Dobney S, Ogunrinde A, Chiasson D, Mullen RT, Teresinski HJ, Singh P, Munro K, Smith SP, Snedden WA. 2014. The calmodulin-like protein CML43 functions as a salicylic-acid-inducible root-specific Ca(2+) sensor in Arabidopsis. The Biochemical journal **457**, 127–36.

Bender KW, Rosenbaum DM, Vanderbeld B, Ubaid M, Snedden WA. 2013. The Arabidopsis calmodulin-like protein, CML39, functions during early seedling establishment. The Plant Journal **76**, 634–47.
Bender KW, Snedden WA. 2013. Calmodulin-related proteins step out from the shadow of their namesake. Plant Physiology **163**, 486–95.
Benn G, Wang C-Q, Hicks DR, Stein J, Guthrie C, Dehesh K. 2014. A key general stress response motif is regulated non-uniformly by CAMTA transcription factors. The Plant Journal **80**, 82–92.
Bigeard J, Colcombet J, Hirt H. 2015. Signaling mechanisms in pattern-triggered immunity (PTI). Molecular plant **8**, 521–39.
Bindreither D, Lackner P. 2009. Structural diversity of calcium binding sites. General physiology and biophysics **28 Spec No**, F82-8.
Bouché N, Fromm H. 2004. GABA in plants: just a metabolite? Trends in Plant Science **9**, 110–115.
Bouché N, Yellin A, Snedden WA, Fromm H. 2005. Plant-Specific Calmodulin-binding Proteins. Annual Review of Plant Biology **56**, 435–466.
Boudsocq M, Sheen J. 2009. Stress Signaling II: Calcium Sensing and Signaling. Abiotic Stress Adaptation in Plants. Dordrecht: Springer Netherlands, 75–90.
Boudsocq M, Willmann MR, McCormack M, Lee H, Shan L, He P, Bush J, Cheng S-H, Sheen J. 2010. Differential innate immune signalling via Ca2+ sensor protein kinases. Nature **464**, 418–422.
Braam J, Davis RW. 1990. Rain-, wind-, and touch-induced expression of calmodulin and calmodulin-related genes in Arabidopsis. Cell **60**, 357–364.
Cazzonelli CI, Nisar N, Roberts AC, Murray KD, Borevitz JO, Pogson BJ. 2014. A chromatin modifying enzyme, SDG8, is involved in morphological, gene expression, and epigenetic responses to mechanical stimulation. Frontiers in Plant Science **5**, 533.
Charpentier M, Sun J, Vaz Martins T, *et al.* 2016. Nuclear-localized cyclic nucleotide-gated channels mediate symbiotic calcium oscillations. Science **352**, 1102–5.
Chehab EW, Eich E, Braam J. 2009. Thigmomorphogenesis: a complex plant response to mechano-stimulation. Journal of Experimental Botany **60**, 43–56.
Chehab EW, Yao C, Henderson Z, Kim S, Braam J. 2012. Arabidopsis touch-induced morphogenesis is jasmonate mediated and protects against pests. Current Biology **22**, 701–6.
Chinchilla D, Bauer Z, Regenass M, Boller T, Felix G. 2006. The Arabidopsis Receptor Kinase FLS2 Binds flg22 and Determines the Specificity of Flagellin Perception. The Plant Cell **18**, 465 LP – 476.
Chinchilla D, Zipfel C, Robatzek S, Kemmerling B, Nürnberger T, Jones JDG, Felix G, Boller T. 2007. A flagellin-induced complex of the receptor FLS2 and BAK1 initiates plant defence. Nature **448**, 497–500.
Cho W, Stahelin R V. 2006. Membrane binding and subcellular targeting of C2 domains. Biochimica et Biophysica Acta (BBA) - Molecular and Cell Biology of Lipids **1761**, 838–849.
Choi J, Huh SU, Kojima M, Sakakibara H, Paek K-H, Hwang I. 2010. The Cytokinin-Activated Transcription Factor ARR2 Promotes Plant Immunity via TGA3/NPR1-Dependent Salicylic Acid Signaling in Arabidopsis. Developmental Cell **19**, 284–295.
Cipollini Jr. DF. 1997. Wind-induced mechanical stimulation increases pest resistance in common bean. Oecologia **111**, 84–90.
Clarke CR, Chinchilla D, Hind SR, Taguchi F, Miki R, Ichinose Y, Martin GB, Leman S, Felix G, Vinatzer BA. 2013. Allelic variation in two distinct Pseudomonas syringae flagellin epitopes modulates the strength of plant immune responses but not bacterial motility. New Phytologist **200**, 847–60.
Dai H, Shin O-H, Machius M, Tomchick DR, Südhof TC, Rizo J. 2004. Structural basis for the evolutionary inactivation of Ca2+ binding to synaptotagmin 4. Nature Structural & Molecular Biology **11**, 844–849.
Dangl JL, Dietrich RA, Richberg MH. 1996. Death Don't Have No Mercy: Cell Death Programs in Plant-Microbe Interactions. The Plant Cell **8**, 1793–1807.
Danna CH, Millet YA, Koller T, Han S-W, Bent AF, Ronald PC, Ausubel FM. 2011. The Arabidopsis flagellin receptor FLS2 mediates the perception of Xanthomonas Ax21 secreted peptides. Proceedings of the National Academy of Sciences **108**, 9286–91.
Day IS, Reddy VS, Shad Ali G, Reddy ASN. 2002. Analysis of EF-hand-containing proteins in Arabidopsis. Genome Biology **3**, research0056.1.
Delk NA, Johnson KA, Chowdhury NI, Braam J. 2005. CML24, regulated in expression by diverse stimuli, encodes a potential Ca2+ sensor that functions in responses to abscisic acid, daylength, and ion stress. Plant Physiology **139**, 240–53.
Dobney S, Chiasson D, Lam P, Smith SP, Snedden WA. 2009. The calmodulin-related calcium sensor CML42 plays a role in trichome branching. The Journal of biological chemistry **284**, 31647–57.

Dodd AN, Kudla J, Sanders D. 2010. The Language of Calcium Signaling. Annual Review of Plant Biology **61**, 593–620.
Doherty CJ, Van Buskirk HA, Myers SJ, Thomashow MF. 2009. Roles for Arabidopsis CAMTA Transcription Factors in Cold-Regulated Gene Expression and Freezing Tolerance. The Plant Cell **21**, 972–984.
Donaldson L, Ludidi N, Knight MR, Gehring C, Denby K. 2004. Salt and osmotic stress cause rapid increases in Arabidopsis thaliana cGMP levels. FEBS Letters **569**, 317–320.
Erickson JR, Sidell BD, Moerland TS. 2005. Temperature sensitivity of calcium binding for parvalbumins from Antarctic and temperate zone teleost fishes. Comparative Biochemistry and Physiology Part A: Molecular & Integrative Physiology **140**, 179–185.
Fang H, Liu Z, Long Y, Liang Y, Jin Z, Zhang L, Liu D, Li H, Zhai J, Pei Y. 2017. The Ca^{2+} /calmodulin2-binding transcription factor TGA3 elevates *LCD* expression and H_2S production to bolster Cr^{6+} tolerance in Arabidopsis. The Plant Journal **91**, 1038–1050.
Finn RD, Attwood TK, Babbitt PC, *et al.* 2017. InterPro in 2017—beyond protein family and domain annotations. Nucleic Acids Research **45**, D190–D199.
Ge SX, Jung D. 2018. ShinyGO: a graphical enrichment tool for animals and plants. bioRxiv.
Gifford JL, Jamshidiha M, Mo J, Ishida H, Vogel HJ. 2013. Comparing the calcium binding abilities of two soybean calmodulins: towards understanding the divergent nature of plant calmodulins. The Plant Cell **25**, 4512–24.
Gifford JL, Walsh MP, Vogel HJ. 2007. Structures and metal-ion-binding properties of the Ca2+-binding helix-loop-helix EF-hand motifs. The Biochemical journal **405**, 199–221.
Gong M, Li Y-J, Dai X, Tian M, Li Z-G. 1997. Involvement of calcium and calmodulin in the acquisition of heat-shock induced thermotolerance in maize seedlings. Journal of Plant Physiology **150**, 615–621.
Halling DB, Liebeskind BJ, Hall AW, Aldrich RW. 2016. Conserved properties of individual Ca2+-binding sites in calmodulin. Proceedings of the National Academy of Sciences **113**, E1216-25.
Hassani-Pak K. 2017. KnetMiner - An integrated data platform for gene mining and biological knowledge discovery. ProQuest Dissertations and Theses.
Heese A, Hann DR, Gimenez-Ibanez S, Jones AME, He K, Li J, Schroeder JI, Peck SC, Rathjen JP. 2007. The receptor-like kinase SERK3/BAK1 is a central regulator of innate immunity in plants. Proceedings of the National Academy of Sciences **104**, 12217–22.
Hepler PK. 2005. Calcium: A Central Regulator of Plant Growth and Development. The Plant Cell **17**, 2142–2155.
Hetherington AM, Brownlee C. 2004. The generation of Ca(2+) signals in plants. Annual Review of Plant Biology **55**, 401–427.
Hoeren FU, Dolferus R, Wu Y, Peacock WJ, Dennis ES. 1998. Evidence for a Role for AtMYB2 in the Induction of the Arabidopsis Alcohol Dehydrogenase Gene (ADH1) by Low Oxygen. Genetics **149**, 479–490.
Houdusse A, Silver M, Cohen C. 1996. A model of Ca2+-free calmodulin binding to unconventional myosins reveals how calmodulin acts as a regulatory switch. Structure **4**, 1475–1490.
Hu W, Yan Y, Tie W, Ding Z, Wu C, Ding X, Wang W, Xia Z, Guo J, Peng M. 2018. Genome-Wide Analyses of Calcium Sensors Reveal Their Involvement in Drought Stress Response and Storage Roots Deterioration after Harvest in Cassava. Genes **9**, 221.
Ichimura K, Mizoguchi T, Yoshida R, Yuasa T, Shinozaki K. 2000. Various abiotic stresses rapidly activate Arabidopsis MAP kinases ATMPK4 and ATMPK6. The Plant Journal **24**, 655–665.
Ishiga Y, Ishiga T, Uppalapati SR, Mysore KS. 2011. Arabidopsis seedling flood-inoculation technique: a rapid and reliable assay for studying plant-bacterial interactions. Plant methods **7**, 32.
Jaffe MJ. 1973. Thigmomorphogenesis: The response of plant growth and development to mechanical stimulation. Planta **114**, 143–157.
Jauregui E, Du L, Gleason C, Poovaiah BW. 2017. W342F Mutation in CCaMK Enhances Its Affinity to Calmodulin But Compromises Its Role in Supporting Root Nodule Symbiosis in Medicago truncatula. Frontiers in Plant Science **8**.
Johnson KA, Sistrunk ML, Polisensky DH, Braam J. 1998. Arabidopsis thaliana responses to mechanical stimulation do not require ETR1 or EIN2. Plant Physiology **116**, 643–9.
Jonak C, Ökrész L, Bögre L, Hirt H. 2002. Complexity, Cross Talk and Integration of Plant MAP Kinase Signalling. Current Opinion in Plant Biology **5**, 415–424.
Jones JDG, Dangl JL. 2006. The plant immune system. Nature **444**, 323–9.
Jurado LA, Chockalingam PS, Jarrett HW. 1999. Apocalmodulin. Physiological Reviews **79**, 661–682.
Kaplan B, Davydov O, Knight H, Galon Y, Knight MR, Fluhr R, Fromm H. 2006. Rapid transcriptome changes induced by cytosolic Ca2+ transients reveal ABRE-related sequences as Ca2+-responsive cis elements in Arabidopsis. The Plant Cell **18**, 2733–48.

Kawasaki H, Nakayama S, Kretsinger RH. 1998. Classification and evolution of EF-hand proteins. Biometals **11**, 277–295.
Kidokoro S, Yoneda K, Takasaki H, Takahashi F, Shinozaki K, Yamaguchi-Shinozaki K. 2017. Different Cold-Signaling Pathways Function in the Responses to Rapid and Gradual Decreases in Temperature. The Plant Cell **29**, 760–774.
Kim MC, Chung WS, Yun D-J, Cho MJ. 2009. Calcium and Calmodulin-Mediated Regulation of Gene Expression in Plants. Molecular Plant **2**, 13–21.
Kim Y, Park S, Gilmour SJ, Thomashow MF. 2013. Roles of CAMTA transcription factors and salicylic acid in configuring the low-temperature transcriptome and freezing tolerance of Arabidopsis. The Plant Journal **75**, 364–376.
Knight H. 1999. Calcium Signaling during Abiotic Stress in Plants. International Review of Cytology **195**, 269–324.
Knight MR, Campbell AK, Smith SM, Trewavas AJ. 1991. Transgenic plant aequorin reports the effects of touch and cold-shock and elicitors on cytoplasmic calcium. Nature **352**, 524–526.
Knight H, Knight MR. 2001. Abiotic stress signalling pathways: specificity and cross-talk. Trends in Plant Science **6**, 262–267.
De Koninck P, Schulman H. 1998. Sensitivity of CaM kinase II to the frequency of Ca2+ oscillations. Science **279**, 227–30.
Köster P, Wallrad L, Edel KH, Faisal M, Alatar AA, Kudla J. 2019. The battle of two ions: Ca 2+ signalling against Na + stress (A Weber, Ed.). Plant Biology **21**, 39–48.
Kretsinger RH. 1976. Calcium-Binding Proteins. Annual Review of Biochemistry **45**, 239–266.
Kretsinger RH, Nockolds CE. 1973. Carp Muscle Calcium-binding Protein. The Journal of biological chemistry **248**, 3313–3326.
Krishnakumar V, Contrino S, Cheng C-Y, Belyaeva I, Ferlanti ES, Miller JR, Vaughn MW, Micklem G, Town CD, Chan AP. 2016. ThaleMine: A Warehouse for Arabidopsis Data Integration and Discovery. Plant & Cell Physiology **58**, pcw200.
Kudla J, Batistic O, Hashimoto K. 2010. Calcium signals: the lead currency of plant information processing. The Plant Cell **22**, 541–63.
Kumar V, Chichili VPR, Zhong L, Tang X, Velazquez-Campoy A, Sheu F-S, Seetharaman J, Gerges NZ, Sivaraman J. 2013. Structural Basis for the Interaction of Unstructured Neuron Specific Substrates Neuromodulin and Neurogranin with Calmodulin. Scientific Reports **3**, 1392.
Kumar S, Mazumder M, Gupta N, Chattopadhyay S, Gourinath S. 2016. Crystal structure of Arabidopsis thaliana calmodulin7 and insight into its mode of DNA binding. FEBS Letters **590**, 3029–3039.
Lange MJP, Lange T. 2015. Touch-induced changes in Arabidopsis morphology dependent on gibberellin breakdown. Nature Plants **1**, 14025.
Leba L-J, Cheval C, Ortiz-Martín I, Ranty B, Beuzón CR, Galaud J-P, Aldon D. 2012. CML9, an Arabidopsis calmodulin-like protein, contributes to plant innate immunity through a flagellin-dependent signalling pathway. The Plant Journal **71**, 976–89.
Lee J-Y, Lee D-H. 2003. Use of Serial Analysis of Gene Expression Technology to Reveal Changes in Gene Expression in Arabidopsis Pollen Undergoing Cold Stress. Plant Physiology **132**, 517–529.
Lee J-Y, Lu H. 2011. Plasmodesmata: the battleground against intruders. Trends in Plant Science **16**, 201–10.
Lee D, Polisensky DH, Braam J. 2005. Genome-wide identification of touch- and darkness-regulated Arabidopsis genes: a focus on calmodulin-like and XTH genes. New Phytologist **165**, 429–44.
Lian K, Gao F, Sun T, van Wersch R, Ao K, Kong Q, Nitta Y, Wu D, Krysan P, Zhang Y. 2018. MKK6 Functions in Two Parallel MAP Kinase Cascades in Immune Signaling. Plant Physiology **178**, 1284 LP – 1295.
Linse S, Brodin P, Drakenberg T, Thulin E, Sellers P, Elmden K, Grundstroem T, Forsen S. 1987. Structure-function relationships in EF-hand calcium-binding proteins. Protein engineering and biophysical studies of calbindin D9k. Biochemistry **26**, 6723–6735.
Liu H-T, Gao F, Li G-L, Han J-L, Liu D-L, Sun D-Y, Zhou R-G. 2008. The calmodulin-binding protein kinase 3 is part of heat-shock signal transduction in Arabidopsis thaliana. The Plant Journal **55**, 760–773.
Liu HT, Li GL, Chang H, Sun DY, Zhou RG, Li B. 2007. Calmodulin-binding protein phosphatase PP7 is involved in thermotolerance in Arabidopsis. Plant, Cell & Environment **30**, 156–164.
Liu L, Li C, Liang Z, Yu H. 2018. Characterization of Multiple C2 Domain and Transmembrane Region Proteins in Arabidopsis. Plant Physiology **176**, 2119–2132.
Liu H-T, Li B, Shang Z-L, Li X-Z, Mu R-L, Sun D-Y, Zhou R-G. 2003. Calmodulin Is Involved in Heat Shock Signal Transduction in Wheat. Plant Physiology **132**, 1186–1195.

Liu J, Whalley HJ, Knight MR. 2015. Combining modelling and experimental approaches to explain how calcium signatures are decoded by calmodulin-binding transcription activators (CAMTAs) to produce specific gene expression responses. New Phytologist **208**, 174–87.
Liu J, Zhu J-K. 1998. A Calcium Sensor Homolog Required for Plant Salt Tolerance. Science **280**, 1943–1945.
Lu D, Wu S, Gao X, Zhang Y, Shan L, He P. 2010. A receptor-like cytoplasmic kinase, BIK1, associates with a flagellin receptor complex to initiate plant innate immunity. Proceedings of the National Academy of Sciences **107**, 496–501.
Ma W, Smigel A, Tsai Y-C, Braam J, Berkowitz GA. 2008. Innate immunity signaling: cytosolic Ca2+ elevation is linked to downstream nitric oxide generation through the action of calmodulin or a calmodulin-like proteins. Plant Physiology **148**, 818–28.
Magnan F, Ranty B, Charpenteau M, Sotta B, Galaud J-P, Aldon D. 2008. Mutations in AtCML9, a calmodulin-like protein from Arabidopsis thaliana, alter plant responses to abiotic stress and abscisic acid. The Plant Journal **56**, 575–89.
Mahajan S, Pandey GK, Tuteja N. 2008. Calcium- and salt-stress signaling in plants: Shedding light on SOS pathway. Archives of Biochemistry and Biophysics **471**, 146–158.
Martí MC, Stancombe MA, Webb AAR. 2013. Cell- and Stimulus Type-Specific Intracellular Free Ca2+ Signals in Arabidopsis. Plant Physiology **163**, 625 LP – 634.
Martin L, Leblanc-Fournier N, Julien J-L, Moulia B, Coutand C. 2010. Acclimation kinetics of physiological and molecular responses of plants to multiple mechanical loadings. Journal of Experimental Botany **61**, 2403–12.
McCormack E, Braam J. 2003. Calmodulins and related potential calcium sensors of Arabidopsis. New Phytologist **159**, 585–598.
McCormack E, Tsai Y-C, Braam J. 2005. Handling calcium signaling: Arabidopsis CaMs and CMLs. Trends in Plant Science **10**, 383–389.
Meese S, Cepeda AP, Gahlen F, Adams CM, Ficner R, Ricci AJ, Heller S, Reisinger E, Herget M. 2017. Activity-Dependent Phosphorylation by CaMKIIδ Alters the Ca2+ Affinity of the Multi-C2-Domain Protein Otoferlin. Frontiers in Synaptic Neuroscience **9**, 13.
Miller JB, Pratap A, Miyahara A, Zhou L, Bornemann S, Morris RJ, Oldroyd GED. 2013. Calcium/Calmodulin-Dependent Protein Kinase Is Negatively and Positively Regulated by Calcium, Providing a Mechanism for Decoding Calcium Responses during Symbiosis Signaling. The Plant Cell **25**, 5053–5066.
Miller G, Schlauch K, Tam R, Cortes D, Torres MA, Shulaev V, Dangl JL, Mittler R. 2009. The plant NADPH oxidase RBOHD mediates rapid systemic signaling in response to diverse stimuli. Science signaling **2**, ra45.
Mishra NS, Tuteja R, Tuteja N. 2006. Signaling through MAP kinase networks in plants. Archives of Biochemistry and Biophysics **452**, 55–68.
Miwa H, Sun J, Oldroyd GED, Allan Downie J. 2006. Analysis of calcium spiking using a cameleon calcium sensor reveals that nodulation gene expression is regulated by calcium spike number and the developmental status of the cell. The Plant Journal **48**, 883–894.
Mody I, De Koninck Y, Otis TS, Soltesz I. 1994. Bridging the cleft at GABA synapses in the brain. Trends in Neurosciences **17**, 517–525.
Moller SG, Kim Y-S, Kunkel T, Chua N-H. 2003. PP7 Is a Positive Regulator of Blue Light Signaling in Arabidopsis. The Plant Cell **15**, 1111–1119.
Morris PC. 2001. MAP kinase signal transduction pathways in plants. New Phytologist **151**, 67–89.
Nakayama S, Kawasaki H, Kretsinger R. 2000. Evolution of EF-Hand Proteins. Calcium Homeostasis. Berlin, Heidelberg: Springer Berlin Heidelberg, 29–58.
Nalefski EA, Falke JJ. 1996. The C2 domain calcium-binding motif: Structural and functional diversity. Protein Science **5**, 2375–2390.
Newman M-A, Sundelin T, Nielsen JT, Erbs G. 2013. MAMP (microbe-associated molecular pattern) triggered immunity in plants. Frontiers in Plant Science **4**, 139.
Nie H, Zhao C, Wu G, Wu Y, Chen Y, Tang D. 2012. SR1, a calmodulin-binding transcription factor, modulates plant defense and ethylene-induced senescence by directly regulating NDR1 and EIN3. Plant Physiology **158**, 1847–59.
Nürnberger T, Kemmerling B. 2006. Receptor protein kinases--pattern recognition receptors in plant immunity. Trends in Plant Science **11**, 519–22.
Ogunrinde A, Munro K, Davidson A, Ubaid M, Snedden WA. 2017. Arabidopsis Calmodulin-Like Proteins, CML15 and CML16 Possess Biochemical Properties Distinct from Calmodulin and Show Non-overlapping Tissue Expression Patterns. Frontiers in Plant Science **8**, 2175.
Orellana S, Yañez M, Espinoza A, Verdugo I, González E, Ruiz-Lara S, Casaretto JA. 2010. The transcription

factor SlAREB1 confers drought, salt stress tolerance and regulates biotic and abiotic stress-related genes in tomato. Plant, Cell & Environment **33**, 2191–2208.
Palta JP. 1996. Role of Calcium in Plant Responses to Stresses: Linking Basic Research to the Solution of Practical Problems. HortScience **31**, 51–57.
Panchy N, Lehti-Shiu M, Shiu S-H. 2016. Topical Review on Gene Duplication Evolution of Gene Duplication in Plants 1[OPEN]. Plant Physiology **171**, 2294–2316.
Park HJ, Kim W-Y, Yun D-J. 2016. A New Insight of Salt Stress Signaling in Plant. Molecules and Cells **39**, 447–459.
Perochon A, Aldon D, Galaud J-P, Ranty B. 2011. Calmodulin and calmodulin-like proteins in plant calcium signaling. Biochimie **93**, 2048–53.
Perruc E, Charpenteau M, Ramirez BC, Jauneau A, Galaud J-P, Ranjeva R, Ranty B. 2004. A novel calmodulin-binding protein functions as a negative regulator of osmotic stress tolerance in Arabidopsis thaliana seedlings. The Plant Journal **38**, 410–420.
Plattner H, Verkhratsky A. 2015. The ancient roots of calcium signalling evolutionary tree. Cell Calcium **57**, 123–132.
Popescu SC, Popescu G V, Bachan S, Zhang Z, Seay M, Gerstein M, Snyder M, Dinesh-Kumar SP. 2007. Differential binding of calmodulin-related proteins to their targets revealed through high-density Arabidopsis protein microarrays. Proceedings of the National Academy of Sciences **104**, 4730–5.
Poux S, Arighi CN, Magrane M, Bateman A, Wei C-H, Lu Z, Boutet E, Bye-A-Jee H, Famiglietti ML, Roechert B. 2016. On expert curation and sustainability: UniProtKB/Swiss-Prot as a case study. bioRxiv, 094011.
Qiu Y, Xi J, Du L, Suttle JC, Poovaiah BW. 2012. Coupling calcium/calmodulin-mediated signaling and herbivore-induced plant response through calmodulin-binding transcription factor AtSR1/CAMTA3. Plant Molecular Biology **79**, 89–99.
Rainaldi M, Yamniuk AP, Murase T, Vogel HJ. 2007. Calcium-dependent and -independent Binding of Soybean Calmodulin Isoforms to the Calmodulin Binding Domain of Tobacco MAPK Phosphatase-1. Journal of Biological Chemistry **282**, 6031–6042.
Ranf S, Eschen-Lippold L, Pecher P, Lee J, Scheel D. 2011. Interplay between calcium signalling and early signalling elements during defence responses to microbe- or damage-associated molecular patterns. The Plant Journal **68**, 100–13.
Rastogi S, Shah S, Kumar R, Vashisth D, Akhtar MQ, Kumar A, Dwivedi UN, Shasany AK. 2019. Ocimum metabolomics in response to abiotic stresses: Cold, flood, drought and salinity (N Baisakh, Ed.). PLoS ONE **14**, e0210903.
Reddy AS. 2001. Calcium: silver bullet in signaling. Plant Science **160**, 381–404.
Reddy ASN, Ali GS, Celesnik H, Day IS. 2011. Coping with Stresses: Roles of Calcium- and Calcium/Calmodulin-Regulated Gene Expression. The Plant Cell **23**, 2010–2032.
Rosli HG, Zheng Y, Pombo MA, Zhong S, Bombarely A, Fei Z, Collmer A, Martin GB. 2013. Transcriptomics-based screen for genes induced by flagellin and repressed by pathogen effectors identifies a cell wall-associated kinase involved in plant immunity. Genome Biology **14**, R139.
Rudd JJ, Franklin-Tong VE. 2001. Unravelling response-specificity in Ca2+ signalling pathways in plant cells. New Phytologist **151**, 7–33.
Sanabria N, Goring D, Nürnberger T, Dubery I. 2008. Self/nonself perception and recognition mechanisms in plants: a comparison of self-incompatibility and innate immunity. New Phytologist **178**, 503–14.
Sanders D, Brownlee C, Harper JF. 1999. Communicating with calcium. The Plant Cell **11**, 691–706.
Sanders D, Pelloux J, Brownlee C, Harper JF. 2002. Calcium at the crossroads of signaling. The Plant Cell.
Scholz SS, Malabarba J, Reichelt M, Heyer M, Ludewig F, Mithöfer A. 2017. Evidence for GABA-Induced Systemic GABA Accumulation in Arabidopsis upon Wounding. Frontiers in Plant Science **8**, 388.
Scholz SS, Reichelt M, Vadassery J, Mithöfer A. 2015. Calmodulin-like protein CML37 is a positive regulator of ABA during drought stress in Arabidopsis. Plant Signaling & Behavior **10**, e1011951.
Schulze B, Mentzel T, Jehle AK, Mueller K, Beeler S, Boller T, Felix G, Chinchilla D. 2010. Rapid heteromerization and phosphorylation of ligand-activated plant transmembrane receptors and their associated kinase BAK1. The Journal of Biological Chemistry **285**, 9444–51.
Schwessinger B, Roux M, Kadota Y, Ntoukakis V, Sklenar J, Jones A, Zipfel C. 2011. Phosphorylation-Dependent Differential Regulation of Plant Growth, Cell Death, and Innate Immunity by the Regulatory Receptor-Like Kinase BAK1 (DS Guttman, Ed.). PLoS Genetics **7**, e1002046.
Scrase-Field SA, Knight MR. 2003. Calcium: just a chemical switch? Current Opinion in Plant Biology **6**, 500–506.

Shin O-H, Han W, Wang Y, Südhof TC. 2005. Evolutionarily conserved multiple C2 domain proteins with two transmembrane regions (MCTPs) and unusual Ca2+ binding properties. The Journal of biological chemistry **280**, 1641–51.
Snedden WA, Fromm H. 2001. Calmodulin as a versatile calcium signal transducer in plants. New Phytologist **151**, 35–66.
Snijder H., Kingma R., Kalk K., Dekker N, Egmond M., Dijkstra B. 2001. Structural investigations of calcium binding and its role in activity and activation of outer membrane phospholipase A from Escherichia coli. Journal of Molecular Biology **309**, 477–489.
Suarez-Rodriguez MC, Adams-Phillips L, Liu Y, Wang H, Su S-H, Jester PJ, Zhang S, Bent AF, Krysan PJ. 2007. MEKK1 is required for flg22-induced MPK4 activation in Arabidopsis plants. Plant Physiology **143**, 661–9.
Subbaiah CC, Sachs MM. 2003. Molecular and Cellular Adaptations of Maize to Flooding Stress. Annals of Botany **91**, 119–127.
Sun Y, Li L, Macho AP, Han Z, Hu Z, Zipfel C, Zhou J-M, Chai J. 2013. Structural basis for flg22-induced activation of the Arabidopsis FLS2-BAK1 immune complex. Science **342**, 624–8.
Szklarczyk D, Franceschini A, Wyder S, *et al.* 2015. STRING v10: protein-protein interaction networks, integrated over the tree of life. Nucleic Acids Research **43**, D447-52.
Tena G, Asai T, Chiu W-L, Sheen J. 2001. Plant mitogen-activated protein kinase signaling cascades. Current Opinion in Plant Biology **4**, 392–400.
Thomma BP, Eggermont K, Penninckx IA, Mauch-Mani B, Vogelsang R, Cammue BP, Broekaert WF. 1998. Separate jasmonate-dependent and salicylate-dependent defense-response pathways in Arabidopsis are essential for resistance to distinct microbial pathogens. Proceedings of the National Academy of Sciences **95**, 15107–11.
Truman W, Sreekanta S, Lu Y, Bethke G, Tsuda K, Katagiri F, Glazebrook J. 2013. The CALMODULIN-BINDING PROTEIN60 family includes both negative and positive regulators of plant immunity. Plant Physiology.
Tsai Y-C, Delk NA, Chowdhury NI, Braam J. 2007. Arabidopsis potential calcium sensors regulate nitric oxide levels and the transition to flowering. Plant Signaling & Behavior **2**, 446–54.
Tsai Y-C, Koo Y, Delk NA, Gehl B, Braam J. 2013. Calmodulin-related CML24 interacts with ATG4b and affects autophagy progression in Arabidopsis. The Plant Journal **73**, 325–35.
Tuteja N, Mahajan S. 2007. Calcium Signaling Network in Plants. Plant Signaling & Behavior **2**, 79–85.
Ueno H. 2000. Enzymatic and structural aspects on glutamate decarboxylase. Journal of Molecular Catalysis B: Enzymatic **10**, 67–79.
Vadassery J, Reichelt M, Hause B, Gershenzon J, Boland W, Mithofer A. 2012. CML42-Mediated Calcium Signaling Coordinates Responses to Spodoptera Herbivory and Abiotic Stresses in Arabidopsis. Plant Physiology **159**, 1159–1175.
Veluchamy S, Hind SR, Dunham DM, Martin GB, Panthee DR. 2014. Natural variation for responsiveness to flg22, flgII-28, and csp22 and Pseudomonas syringae pv. tomato in heirloom tomatoes. PLoS ONE **9**, e106119.
La Verde V, Dominici P, Astegno A, La Verde V, Dominici P, Astegno A. 2018. Towards Understanding Plant Calcium Signaling through Calmodulin-Like Proteins: A Biochemical and Structural Perspective. International Journal of Molecular Sciences **19**, 1331.
Verhertbruggen Y, Marcus SE, Chen J, Knox JP. 2013. Cell Wall Pectic Arabinans Influence the Mechanical Properties of Arabidopsis thaliana Inflorescence Stems and Their Response to Mechanical Stress. Plant & Cell Physiology **54**, 1278–1288.
Virdi AS, Singh S, Singh P. 2015. Abiotic stress responses in plants: roles of calmodulin-regulated proteins. Frontiers in Plant Science **6**, 809.
Voigt CA. 2014. Callose-mediated resistance to pathogenic intruders in plant defense-related papillae. Frontiers in Plant Science **5**, 168.
Wagner S, De Bortoli S, Schwarzländer M, Szabò I. 2016. Regulation of mitochondrial calcium in plants versus animals. Journal of Experimental Botany **67**, 3809–3829.
Wan D, Li R, Zou B, Zhang X, Cong J, Wang R, Xia Y, Li G. 2012. Calmodulin-binding protein CBP60g is a positive regulator of both disease resistance and drought tolerance in Arabidopsis. Plant Cell Reports **31**, 1269-81.
Wang X, Sager R, Cui W, Zhang C, Lu H, Lee J-Y. 2013. Salicylic acid regulates Plasmodesmata closure during innate immune responses in Arabidopsis. The Plant Cell **25**, 2315–29.
Wang L, Tsuda K, Sato M, Cohen JD, Katagiri F, Glazebrook J. 2009. Arabidopsis CaM binding protein CBP60g contributes to MAMP-induced SA accumulation and is involved in disease resistance against Pseudomonas syringae. PLoS Pathogens **5**, e1000301.
Wang Y, Wang B, Gilroy S, Wassim Chehab E, Braam J. 2011. CML24 is Involved in Root Mechanoresponses and Cortical Microtubule Orientation in Arabidopsis. Journal of Plant Growth Regulation **30**, 467–479.

Whalley HJ, Knight MR. 2013. Calcium signatures are decoded by plants to give specific gene responses. New Phytologist **197**, 690–3.
White PJ, Broadley MR. 2003. Calcium in Plants. Annals of Botany **92**, 487–511.
Yamada K, Yamaguchi K, Shirakawa T, *et al.* 2016. The Arabidopsis CERK1-associated kinase PBL27 connects chitin perception to MAPK activation. The EMBO Journal **35**, 2468–2483.
Yamazaki T, Takata N, Uemura M, Kawamura Y. 2010. Arabidopsis synaptotagmin SYT1, a type I signal-anchor protein, requires tandem C2 domains for delivery to the plasma membrane. The Journal of biological chemistry **285**, 23165–76.
Yang T, Chaudhuri S, Yang L, Du L, Poovaiah BW. 2010*a*. A Calcium/Calmodulin-regulated Member of the Receptor-like Kinase Family Confers Cold Tolerance in Plants. Journal of Biological Chemistry **285**, 7119–7126.
Yang Z, Lasker K, Schneidman-Duhovny D, Webb B, Huang CC, Pettersen EF, Goddard TD, Meng EC, Sali A, Ferrin TE. 2012. UCSF Chimera, MODELLER, and IMP: An integrated modeling system. Journal of Structural Biology **179**, 269–278.
Yang T, Shad Ali G, Yang L, Du L, Reddy ASN, Poovaiah BW. 2010*b*. Calcium/calmodulin-regulated receptor-like kinase CRLK1 interacts with MEKK1 in plants. Plant Signaling & Behavior **5**, 991–994.
Yang X, Wang S-S, Wang M, Qiao Z, Bao C-C, Zhang W. 2014. Arabidopsis thaliana calmodulin-like protein CML24 regulates pollen tube growth by modulating the actin cytoskeleton and controlling the cytosolic Ca(2+) concentration. Plant Molecular Biology **86**, 225–36.
Yao J, Gaffaney JD, Kwon SE, Chapman ER. 2011. Doc2 Is a Ca2+ Sensor Required for Asynchronous Neurotransmitter Release. Cell **147**, 666–677.
Yoo JH, Park CY, Kim JC, *et al.* 2005. Direct interaction of a divergent CaM isoform and the transcription factor, MYB2, enhances salt tolerance in arabidopsis. The Journal of biological chemistry **280**, 3697–706.
Yoshida T, Fujita Y, Sayama H, Kidokoro S, Maruyama K, Mizoi J, Shinozaki K, Yamaguchi-Shinozaki K. 2010. AREB1, AREB2, and ABF3 are master transcription factors that cooperatively regulate ABRE-dependent ABA signaling involved in drought stress tolerance and require ABA for full activation. The Plant Journal **61**, 672–685.
Yuan P, Jauregui E, Du L, Tanaka K, Poovaiah B. 2017. Calcium signatures and signaling events orchestrate plant–microbe interactions. Current Opinion in Plant Biology **38**, 173–183.
Zeng H, Xu L, Singh A, Wang H, Du L, Poovaiah BW. 2015. Involvement of calmodulin and calmodulin-like proteins in plant responses to abiotic stresses. Frontiers in Plant Science **6**, 600.
Zhang J, Li W, Xiang T, *et al.* 2010. Receptor-like Cytoplasmic Kinases Integrate Signaling from Multiple Plant Immune Receptors and Are Targeted by a Pseudomonas syringae Effector. Cell Host & Microbe **7**, 290–301.
Zhang W, Zhou R-G, Gao Y-J, Zheng S-Z, Xu P, Zhang S-Q, Sun D-Y. 2009. Molecular and Genetic Evidence for the Key Role of AtCaM3 in Heat-Shock Signal Transduction in Arabidopsis. Plant Physiology **149**, 1773 LP – 1784.
Zhou J, Wu S, Chen X, Liu C, Sheen J, Shan L, He P. 2014. The Pseudomonas syringae effector HopF2 suppresses Arabidopsis immunity by targeting BAK1. The Plant Journal **77**, 235–45.
Zhou Y, Xue S, Yang JJ. 2013. Calciomics: integrative studies of Ca2+-binding proteins and their interactomes in biological systems. Metallomics : integrated biometal science **5**, 29–42.
Zhu J-K. 2002. Salt and Drought Stress Signal Transduction in Plants. Annual Review of Plant Biology **53**, 247–273.
Zielinski RE. 1998. Calmodulin and Calmodulin-Binding Proteins in Plants. Annual Review of Plant Physiology and Plant Molecular Biology **49**, 697–725.

Chapter 2:

A calmodulin and calmodulin-like protein network integrates touch and pathogen responses in *Arabidopsis thaliana*

I would like to acknowledge the following people for contributing to the results for this chapter: Dr. Nathan Miller, Savana Lipps, Gabrielle Li, and Simon Gilroy.

I was responsible for generating all of the results. Savana Lipps assisted with pathogenesis assays and imaging. Gabrielle Li assisted with qPCR and genotyping. Nathan Miller designed the image-analysis toolkit for the touch response robot. Simon Gilroy and I wrote all parts of the manuscript.

Summary

- Plants respond to mechanical stimuli with a suite of physiological responses including reduction in overall growth, hardening of supporting tissues, the darkening of leaves, and delay in flowering time.
- Molecular responses to mechanical stimulation have been noted to relate to Ca^{2+}-dependent signal transduction, with induction of calmodulin (*CAM*) and calmodulin-like (*CML*) genes.
- I therefore mined the publicly available transcriptomics data and then used network inference tools to generate a molecular network of *CAMs* and *CMLs* that may connect the plant's molecular and physiological responses to touch.
- I used knockout lines in each of the candidate touch-related *CAM* and *CML* genes from this analysis and monitored alterations in their responses to touch.
- In addition, as the physiological responses to repeated touch stimulus have been noted to be associated with an improvement in the response to pathogen attack, I used network inference tools to create a molecular pathogen-response network and monitored equivalent molecular and physiological measures of pathogen defense in these mutants.
- I found that within my touch-focused network of 12 touch-responsive *CAM* and *CML* genes, mutants showed disruption in touch or pathogen response, with a broad tendency for upregulation of pathogen response marker genes and suppression of touch-related markers. At a physiological level, 4 showed increased defense capacity and 4 were significantly compromised in defense. In addition, *CAM2*, *CML5*, *CML12*, *CML24*, *CML27*, *CML40*, *CML44*, *CML46*, and *CML49* all exhibited touch insensitivity. Of these, 5 mutants showed a constitutive reduction in plant size that did not respond to touch, with only the mutant in *CAM2* showing wild-type-like unstimulated growth and subsequent touch insensitivity.
- These findings provide evidence for the involvement of a subset of the *CAM*/*CML* gene family in coordinating the plant responses to the seemingly distinct stimuli of touch and pathogen attack.

INTRODUCTION

Plants are constantly bombarded by a host of diverse signals from fluttering in the wind, to attack by an insect, or the drying of the soil. These stimuli initiate a series of cellular perception and signaling events that ultimately trigger highly adaptive downstream responses. For instance, plants exhibit thigmomorphogenesis, i.e., altered growth and development in response to touch stimuli. Such stimuli do not arrive in isolation and so the plant must trigger multiple, parallel signaling networks in order to process and integrate this array of information to the most appropriate suite of responses. These stimuli can be vastly different in nature, yet, while, e.g., the biotic stimulus of a pathogen attack and the abiotic signal arising from the mechanical force of the wind seem very different, they do appear connected within the plant's response systems. Thus, mechanically stimulated plants appear better able to defend themselves against pathogens (Gus-Mayer *et al.*, 1998; Benikhlef *et al.*, 2013; Tomas-Grau *et al.*, 2017). Indeed, the phenomenon of cross-protection/cross-tolerance, where one stimulus protects a plant against a seemingly disconnected stress, is a well-reported phenomenon (Pastori and Foyer, 2002; Mittler, 2006; Foyer *et al.*, 2016).

One possibility is that some of the outputs of, e.g., the mechanical response system, such as deposition of more strengthening elements within the wall, incidentally, provide barriers to pathogen entry, i.e., cross-tolerance is an accidental output of an inherently mechanical response system. Alternatively, cross-talk between the molecular signaling networks triggered by each "independent" signaling input may lead to these cross-tolerance outputs being hardwired into both signaling networks. In this latter case, shared signaling mechanisms could likely yield the information exchange between the pathways. Indeed, such shared systems through, e.g., hormonal regulation are thought to operate to optimize the tradeoffs between prioritizing one signal response pathway over another (Berens *et al.*, 2019). For example, there is a well-documented tradeoff

between eliciting immune responses or adaptation to abiotic stress, such as an overabundance of salt, and the maintenance of vegetative growth (Huot *et al.*, 2014; Karasov *et al.*, 2017).

Many molecular regulators have been proposed to play roles in both mechanical and pathogen response signaling. Thus, common hormones (e.g., salicylic acid (SA), jasmonic acid (JA), ethylene (Chehab *et al.*, 2009; Tsuda *et al.*, 2008; Yi *et al.*, 2014; Mersmann *et al.*, 2010; Chehab *et al.*, 2012), signal transduction machinery (e.g., mitogen-activated protein kinase) (Wu *et al.*, 2014; Mizoguchi *et al.*, 1996; Ichimura *et al.*, 2000), and second messengers, such as Ca^{2+} (Toriyama and Jaffe, 1972; Knight *et al.*, 1991; Legué *et al.*, 1997; Grant *et al.*, 2000; Lecourieux *et al.*, 2006; Nakagawa *et al.*, 2007; Monshausen *et al.*, 2009; Kwaaitaal *et al.*, 2011), have all been found to work within both the touch- and pathogen-response systems, although their roles have been identified independently in each signaling system. For Ca^{2+} signaling to operate specifically in both touch and pathogen responses, the frequency, amplitude, duration and localization of the change in $[Ca^{2+}]$ is thought to define stimulus-specific information, the so-called 'calcium signature' of the stimulus (McAinsh and Pittman, 2009; Dodd *et al.*, 2010). This signature is then decoded by Ca^{2+}-response proteins to trigger specific outputs leading to the appropriate downstream response. In this scenario, the molecular decoding system for the pathogen response would be tuned to a different Ca^{2+} signature than that encoding the touch signal and, so, the same second messenger, Ca^{2+}, can elicit specific downstream responses to two different inputs.

For the touch response, amongst the earliest molecularly identified response elements were the Arabidopsis touch-induced genes, named *TOUCH1-3* (*TCH1-3*), that encode calmodulin and CaM-like proteins (CMLs). Thus, *TCH1* is CaM isoform 2 (*CAM2*), *TCH2* is *CML24* and *TCH3*, *CML12* (Braam and Davis, 1990; Ma *et al.*, 2008), highlighting the likely role of the CaM/CML superfamily in decoding touch signals in the plant. Consistent with these ideas, *cml24* mutants

show altered waving and thigmotropic responses that have been linked to the touch sensing apparatus of the root (Wang *et al.*, 2011; Zha *et al.*, 2016; reviewed in Toyota and Gilroy, 2013).

In the pathogen response, e.g., CML8, CML9, CML41 and CML43 are all thought to act as positive regulators of defense (Leba *et al.*, 2012; Bender *et al.*, 2014; Zhu *et al.*, 2016; Xu *et al.*, 2017), whereas CML46 and CML47 operate redundantly as negative regulators of immune function (Lu *et al.*, 2018). Indeed, modeling has suggested a strong causal link between Ca^{2+} signal dynamics, CaM action and patterns of downstream defense gene induction (Lenzoni *et al.*, 2018). Intriguingly for the ideas of cross-talk between the touch and pathogen systems, despite *CML24* being an archetypical touch response gene, disruption of CML24 function also leads to reduced hypersensitive response and impaired pathogen triggered NO production (Ma *et al.*, 2008).

I therefore asked how far the CaM and CML families might provide insight into the cross-talk between the mechanical and pathogen response networks. Lee *et al*. (2005) previously identified 10 *CAM* and *CML* genes as showing >two-fold touch-inducible transcription, although for most of these genes a link to mechanical response outputs has still yet to be made. I analyzed the responses of mutants in all members of this putative touch response network. I report that mutants in these genes show altered mechano-response at levels from disrupted thigmomporphogenesis to a general suppression of molecular responses to touch. Of these genes chosen for their mechanical responses, I also found that *CAM2*, *CML5*, *CML9*, *CML12*, *CML24* and *CML40* showed alterations in pathogen response, suggesting that these genes may form an intersection between the flow of Ca^{2+}-response information stemming from both touch and pathogen perception and signaling systems.

RESULTS

Bioinformatics Analysis

Lee *et al*. (2005) identified 10 *CAM*s and *CML*s as showing significant touch induction to >2-fold. In addition, in the analysis of Lee *et al*. (2005), *CML9* showed induction to 1.98-fold ($p = 0.0013$) and so I also included this gene in my analyses. Mutants in *CML24* and *12* have been reported to show thigmotropic phenotypes, whereas *CAM2* mutants showed no such changes (Wang *et al.*, 2011; Zha *et al.*, 2016), suggesting that induction by touch alone may not be a strong predicter of genes with touch-related mutant phenotypes. Therefore, I used these genes as a starting point to ask if they likely formed a coherent touch responsive network using bioinformatics. I used the functional protein network inference tool STRING 11.0 (Szklarczyk *et al.*, 2019) to generate a putative interconnectivity network, shown in **Figure 2.1**. Such analysis suggested these CaMs and CMLs form a tightly linked genetic network, with *NOA1* as an important hub connecting all but *CML46*. This coherent network suggested that further genetic analysis of these CaMs and CMLs could yield insight into a potentially common role in touch sensing and response.

Additionally, **Figure 2.1** shows that when we seed STRING with the putative touch genes from Lee *et al*. (2005), no additional *CAM*s or *CML*s (apart from *CAM3* and *CAM5*, which encode the same CaM isoform as *CAM2*) are a part of this network. This indicates that their analysis was correct; otherwise, if there were other *CAM*s or *CML*s involved in this kind of response, they would be expected to appear in the immediate vicinity of the touch genes in the network. I therefore systematically analyzed mutants in all these touch responsive *CAM*s and *CML*s for alterations in touch response using a suite of molecular markers for touch response as well as effects on overall thigmomorphogenesis. I also included a *CAM7* mutant in my analyses due to the high sequence

similarity of CaM7 to CaM2 (differing by a single amino acid) (Kumar *et al.*, 2016) but it did not show touch induction in the Lee *et al.* (2005) analysis.

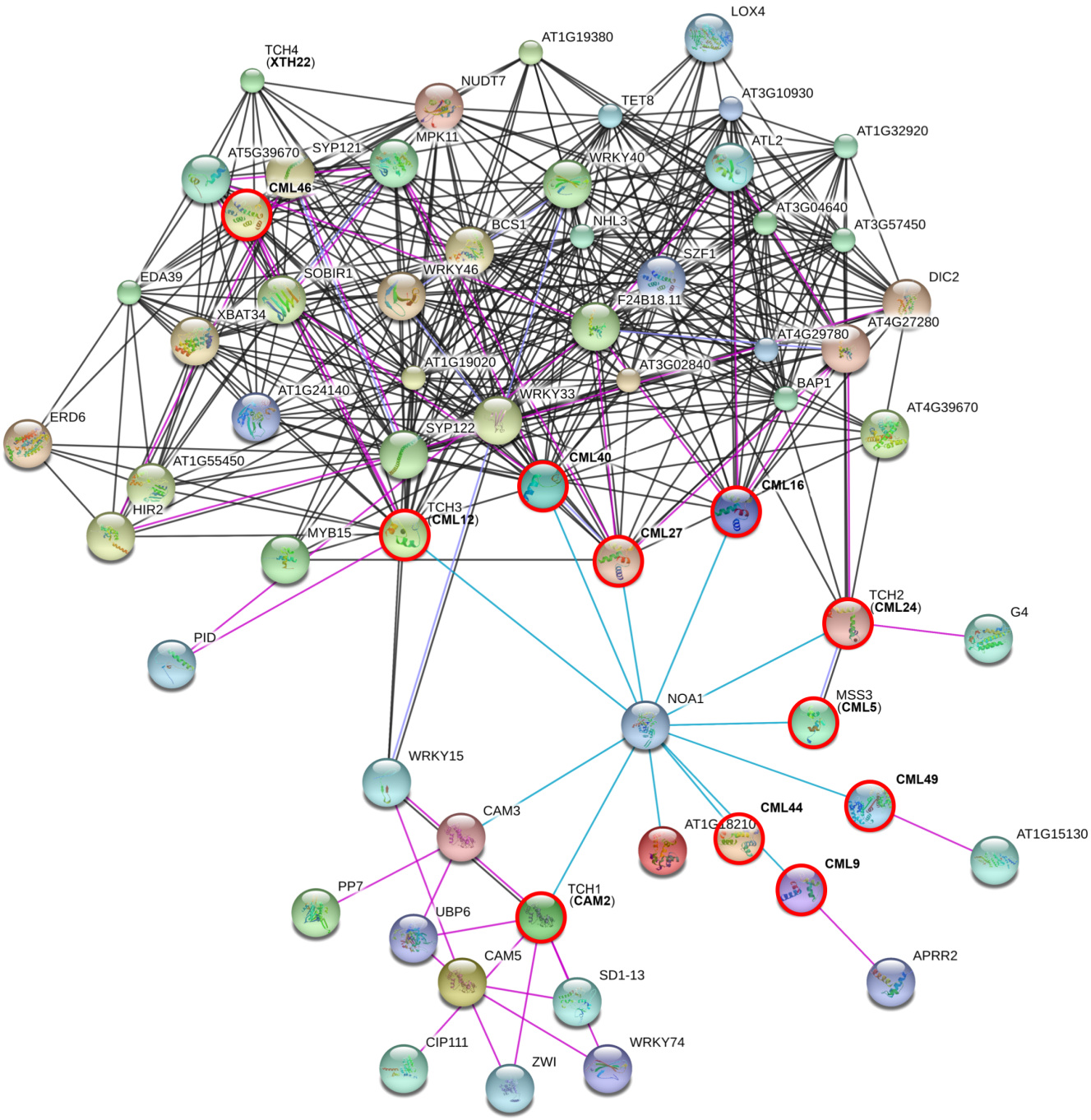

Figure 2.1 CaM/CML genes upregulated in response to touch interact with numerous targets from various pathways. Interaction network of ≥2-fold touch-inducible CaMs/CMLs from Lee, *et al*., (2005) (**bold names**; listed in **Supplementary Table S2.1**) and their experimentally-determined interaction partners (listed in **Supplementary Table S2.2**). Developed using STRING v11. Black lines represent connections based upon co-expression analyses; violet lines are from experimental biochemical data; blue lines are from Biocarta, BioCyc, GO, KEGG, and Reactome databases.

Molecular Response to Touch

I first monitored molecular markers for touch response (a 100g aluminum rod was rested under its own weight on seedlings, for 3s). **Figure 2.2** shows that with such a treatment on wild type plants, 30 mins after touch stimulation, the classic touch response markers *TCH1-TCH4* were induced between ~4.5- and ~20-fold. I then assayed mutants in all 11 of the touch-upregulated genes described above along with *CAM7* mutants for response in this system. Two mutant alleles were acquired from ABRC for all subsequent analyses. In **Figure 2.2**, it is shown that in all cases, even in the absence of the touch stimulus, mutants in the touch-network genes led to suppression of at least one touch responsive marker gene. Upon touch stimulation, most of the mutants showed suppression of the touch-inducible markers and even when induction occurred, such as with *TCH2*, the level of induction was significantly below that seen in wild type (Col-0) in nearly all mutant backgrounds at 30 mins (with the exception of, e.g., *TCH2* in the *cam7*, *cml5*, *cml9*, and *cml40*

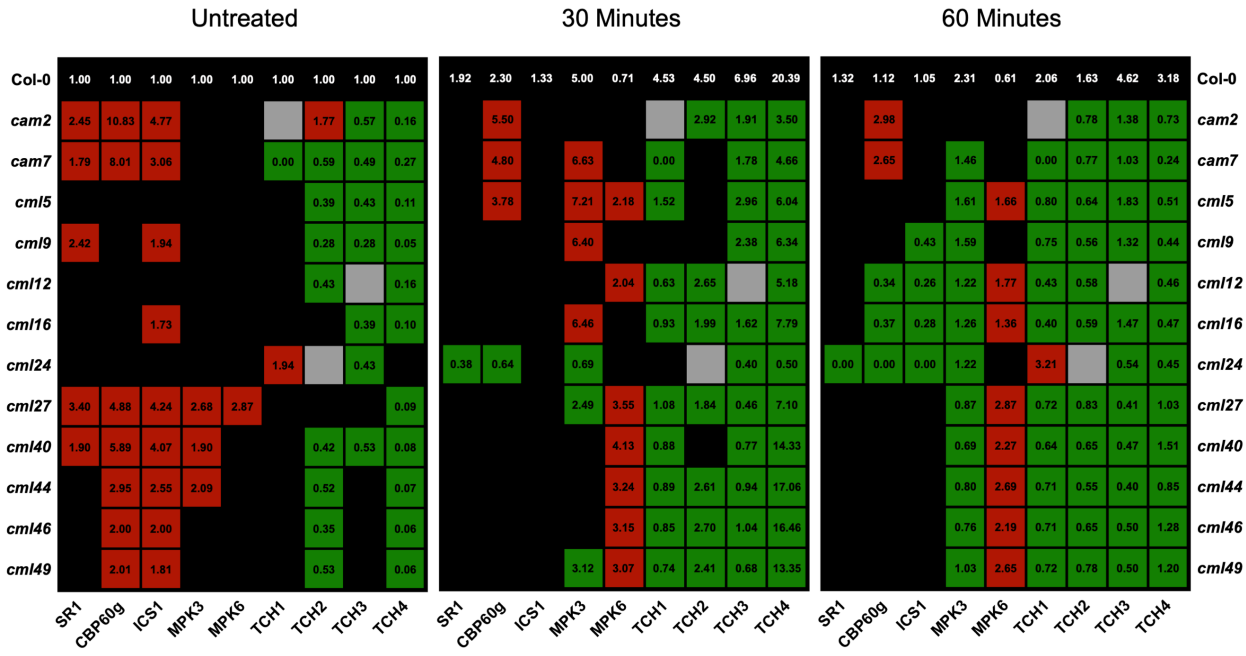

Figure 2.2 *CaM* and *CML* mutant plants differentially express pathogen and touch-responsive genes after touch stimulus.
Fold-expression ($2^{-\Delta\Delta Ct}$) values are relative to untreated Col-0: Red > Col-0; green < Col-0; black represents values that are not significantly different from Col-0 (2-way ANOVA; Dunnett's Test; $p < 0.05$); grey indicates the knockout for the indicated marker gene. $n \geq 12$ biological replicates with 4 technical replicates from 2 independent experiments. As touch and flg22 treatments were performed in parallel, the untreated control is the same for both and so the same untreated sample data is shown in **Figures 2.2 and 2.5**.

mutants) and in all mutant lines at 60 minutes post-touch stimulation. Thus, mutants in these touch responsive *CAM*s and *CML*s disrupt basal expression of molecular markers for touch response and also suppress subsequent touch-responsive induction of these markers, consistent with their potential role in the touch signaling network.

Physiological Response to Touch

In addition to molecular responses to touch, plants often respond to mechanical stress with thigmomorphogenesis-related reduction in vegetative growth (Chehab *et al.*, 2012). In most cases this effect plays out over many hours to days and so imposing a uniform mechanical stress over these periods is challenging, especially when needing to compare the quantitative responses of multiple mutants over time against each other. Therefore, a touch stimulation robot based on the three-axis movement mechanism from a computer numerical control (CNC) milling machine, the

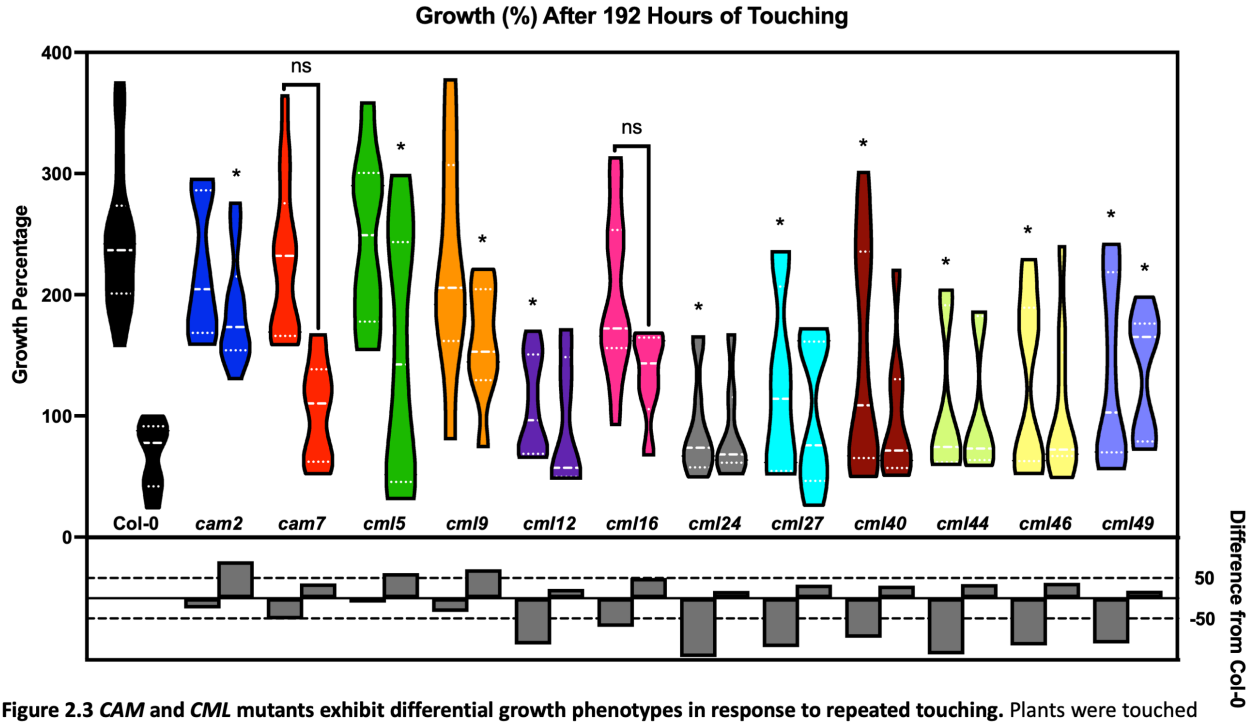

Figure 2.3 *CAM* and *CML* mutants exhibit differential growth phenotypes in response to repeated touching. Plants were touched at 5 minute intervals over 8 days using the Automated Botanical Contact Device. Increased growth over the 8 days is reported as growth percentage (x100). The difference between untouched (left bar) and touched (right bar) from Col-0 for each genotype is reported as percentage change (x100) and indicated by the white brick bars. Each mutant, except *cam7* exhibited a significant difference in percentage change, compared to Col-0 (2-way ANOVA; Dunnett's Test; $p < 0.05$).

Automated Botanical Contact Device (ABCD), that intermittently drew a plastic sheet over the plants as they grew, providing a relatively gentle, controlled mechanical stimulation, was created to address this issue. A full description of the development and implementation of this apparatus is presented in **Appendix I**. This approach allowed me to grow a large number of plants in flats, with a touch stimulated row growing beside its unstimulated control (a row where the plastic sheet providing the touch contact had been removed). Twenty-day-old plants were grown and then the machine was programmed to stimulate them, from then-on, every 5 mins. Images of growing plants were collected, continuously, using an automated Raspberry Pi camera system.

Figure 2.3 summarizes responses after 8 days of stimulation (the time course data for each mutant is shown in **Supplementary Figures S2.1-S2.12**). In wild type, such repetitive mechanical stimulation led to the expected reduced rosette growth to ~35% of untouched controls at day 8. The mutants showed 3 classes of response: (1) rosette growth that mirrored the untouched growth rate and touch sensitivity of wild type (e.g. *cml16* and *cam7* – the gene chosen because it did not show touch-responsiveness in Lee *et al*., (2005)), (2) growth where untouched rates resembled wild type but touch sensitivity was significantly reduced (i.e., growth rates were less touch inhibited than wild type (*cam2*, *cml5*, and *cml9*), and (3) growth that was slower than wild type in untouched conditions but that subsequently did not respond to touch with further inhibition (*cml12*, *cml24*, *cml27*, *cml40*, *cml44*, *cml46*, and *cml49*).

Response to Pathogen

As noted above, plants receiving mechanical stimulation have been noted to show enhanced defense responses and so I was interested in whether these *CAM* and *CML* genes selected for their relationships to touch might also play roles in pathogen response. To ask this question, I, again,

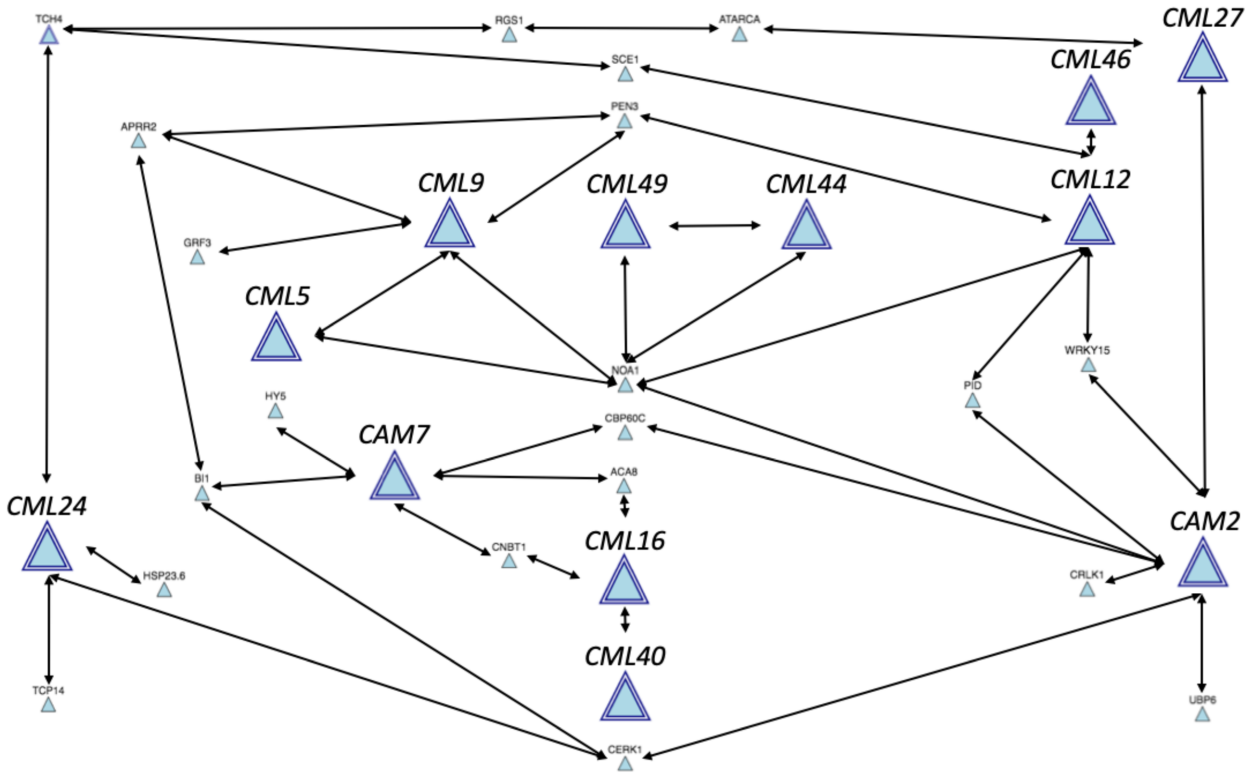

Figure 2.4 CaM/CML genes upregulated in response to touch are also involved in pathogen responses. Genetic network diagram developed using KNetMiner connecting touch-responsive genes in **Figure 2.1** to pathogen responses. Genes found to be upregulated at least 2-fold in response to mechanical stimuli are enlarged, as is *CAM7*. Genes connecting touch-responsive genes to pathogen responses are smaller. Arrows denote experimentally-determined connections.

first adopted a bioinformatics-driven approach. Whereas STRING constructs a network of interactions between genes based solely on user-selectable combinations experimentally-determined relationships, it does not allow queries based upon gene ontology or known descriptions of the kinds of interactions in which they are involved. While the data supporting the existence of these interactions may be contained, however cryptically, in STRING networks, that information is not a part of the query interface. The network inference tool, KnetMiner, which mines the Ondex knowledge environment (Hassani-Pak *et al.*, 2016; Brandizi *et al.*, 2018), on the other hand, allows ontology-based search terms to add depth to the network analysis. Therefore, to determine whether a coherent network integrating the – previously-described – touch genes and the plant responses to pathogens could be formed, I input the *CAM* and *CML*s of the touch network

into KnetMiner and applied the ontology searches "pathogen response," "defense response," "flg22," "defense-related protein," and "plant-pathogen interaction". The output from this query is shown in **Figure 2.4**. This figure also connects *CAM7* (center-left of the network figure) to the touch-responsive *CAM*s and *CML*s. This network supports the hypothesis that these touch-related *CAM*s and *CML*s may be involved in defense responses, as I was able to generate a coherent network from these touch-network genes with extensive putative links to defense. Had the hypothesis been false, I would have expected only one or two of the links to pathogen-responses to appear. Therefore, I proceeded to test all the mutants in these genes for altered defense capacity.

Molecular Response to Pathogen Treatment

I used the microbe associated molecular pattern (MAMP) flg22 to elicit an immune response (pattern-triggered immunity, PTI) in wild type and the touch-network mutants, and qPCR

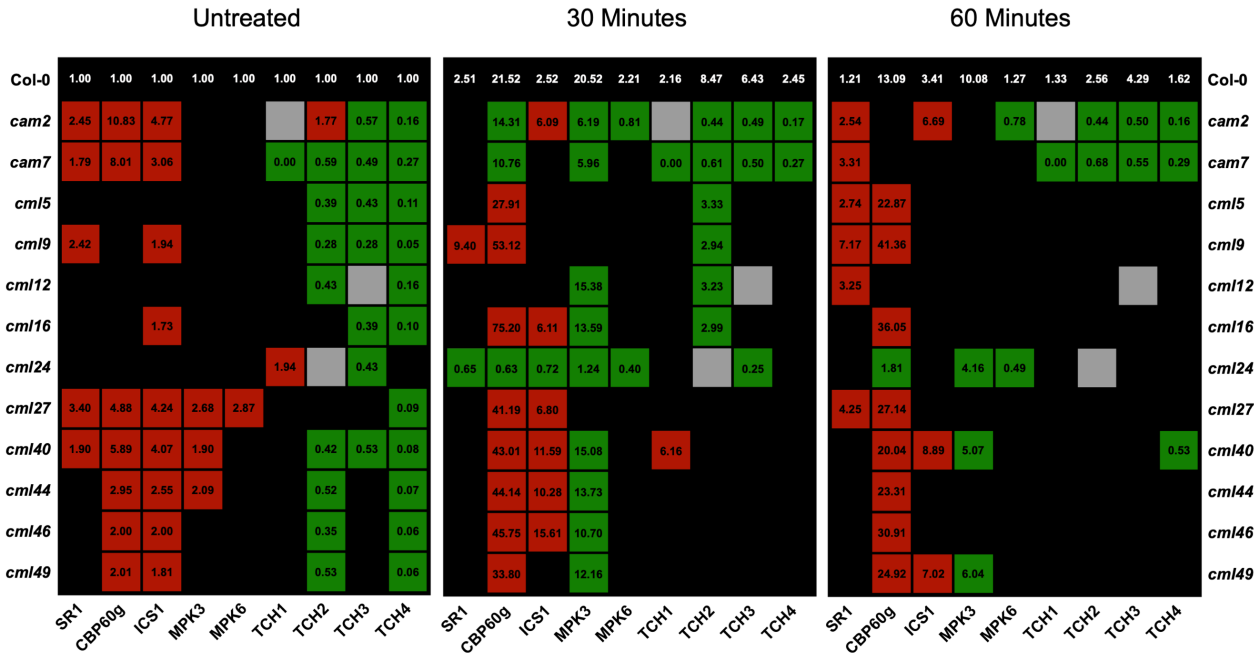

Figure 2.5 *CaM* and *CML* mutant plants differentially express pathogen and touch-responsive genes after treatment with 1 µM flg22. Fold-expression ($2^{-\Delta\Delta Ct}$) values are relative to untreated Col-0: Red > Col-0; green < Col-0; black represents values that are not significantly different from Col-0 (2-way ANOVA; Dunnett's Test; $p < 0.05$); grey indicates the knockout for the indicated marker gene. $n \geq 12$ biological replicates with 4 technical replicates from 2 independent experiments. As touch and flg22 treatments were performed in parallel, the untreated control is the same for both and so the same untreated sample data is shown in **Figures 2.2 and 2.5**.

to monitor the levels of PTI-related marker genes in these backgrounds. **Figure 2.5** shows that, in Col-0, the expression of genes related to immune response and salicylic acid production such as *SR1, CBP60g* and *ICS1* and defense signal response genes such as *MPK3* and *MPK6* reach from between ~2.5- to ~21.5-fold induction 30 mins after flg22 treatment. This response defined the extent and kinetics of the expected MAMP-induced molecular response.

Even before flg22 treatment, several of the mutant plants, (*cam2*, *cam7*, *cml9*, *cml27*, *cml40*, *cml44*, *cml46* and *cml49*) exhibited significantly increased basal expression of at least one of the pathogen-response marker genes – *SR1*, *CBP60g*, or *ICS1* – relative to Col-0. For all of these but the *cam2*, *cam7* and *cml24* mutants, expression of the marker genes significantly increased after flg22 treatment, indicating a response to flg22 mirroring Col-0, but often to much higher levels. For example, the 2.4-fold basal induction of *SR1* in *cml9* over wild type levels was increased to 9.4-fold at 30 mins after flg22 treatment, a level sustained at 7.2-fold at 60 mins. In the same background, *CPB60g* was induced to 40-50-fold above wild type levels by flg22 treatment. *cam2* and *cam7* exhibited a slightly different pattern, as both mutants showed elevated untreated levels of several of the defense markers and sustained these already elevated levels at 30 and 60 mins of flg22 treatment. These levels were maintained without clear further induction due to MAMP addition. The induction of the defense response markers *MPK3* and *MPK6* also was suppressed after flg22 treatment in *cam2*. These results indicate that CaM2 and CaM7 may negatively regulate the molecular response to flg22, potentially acting through the MPK3/MPK6 pathway. Additionally, *cml24* stood out in this analysis as it exhibited wild type levels of expression of pathogen-response marker genes in untreated samples. However, the expression of these genes decreased significantly after flg22 treatment, relative to Col-0.

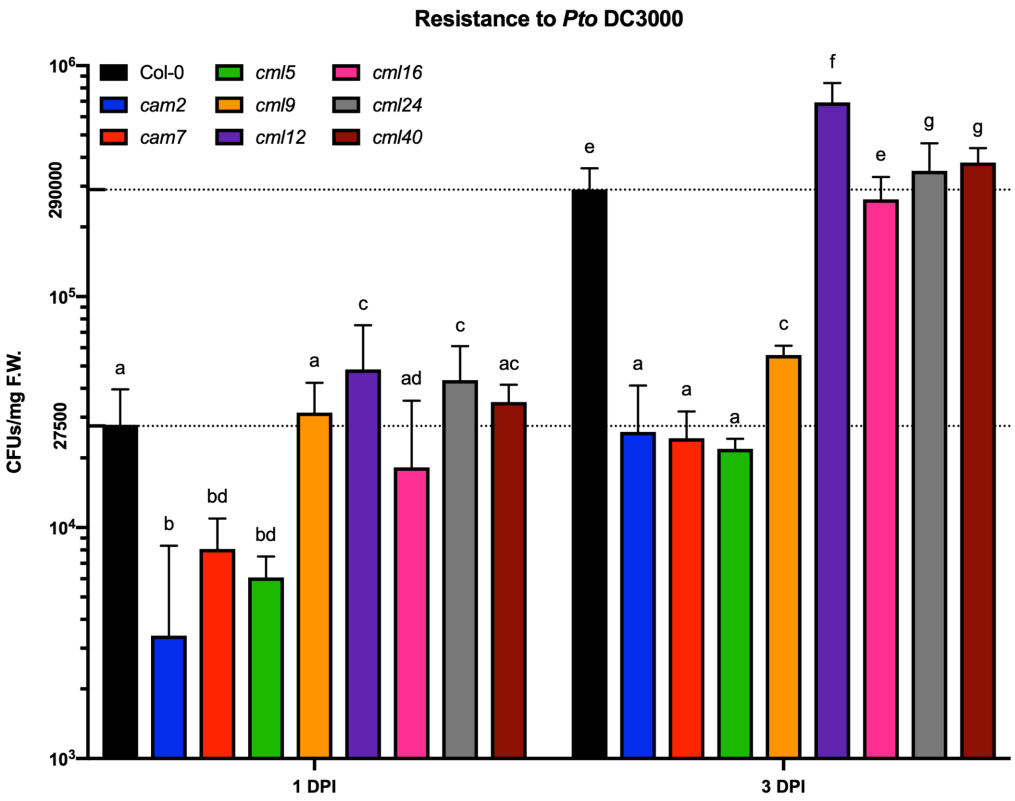

Figure 2.6 *CAM* and *CML* mutants exhibit differential ability to suppress internal pathogen proliferation. Plants were flooded with *Pto* DC3000 (OD_{595} = 0.4), harvested 1 and 3 days post-inoculation (DPI), and extractable bacteria (CFUs/mg F.W.) were counted. Results represent mean ± s.d.; n = 12 biological replicates, each with 4 technical replicates from 3 independent experiments. Columns with the same letter are not statistically different from Col-0 at the given time point (2-way ANOVA; Dunnett's Test; $p < 0.05$).

Physiological Response to Pathogen Treatment

To assay how well each mutant line survived after infection by *Pseudomonas syringae* pv. *tomato* DC3000 (*Pto* DC3000), I carried out pathogen treatments, assaying survival time (to complete loss of green tissue) as an initial index of defense capacity. Under my assay conditions, Col-0 seedlings exhibited a complete loss of green tissue at 6 days post-infection (DPI; **Supplementary Figure S2.13**). *cam2*, *cam7*, *cml5*, and *cml9* showed an increase in longevity after exposure to *Pto* DC3000, surviving approximately 3 DPI longer than Col-0. Conversely, *cml12*, *cml16*, *cml24* and *cml40* exhibited a decrease in longevity, surviving between 1 and 2 days less than Col-0.

To confirm these observed changes in defense capabilities, I also monitored the ability of those mutants from the survival assays that showed significant resistance or susceptibility, to

defend against seedling flood inoculation with *Pto* DC3000. **Figure 2.6** shows that differences in resistance were evident in as short as 1 DPI but were most clear at 3 DPI. Under these conditions, at 3 DPI, *cam2*, *cam7*, *cml5*, and *cml9* plants all exhibited significantly fewer extractable bacteria after inoculation at day 0, indicating increased resistance, whereas *cml12*, *cml24*, and *cml40*, exhibited a significant reduction in resistance. With the exception of *cml16*, which exhibited resistance at the same level as Col-0, these results confirmed the expectations from the time-to-death assay.

Touch and Pathogen Responses Share Molecular Responsiveness

The above analyses suggest that mutants in genes selected for their relationship to touch response also show disruptions in pathogen response. I therefore asked how specifically the well-defined markers of pathogen (*ICS1*, *CPB60g*, *SR1*, *MPK3*, *MPK6*) and touch response (*TCH1*, *TCH2*, *TCH3*, *TCH4*) relate to each of these stimuli. **Figure 2.5** shows that in wild type, touch response markers are upregulated by flg22 treatment. Thus, the canonical touch-responsive genes *TCH1*, *TCH2*, *TCH3*, and *TCH4* all increase in expression after flg22 treatment in Col-0. *TCH2* is the most highly-expressed *TCH* gene, reaching peak induction of ~8.5-fold at 30 mins after flg22 treatment. Similarly, **Figure 2.2** shows that defense response genes are also induced by touch in wild type plants, with e.g., 5-fold induction of *MPK3* and 2.5-fold of *CPB60g* at 30 mins after touch stimulation.

DISCUSSION

Touch stimulation is known to trigger Ca^{2+} changes that are thought, in turn, to trigger downstream responses (Toyota and Gilroy, 2013; Monshausen and Haswell, 2013). Although the mechanosensors, likely mechanosensitive ion channels, responsible for these changes remain unknown, some downstream signaling elements are now characterized, including hormones, e.g., JA and GA (Chehab *et al.*, 2012; Lange and Lange, 2015) and, of particular relevance to this work, Ca^{2+}-responsive proteins, such as CaM/CML superfamily members (Toyota and Gilroy, 2013).

Although 3 out of the 4 original touch-induced genes identified in the 1990s were CaM or CMLs (*TCH1*/*CAM2; TCH2/CML24; TCH3/CML12*), direct evidence for the role of *CML24* and *CML12* in mediating touch responses via root thigmotropic and wave responses has only relatively recently been found (Wang *et al.*, 2011; Zha *et al.*, 2016). The results in this study, using the 11 touch-responsive CaM and CMLs identified in Lee *et al*. (2005), provide evidence for a functional role for all of these genes in the physiological and/or molecular responses to touch stimulation. Thus, mutants in *CAM2* (*TCH1*) disrupt basal, unstimulated touch response gene expression, with suppression of *TCH3* and *TCH4* and induction of *TCH2* relative to wild type. Further, *cam2* mutants show insensitivity of growth inhibition by touch, however, mutants in *CAM7* (chosen as it did not show touch-induction in the Lee *et al.* (2005) analysis and as CaM7 differs from CaM2 by a single amino acid) showed wild-type-like growth inhibition to touch, suggesting a higher degree of specificity in the touch-response system. Similarly, *cml12* mutants downregulate *TCH2* and *TCH4* basal levels, whereas *cml24* mutants upregulate *TCH1* and downregulate *TCH3*. Both *cml12* and *cml24* mutants downregulate further touch-induction of these markers and both show a constitutive restriction in growth and insensitivity to the triggering of any subsequent further

reduction in growth by touch stimulation. Thus, mutants in all three of these *TCH* genes affect touch responses, although the specific outcomes of their knockouts are not identical.

However, taking all the CaMs and CML mutants I analyzed together does reveal some broad themes, although again, individual CaM or CMLs may break specific elements of these general patterns. At a molecular level, knockouts in the touch-induced CaM/CMLs lead to repression of basal levels of touch-induced genes and subsequent suppression of further induction by touch. These effects are most obvious for the basal and inducible levels of *TCH2* (*CML24*) and *TCH4* (*XTH22*). A notable exception is the *cml24* mutant, where *TCH1* (*CAM2*) expression is upregulated at basal levels and shows higher touch induction than wild type over 60 mins. There is a reciprocal basal induction of *TCH2* (*CML24*) in the *cam2* background, suggesting there may be some co-regulation or other sort of genetic linkage between these two touch-related genes. These observations are consistent with this suite of CaMs and CMLs that I targeted as they show induction by touch stimulation (Lee *et al.*, 2005) being part of an integrated Ca^{2+} response network playing roles as positive regulators of the molecular response to touch.

However, although disruption of the levels of touch response genes in these mutant backgrounds correlates well with their subsequent alteration of thigmomorphogenesis, they do not all lead to the same outcome of touch-insensitivity, i.e., only mutations in *CAM2*, *CML5* and *CML9* result in wild type untouched growth, but touch-insensitive vegetative growth over 8 days of mechanical stimulation. Other mutants exhibited gross reduction in vegetative growth in both untouched and touched plants, perhaps obscuring the true impact their mutant backgrounds had on touch-sensitivity. For example, mutations in *CML24* and *CML44* led to untouched and touched vegetative growth that was not significantly greater than that of touched Col-0 plants over 8 days of mechanical stimulation (**Supplementary Figures S2.7 and S2.10**, respectively). The expected

outcome, significant reduction in touch-sensitivity, therefore, might not have been observable, as maximal growth was severely diminished, due to their mutations. In fact, this relative dwarfing of *CML* mutants was the most common growth phenotype.

Part of an answer to these observations may lie in my finding that this CaM and CML-based network also appears to play a role in pathogen defense and so may be exhibiting tradeoffs between the two (pathogen- and touch-) response pathways and vegetative growth. Thus, in the mutants of these genes originally selected for their relationship to touch response, defense-related marker gene expression is also disrupted. In 9 of the 12 mutants analyzed (*cam2*, *cam7*, *cml9*, *cml16*, *cml27*, *cml40*, *cml44*, *cml46*, and *cml49*) basal levels of one or more defense marker genes was elevated above wild type levels (**Figure 2.5**), with the most common theme of increase in *CBP60g*, a positive regulator of the expression of a key enzyme in SA production, *ICS1*. Consistent with this observation, *ICS1* itself is also induced, suggesting SA-dependent signaling may be activated in these lines. Further, these mutants generally showed increased induction of these two genes due to flg22 stimulation at 30 mins and also to a lesser extent at 60 mins.

Again, as with touch responses, a notable exception here is *cml24*, which showed wild type levels of defense genes prior to flg22 treatment but suppressed induction after treatment with the elicitor (**Figure 2.5**). These molecular responses correlated well with subsequent compromised defense abilities in *cml24* mutants. CML24 has been previously linked to both touch and defense responses, with loss of function mutants showing disrupted thigmotropism and root waving (Wang *et al.*, 2011; Zha *et al.*, 2016) and impaired hypersensitivity and MAMP-induced NO production (Ma *et al.*, 2008), consistent with the disrupted defense responses seen in my assays. My analyses suggest that CML24 may be unique among the members of my touch-induced CAM and CML network in being integral to both touch-induction and MAMP-induction of defense genes such as

CPB60g. Most other members of the touch-network appear more involved in repressing the MAMP-induced response system triggering these defense responses, with little effect on the touch regulation of these defense genes. CML24 is emerging as a major hub in biotic and abiotic signaling systems, e.g., playing roles in hormone and circadian responses (e.g., (La Verde *et al.*, 2018; Martí Ruiz *et al.*, 2018) (see **Chapter 1**). Taken together with my observations, these reports indicate that CML24 could be a major integration point across much of stress and developmental signaling.

My analyses also show that *CML16*, which is part of the touch-responsive network and found to be upregulated after 30 mins of treatment with *Spodoptera littoralis* oral secretions (Vadassery *et al.*, 2012), tentatively suggesting a role in defense, exhibited nearly wild type physiological responses to touch and pathogen treatments. Although expression of touch-response marker genes was significantly lower after touch treatment and expression of some pathogen-response marker genes was significantly higher than Col-0 after flg22 treatment (**Figures 2.2** and **2.5**), these patterns did not lead to deviation from wild type physiological pathogen- or touch-responses (**Figures 2.3** and **2.6**). It is possible that the roles(s) of CML16 are being masked by functional redundancy with some other CML, although its position in the genetic network shown in **Figure 2.1** does not highlight it as an obvious outlier.

The other clear feature from the analyses of molecular responses to flg22 induction of "touch-related" CaM and CML mutants is that, although basal levels of *MPK6* are wild type (except for a small induction in *cml27*), after flg22 addition, there is a general increase in the expression of this gene, which is especially obvious at 60 mins. MPK6 is an important defense regulator and so these results would suggest that the role of many of the touch-related CaMs and CMLs is normally to repress this gene, perhaps to favor mechanical signaling. *MPK3* and *MPK6*

are closely related in defense signaling (Nühse *et al.*, 2000; Takahashi *et al.*, 2007) but *MPK3* shows slightly different kinetics in my experiments, with transient induction in some but not all mutants but then widespread repression at 60 mins of flg22 treatment, again broadly consistent with a model where the touch-network CaM/CMLs normally favor touch responses by regulating the MPK-related defense pathway.

Touch stimulation, on the other hand, is known to induce MPK6 biochemical activity but not through gene induction (Ichimura *et al.*, 2000; Colcombet and Hirt, 2008) and *MPK6* does not show-up in the touch-responsive transcriptomes (Kimbrough *et al.*, 2004; Lee *et al.*, 2005) (**Supplementary Table S2.1** and **S2.2**). Indeed, my data suggests *MPK6* is normally suppressed in response to touch. However, in the *CAM*/*CML* mutant backgrounds, this repression is converted to induction. Additionally, *MPK3* has been reported to show transcriptional induction upon touch stimulation (Mizoguchi *et al.*, 1996), which is confirmed in my wild type response data. However, in contrast to *MPK6*, *MPK3* shows mostly normal touch induction at 30 mins in the mutants (with a small but significant over-induction in *cam2*, *cml5*, *cml9* and *cml16*) but then suppression of the normal induction seen at 60 mins in all but the *cam2* mutants. In these mutants flg22 induction of *MPK3* is also repressed at 30 mins, suggesting an inhibition, or delay in initiating the pathogen response system. Taken together, these results for *MPK3* and *MPK6* suggest that the touch-responsive CaM/CML network may be directly involved in regulating the level of these MAP kinases, providing a potential mechanism to balance their activities and so the downstream touch vs defense response.

In summary, the bioinformatics analysis of the 11 touch-inducible *CAMs* and *CMLs* from Lee *et al.* (2005), and *CAM7*, placed each of them within a pathogen-responsive network (**Figure 2.4**). After analyzing the molecular and physiological responses of two alleles for each of the single

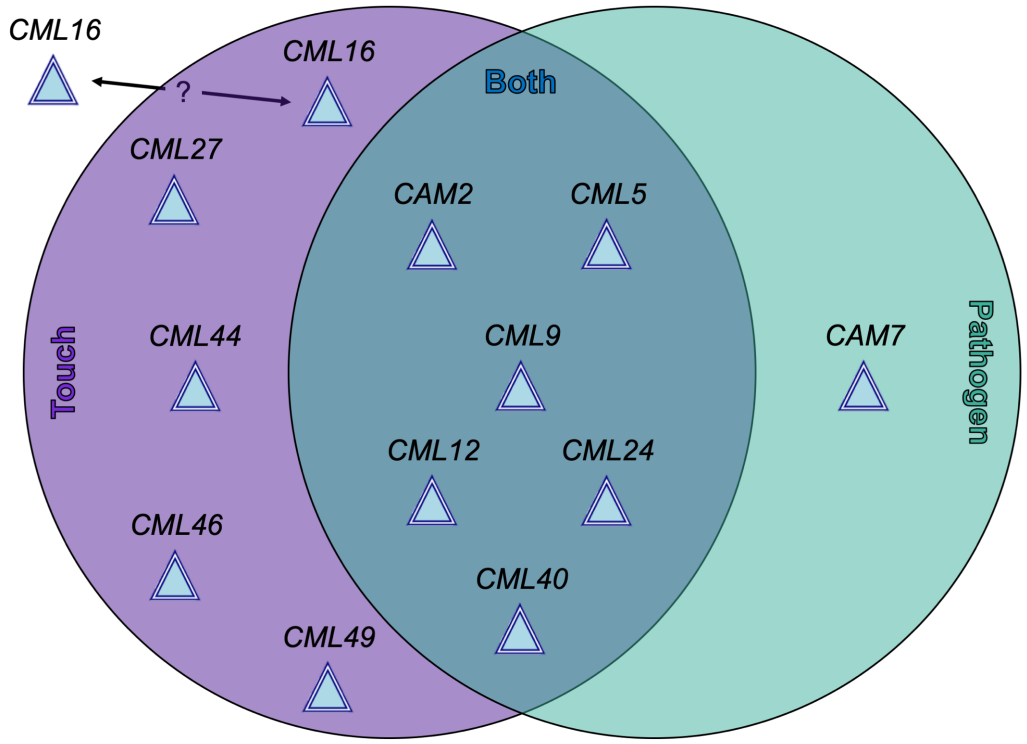

Figure 2.7 *CAM/CML* genes are touch-responsive, pathogen-responsive, or both.
Bioinformatic network analysis of the 11 touch-inducible *CAMs* and *CMLs* from Lee *et al.* (2005), and *CAM7*, placed each gene within a pathogen-responsive network (**Figure 2.4**). Although the molecular analysis of mutants in these genes presented evidence of alterations in touch- and pathogen-responsiveness, the ultimate outputs – thigmomorphogenesis and pathogenesis – revealed that not all of the genes should be considered to be involved both sets of responses. The molecular and physiological analyses indicate that *CAM7* is involved in the pathogen-response; *CML27*, *CML44*, *CML46*, and *CML49* are involved in touch-responses; and *CAM2*, *CML5*, *CML9*, *CML12*, *CML24*, and *CML40* are involved in the responses to both stimuli. These results also indicate that *CML16* might be involved in touch-responses or may not fit into any of these categories.

mutants in each of these genes to touch and pathogen stimuli, the involvement of every gene, in both responses, was not clearly discernible. However, the effects of the loss of a single regulatory element (i.e. an individual *CAM* or *CML*) can be masked by a robust compensatory network, unless the lost element is a critical component, such as a hub for several inputs (Albert, 2005). Thus, although each of the single mutants do exhibit clear alterations in molecular responses to these stimuli, their effects on whole plant physiology appear more cryptic. **Figure 2.7** provides a summary of these findings. Importantly, mutants in *CAM2*, *CML5*, *CML9*, *CML12*, *CML24*, and *CML40* exhibit distinct molecular and physiological responses to both touch an pathogen stimuli, and, therefore, these genes are classified as participating in the responses to both.

MATERIALS AND METHODS

Plant Material and Growth Conditions

The lines listed in **Supplementary Table S2.1** were acquired from the *Arabidopsis* Biological Resource Center at Ohio State University. Seeds were imbibed with sterile H_2O (20 mins), sterilized with 70% (v/v) ethanol (1 min), 20% (v/v) bleach (2 mins), and washed three times with sterile H_2O. Sterile seeds were sown onto Petri plates containing ½-strength Linsmaier and Skoog (LS) Modified Basal Medium (PhytoTechnology Laboratories), 1.0% (w/v) Phytagel (Sigma Life Science) and 1.0% (w/v) sucrose (growth medium, hereafter). After the plants were grown for 21 days in 16 hours light/8 hours dark (long-day) photoperiod under 100 μE m^{-2} sec^{-1} at 22˚C in a plant-growth chamber, the location of each insertion was verified by PCR amplification of gene-specific and T-DNA-specific primers (**Supplementary Table S2.3**). Neither allele of any mutant showed obvious gross alteration of vegetative development when grown at 22˚C (8, 12, or 24-hour photoperiod), although some mutants grew more slowly, as documented in the results section.

Physiological Response to Pathogen and Touch Stimuli

Bacterial Growth

Pseudomonas syringae pv tomato DC3000 (*Pto* DC3000), resistant to rifampicin (Rif) (Debener *et al.*, 1991; Grant *et al.*, 1995) and virulent to Col-0, was stored as a glycerol stock at -80˚C. Liquid shake cultures (LB with Rif) were prepared 48 h before inoculation and cultivated at 28°C in a shaker-incubator at 250 rpm. Inoculum was prepared by harvesting cells from shake culture by centrifugation (5000 rpm for 10 min), resuspending cells, washing the pellets two times in sterile H_2O and resuspending in sterile H_2O to an OD_{595nm} = 0.4 (~3.2 x 10^8 CFU/mL of bacteria). Silwet L-77 surfactant (Lehle Seeds) was added to the inoculum at a concentration of 0.025% (v/v)

to ensure uniform infiltration through stomatal apertures (Zidack *et al.*, 1992; Clough and Bent, 1998; Ishiga *et al.*, 2011).

Pathogenesis

Pathogenesis assays (0, 1, and 3 days) were performed essentially as in Ishiga *et al*. (2011). Fourteen-day-old seedlings were grown in 12-well plates containing growth medium and grown in 16 hours light/8 hours dark under 100 µE m^{-2} sec^{-1} at 22˚C. Each plate contained 4 technical repetitions of three genotypes: Col-0 and two mutants. Seedlings were flooded with 1 mL of *Pto* DC3000 and incubated for 3 mins at RT and the medium decanted. At 0 (immediate), 1, and 3 days post-infection (DPI), seedlings were harvested, treated with 1 mL of 5.0% (v/v) H_2O_2 for 5 mins to remove external bacteria and washed with 1 mL of sterile H_2O three times. Tissue was homogenized (Spex SamplePrep MiniG 1600) for 5 mins at 1500 strokes/min and number of colony-forming units were determined by serial dilutions on LB agar plates containing 50 µg/mL Rif. 0 DPI seedlings yielded no bacterial growth, indicating the efficacy of the H_2O_2 surface-sterilization. One-way ANOVA analyses were performed to compare the differences between the means of bacterial growth in Col-0 and those in the mutant plants, at 1- and 3-DPI. For these experiments, Tukey's Test for multiple comparisons was used and the results were considered significant if the p-value was < 0.05.

Automated Botanical Contact Device

Seeds from each plant line were imbibed for 20 min in sterile H_2O and sown into a single hole cut into the center of a black acrylic square (75 mm L x 75 mm W x 4.5 mm H) resting on #1801 pots containing Fafard Germination Mix (Sun Gro Horticulture). The squares were labeled with QR

codes encoding the genotype and position. The pots were randomized in pairs (one mechanically stimulated row next to one unstimulated row) and grown for 21 days in the Automated Botanical Contact Device (ABCD) under normal growth conditions, before starting touch simulation (see **Appendix I** for technical description of the ABCD).

On day 20 after germination, rosettes were imaged from above by an array of Raspberry Pi Camera Modules (picamera, Adafruit). With each camera monitoring 9 seedlings in a 3x3 arrangement. Touch stimulation by 1 cm fingers cut into acrylic sheets began at 21 days after germination. Images were uploaded to CyVerse (https://de.cyverse.org) and analyzed by the phytoMorph Image Phenomics Tool Kit module Overhead Plant Tracker.

Multiple *t*-tests were performed to compare the mean of each time point in Col-0 to the mean of each timepoint in the mutant plants, in untouched and touched samples. The results were considered significant if the p-value was < 0.05. For those timepoints where the difference between the means of untouched and/or touched Col-0 and mutant plant growth percentage were significant, the difference between mean untouched Col-0 (U_{WT}) and mean untouched mutant (U_{mutant}) and the difference between mean touched Col-0 (T_{WT}) and mean touched mutant, (T_{mutant}) at each timepoint was calculated. $(U_{WT}-U_{mutant}+T_{WT}-T_{mutant})/2$ was used to denote the divergence of mean growth of the mutants from Col-0 for both untouched and touched plants providing a measure of the "Sensitivity" to touch that also allowed for the fact that some mutants grew more slowly than wild type plants (**Supplementary Figures S2.1-2.12**). Negative "Sensitivity" values indicate mutants that are less sensitive to touch than Col-0. Positive "Sensitivity" values indicate mutants that are more sensitive.

Molecular Response to Pathogen and Touch Stimuli

Plant Growth

Seeds from each plant line were planted in 12-well plates containing growth medium without Phytagel (liquid growth medium) and grown under normal growth conditions, essentially as in Danna *et al*. (2011). Two plates were made for each genotype: one for the control and one for treatment. At least 4 technical repetitions, per treatment, per genotype, were performed for 3 independent biological replicates. On day 8 of growth, an additional 1 mL of growth medium was added to the wells to replenish the volume taken-up by the plants (Danna *et al.*, 2011).

MAMP and Touch Treatment for Gene Expression Analysis

To assay the molecular response to flg22 elicitation, ten-day-old seedlings of each genotype were treated with 1 μM flg22 suspended in 20 μL of liquid growth medium. The flg22 solution was slowly, gently dispensed on the side of each well of the 12-well plates, to avoid eliciting a mechanical response. For the control, ½ LS medium (without flg22) was used. To assay the molecular response to touch, a 100g aluminum rod, machined to fit into a single well of the 12-well plates, was rested onto the 10-day-old seedlings for 3s. For both treatments, samples were harvested at 0-, 30-, and 60-mins after treatment, snap-frozen in N_2(l) and stored at -80º C until RNA isolation.

Tissue Extraction, RNA Isolation and Reverse-Transcription qPCR

The plant samples were homogenized (Spex SamplePrep MiniG 1600) in RLT buffer containing ß-mercaptoethanol, using three or four 2.4 mm tungsten beads and total RNA isolated using the

RNeasy kit (Qiagen) according to the manufacturer's instructions. Genomic DNA was removed using Turbo DNAse treatment (Invitrogen) according to the manufacturer's instructions.

Quantitative PCR was performed in 96-well optical PCR plates (ABgene, Portsmouth, NH, USA), with a 7500 Real Time PCR System (Applied Biosystems, Waltham, MA, USA) using the Luna One-Step qPCR Master Mix (New England Biolabs, Ipswitch, MA, USA), with the following parameters: 1 cycle of 10 mins at 95˚C; 40 cycles of 15 s at 95˚C, 15 s at 58˚C, and 15 s at 65˚C; and 1 cycle of dissociation from 58-95˚C with 1˚C increments. Relative expression was normalized to *UBQ10* expression in untreated Col-0 samples and quantified using the $2^{-\Delta\Delta Ct}$ method (Livak and Schmittgen, 2001; Choi and Roberts, 2007; Schmittgen and Livak, 2008). Primers specific to *SR1*, *CBP60g*, *ICS1*, *MPK3*, *MPK6*, *TCH1*, *TCH2*, *TCH3*, and *TCH4* are shown in **Supplementary Table S2.4**).

Data was analyzed using Prism Statistical Software V8.0 (GraphPad Software, La Jolla, CA, USA) using two-way ANOVA and Dunnett's Test for multiple comparisons with a significance threshold of p-value < 0.05.

LITERATURE CITED

Albert, R. (2005) Scale-free networks in cell biology. *J. Cell Sci.*, **118**, 4947 LP – 4957.

Asai, T., Tena, G., Plotnikova, J., Willmann, M.R., Chiu, W.-L., Gomez-Gomez, L., Boller, T., Ausubel, F.M. and Sheen, J. (2002) MAP kinase signalling cascade in Arabidopsis innate immunity. *Nature*, **415**, 977–983.

Bender, K.W., Dobney, S., Ogunrinde, A., et al. (2014) The calmodulin-like protein CML43 functions as a salicylic-acid-inducible root-specific Ca(2+) sensor in Arabidopsis. *Biochem. J.*, **457**, 127–36.

Benikhlef, L., L'Haridon, F., Abou-Mansour, E., Serrano, M., Binda, M., Costa, A., Lehmann, S. and Métraux, J.-P. (2013) Perception of soft mechanical stress in Arabidopsis leaves activates disease resistance. *BMC Plant Biol.*, **13**, 133.

Berens, M.L., Wolinska, K.W., Spaepen, S., et al. (2019) Balancing trade-offs between biotic and abiotic stress responses through leaf age-dependent variation in stress hormone cross-talk. *Proc. Natl. Acad. Sci.*, **116**, 2364 LP – 2373.

Braam, J. and Davis, R.W. (1990) Rain-, wind-, and touch-induced expression of calmodulin and calmodulin-related genes in Arabidopsis. *Cell*, **60**, 357–364.

Brandizi, M., Singh, A., Rawlings, C. and Hassani-Pak, K. (2018) Towards FAIRer Biological Knowledge Networks Using a Hybrid Linked Data and Graph Database Approach. *J. Integr. Bioinform.*, **15**.

Chehab, E.W., Eich, E. and Braam, J. (2009) Thigmomorphogenesis: a complex plant response to mechano-stimulation. *J. Exp. Bot.*, **60**, 43–56.

Chehab, E.W., Yao, C., Henderson, Z., Kim, S. and Braam, J. (2012) Arabidopsis touch-induced morphogenesis is jasmonate mediated and protects against pests. *Curr. Biol.*, **22**, 701–6.

Choi, W.-G. and Roberts, D.M. (2007) Arabidopsis NIP2;1, a major intrinsic protein transporter of lactic acid induced by anoxic stress. *J. Biol. Chem.*, **282**, 24209–18.

Clough, S.J. and Bent, A.F. (1998) Floral dip: a simplified method forAgrobacterium-mediated transformation ofArabidopsis thaliana. *Plant J.*, **16**, 735–743.

Colcombet, J. and Hirt, H. (2008) Arabidopsis MAPKs: a complex signalling network involved in multiple biological processes. *Biochem. J.*, **413**, 217–26.

Danna, C.H., Millet, Y.A., Koller, T., Han, S.-W., Bent, A.F., Ronald, P.C. and Ausubel, F.M. (2011) The Arabidopsis flagellin receptor FLS2 mediates the perception of Xanthomonas Ax21 secreted peptides. *Proc. Natl. Acad. Sci.*, **108**, 9286–91.

Debener, T., Lehnackers, H., Arnold, M. and Dangl, J.L. (1991) Identification and molecular mapping of a single Arabidopsis thaliana locus determining resistance to a phytopathogenic Pseudomonas syringae isolate. *Plant J.*, **1**, 289–302.

Dodd, A.N., Kudla, J. and Sanders, D. (2010) The Language of Calcium Signaling. *Annu. Rev. Plant Biol.*, **61**, 593–620.

Du, L., Ali, G.S., Simons, K.A., Hou, J., Yang, T., Reddy, A.S.N. and Poovaiah, B.W. (2009) Ca2+/calmodulin regulates salicylic-acid-mediated plant immunity. *Nature*, **457**, 1154–1158.

Foyer, C.H., Rasool, B., Davey, J.W. and Hancock, R.D. (2016) Cross-tolerance to biotic and abiotic stresses in plants: a focus on resistance to aphid infestation. *J. Exp. Bot.*, **67**, 2025–2037.

Grant, M., Brown, I., Adams, S., Knight, M., Ainslie, A. and Mansfield, J. (2000) The RPM1 plant disease resistance gene facilitates a rapid and sustained increase in cytosolic calcium that is necessary for the oxidative burst and hypersensitive cell death. *Plant J.*, **23**, 441–450.

Grant, M.R., Godiard, L., Straube, E., Ashfield, T., Lewald, J., Sattler, A., Innes, R.W. and Dangl, J.L. (1995) Structure of the Arabidopsis RPM1 Gene Enabling Dual Specificity Disease Resistance. *Science (80-.).*, **269**, 843–846.

Gus-Mayer, S., Naton, B., Hahlbrock, K. and Schmelzer, E. (1998) Local mechanical stimulation induces components of the pathogen defense response in parsley. *Proc. Natl. Acad. Sci.*, **95**, 8398–403.

Hassani-Pak, K., Castellote, M., Esch, M., Hindle, M., Lysenko, A., Taubert, J. and Rawlings, C. (2016) Developing integrated crop knowledge networks to advance candidate gene discovery. *Appl. Transl. Genomics*, **11**, 18–26.

Huot, B., Yao, J., Montgomery, B.L. and He, S.Y. (2014) Growth-defense tradeoffs in plants: a balancing act to optimize fitness. *Mol. Plant*, **7**, 1267–1287.

Ichimura, K., Mizoguchi, T., Yoshida, R., Yuasa, T. and Shinozaki, K. (2000) Various abiotic stresses rapidly activate Arabidopsis MAP kinases ATMPK4 and ATMPK6. *Plant J.*, **24**, 655–665.

Ishiga, Y., Ishiga, T., Uppalapati, S.R. and Mysore, K.S. (2011) Arabidopsis seedling flood-inoculation technique: a rapid and reliable assay for studying plant-bacterial interactions. *Plant Methods*, **7**, 32.

Karasov, T.L., Chae, E., Herman, J.J. and Bergelson, J. (2017) Mechanisms to Mitigate the Trade-Off between Growth and Defense. *Plant Cell*, **29**, 666 LP – 680.

Kimbrough, J.M., Salinas-Mondragon, R., Boss, W.F., Brown, C.S. and Sederoff, H.W. (2004) The fast and transient transcriptional network of gravity and mechanical stimulation in the Arabidopsis root apex. *Plant Physiol.*, **136**, 2790–805.

Knight, M.R., Campbell, A.K., Smith, S.M. and Trewavas, A.J. (1991) Transgenic plant aequorin reports the effects of touch and cold-shock and elicitors on cytoplasmic calcium. *Nature*, **352**, 524–526.

Kumar, S., Mazumder, M., Gupta, N., Chattopadhyay, S. and Gourinath, S. (2016) Crystal structure of Arabidopsis thaliana calmodulin7 and insight into its mode of DNA binding. *FEBS Lett.*, **590**, 3029–3039.

Kwaaitaal, M., Huisman, R., Maintz, J., Reinstädler, A. and Panstruga, R. (2011) Ionotropic glutamate receptor (iGluR)-like channels mediate MAMP-induced calcium influx in *Arabidopsis thaliana*. *Biochem. J.*, **440**, 355–373.

Lange, M.J.P. and Lange, T. (2015) Touch-induced changes in Arabidopsis morphology dependent on gibberellin breakdown. *Nat. Plants*, **1**, 14025.

Leba, L.-J., Cheval, C., Ortiz-Martín, I., Ranty, B., Beuzón, C.R., Galaud, J.-P. and Aldon, D. (2012) CML9, an Arabidopsis calmodulin-like protein, contributes to plant innate immunity through a flagellin-dependent signalling pathway. *Plant J.*, **71**, 976–89.

Lecourieux, D., Ranjeva, R. and Pugin, A. (2006) Calcium in plant defence-signalling pathways. *New Phytol.*, **171**, 249–269.

Lee, D., Polisensky, D.H. and Braam, J. (2005) Genome-wide identification of touch- and darkness-regulated Arabidopsis genes: a focus on calmodulin-like and XTH genes. *New Phytol.*, **165**, 429–44.

Legué, V., Blancaflor, E., Wymer, C., Perbal, G., Fantin, D. and Gilroy, S. (1997) Cytoplasmic free Ca2+ in Arabidopsis roots changes in response to touch but not gravity. *Plant Physiol.*, **114**, 789–800.

Lenzoni, G., Liu, J. and Knight, M.R. (2018) Predicting plant immunity gene expression by identifying the decoding mechanism of calcium signatures. *New Phytol.*, **217**, 1598–1609.

Livak, K.J. and Schmittgen, T.D. (2001) Analysis of Relative Gene Expression Data Using Real-Time Quantitative PCR and the 2−ΔΔCT Method. *Methods*, **25**, 402–408.

Lu, Y., Truman, W., Liu, X., Bethke, G., Zhou, M., Myers, C., Katagiri, F. and Glazebrook, J. (2018) Different modes of negative regulation of plant immunity by calmodulin-related genes. *Plant Physiol.*, pp.01209.2017.

Ma, W., Smigel, A., Tsai, Y.-C., Braam, J. and Berkowitz, G.A. (2008) Innate immunity signaling: cytosolic Ca2+ elevation is linked to downstream nitric oxide generation through the action of calmodulin or a calmodulin-like proteins. *Plant Physiol.*, **148**, 818–28.

Martí Ruiz, M.C., Hubbard, K.E., Gardner, M.J., et al. (2018) Circadian oscillations of cytosolic free calcium regulate the Arabidopsis circadian clock. *Nat. Plants*, **4**, 690–698.

McAinsh, M.R. and Pittman, J.K. (2009) Shaping the calcium signature. *New Phytol.*, **181**, 275–294.

Mersmann, S., Bourdais, G., Rietz, S. and Robatzek, S. (2010) Ethylene signaling regulates accumulation of the FLS2 receptor and is required for the oxidative burst contributing to plant immunity. *Plant Physiol.*, **154**, 391–400.

Mittler, R. (2006) Abiotic stress, the field environment and stress combination. *Trends Plant Sci.*, **11**, 15–19.

Mizoguchi, T., Irie, K., Hirayama, T., Hayashida, N., Yamaguchi-Shinozaki, K., Matsumoto, K. and Shinozaki, K. (1996) A gene encoding a mitogen-activated protein kinase kinase kinase is induced simultaneously with genes for a mitogen-activated protein kinase and an S6 ribosomal protein kinase by touch, cold, and water stress in Arabidopsis thaliana. *Proc. Natl. Acad. Sci.*, **93**, 765–9.

Monshausen, G.B., Bibikova, T.N., Weisenseel, M.H. and Gilroy, S. (2009) Ca2+ regulates reactive oxygen species production and pH during mechanosensing in Arabidopsis roots. *Plant Cell*, **21**, 2341–56.

Monshausen, G.B. and Haswell, E.S. (2013) A force of nature: molecular mechanisms of mechanoperception in plants. *J. Exp. Bot.*, **64**, 4663–80.

Nakagawa, Y., Katagiri, T., Shinozaki, K., et al. (2007) Arabidopsis plasma membrane protein crucial for Ca2+ influx and touch sensing in roots. *Proc. Natl. Acad. Sci.*, **104**, 3639–44.

Nühse, T.S., Peck, S.C., Hirt, H. and Boller, T. (2000) Microbial elicitors induce activation and dual phosphorylation of the Arabidopsis thaliana MAPK 6. *J. Biol. Chem.*, **275**, 7521–6.

Pastori, G.M. and Foyer, C.H. (2002) Common Components, Networks, and Pathways of Cross-Tolerance to Stress. The Central Role of "Redox" and Abscisic Acid-Mediated Controls. *Plant Physiol.*, **129**, 460 LP – 468.

Schmittgen, T.D. and Livak, K.J. (2008) Analyzing real-time PCR data by the comparative CT method. *Nat. Protoc.*, **3**, 1101–1108.

Szklarczyk, D., Gable, A.L., Lyon, D., et al. (2019) STRING v11: protein–protein association networks with increased coverage, supporting functional discovery in genome-wide experimental datasets. *Nucleic Acids Res.*, **47**, D607–D613.

Takahashi, F., Yoshida, R., Ichimura, K., Mizoguchi, T., Seo, S., Yonezawa, M., Maruyama, K., Yamaguchi-Shinozaki, K. and Shinozaki, K. (2007) The Mitogen-Activated Protein Kinase Cascade MKK3–MPK6 Is an Important Part of the Jasmonate Signal Transduction Pathway in Arabidopsis. *Plant Cell*, **19**, 805 LP – 818.

Tomas-Grau, R.H., Requena-Serra, F.J., Hael-Conrad, V., Martínez-Zamora, M.G., Guerrero-Molina, M.F. and Díaz-Ricci, J.C. (2017) Soft mechanical stimulation induces a defense response against Botrytis cinerea in strawberry. *Plant Cell Rep.*, **37**, 239–250.

Toriyama, H. and Jaffe, M.J. (1972) Migration of Calcium and Its Role in the Regulation of Seismonasty in the Motor Cell of Mimosa pudica L. *Plant Physiol.*, **49**, 72–81.

Toyota, M. and Gilroy, S. (2013) Gravitropism and mechanical signaling in plants. *Am. J. Bot.*, **100**, 111–125.

Tsuda, K., Sato, M., Glazebrook, J., Cohen, J.D. and Katagiri, F. (2008) Interplay between MAMP-triggered and SA-mediated defense responses. *Plant J.*, **53**, 763–775.

Vadassery, J., Scholz, S.S. and Mithöfer, A. (2012) Multiple calmodulin-like proteins in Arabidopsis are induced by insect-derived (Spodoptera littoralis) oral secretion. *Plant Signal. Behav.*, **7**, 1277–80.

Verde, V. La, Dominici, P., Astegno, A., Verde, V. La, Dominici, P. and Astegno, A. (2018) Towards Understanding Plant Calcium Signaling through Calmodulin-Like Proteins: A Biochemical and Structural Perspective. *Int. J. Mol. Sci.*, **19**, 1331.

Wang, Y., Wang, B., Gilroy, S., Wassim Chehab, E. and Braam, J. (2011) CML24 is Involved in Root

Mechanoresponses and Cortical Microtubule Orientation in Arabidopsis. *J. Plant Growth Regul.*, **30**, 467–479.

Wu, S., Shan, L. and He, P. (2014) Microbial signature-triggered plant defense responses and early signaling mechanisms. *Plant Sci.*, **228**, 118–26.

Xu, B., Cheval, C., Laohavisit, A., Hocking, B., Chiasson, D., Olsson, T.S.G., Shirasu, K., Faulkner, C. and Gilliham, M. (2017) A calmodulin-like protein regulates plasmodesmal closure during bacterial immune responses. *New Phytol.*, **215**, 77–84.

Yi, S.Y., Shirasu, K., Moon, J.S., Lee, S.-G. and Kwon, S.-Y. (2014) The activated SA and JA signaling pathways have an influence on flg22-triggered oxidative burst and callose deposition. B. S. Kim, ed. *PLoS One*, **9**, e88951.

Zha, G., Wang, B., Liu, J., Yan, J., Zhu, L. and Yang, X. (2016) Mechanical touch responses of Arabidopsis TCH1-3 mutant roots on inclined hard-agar surface**. *Int. Agrophysics*, **30**, 105–111.

Zheng, X.-Y., Zhou, M., Yoo, H., Pruneda-Paz, J.L., Spivey, N.W., Kay, S.A. and Dong, X. (2015) Spatial and temporal regulation of biosynthesis of the plant immune signal salicylic acid. *Proc. Natl. Acad. Sci.*, **112**, 9166–73.

Zhu, X., Robe, E., Jomat, L., Aldon, D., Mazars, C. and Galaud, J.-P. (2016) CML8, an Arabidopsis Calmodulin-Like Protein, Plays a Role in *Pseudomonas syringae* Plant Immunity. *Plant Cell Physiol.*, **58**, pcw189.

Zidack, N.K., Backman, P.A. and Shaw, J.J. (1992) Promotion of bacterial infection of leaves by an organosilicone surfactant: Implications for biological weed control. *Biol. Control*, **2**, 111–117.

SUPPLEMENTARY TABLES AND FIGURES

Supplementary Table S2.1: Genes Upregulated ≥2-Fold In Response to Touch, as Determined by Microarray (Lee *et al.*, 2005) For each gene, two T-DNA insertion alleles were ordered from ABRC (except *cml24*, for which the *cml24-4* loss of function point mutant was used).

Gene ID	Accession Number	Other ID	First Insertion	Second Insertion
CAM2	At2g41110	TCH1	SALK_066990	SALK_114166
CAM7	At3g43810	ZBF3	SALK_074336 (*cam7-1*)	SALKseq_128513
CML5	At2g43290	MSS3	SALKseq_065778	GK-061E12 (N405820)
CML9	At3g51920	-----	SALK_006380	SALK_033724
CML12	At2g41100	TCH3	SALK_090554 *(cml12-2)*	SALK_122731.26.30.x
CML16	At3g25600	-----	SALK_024662	SALK_051864
CML24	At5g37770	TCH2	SALK_054200.101	*cml24-4* (point mutant)
CML27	At1g18210	-----	SALK_075633	SALK_029003
CML40	At3g01830	-----	WiscDsLoxHs205_02C	SALK_152226
CML44	At1g21550	-----	SALK_107191	SALK_027844.37.85.x
CML46	At5g39670	CML45	SALK_127471	SALK_057550.54.95.x
CML49	At3g10300	-----	SALK_090873	SALK_035905

Supplementary Table S2.2: Genes Found to be Associated with Genes in **Table 1** by Bioinformatics Analysis, with Regard to both Pathogen and Touch Responses.

Gene ID	Accession Number	Gene ID	Accession Number	Gene ID	Accession Number
MPK11	At1g01560	SYP121	At3g11820	WRKY53	At4g23810
ERD6	At1g08930	PBP1	At3g16420	DIC2	At4g24570
SEC31A	At1g18830	------	At3g19010	------	At4g27280
CPK1	At1g18890	ZAT7	At3g46090	NHL3	At5g06320
CAM4	At1g66410	NOA1	At3g47450	------	At5g10695
MATE	At2g04050	------	At3g57450	------	At5g25440
CAM5	At2g27030	------	At3g61080	------	At5g35735
NHL13	At2g27080	SEC31B	At3g63460	------	At5g48540
SOBIR1	At2g31880	XBAT34	At4g14365	------	At5g66070
------	At2g39650	CML8	At4g14640		
------	At2g39920	APRR2	At4g18020		

Supplementary Table S2.3: Primers used for genotyping.
T-DNA-specific primers appear at the bottom.

Gene ID	Primer Sequence (5' to 3') Insert 1	Primer Sequence (5' to 3') Insert 2
CAM2	F - TTTTAACCAGCAAAAACCAGC	F - ATTCGTAGCACACGAATCGTC
	R - CTCTTCTCATGTCAACCTGGC	R - CCGATAAGCATCTTCTTGCTTC
CAM7	F - TTTCCGAAATACATGCGATAAC	F - Same as *CAM7* LP1
	R - TGTGCAGAGATTCACGATCAC	R - Same as *CAM7* RP1
CML5	F - TAGAGCTGCGAAACAAGAAGC	F - AAGACAGAGTTGCGAGTACGC
	R - TCCGTCAACGATGTTACCTTC	R - ACATGTGGAAGAAACCGTGAG
CML9	F - TGAGCGATGTTGACATCTTTG	F - Same as *CML9* LP1
	R - TTTGGTTTGGTTCGAATTTTG	R - Same as *CML9* RP1
CML12	F - TTACTTGCTCAAGCCATCCC	F - CGACAAAAGCTGATCTTCAGG
	R - AATCCGCTTCGTTCATCAAG	R - CAAGATAACAGCGCTTCGAAC
CML16	F - TGCAACTGTCTCAACCAAGTG	F - TTTCATGTGTCCACTGTCCAG
	R - TCTTCTTTCTCCATCAATGGC	R - TTCTGTTGAACCAAATCGACC
CML24	F - CAAAATAGAGAGAGCATTTGAGAAAC	F – N/A (Point mutation)
	R - TACGAATCATCACCGTCGAC	R – N/A (Point mutation)
CML27	F - TTCGTCGAGGTTGATGTAACC	F - TCGAAATTAACATTCCCATCG
	R - AACAATCACACCGCGTAAAAG	R - GCCCCTCCAACTTTTATTTTC
CML40	F - GTCAACGGAAACTTCGTCGT	F - TGGCTAATTCATTGGTTACGC
	R - ATTGCATCATGGCCCTAAAC	R - TGAGAGCCAAACACTTTTTCC
CML44	F - TTCACAGGGAAAAATCCACTG	F - AACACACAAATTCTCGTTGGG
	R - ATCTCCGTTCACATCGAACAC	R - ACGGAAGAGATTAAAGCGGAG
CML46	F - AACTTCCTCTCTTTTGCCTCG	F - CGATTTGGTTTAGAAAACAAATAAAAC
	R - AGTGATGGAGAGCTCTTGCAC	R - ATGTTTTGGAGGAGATGTTGG
CML49	F - GACCAATCTTCCTGACATTGC	F - GATAACGCCGTATCCTTCTCC
	R - TGGACTTGTTGTTGGTTCATG	R - ACATTGTGGCTTGTTTCCAAG
LBb1.3	F - ATTTTGCCGATTTCGGAAC	
GABI-KAT	F - ATAATAACGCTGCGGACATCTACATTTT	
WiscDsLox	F - AACGTCCGCAATGTGTTATTAAGTTG	

Supplementary Table S2.4: Primers used for qPCR analyses.

Gene ID	Primer Sequence (5' to 3')	Reference to Pathogen or Touch Responsiveness
UBQ10	F - CACACTCCACTTGGTCTTGCGT	-
	R - TGGTCTTTCCGGTGAGAGTCTTCA	
SR1	F - TTCCGAGGTTACAAGGGAAG	**Du et al., (2009)**
	R - CCCCCACTGACCAAATTATC	
CBP60g	F - AATAACGAGGAGGATGAGAACG	**Zheng et al., (2015)**
	R - TCAGACACGGTAAGAAACATCG	
ICS1	F - TTCCAGCAGAAGAAGCAAGG	**Zheng et al., (2015)**
	R - GATCCCGACTGCAAATTCAC	
PR1	F - ATGTGCCAAAGTGAGGTGTAA	**Asai et al., (2002)**
	R - TTCACATAATTCCCACGAGCA	
PR5	F – AGGAACAATTGCCCTACCACC	**Asai et al., (2002)**
	R - TCCTTGACCGGCGAGAGTT	
TCH1	F - ACCAGAACGGTTTCATCTC	**Braam and Davis, (1990)**
	R - GATCTGACCATCACCATCAA	
TCH2	F - AGAAGATGATGAGTAATGGTGGTG	**Braam and Davis, (1990)**
	R - CGCCGTCACTAAAATTAATCTGC	
TCH3	F - CATAGCGGTCGGGGTTG	**Braam and Davis, (1990)**
	R - TGTCAGACCCTATTGGCATAAAG	
TCH4	F - GCAGAGGAACTACATGATCTATAA	**Braam and Davis, (1990)**
	R - TCTTGTTCCTCTCTCAACTC	
MPK3	F - TGACGTTTGACCCCAACAGA	**Asai et al., (2002)**
	R - CTGTTCCTCATCCAGAGGCTG	
MPK6	F - CCGACAGTGCATCCTTTAGCT	**Asai et al., (2002)**
	R - TGGGCCAATGCGTCTAAAAC	

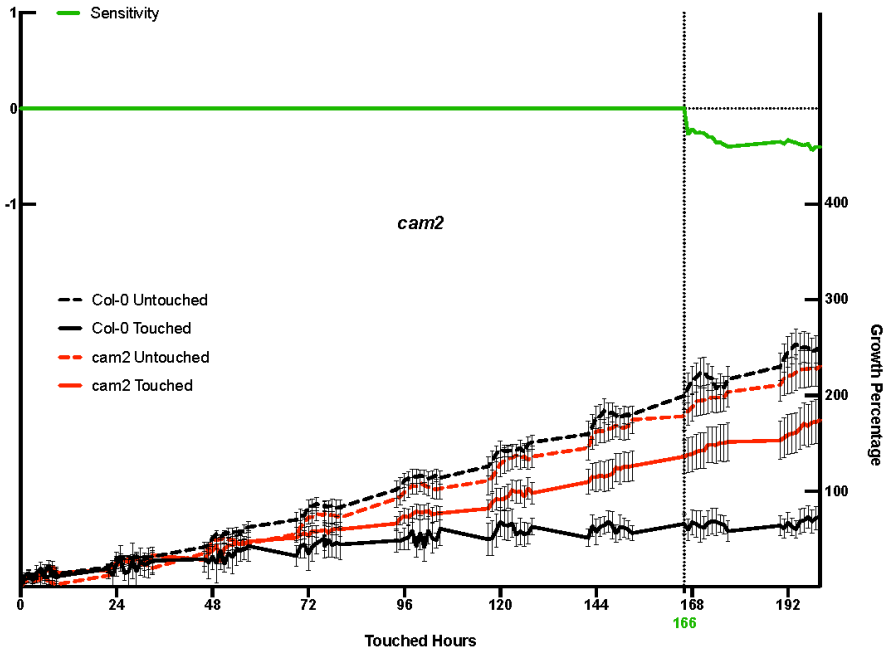

Supplementary Figure S2.1 *cam2* is significantly less sensitive to repeated touch stimulus than Col-0. Plants were touched every 5 minutes for >8 days and imaged every hour. Percent growth was extracted from images at each time point ($\Delta A/A_0$). Sensitivity (green trace) is a measure of divergence of the mean growth at each time point from Col-0 for both untouched and touched measures, denoting sensitivity to some stress or force (e.g. touch). *cam2* plants exhibit no significant difference in growth of untouched plants, but are less sensitive to touch stimulus, exhibiting decreased growth inhibition due to touch, relative to Col-0.

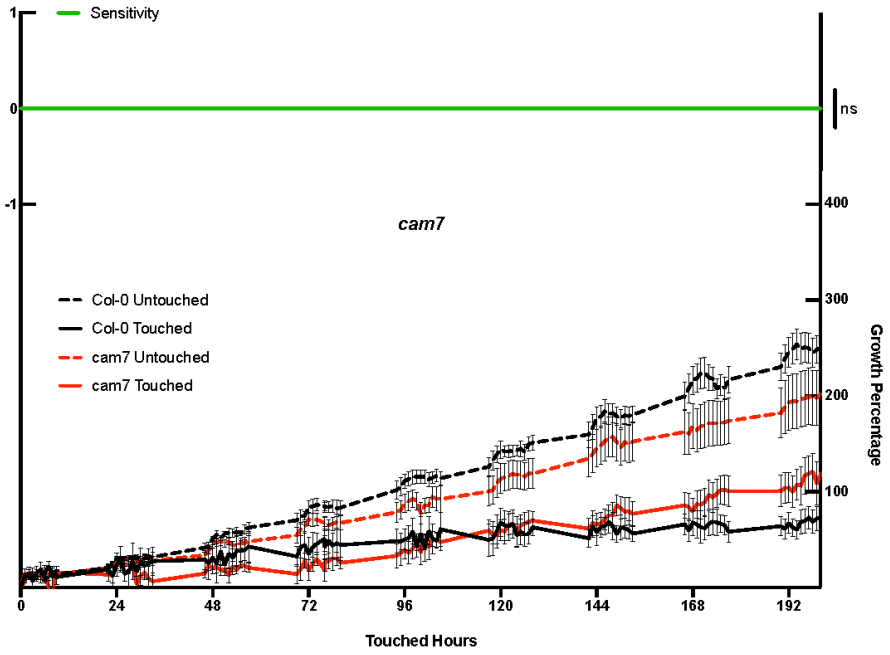

Supplementary Figure S2.2 *cam7* is not significantly less sensitive to repeated touch stimulus than Col-0. Plants were touched every 5 minutes for >8 days and imaged every hour. Percent growth was extracted from images at each time point ($\Delta A/A_0$). Sensitivity (green trace) is a measure of divergence of the mean growth at each time point from Col-0 for both untouched and touched measures, denoting sensitivity to some stress or force (e.g. touch). There is no significant difference between the mean untouched or touched values, compared to Col-0.

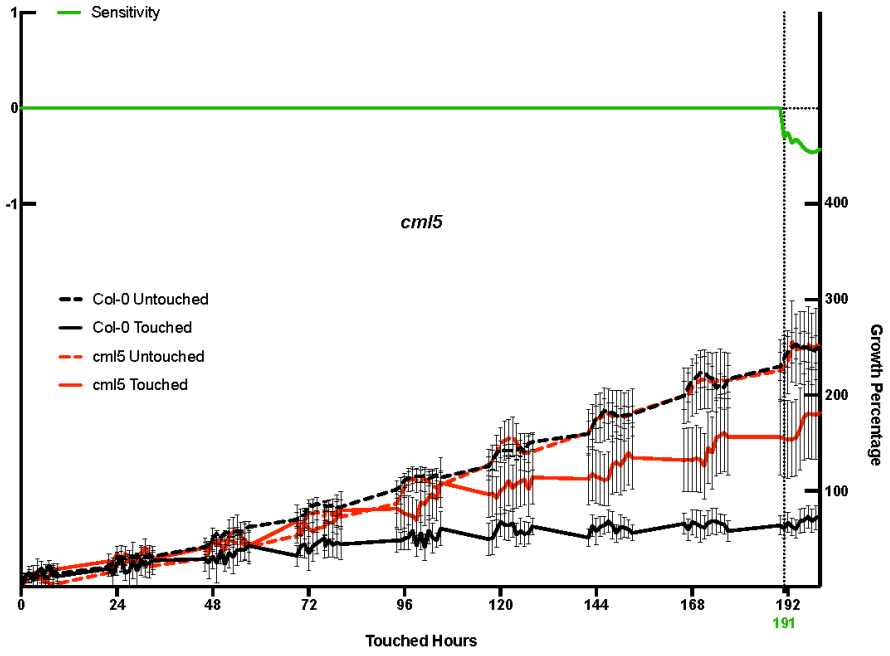

Supplementary Figure S2.3 *cml5* is significantly less sensitive to repeated touch stimulus than Col-0. Plants were touched every 5 minutes for >8 days and imaged every hour. Percent growth was extracted from images at each time point ($\Delta A/A_0$). Sensitivity (green trace) is a measure of divergence of the mean growth at each time point from Col-0 for both untouched and touched measures, denoting sensitivity to some stress or force (e.g. touch). *cml5* plants exhibit no significant difference in growth of untouched plants, but are less sensitive to touch stimulus, exhibiting decreased growth inhibition due to touch, relative to Col-0.

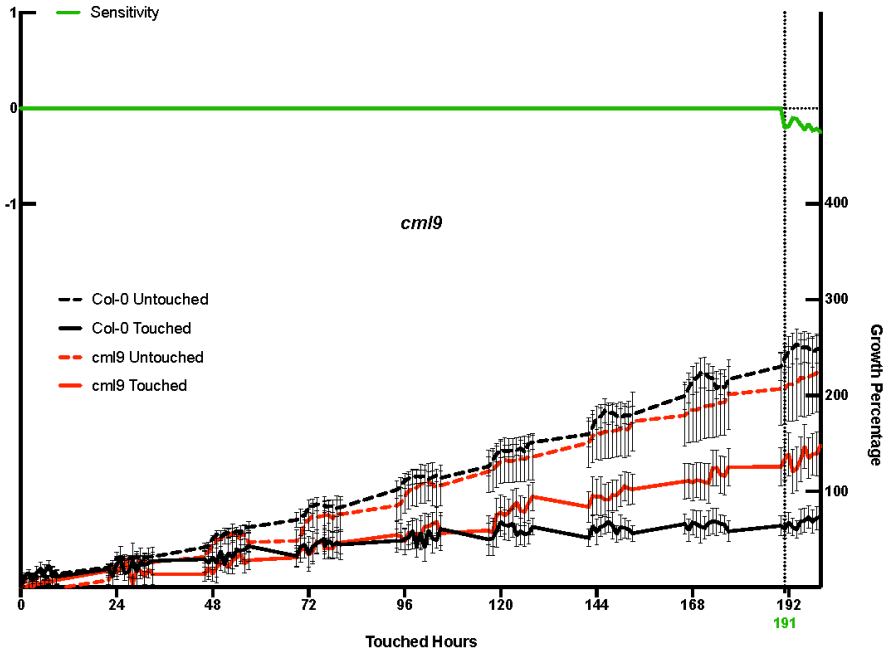

Supplementary Figure S2.4 *cml9* issignificantly less sensitive to repeated touch stimulus than Col-0. Plants were touched every 5 minutes for >8 days and imaged every hour. Percent growth was extracted from images at each time point ($\Delta A/A_0$). Sensitivity (green trace) is a measure of divergence of the mean growth at each time point from Col-0 for both untouched and touched measures, denoting sensitivity to some stress or force (e.g. touch). *cml9* plants exhibit no significant difference in growth of untouched plants, but are less sensitive to touch stimulus, exhibiting decreased growth inhibition due to touch, relative to Col-0.

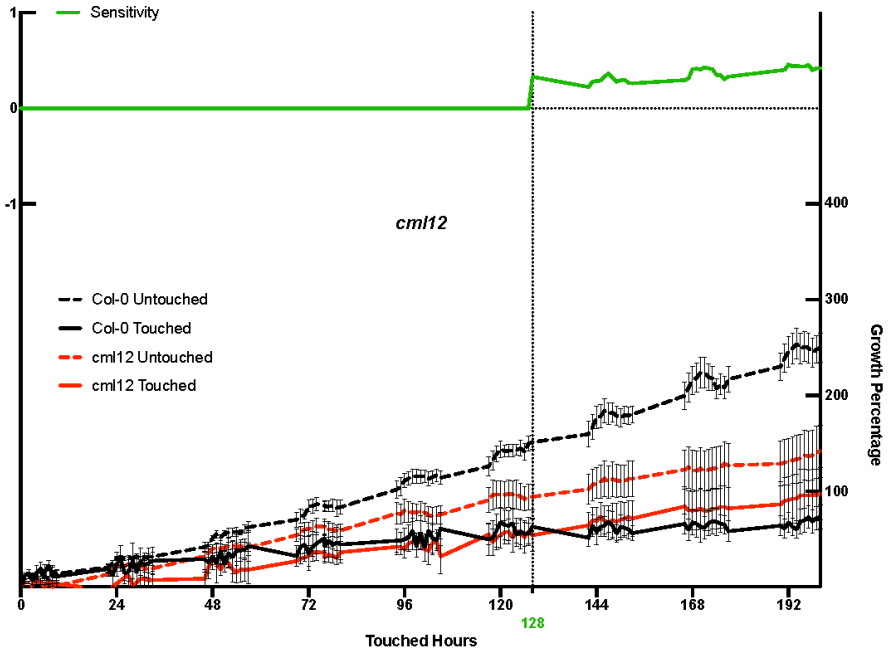

Supplementary Figure S2.5 *cml12* exhibits significantly altered growth phenotypes, in untouched and touched plants, relative to Col-0. Plants were touched every 5 minutes for >8 days and imaged every hour. Percent growth was extracted from images at each time point ($\Delta A/A_0$). Sensitivity (green trace) is a measure of divergence of the mean growth at each time point from Col-0 for both untouched and touched measures, denoting sensitivity to some stress or force (e.g. touch). *cml12* plants exhibit reduced growth in untouched plants and decreased growth inhibition due to touch, relative to Col-0.

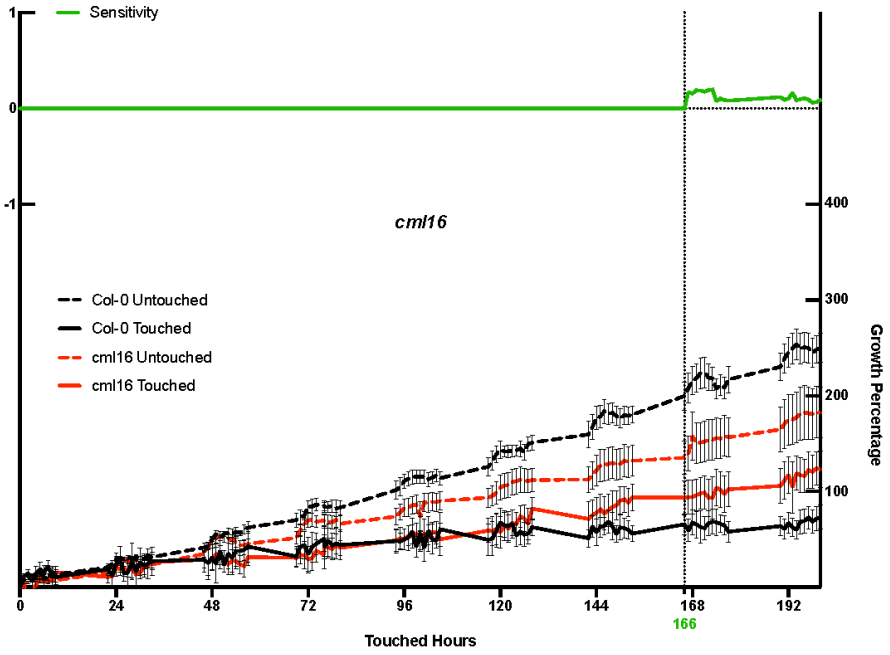

Supplementary Figure S2.6 *cml16* exhibits significantly altered growth phenotypes, in untouched and touched plants, relative to Col-0. Plants were touched every 5 minutes for >8 days and imaged every hour. Percent growth was extracted from images at each time point ($\Delta A/A_0$). Sensitivity (green trace) is a measure of divergence of the mean growth at each time point from Col-0 for both untouched and touched measures, denoting sensitivity to some stress or force (e.g. touch). *cml16* plants exhibit reduced growth in untouched plants and decreased growth inhibition due to touch, relative to Col-0.

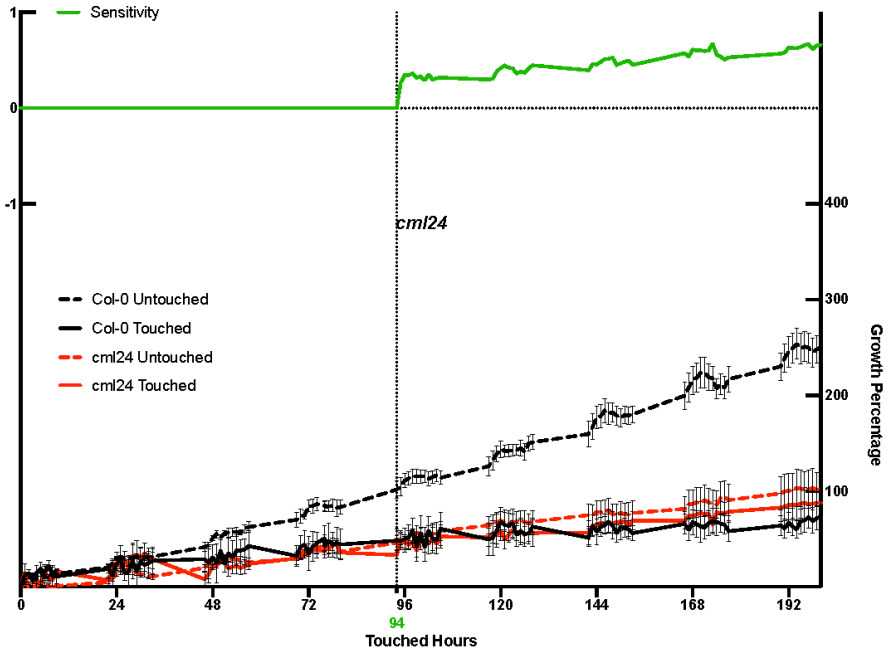

Supplementary Figure S2.7 *cml24* exhibits significantly altered growth phenotypes, in untouched and touched plants, relative to Col-0. Plants were touched every 5 minutes for >8 days and imaged every hour. Percent growth was extracted from images at each time point ($\Delta A/A_0$). Sensitivity (green trace) is a measure of divergence of the mean growth at each time point from Col-0 for both untouched and touched measures, denoting sensitivity to some stress or force (e.g. touch). *cml24* plants exhibit reduced growth in untouched plants and decreased growth inhibition due to touch, relative to Col-0.

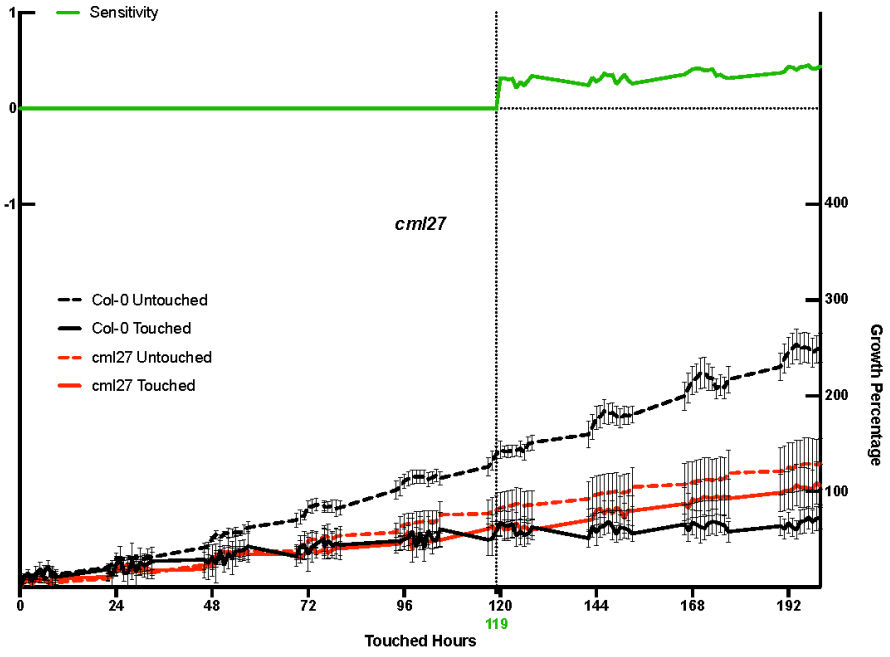

Supplementary Figure S2.8 *cml27* exhibits significantly altered growth phenotypes, in untouched and touched plants, relative to Col-0. Plants were touched every 5 minutes for >8 days and imaged every hour. Percent growth was extracted from images at each time point ($\Delta A/A_0$). Sensitivity (green trace) is a measure of divergence of the mean growth at each time point from Col-0 for both untouched and touched measures, denoting sensitivity to some stress or force (e.g. touch). *cml27* plants exhibit reduced growth in untouched plants and decreased growth inhibition due to touch, relative to Col-0.

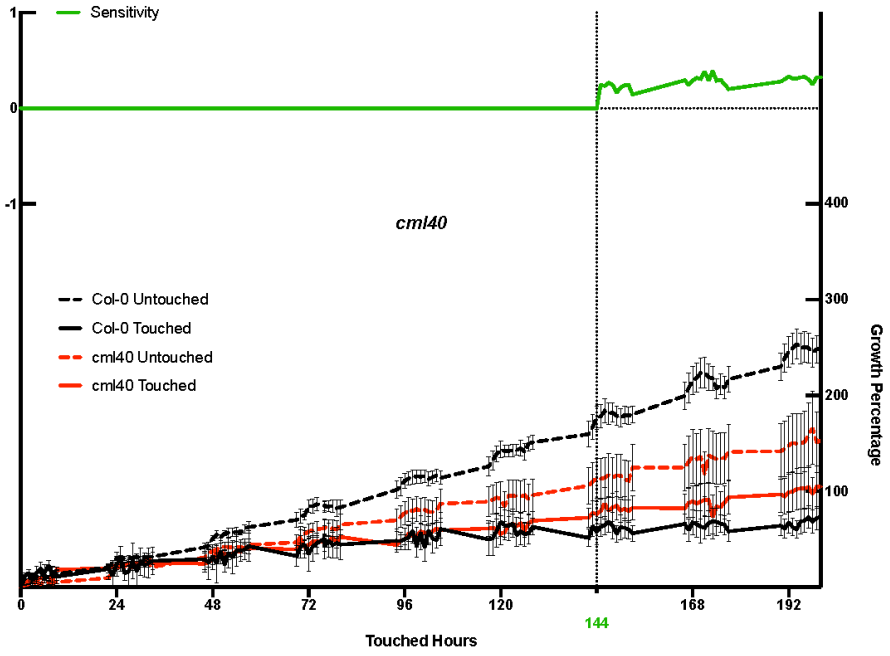

Supplementary Figure S2.9 *cml40* exhibits significantly altered growth phenotypes, in untouched and touched plants, relative to Col-0. Plants were touched every 5 minutes for >8 days and imaged every hour. Percent growth was extracted from images at each time point ($\Delta A/A_0$). Sensitivity (green trace) is a measure of divergence of the mean growth at each time point from Col-0 for both untouched and touched measures, denoting sensitivity to some stress or force (e.g. touch). *cml40* plants exhibit reduced growth in untouched plants and decreased growth inhibition due to touch, relative to Col-0.

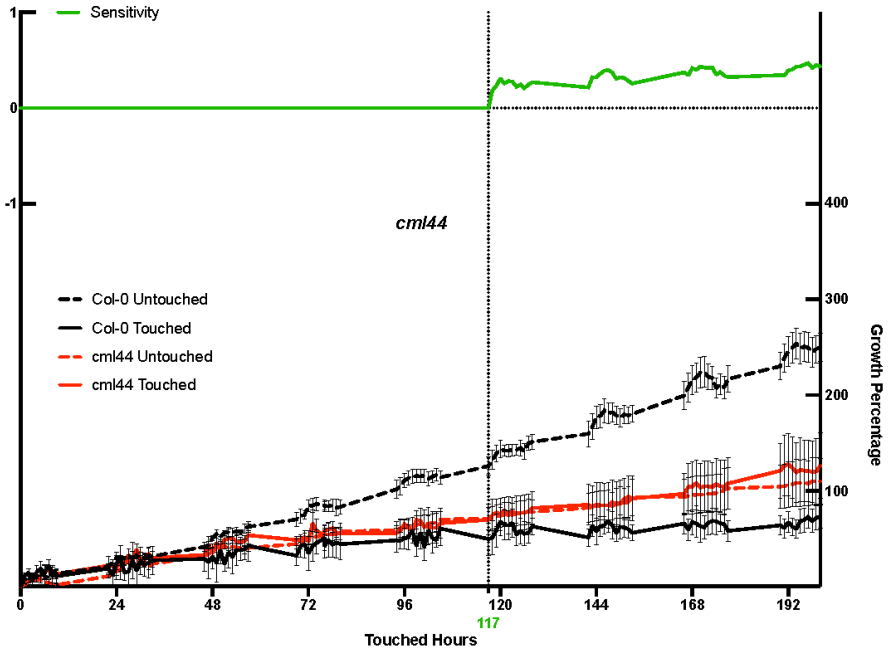

Supplementary Figure S2.10 *cml44* exhibits significantly altered growth phenotypes, in untouched and touched plants, relative to Col-0. Plants were touched every 5 minutes for >8 days and imaged every hour. Percent growth was extracted from images at each time point ($\Delta A/A_0$). Sensitivity (green trace) is a measure of divergence of the mean growth at each time point from Col-0 for both untouched and touched measures, denoting sensitivity to some stress or force (e.g. touch). *cml44* plants exhibit reduced growth in untouched plants and decreased growth inhibition due to touch, relative to Col-0.

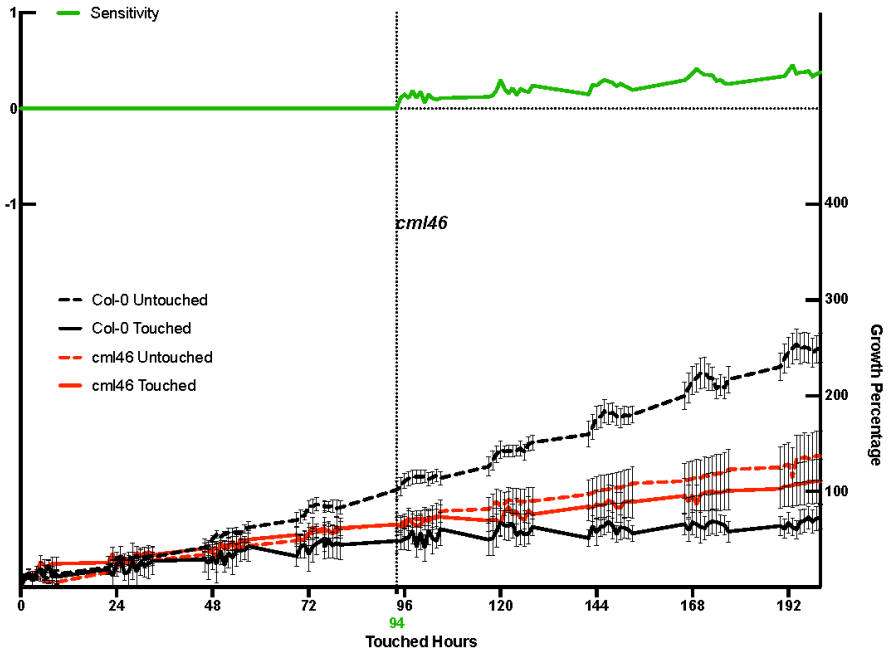

Supplementary Figure S2.11 *cml46* exhibits significantly altered growth phenotypes, in untouched and touched plants, relative to Col-0. Plants were touched every 5 minutes for >8 days and imaged every hour. Percent growth was extracted from images at each time point ($\Delta A/A_0$). Sensitivity (green trace) is a measure of divergence of the mean growth at each time point from Col-0 for both untouched and touched measures, denoting sensitivity to some stress or force (e.g. touch). *cml46* plants exhibit reduced growth in untouched plants and decreased growth inhibition due to touch, relative to Col-0.

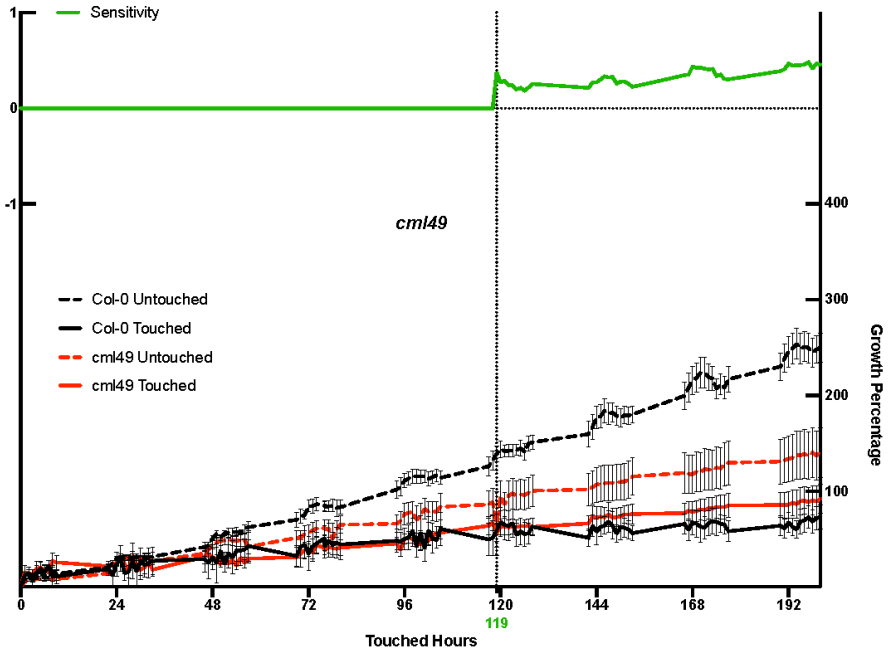

Supplementary Figure S2.12 *cml49* exhibits significantly altered growth phenotypes, in untouched and touched plants, relative to Col-0. Plants were touched every 5 minutes for >8 days and imaged every hour. Percent growth was extracted from images at each time point ($\Delta A/A_0$). Sensitivity (green trace) is a measure of divergence of the mean growth at each time point from Col-0 for both untouched and touched measures, denoting sensitivity to some stress or force (e.g. touch). *cml49* plants exhibit reduced growth in untouched plants and decreased growth inhibition due to touch, relative to Col-0.

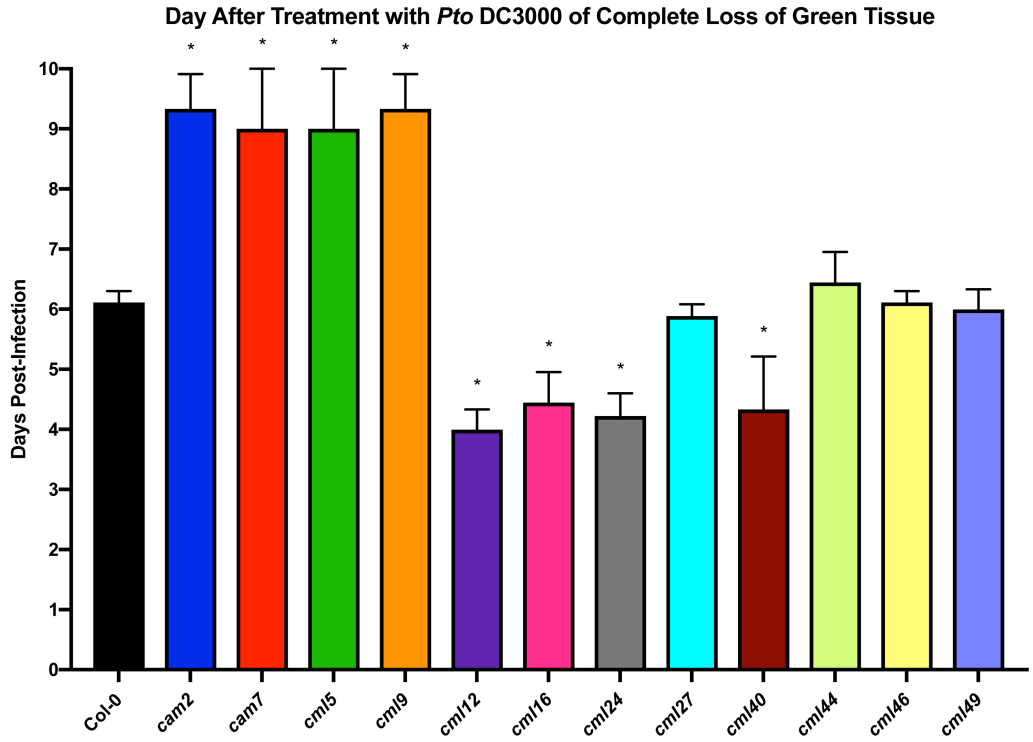

Supplementary Figure S2.13 *CAM* and *CML* mutants exhibit differential ability to suppress internal pathogen proliferation. Plants were flooded with *Pto* DC3000 (OD_{595} = 0.4) and monitored until all green tissue was lost. Results represent mean ± s.d.; n = 9 biological replicates; 3 replicates from 3 independent experiments. Columns with the same letter are not statistically different from Col-0 at the given time point (2-way ANOVA; Dunnett's Test; $p < 0.05$).

Chapter 3:

CaM2 and CaM7 regulate salicylic acid-dependent and -independent plant immunity in *Arabidopsis thaliana*

This chapter has been formatted for submission to the *Plant Journal*.

I would like to acknowledge the following people for contributing to the results for this chapter: Rebekah Holtsclaw, Savana Lipps, Gabrielle Li, Dr. Abraham Koo, and Simon Gilroy. I was responsible for generating all of the results. Rebekah Holtsclaw and Abraham Koo were responsible for the salicylic acid measurements. Savana Lipps assisted with pathogenesis and callose deposition measurements. Gabrielle Li assisted with qPCR and generation of the double mutant. Simon Gilroy and I wrote all parts of the manuscript.

Summary

Phytopathogens produce microbe-associated molecular patterns (MAMPs) that induce plant defenses by binding to pattern-recognition receptors at the plasma membrane. This perception precipitates Ca^{2+} fluxes that initiate signaling cascades, coordinating a multi-pronged approach to defeating infectious pathogens. One component of this response network involves calcium-bound calmodulin regulation of the production of salicylic acid and subsequent defense-related transcripts. Loss-of-function alleles of *CAM2* and *CAM7* led to the constitutive expression of genes that regulate SA production coupled with upregulation of SA response genes such as *PR1.* These observations imply that CAM2 and CAM7 may cooperate to negatively regulate plant immunity in a SA-dependent manner. However, *cam2* and *cam7* plants produced WT SA levels and *cam2 cam7* plants produced significantly less SA than WT, both before and after MAMP (flg22) treatment. Nonetheless, *cam2*, *cam7*, and *cam2 cam7* plants all exhibited resting *PR1* expression at approximately 35-fold higher levels than WT, with no significant change after MAMP treatment. Taken together, these results suggest that SA is not required for *PR1* induction, in these mutants. All of these *CAM* mutant lines also exhibit significantly increased disease resistance to *Pseudomonas syringae*, indicating that a suite of responses typified by early *PR1* induction in these backgrounds is sufficient to inhibit disease progression. These results suggest that, while CAM2 and CAM7 may play a role in negatively regulating SA-production-related transcripts, their activity in repressing *PR1* expression – and plant immunity – can also operate through a SA-independent mechanism.

Significance Statement

We show that the CaM2 and CaM7 isoforms of calmodulin operate as negative regulators of the plant pattern triggered immunity (PTI) system. Although they act to modulate salicylic acid production, their effects on immune function also operate through a salicylic acid-independent pathway.

INTRODUCTION

The calcium ion is an important second messenger in most organisms, where it is required for adaptive responses to many stimuli (Berridge *et al.*, 2000; Clapham, 2007; Poovaiah and Du, 2018). The Ca^{2+} flux machinery is thought to generate differential elevations of $[Ca^{2+}]_{cyt}$ in response to diverse stimuli, with the frequency, amplitude, duration and localization of the change in $[Ca^{2+}]_{cyt}$ defining stimulus-specific information, the so-called 'calcium signature' of the stimulus (McAinsh and Pittman, 2009; Dodd *et al.*, 2010). This system then requires the cell to have a network of Ca^{2+} responsive proteins that can decode the information within these signatures.

It is known that Ca^{2+}-binding proteins (CaBPs), like calmodulin (CaM), are required for connecting elevations in $[Ca^{2+}]_{cyt}$ to specific downstream responses (Hashimoto and Kudla, 2011). The details of the biochemical interactions behind decoding each calcium signature, however, have remained largely elusive. Recent work using mathematical modeling approaches has described possible mechanisms by which calcium signatures produced during plant immune responses may be decoded through the interactions of the Ca^{2+} signature and the dynamics of interactions between CaMs and target regulators of salicylic acid (SA) production. Indeed, this model can predict the empirically verified patterns of gene expression generated by different Ca^{2+} signatures (Lenzoni *et al.*, 2018). These findings suggest that interactions at the level of CaM and CaBP dynamics are likely key players in signal decoding and the triggering of immune responses. Consistent with these ideas, pathogen attack has been demonstrated by many researchers to both increase $[Ca^{2+}]_{cyt}$ and rely on the activity of a range of CaBPs to initiate plant immunity (e.g., (Kim *et al.*, 2002; Dodd *et al.*, 2010; Galon *et al.*, 2010; Kudla *et al.*, 2010; Seybold *et al.*, 2014; Tsuda and Somssich, 2015).

During the interaction between pathogenic bacteria and plants, particular microbe-associated molecular patterns (MAMPs) act as elicitors of plant defense responses through the process of pattern-triggered immunity (PTI) (Jones and Dangl, 2006; Veluchamy *et al.*, 2014; Suarez-Rodriguez *et al.*, 2007; Ranf *et al.*, 2011). A hallmark of early PTI responses is the rapid increase in $[Ca^{2+}]_{cyt}$ immediately after bacterial (or MAMP) elicitation (Knight *et al.*, 1991; Blume *et al.*, 2000; Ranf *et al.*, 2011) with subsequent production of defense compounds and hormones, such as salicylic acid (SA) (Yi *et al.*, 2014; Hilleary and Gilroy, 2018). During PTI in *Arabidopsis thaliana,* a signal responsive protein, SR1 (CaM-binding transcription activator 3, CAMTA3), functions as a transcription factor that negatively regulates isochorismate synthase 1 (ICS1; salicylic acid induction deficient 2, *SID2*), a key enzyme required for flagellin-dependent SA production (Du *et al.*, 2009). In parallel, the transcription factor CaM-binding protein 60-like g (CBP60g) positively regulates *ICS1* production and, therefore, SA-mediated plant immunity (Wang *et al.*, 2009). These CaM-binding transcription factors provide targets for the involvement of CaM in this process. These observations highlight a potentially central role for Ca^{2+}/CaM-based signaling in the regulation of immune response, with the overall defense outcome likely reflecting a balance between stimulatory and repressive components of the regulatory network.

The Arabidopsis genome contains seven *CAM*s that encode four CaM isoforms: CaM1/CaM4, CaM2/CaM3/CaM5, CaM6, and CaM7 (La Verde *et al.*, 2018). Amongst the CaMs, CaM2 and CaM7 have been previously linked to defense and CaM2 and CaM7 differ by a single amino acid (Kumar *et al.*, 2016). For example, CaM2 interacts with proteins that are associated with the machinery of SA-dependent gene expression (Choi *et al.*, 2010; Fang *et al.*, 2017) and CaM7 participates in non-host resistance (Campe *et al.*, 2016), whereas the other CaMs do not.

We therefore set out to examine the extent to which CaM2 and CaM7 are involved in common versus specific elements of the regulation of SA production and downstream defense responses. We report that CaM2 and CaM7 are indeed important for regulating plant immune responses ranging from the control of MAMP-induced gene expression to defense against *Pseudomonas syringae* pv. *tomato* DC3000 (*Pto* DC3000), but they also play independent roles in, e.g., regulating callose deposition, indicating both overlapping and distinct signaling activities. Despite their effects on the regulation of SA synthesis-related transcripts, both CaM2 and CaM7 appear to also play roles in SA-independent immune responses, suggesting they could coordinate the action of multiple pathways within the regulatory networks underlying the immune response.

RESULTS

cam2, *cam7*, and *cam2 cam7* Mutations Result in Significant Alterations in SA-Related Defense Transcripts

Before assessing how mutants in *CAM2* and *CAM7* affected defense responses to pathogen or flg22 treatment, we first asked whether there were constitutive effects of these mutant backgrounds on defense-related events. This is a key question as many mutants that trigger constitutive defense responses also show grossly disrupted development (Karasov *et al.*, 2017), making it hard to understand whether differences in relation to wild type reflect specific disruption of defense processes or secondary effects from altered growth habit. Neither the single mutants (*cam2-1*, SALK_114166, *cam7-1*, SALKseq_128513; **Figure 3.1a, 3.1b**) nor the *cam2*-1/cam7-*1* double mutants (*cam2 cam7*) showed obvious vegetative growth phenotypes, suggesting that comparison to wild type responses to defense elicitation would likely be more robust. qPCR indicated that the *cam2* and *cam7* alleles were knockouts. However, unexpectedly, *CAM2* transcript was also

undetectable in the *cam7* mutant background. Data from *cam2-1* and *cam7-1* are shown (**Figure 3.1c**) but identical results were obtained from the second allele of each (**Supplementary Figure S3.1c**). CAM7 has been shown to act directly as a transcription factor (Kumar *et al.*, 2016) and the promoter of *CAM2* does have a putative CAM7 target site within it suggesting a potential mechanism behind this CAM7 effect (see discussion below).

In response to flg22, wild type plants showed ~two-fold induction of the defense response marker gene *PR1* detectable at 30-60 mins after treatment and accumulation to >100-fold of basal levels over 24h (**Figure 3.2a**). However, untreated *cam2*, *cam7*, and *cam2 cam7* mutants already expressed *PR1* at levels significantly above untreated wild type (>35-fold; 2-way ANOVA; Dunnett's test; $p<0.05$). These levels remained elevated and unchanged throughout 24h of treatment with 1μM flg22. These results indicate that these *CAM* mutant backgrounds lead to a

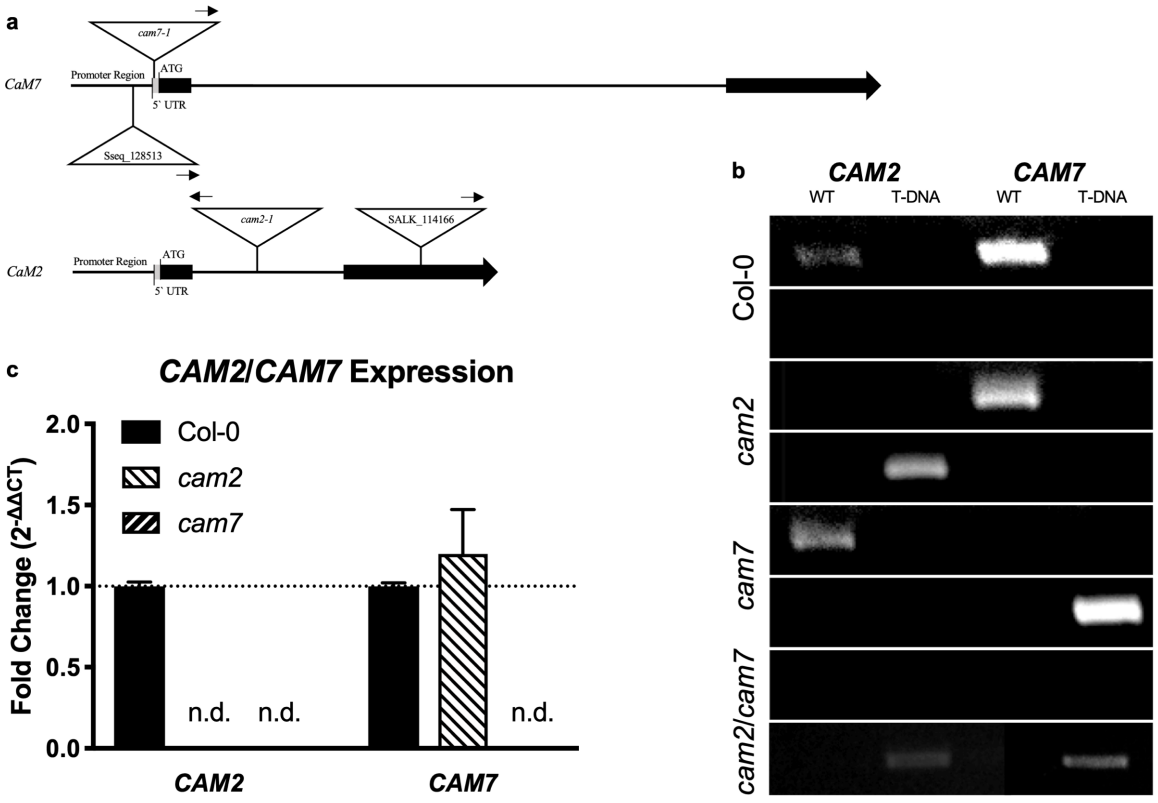

Figure 3.1 Identification of RNA null alleles of *cam2*, *cam7*, and recovery of *cam2 cam7* double mutant plants . (**a**) Gene diagrams for *CAM2* and *CAM7*, indicating the locations of T-DNA insertions. (**b**) Gel electrophoresis after PCR with WT- and T-DNA-specific *CAM2* and *CAM7* primers indicating homozygosity of each insertional mutant. (**c**) Transcript level of *CAM2* and *CAM7* in the *cam2* and *cam7* backgrounds indicating each mutant as an RNA-null and that there was no expression of *CAM2* in the *cam7* background.

sustained increase in defense gene induction that approaches levels seen upon flg22 response but that is itself no longer responsive to defense elicitor induction.

PR1 gene expression in defense responses is generally thought to be elicited by SA-mediated events (Seyfferth and Tsuda, 2014). To explore a potential upstream cause of the elevated level of expression of *PR1* in *cam2*, *cam7*, and *cam2 cam7* mutants, we therefore assayed the expression of the SA-production/regulatory genes: *SR1*, *CBP60g*, and *ICS1*. In untreated *cam2* and *cam7* mutants (but not *cam2 cam7*, see below), *ICS1* was already expressed above the maximum levels seen in flg22-treated wild type plants (**Figure 3.2b**). At 30- and 60-mins after addition of 1µM flg22, this increased *ICS1* expression was unaltered. These results indicate loss of function

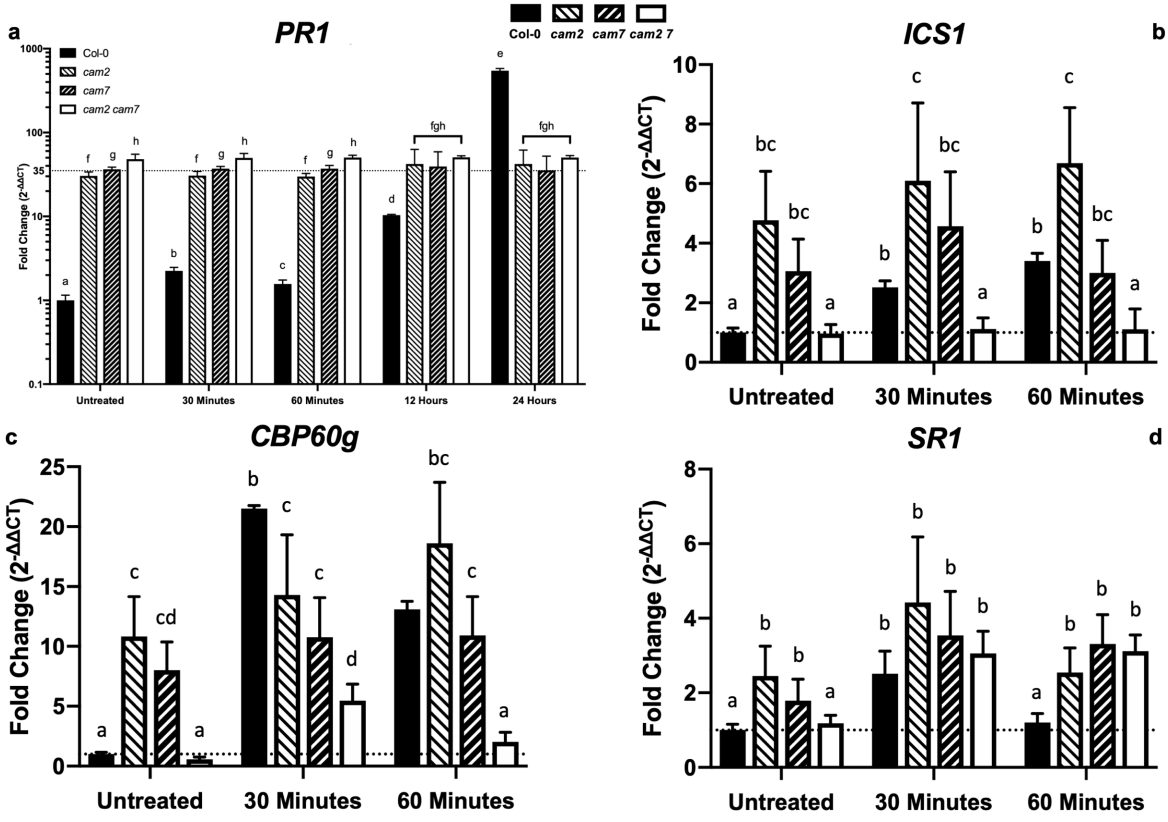

Figure 3.2 *cam2*, *cam7*, and *cam2 cam7* plants exhibit altered defense-related gene expression. Transcript levels of 10-day-old seedlings treated with 1 µM flg22 for 0 (untreated), 30, and 60 minutes. (**a**) Transcript level of *PR1*. (**b**) Transcript level of *ICS1*. (**c**) Transcript level of *CBP60g*. (**d**) Transcript level of *SR1*. Fold-change ($2^{-\Delta\Delta Ct}$) values are relative to untreated Col-0. Results represent mean ± s.d.; n = 3 biological replicates with 4 technical replicates from 3 independent experiments. Columns with asterisks (*) are statistically different from Col-0 at the given time point (2-way ANOVA; Dunnett's Test; $p < 0.05$).

in *CAM2* and *CAM7* leads to disruption of the regulation normally imposed on *ICS1* and potentially an uncoupling from flg22-dependent controls.

Increased *ICS1* expression could possibly be explained by upregulation of the expression of the *ICS1* positive transcriptional regulator CBP60g, downregulation of the expression of the *ICS1* negative regulator SR1, or both. Both *CPB60g* and *SR1* showed induction over 30-60 mins of flg22 treatment in wild type plants (**Figure 3.2c and 3.2d,** respectively), but akin to their induction of *ICS1* expression, the untreated *cam2* and *cam7* plants exhibited significant upregulation of these genes relative to wild type levels and this induction was again sustained throughout measurements at 30-60 mins of flg22 treatment.

Unlike the single mutants, the *cam2 cam7* double mutant plants exhibited wild type levels of *ICS1* that did not change upon flg22 treatment. *CBP60g* did show induction with flg22 treatment but at all timepoints was significantly suppressed relative to wild type. *SR1* levels mirrored wild type in untreated *cam2 cam7* and induction was observed at 30 mins post-flg22 treatment but these *SR1* levels were significantly above wild type at 60 mins after flg22 treatment, when *SR1* had returned to basal expression levels in wild type.

*S*alicylic Acid Levels are Altered in *cam2*, *cam7* and *cam2 cam7* Mutants

The above results are broadly consistent with mutants in *CAM2* and *CAM7* acting through disruption of SA production. To directly test this idea, we monitored SA levels in the CaM mutant backgrounds. Despite elevated levels of ICS1, *cam2* and *cam7* mutants showed basal levels of SA and induction of SA accumulation over 24h that were identical to wild type plants (**Figure 3.3**). *cam7* mutants did accumulate a significant ~40% increase in SA level at 24h post-flg22 treatment

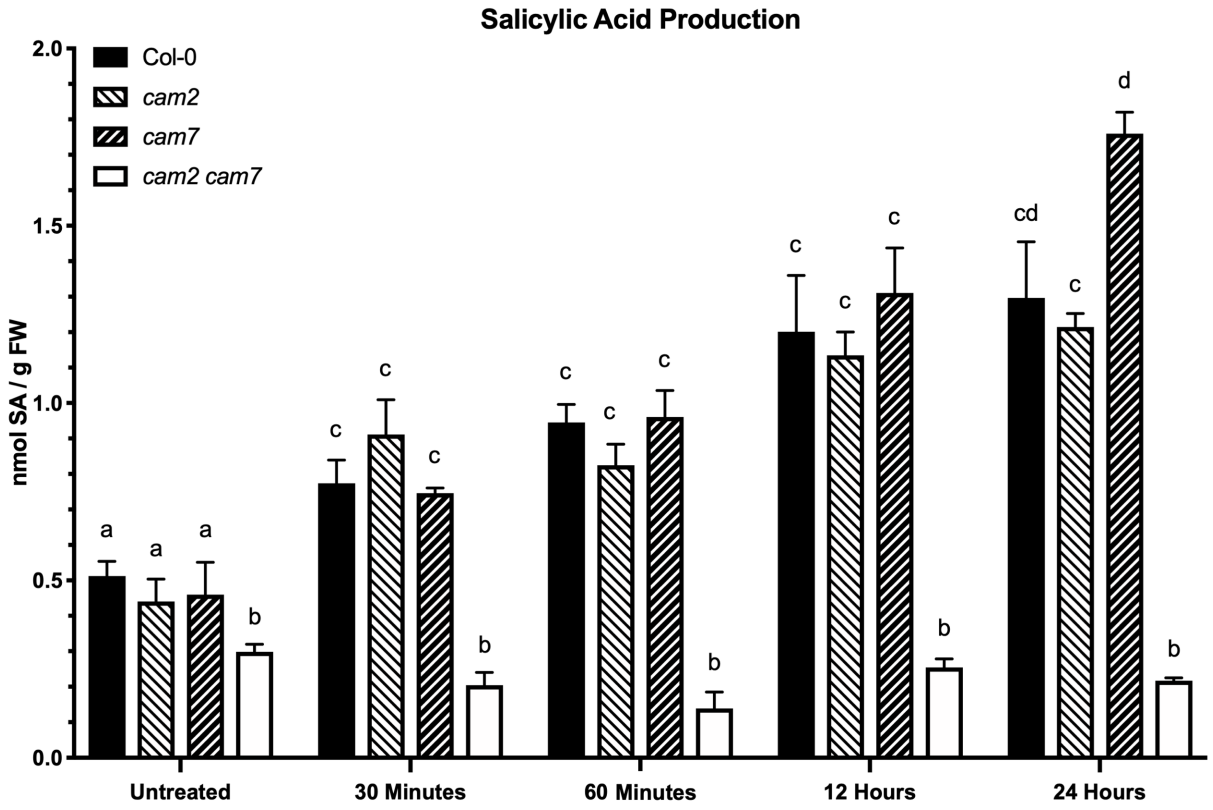

Figure 3.3 *cam2 cam7* plants exhibit reduced salicylic acid production levels. Salicylic acid (SA) production of 10-day-old seedlings treated with 1 µM flg22 for 0 (untreated), 30, 60 minutes, 12, and 24 hours. *cam2* and *cam7* plants produce wild type levels of SA at all time points. However, *cam2 cam7* plants produce significantly less SA in untreated and treated samples, at all time points, indicating that *cam2 cam7* plants are deficient in defense-related SA production. Results represent mean ± s.e.m.; n = 12 biological replicates from 3 independent experiments. Columns with the same letter are not statistically different (2-way ANOVA; Dunnett's Test; $p < 0.05$).

over *cam2* but neither were significantly different from the wild type level. *cam2 cam7* double mutants showed significantly reduced SA levels that did not change with flg22 treatment.

These results indicate that the molecular markers for defense response (e.g. *PR1*) and regulation through SA (e.g. *ICS1*) do not lead to increased SA levels in the *CAM* mutant backgrounds. We therefore sought to define the impact of these mutants on the defense response systems of the plant to ask how disruption of *CAM2* and *CAM7* affected the physiological outputs of defense signaling.

cam2, cam7 and *cam2 cam7* Mutants Exhibit Altered Callose Deposition Phenotypes

Callose is a β-1,3 glucan cell-wall constituent closely linked to defense responses within the plant (Piasecka *et al.*, 2015). Callose production can be visualized as local deposits or papillae that stain with aniline blue. Therefore, we used the density of papillae as one measure of defense response. Untreated 14-day-old wild type plants produced ~1 callose papilla mm^{-2}, increasing to ~14 mm^{-2} after 24 hrs of treatment with 1μM flg22 (**Figure 3.4a**). Untreated *cam2* plants produced ~8 callose papillae mm^{-2}, with no significant change after flg22 treatment. On the other hand, untreated *cam7* and *cam2 cam7* plants were not different from wild type Col-0 but deposited significantly less callose after flg22 treatment.

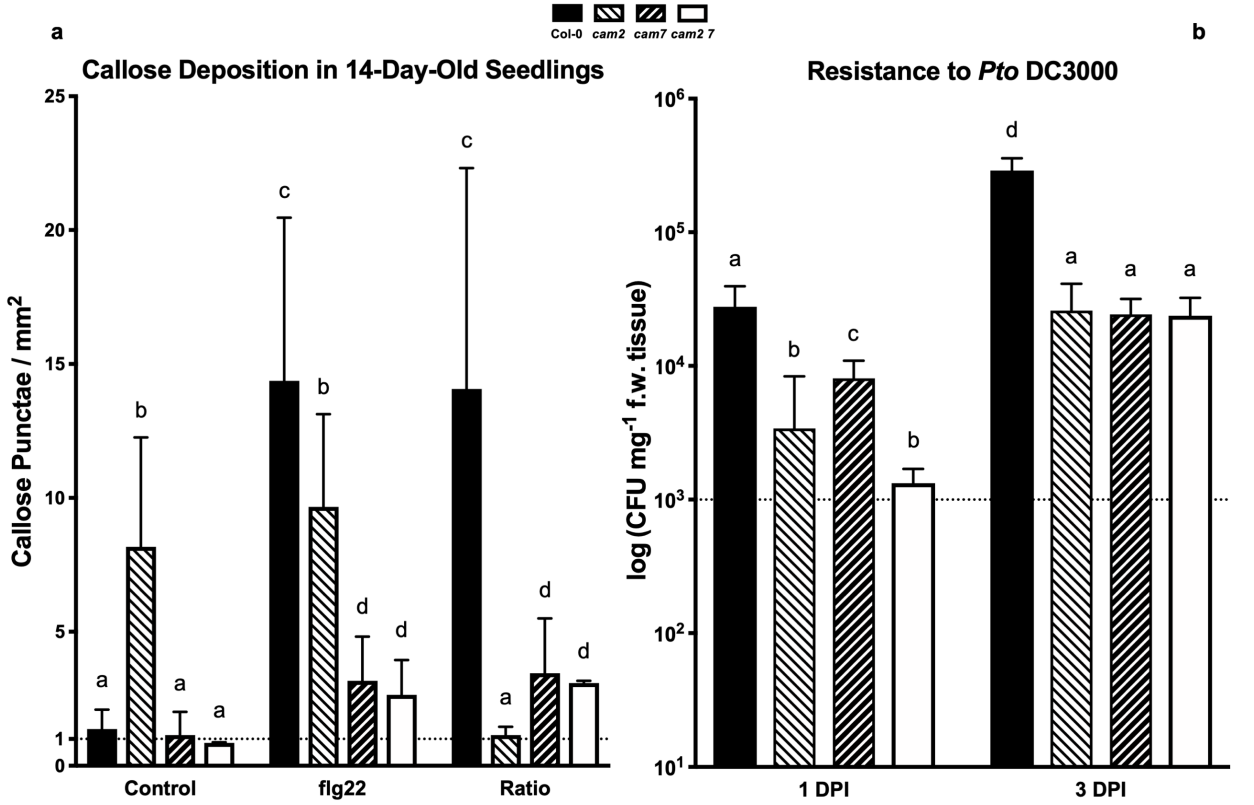

Figure 3.4 *cam2*, *cam7*, and *cam2 cam7* plants exhibit altered callose deposition and pathogen resistance phenotypes. (**a**) Col-0 deposits ~15-fold more papillae after treatment with 1 μM flg22 than before. Untreated *cam2* plants produce ~8 papillae mm^{-2}, with no significant change after flg22 treatment. Untreated *cam7* and *cam2 cam7* plants were not different from Col-0 but deposited significantly less callose after flg22 treatment. (**b**) *cam2*, *cam7*, and *cam2 cam7* plants were significantly more resistant to *Pto* DC3000 at 1 and 3 days post-infection. Results represent mean ± s.d.; n ≥ 12 biological replicates from 3 independent experiments. Columns with the same letter are not statistically different (2-way ANOVA; Dunnett's Test; $p < 0.05$).

cam2, *cam7*, and *cam2 cam7* Mutants Exhibit Increased Resistance to *Pseudomonas syringae* pv tomato DC3000

The ultimate measure of defense is the ability to suppress pathogen proliferation within the plant. Therefore, we monitored the ability of the wild type and the *CAM* mutants to defend against challenge with the bacterial pathogen *Pto* DC3000 (**Figure 3.4b**). *cam2*, *cam7* and *cam2 cam7* all exhibited significantly reduced bacterial growth, showing up to an order of magnitude fewer extractable bacterial Colony Forming Units (CFUs) per mg fresh weight whole seedlings at both 1 and 3 days-post-inoculation (DPI). This result suggests increased resistance to *Pto* DC3000 in *cam2*, *cam7*, and *cam2 cam7* plants.

DISCUSSION

Calmodulin appears as a central player in many of the models of plant immune response. However, Arabidopsis has 7 CaM genes that encode 4 different proteins (La Verde *et al.*, 2018) and so the potential exists for complex regulatory loops involving different isoforms. CaM2 and CaM7 differ by a single amino acid (Kumar *et al.*, 2016), yet this lone change appears to have important effects on sub-functionalization, with CaM7 directly binding DNA and acting as a transcription factor, an activity not shared by CaM2 (Kumar *et al.*, 2016). Our analyses, however, suggest that CaM2 and CaM7 do share some regulatory roles within the plant defense system. For example, *cam2*, *cam7* and *cam2 cam7* double mutants all show elevated *PR1* expression (**Figure 3.2a**, **Supplementary Figure S3.4a**) and enhanced whole plant defense (**Figure 3.4b**), suggesting parallel regulatory actions. For both this induction of *PR1* and resistance to the hemibiotrophic phytobacterium *Pto* DC3000, the effect of the double is not significantly different from the single mutants, with no obvious additive or synergistic action. This might suggest both CaM2 and CaM7 operate in the

same pathway to the modulation of defense signaling. Indeed, CaM7 has been shown to be a direct transcriptional activator, binding Z- (Kushwaha *et al.*, 2008), E- and T/G-box DNA (Abbas *et al.*, 2014) and inspection of the promoter region of *CAM2* shows it to contain two E-box DNA motifs at 619 and 401 base pairs upstream of the transcriptional start site, indicating that *CAM2* may be transcriptionally regulated by CAM7. This idea is consistent with the lack of detectable *CAM2* transcript in the *cam7* mutant background. Thus, *cam7* phenotypes could effectively operate through repression of *CAM2*, i.e., the *cam7* phenotype would in effect be a *cam2* loss-of-function phenotype. However, our other phenotyping suggests this is unlikely to be the case with e.g., differential effects of *cam2* and *cam7* on defense-related events such as callose deposition (**Figure 3.4a**) and *SR1* (**Figure 3.2d**, **Supplementary Figure S3.4d**) and *PR5* (**Supplementary Figures S3.5a, S3.6a**) expression. Indeed, in non-host resistance to the fungal pathogens *Phakopsora pachyrhizi* and *Blumeria graminis f.sp. hordei*, *cam7* but not *cam2* mutants were reported to show reduced defense responses (Campe *et al.*, 2016). In contrast, in our experiments, we observed that loss-of-function in *CAM2* and *CAM7* led to enhanced defense against a bacterial pathogen, raising the intriguing possibility that these calmodulins act as regulators across the different pathways of defense response, perhaps switching the level of output between each, as needed.

In the *cam2*, *cam7*, and *cam2 cam7* backgrounds, *PR1* levels are significantly upregulated, with induction uncoupled from flg22 response (**Figure 3.2a**). This high background *PR1* expression is consistent with the constitutively elevated *ICS1* expression and, therefore, SA production. However, SA production was unaltered in *cam2* and *cam7* single mutants, relative to Col-0, and was reduced in the *cam2 cam7* double mutant even though *ICS1* expression appeared constitutively activated in the single mutants and repressed in the double. *ICS1* expression is positively regulated by CPB60g and repressed through a SR1-mediated pathway (Seyfferth and

Tsuda, 2014). Both CPB60g and SR1 are known to require CaM binding for their regulatory activity, providing a potential link to CaM2 and CaM7 action. Thus, *SR1* mutants are known to show increased resistance to *Pto* DC3000 and an avirulent *Pto* strain (*AvrRpt2*; Du et al., 2009). Furthermore, *SR1* mutants exhibited increased SA production as the result of upregulation of several positive regulators of *ICS1* and, therefore, SA biosynthesis. Mutations in various locations in the CaM-binding domain of SR1 compromised their function, demonstrating that Ca^{2+}/CaM-binding is required for SR1-mediated suppression of plant immunity. Similarly, *cbp60g* mutants have reduced flg22-responsive *ICS1* transcript abundance, produce less SA and are less resistant to virulent *Pto* DC3000, *Pseudomonas syringae* pv. Maculicola (*Psm* ES4326) and avirulent *Pto* DC3000 *hrcC* (Wang *et al.*, 2009). As with SR1, mutating residues in the CaM-binding domain of CBP60g compromised its function and inhibited MAMP-induced SA accumulation. Thus, CaM action on both SR1 and CBP60g would be expected to enhance ICS1 activity and so increase SA levels, leading to the prediction that CaM mutants should show impaired defense and lower SA accumulation. However, our results show that both *cam2* and *cam7* mutants exhibit unaltered SA levels and enhanced defense to *Pto* DC3000. Therefore, actions of CAM2 and CAM7 outside of their roles as potential regulators of SR1 and CBP60g proteins are likely to be in operation. In *cam2* and *cam7* lines, both *CPB60g* and *SR1* are upregulated (**Figure 3.2c**, **3.2d**). However, the induction of *CPB60g* is much higher than *SR1* and this shift in the balance of CaM-dependent regulation of *CPB60g* and *SR1* expression towards the side of activation of *ICS1* transcription would be expected to support constitutive elevation in resting SA levels in these backgrounds, i.e., the loss of CaM2 or CaM7 shifts the balance of the response network to, in this case, constitutive *ICS1* expression and, therefore, SA-mediated defense.

However, our results point to a role for SA-independent events. Constitutive *ICS1* expression would be expected to precipitate constitutive production of SA and, thereafter, upregulation of *PR1* expression. While our results do indicate induction of *ICS1* above maximal wild type levels paired with upregulation of *PR1*, these levels are uncoupled from the canonical SA-dependent response. One explanation may be that the pool of chorismate available within the cells is not sufficient to increase isochorismate – and, therefore, SA – production, beyond wild type levels, even though *ICS1* transcription is enhanced in the *cam2* and *cam7* mutants. Furthermore, SA may simply be degraded when produced above wild type levels in the absence of clear pathogen elicitation. As there is no significant increase in SA-related transcripts in these mutants after flg22 treatment, perhaps the feedback required to sustain SA levels within the cells is not present.

A possible explanation for the relatively high level of *PR1* expression in the *cam2*, *cam7*, and *cam2 cam7* mutants, regardless of SA input, is that the level of defense response may be set by numerous regulators and transcription factors, many of which can be found in the TGA and 'WRKYGQK' (WRKY) transcription factor families (Seyfferth and Tsuda, 2014). CaM2 has been found to be intimately linked to TGA3 and its regulatory relationship to *PR1* (Choi *et al.*, 2010; Fang *et al.*, 2017). However, it is still perhaps surprising that a mutation in CaM2 (or indeed CaM7) would have such a pronounced effect on *PR1* expression and disease resistance given the complex web of regulators controlling these responses. For instance, it was shown that the activity of TGA2, TGA5, and TGA6 also lead to repression of *PR1* in non-stress conditions (Rochon *et al.*, 2006). TGA2, TGA5, and TGA6 were also shown to be essential to the elicitor-triggered induction of *PR1* expression and the induction of systemic acquired resistance (SAR) through their interaction with the SA receptor NPR1 (Zhang *et al.*, 2003; Mou *et al.*, 2003). WRKY50 has also been shown

to enhance *PR1* expression (Hussain *et al.*, 2018), especially when in combination with *tga2* and *tga5* mutations (but not *tga3*).

This complex, interconnected web of regulation would be expected to yield a robust network where loss of a single regulatory element would not be predicted to lead to wholesale reprogramming of control unless the lost element is a critical, highly interconnected hub for the network (Albert, 2005). Hub-like effects of CaM2 and CaM7 would suggest widespread roles over and above transcriptional regulation of *PR1* through e.g., interactions such as with TGA3. This idea is consistent with the significant increases in defense response to *Pto* DC3000 in the *cam2, cam7* and *cam2 cam7* mutants, implying a substantial shift in the poise of the uninduced defense system (**Figure 3.4b**). Our results from the *cam2*, *cam7*, and *cam2 cam7* mutants suggest that enhanced defense (**Figure 3.4b**) does not in this case correlate with increased SA production (**Figure 3.3**). Salicylic acid-independent *PR1* induction has been reported, for instance, through the MAP kinase regulatory pathway. Thus, although transient activation of *MPK3* and *MPK6* does not affect *PR1* levels, their constitutive induction does (Seyfferth and Tsuda, 2014). However, this mechanism seems less likely for the *cam2 cam7* effect we report, as *MPK3* and *MPK6* expression remained at wild type levels in this background (**Supplementary Figures S3.5c** and **S3.5d**, respectively). These observations suggest either the operation of an additional, yet-to-be-characterized SA-independent pathway to *PR1* transcription, or that CaM2 and CaM7 are operating in the MAP Kinase pathway downstream of MPK3 and MPK6.

Constitutively defended plants tend to exhibit a tradeoff between vegetative growth and defense, being smaller and often exhibiting more general stress-related phenotypes (Huot *et al.*, 2014; Karasov *et al.*, 2017). Yet, in the case of *cam2*, *cam7* and *cam2 cam7* mutants, there is no obvious reduction in vegetative growth and development. One proposed mechanism for the

tradeoff between growth and defense is through antagonistic interactions between hormone regulatory pathways (Karasov *et al.*, 2017). Such tradeoffs related to SA are likely to be complex, e.g., SA is reported to be able to both retard and stimulate growth depending on conditions (Rivas-San Vicente and Plasencia, 2011). However, our results imply that the defense pathways being modulated by CaM2- and CaM7-dependent events can operate via an SA-independent pathway, as, in the *cam2*, *cam7*, and *cam2 cam7* mutants, defense is upregulated but SA levels are either unchanged or repressed, relative to Col-0 (**Figure 3.3**). By bypassing this hormone, the constitutive defense posture in the *cam2*, *cam7*, and *cam2 cam7* mutants may also bypass some of the trade-offs associated with induction of SAR.

MATERIALS AND METHODS

Plant Material and Growth Conditions

We acquired *Arabidopsis thaliana* lines harboring each of two previously-characterized loss-of-function alleles in both *CaM2* (*cam2-1*/SALK_066990 and SALK_114166) and *CaM7* (*cam7-1*/SALK_074336 and SALKseq_128513) (**Figure 3.1a**) from the *Arabidopsis* Biological Resource Center at Ohio State University. Seeds were imbibed with sterile H_2O (20 mins), sterilized with 70% (v/v) ethanol (1 min), 20% (v/v) bleach (2 mins), and washed three times with sterile H_2O. Sterile seeds were sown onto petri plates containing ½-strength Linsmaier and Skoog (LS) Modified Basal Medium (PhytoTechnology Laboratories), 1.0% (v/v) phytagel (Sigma Life Science) and 1.0% (w/v) sucrose (growth medium, hereafter). After the plants were grown for 21 days in 16 hours light/8 hours dark (long-day) photoperiod under 100 $\mu E\ m^{-2}\ sec^{-1}$ at 22˚C in a plant-growth chamber (normal growth conditions, hereafter), the location of each insertion was verified by PCR amplification of gene-specific and T-DNA-specific primers (**Figure 3.1b**,

Supplementary Table S3.1). To confirm that the lines were *bona fide cam2* and *cam7* null mutants, we quantified *CAM2* and *CAM7* transcript accumulation in wild type (Col-0) and the T-DNA insertion lines via qPCR. This analysis indicated that both *cam2* alleles and both *cam7* alleles accumulated no *CAM2* and *CAM7* transcript, respectively. Additionally, *cam7* plants accumulated no detectable *CAM2* transcript, as well (**Figure 3.1c**).

We also generated crosses between homozygous *cam2-1* and *cam7-1* plants. We used reciprocal crosses between demasculinized *cam2-1* flowers with *cam7-1* pollen, and demasculinized *cam7-1* flowers with *cam2-1* pollen and were able to recover homozygous *cam2 cam7* double mutant seed from both sets of crosses (**Figure 3.1b**).

MAMP Treatment and Tissue Collection

To determine the plant responses to MAMP treatments, seeds from each confirmed knockout line were planted in 12-well plates (Greiner Bio-One, Monroe, NC, USA) containing growth medium and grown for 10-14 days, depending on the experimental design, in long-day photoperiod as described above. Paired replicate plates were made for each genotype: one for the control and one for flg22 treatment. At least 4 technical repetitions per treatment, per genotype were analyzed. Each experiment was repeated 3 times.

To measure the molecular response to MAMP elicitation, 10-day-old *Arabidopsis* seedlings were treated with 1 μM flg22 suspended in liquid growth medium (growth medium without Phytagel). The flg22 solution was slowly and gently dispensed on the side of each well of 12-well plates to avoid eliciting a mechanical response. For the control, liquid growth medium (without flg22) was used. After treatment, the seedlings were harvested at 30 and 60 mins or 12 and 24h post-treatment, frozen in N_2(l) and stored at -80º C until RNA isolation.

RNA Isolation and Reverse-Transcription qPCR

The total RNA from plant samples was isolated using the RNeasy Plant Mini kit (Qiagen, Valencia, CA, USA). Plant samples were homogenized (Spex SamplePrep MiniG 1600) at 1500 strokes/min, per the manufacturer's instructions. RNA samples were treated with the TURBO DNase kit (Ambion, Waltham, MA, USA) to degrade genomic DNA.

SR1, *CBP60g*, *ICS1*, *PR1*, *PR5*, *MPK3* and *MPK6*, were then monitored by qPCR. Primers specific to sequences within each of these genes (**Supplementary Table S3.2**) were added to individual aliquots of Luna One-Step qPCR Master Mix (New England Biolabs, Ipswitch, MA, USA), according to the manufacturer's protocol. The master mixes and RNA samples were aliquoted into 96-well optical PCR plates (ABgene, Portsmouth, NH, USA), and qPCR performed using a 7500 Real Time PCR System (Applied Biosystems, Waltham, MA, USA) with the following parameters: 1 cycle of 10 mins at 95˚C; 40 cycles of 15 s at 95˚C, 15 s at 58˚C, and 15 s at 65˚C; and 1 cycle of dissociation from 58-95˚C with 1˚C increments. Relative expression was quantified using the $2^{-\Delta\Delta Ct}$ method (Livak and Schmittgen, 2001; Choi and Roberts, 2007; Schmittgen and Livak, 2008).

Expression of the marker genes was normalized to *UBQ10* expression in untreated Col-0 samples. Expression data was analyzed using Prism Statistical Software V8.0 (GraphPad Software, La Jolla, CA, USA). Two-way ANOVA analyses were performed to compare the differences between the means of each marker gene in response to each stimulus in Col-0 and those in the mutant plants, within each time point. For these experiments, Dunnett's Test for multiple comparisons was used and the results were considered significant if the p-value was < 0.05.

Callose Deposition

Callose staining was adapted from Clay et al. (2009) and Schenk et al. (2014). Leaves were detached from 2-week-old Arabidopsis plants and placed in 12-well cell culture plates (Greiner Bio-One, Monroe, NC, USA) and treated for 24h in a 1 μM solution of flg22. Samples were cleared in 1:3 acetic acid/ethanol (v/v) overnight, washed in 150 mM K_2HPO_4 for 30 mins and stained for 12h in a solution of 150 mM K_2HPO_4 and 0.01% (v/v) aniline blue in the dark at 4˚C. Stained leaves were then washed in ddH_2O and embedded in 50% (v/v) glycerol. Callose deposits were quantified by confocal laser scanning microscope using a Zeiss LSM 710 inverted confocal microscope equipped with a 5x/0.16 EC Plan-Neofluar objective, Ex 405 nm, Em 480-570 nm. One hundred images of each leaf (total area 1700.38 μm x 1700.38 μm) were stitched together, using ImageJ software (Schindelin *et al.*, 2012; Schindelin *et al.*, 2015), to create a single image of the whole leaf. Callose deposits were counted using the "Analyze Particles" function of ImageJ with manual verification. Two-way ANOVA analyses were performed to compare the differences between the means of each callose measurement in Col-0 and those of in the mutant plants, before and after flg22 treatment. For these experiments, Tukey's Test for multiple comparisons was used and the results were considered significant if the p-value was < 0.05.

Salicylic Acid Measurement

Plants were grown, treated, and harvested as done for MAMP treatment assay of 10-day-old plants. SA content in seedlings was measured using ultra performance liquid chromatography electrospray ionization tandem mass spectrometry (UPLC-ESI-MS/MS) method as previously described (Koo *et al.*, 2011; Smith *et al.*, 2014), with minor modifications. Briefly, ~60-100 mg of tissue was flash-frozen in a tube containing metal beads using $N_2(l)$, then ground to a fine powder using a tissue

homogenizer (TissueLyser II, Qiagen, Venlo, Netherlands). The ground tissue was then vortexed for 5 mins at 4˚C with 150 µL of extraction buffer (70% methanol/water (v/v) with 0.5% acetic acid) containing a known amount of an internal standard, deuterium-labeled SA (d4-SA). The mixture was transferred to a microcentrifuge tube and centrifuged at 14,000 rpm for 20 min at 4°C. Seven µL of the resulting supernatant was separated on an Ascentis Express HPLC C18 column (2.7 µm, 5 cm x 2.1 mm; Supelco, Bellefonte, PA, USA) attached to an Acquity UPLC H-Class system (Waters) using a 3-min gradient program consisting of 0.1% (v/v) aqueous formic acid and methanol as mobile phase (0.4 mL/min flow rate at 40°C).

Bacterial Growth

Pseudomonas syringae pv tomato DC3000 (*Pto* DC3000), resistant to rifampicin (Rif) (Debener *et al.*, 1991; Grant *et al.*, 1995) was stored as a glycerol stock at -80˚C. Liquid shake cultures (LB with Rif) were prepared 48 h before inoculation (28°C, 250 rpm orbital shaker). Inoculum was prepared by harvesting cells from the shake culture by centrifugation (5000 rpm for 10 min), resuspending cells, washing the pellets two times in H_2O and resuspending in H_2O for inoculation. The concentration of cells was adjusted to an OD_{595nm} = 0.4 (~3.2 x 10^8 CFU/mL of bacteria). 0.025% (v/v) Silwet L-77 surfactant (Lehle Seeds) was then added to aid infiltration into the plant (Zidack *et al.*, 1992; Clough and Bent, 1998; Ishiga *et al.*, 2011).

Pathogenesis

Pathogenesis assays (0, 1, and 3 days) were performed on 14-day-old seedlings essentially as in Ishiga et al. (2011). Briefly, each 12 well plate contained 4 technical repetitions of three genotypes: Col-0 and two mutants. Seedlings were flooded with 1 mL of *Pto* DC3000 and incubated for 3

mins at RT and the medium was decanted. At 0 (immediate), 1, and 3 days post-infection (DPI), seedlings were harvested, treated with 1 mL of 5.0% (v/v) H_2O_2 for 5 mins to remove external bacteria and washed with 1 mL of H_2O three times. Tissue was homogenized (Spex SamplePrep MiniG 1600) for 5 mins at 1500 strokes/min and serial dilutions of lysate were performed on LB agar plates containing 50 μg/mL Rif. 0 DPI seedlings yielded no bacterial growth, confirming the efficacy of the H_2O_2 surface-sterilization. One-way ANOVA analyses were performed to compare the differences between the means of bacterial growth in Col-0 and those in the mutant plants, at 1- and 3-DPI. For these experiments, Tukey's Test for multiple comparisons was used and the results were considered significant if the p-value was < 0.05.

ACKNOWLEDGEMENTS

The authors thank Drs. Richard Hilleary and Arthur Poitout for helpful discussions. This work was supported by NSF: MCB-1329273, IOS-1557899 to SG and IOS-1557439 to AK.

LITERATURE CITED

Abbas, N., Maurya, J.P., Senapati, D., Gangappa, S.N. and Chattopadhyay, S. (2014) Arabidopsis CAM7 and HY5 physically interact and directly bind to the HY5 promoter to regulate its expression and thereby promote photomorphogenesis. *Plant Cell*, **26**, 1036–52.

Albert, R. (2005) Scale-free networks in cell biology. *J. Cell Sci.*, **118**, 4947 LP – 4957.

Asai, T., Tena, G., Plotnikova, J., Willmann, M.R., Chiu, W.-L., Gomez-Gomez, L., Boller, T., Ausubel, F.M. and Sheen, J. (2002) MAP kinase signalling cascade in Arabidopsis innate immunity. *Nature*, **415**, 977–983.

Berridge, M.J., Lipp, P. and Bootman, M.D. (2000) The versatility and universality of calcium signalling. *Nat. Rev. Mol. Cell Biol.*, **1**, 11–21.

Blume, B., Nurnberger, T., Nass, N. and Scheel, D. (2000) Receptor-Mediated Increase in Cytoplasmic Free Calcium Required for Activation of Pathogen Defense in Parsley. *Plant Cell*, **12**, 1425.

Campe, R., Langenbach, C., Leissing, F., Popescu, G. V., Popescu, S.C., Goellner, K., Beckers, G.J.M. and Conrath, U. (2016) ABC transporter PEN3/PDR8/ABCG36 interacts with calmodulin that, like PEN3, is required for Arabidopsis nonhost resistance. *New Phytol.*, **209**, 294–306.

Cheng, F., Blackburn, K., Lin, Y., Goshe, M.B. and Williamson, J.D. (2009) Absolute Protein Quantification by LC/MS E for Global Analysis of Salicylic Acid-Induced Plant Protein Secretion Responses. *J. Proteome Res.*, **8**, 82–93.

Chinchilla, D., Bauer, Z., Regenass, M., Boller, T. and Felix, G. (2006) The Arabidopsis Receptor Kinase FLS2 Binds flg22 and Determines the Specificity of Flagellin Perception. *Plant Cell*, **18**, 465 LP – 476.

Choi, J., Huh, S.U., Kojima, M., Sakakibara, H., Paek, K.-H. and Hwang, I. (2010) The Cytokinin-Activated Transcription Factor ARR2 Promotes Plant Immunity via TGA3/NPR1-Dependent Salicylic Acid Signaling in Arabidopsis. *Dev. Cell*, **19**, 284–295.

Choi, W.-G. and Roberts, D.M. (2007) Arabidopsis NIP2;1, a major intrinsic protein transporter of lactic acid induced by anoxic stress. *J. Biol. Chem.*, **282**, 24209–18.

Clapham, D.E. (2007) Calcium Signaling. *Cell*, **131**, 1047–1058.

Clay, N.K., Adio, A.M., Denoux, C., Jander, G. and Ausubel, F.M. (2009) Glucosinolate metabolites required for an Arabidopsis innate immune response. *Science (80-.).*, **323**, 95–101.

Clough, S.J. and Bent, A.F. (1998) Floral dip: a simplified method forAgrobacterium-mediated transformation ofArabidopsis thaliana. *Plant J.*, **16**, 735–743.

Debener, T., Lehnackers, H., Arnold, M. and Dangl, J.L. (1991) Identification and molecular mapping of a single Arabidopsis thaliana locus determining resistance to a phytopathogenic Pseudomonas syringae isolate. *Plant J.*, **1**, 289–302.

Dodd, A.N., Kudla, J. and Sanders, D. (2010) The Language of Calcium Signaling. *Annu. Rev. Plant Biol.*, **61**, 593–620.

Du, L., Ali, G.S., Simons, K.A., Hou, J., Yang, T., Reddy, A.S.N. and Poovaiah, B.W. (2009) Ca2+/calmodulin regulates salicylic-acid-mediated plant immunity. *Nature*, **457**, 1154–1158.

Fang, H., Liu, Z., Long, Y., et al. (2017) The Ca^{2+} /calmodulin2-binding transcription factor TGA3 elevates *LCD* expression and H_2S production to bolster Cr^{6+} tolerance in Arabidopsis. *Plant J.*, **91**, 1038–1050.

Galon, Y., Aloni, R., Nachmias, D., et al. (2010) Calmodulin-binding transcription activator 1 mediates auxin signaling and responds to stresses in Arabidopsis. *Planta*, **232**, 165–178.

Grant, M.R., Godiard, L., Straube, E., Ashfield, T., Lewald, J., Sattler, A., Innes, R.W. and Dangl, J.L. (1995) Structure of the Arabidopsis RPM1 Gene Enabling Dual Specificity Disease Resistance. *Science (80-.).*, **269**, 843–846.

Hashimoto, K. and Kudla, J. (2011) Calcium decoding mechanisms in plants. *Biochimie*, **93**, 2054–2059.

Hilleary, R. and Gilroy, S. (2018) Systemic signaling in response to wounding and pathogens. *Curr. Opin. Plant Biol.*, **43**, 57–62.

Huot, B., Yao, J., Montgomery, B.L. and He, S.Y. (2014) Growth-defense tradeoffs in plants: a balancing act to optimize fitness. *Mol. Plant*, **7**, 1267–1287.

Hussain, R.M.F., Sheikh, A.H., Haider, I., Quareshy, M. and Linthorst, H.J.M. (2018) Arabidopsis WRKY50 and TGA Transcription Factors Synergistically Activate Expression of PR1. *Front. Plant Sci.*, **9**, 930.

Ishiga, Y., Ishiga, T., Uppalapati, S.R. and Mysore, K.S. (2011) Arabidopsis seedling flood-inoculation technique: a rapid and reliable assay for studying plant-bacterial interactions. *Plant Methods*, **7**, 32.

Jones, J.D.G. and Dangl, J.L. (2006) The plant immune system. *Nature*, **444**, 323–9.

Karasov, T.L., Chae, E., Herman, J.J. and Bergelson, J. (2017) Mechanisms to Mitigate the Trade-Off between Growth and Defense. *Plant Cell*, **29**, 666 LP – 680.

Kim, M.C., Panstruga, R., Elliott, C., Müller, J., Devoto, A., Yoon, H.W., Park, H.C., Cho, M.J. and Schulze-Lefert, P. (2002) Calmodulin interacts with MLO protein to regulate defence against mildew in barley. *Nature*, **416**, 447–451.

Knight, M.R., Campbell, A.K., Smith, S.M. and Trewavas, A.J. (1991) Transgenic plant aequorin reports the effects of touch and cold-shock and elicitors on cytoplasmic calcium. *Nature*, **352**, 524–526.

Koo, A.J.K., Cooke, T.F. and Howe, G.A. (2011) Cytochrome P450 CYP94B3 mediates catabolism and inactivation of the plant hormone jasmonoyl-L-isoleucine. *Proc. Natl. Acad. Sci.*, **108**, 9298 LP – 9303.

Kudla, J., Batistic, O. and Hashimoto, K. (2010) Calcium signals: the lead currency of plant information processing. *Plant Cell*, **22**, 541–63.

Kumar, S., Mazumder, M., Gupta, N., Chattopadhyay, S. and Gourinath, S. (2016) Crystal structure of Arabidopsis thaliana calmodulin7 and insight into its mode of DNA binding. *FEBS Lett.*, **590**, 3029–3039.

Kushwaha, R., Singh, A. and Chattopadhyay, S. (2008) Calmodulin7 plays an important role as transcriptional regulator in Arabidopsis seedling development. *Plant Cell*, **20**, 1747–59.

Lenzoni, G., Liu, J. and Knight, M.R. (2018) Predicting plant immunity gene expression by identifying the decoding mechanism of calcium signatures. *New Phytol.*, **217**, 1598–1609.

Livak, K.J. and Schmittgen, T.D. (2001) Analysis of Relative Gene Expression Data Using Real-Time Quantitative PCR and the $2^{-\Delta\Delta CT}$ Method. *Methods*, **25**, 402–408.

McAinsh, M.R. and Pittman, J.K. (2009) Shaping the calcium signature. *New Phytol.*, **181**, 275–294.

Mou, Z., Fan, W. and Dong, X. (2003) Inducers of Plant Systemic Acquired Resistance Regulate NPR1 Function through Redox Changes. *Cell*, **113**, 935–944.

Piasecka, A., Jedrzejczak-Rey, N. and Bednarek, P. (2015) Secondary metabolites in plant innate immunity: conserved function of divergent chemicals. *New Phytol.*, **206**, 948–964.

Poovaiah, B.W. and Du, L. (2018) Calcium signaling: decoding mechanism of calcium signatures. *New Phytol.*, **217**, 1394–1396.

Ranf, S., Eschen-Lippold, L., Pecher, P., Lee, J. and Scheel, D. (2011) Interplay between calcium signalling and early signalling elements during defence responses to microbe- or damage-associated molecular patterns. *Plant J.*, **68**, 100–13.

Ranty, B., Aldon, D. and Galaud, J.-P. (2006) Plant calmodulins and calmodulin-related proteins: multifaceted relays to decode calcium signals. *Plant Signal. Behav.*, **1**, 96–104.

Rivas-San Vicente, M. and Plasencia, J. (2011) Salicylic acid beyond defence: its role in plant growth and development. *J. Exp. Bot.*, **62**, 3321–3338.

Rochon, A., Boyle, P., Wignes, T., Fobert, P.R. and Després, C. (2006) The Coactivator Function of Arabidopsis NPR1 Requires the Core of Its BTB/POZ Domain and the Oxidation of C-Terminal Cysteines. *Plant Cell*, **18**, 3670 LP – 3685.

Schenk, S.T., Hernández-Reyes, C., Samans, B., et al. (2014) N-Acyl-Homoserine Lactone Primes Plants for Cell Wall Reinforcement and Induces Resistance to Bacterial Pathogens via the Salicylic Acid/Oxylipin Pathway. *Plant Cell*, **26**, 2708–2723.

Schindelin, J., Arganda-Carreras, I., Frise, E., et al. (2012) Fiji: an open-source platform for biological-image analysis. *Nat. Methods*, **9**, 676–682.

Schindelin, J., Rueden, C.T., Hiner, M.C. and Eliceiri, K.W. (2015) The ImageJ ecosystem: An open platform for biomedical image analysis. *Mol. Reprod. Dev.*, **82**, 518–529.

Schmittgen, T.D. and Livak, K.J. (2008) Analyzing real-time PCR data by the comparative CT method. *Nat. Protoc.*, **3**, 1101–1108.

Seybold, H., Trempel, F., Ranf, S., Scheel, D., Romeis, T. and Lee, J. (2014) Ca2+ signalling in plant immune response: from pattern recognition receptors to Ca2+ decoding mechanisms. *New Phytol.*, **204**, 782–790.

Seyfferth, C. and Tsuda, K. (2014) Salicylic acid signal transduction: the initiation of biosynthesis, perception and transcriptional reprogramming. *Front. Plant Sci.*, **5**, 697.

Smith, J.M., Leslie, M.E., Robinson, S.J., et al. (2014) Loss of Arabidopsis thaliana Dynamin-Related Protein 2B reveals separation of innate immune signaling pathways. *PLoS Pathog.*, **10**, e1004578.

Suarez-Rodriguez, M.C., Adams-Phillips, L., Liu, Y., Wang, H., Su, S.-H., Jester, P.J., Zhang, S., Bent, A.F. and Krysan, P.J. (2007) MEKK1 is required for flg22-induced MPK4 activation in Arabidopsis plants. *Plant Physiol.*, **143**, 661–9.

Tsuda, K. and Somssich, I.E. (2015) Transcriptional networks in plant immunity. *New Phytol.*, **206**, 932–947.

Veluchamy, S., Hind, S.R., Dunham, D.M., Martin, G.B. and Panthee, D.R. (2014) Natural variation for responsiveness to flg22, flgII-28, and csp22 and Pseudomonas syringae pv. tomato in heirloom tomatoes. *PLoS One*, **9**, e106119.

Verde, V. La, Dominici, P., Astegno, A., Verde, V. La, Dominici, P. and Astegno, A. (2018) Towards Understanding Plant Calcium Signaling through Calmodulin-Like Proteins: A Biochemical and Structural Perspective. *Int. J. Mol. Sci.*, **19**, 1331.

Wang, L., Tsuda, K., Sato, M., Cohen, J.D., Katagiri, F. and Glazebrook, J. (2009) Arabidopsis CaM binding protein CBP60g contributes to MAMP-induced SA accumulation and is involved in disease resistance against Pseudomonas syringae. *PLoS Pathog.*, **5**, e1000301.

Yi, S.Y., Shirasu, K., Moon, J.S., Lee, S.-G. and Kwon, S.-Y. (2014) The activated SA and JA signaling pathways have an influence on flg22-triggered oxidative burst and callose deposition. B. S. Kim, ed. *PLoS One*, **9**, e88951.

Zhang, Y., Tessaro, M.J., Lassner, M. and Li, X. (2003) Knockout Analysis of Arabidopsis Transcription Factors TGA2, TGA5, and TGA6 Reveals Their Redundant and Essential Roles in Systemic Acquired Resistance. *Plant Cell*, **15**, 2647 LP – 2653.

Zheng, X.-Y., Zhou, M., Yoo, H., Pruneda-Paz, J.L., Spivey, N.W., Kay, S.A. and Dong, X. (2015) Spatial and temporal regulation of biosynthesis of the plant immune signal salicylic acid. *Proc. Natl. Acad. Sci.*, **112**, 9166–73.

Zidack, N.K., Backman, P.A. and Shaw, J.J. (1992) Promotion of bacterial infection of leaves by an organosilicone surfactant: Implications for biological weed control. *Biol. Control*, **2**, 111–117.

SUPPLEMENTARY TABLES AND FIGURES

Supplementary Table S1. Primers used for genotyping.

Gene ID	Primer Sequence (5' to 3') Insert 1	Primer Sequence (5' to 3') Insert 2
CAM2	F - TTTTAACCAGCAAAAACCAGC	F - ATTCGTAGCACACGAATCGTC
	R - CTCTTCTCATGTCAACCTGGC	R - CCGATAAGCATCTTCTTGCTTC
CAM7	F - TTTCCGAAATACATGCGATAAC	F - Same as *CAM7* LP1
	R – TGTGCAGAGATTCACGATCAC	R - Same as *CAM7* RP1
LBb1.3	F - ATTTTGCCGATTTCGGAAC	

Supplementary Table S2. Primers used for qPCR analyses.

Gene ID	Primer Sequence (5' to 3')	Reference to Pathogen Responsiveness
UBQ10	F - CACACTCCACTTGGTCTTGCGT	-
	R - TGGTCTTTCCGGTGAGAGTCTTCA	
SR1	F - TTCCGAGGTTACAAGGGAAG	**Du et al., (2009)**
	R - CCCCCACTGACCAAATTATC	
CBP60g	F - AATAACGAGGAGGATGAGAACG	**Zheng et al., (2015)**
	R - TCAGACACGGTAAGAAACATCG	
ICS1	F - TTCCAGCAGAAGAAGCAAGG	**Zheng et al., (2015)**
	R - GATCCCGACTGCAAATTCAC	
PR1	F - ATGTGCCAAAGTGAGGTGTAA	**Asai et al., (2002)**
	R - TTCACATAATTCCCACGAGCA	
PR5	F – AGGAACAATTGCCCTACCACC	**Asai et al., (2002)**
	R - TCCTTGACCGGCGAGAGTT	
MPK3	F - TGACGTTTGACCCCAACAGA	**Asai et al., (2002)**
	R - CTGTTCCTCATCCAGAGGCTG	
MPK6	F - CCGACAGTGCATCCTTTAGCT	**Asai et al., (2002)**
	R - TGGGCCAATGCGTCTAAAAC	

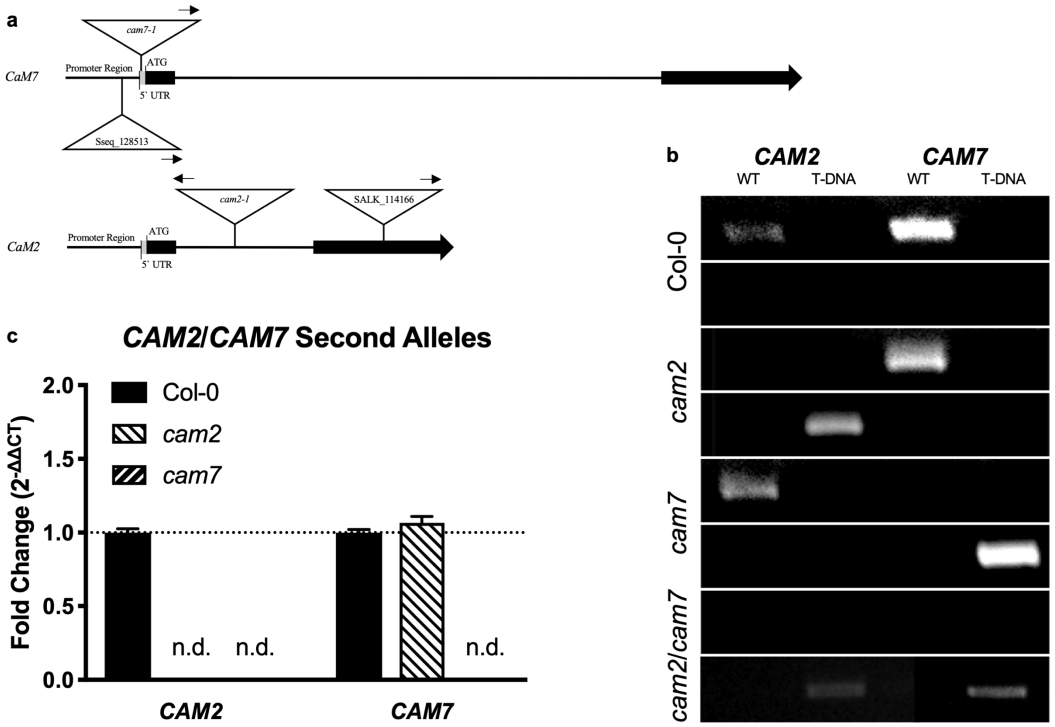

Supplementary Figure S3.1 Identification of RNA null alleles of *cam2*, *cam7*, and recovery of *cam2 cam7* double mutant plants . (**a**) Gene diagrams for *CAM2* and *CAM7*, indicating the locations of T-DNA insertions. (**b**) Gel electrophoresis after PCR with WT- and T-DNA-specific *CAM2* and *CAM7* primers indicating homozygosity of each insertional mutant. (**c**) Transcript level of *CAM2* and *CAM7* in the *cam2* and *cam7* backgrounds indicating each mutant as an RNA-null and that there was no expression of *CAM2* in the *cam7* background.

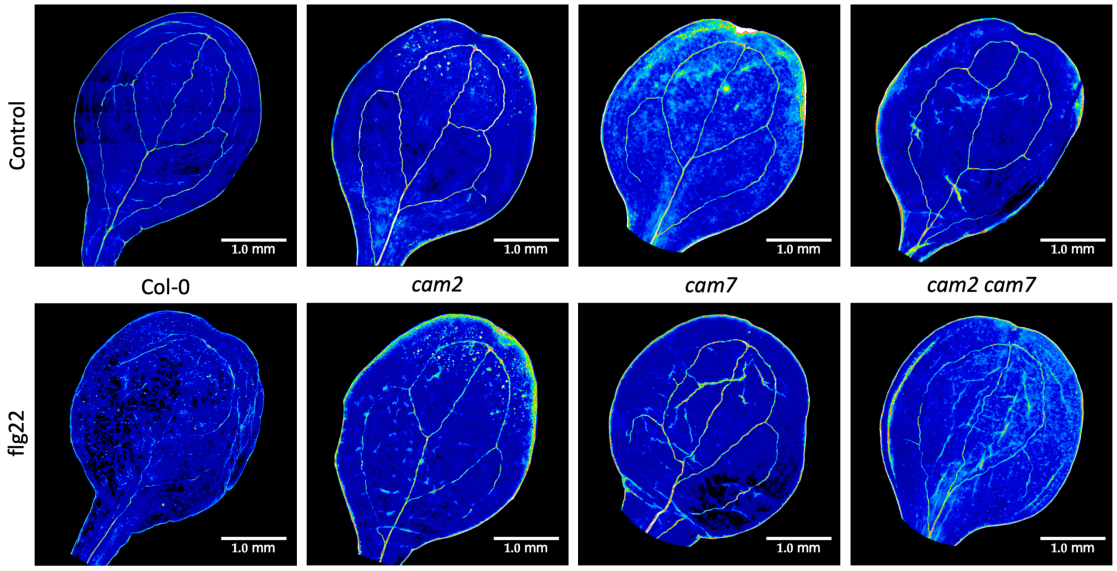

Supplementary Figure S3.2 *cam2*, *cam7*, and *cam2 cam7* mutations alter the deposition of callose in response to flg22. Col-0 deposits ~15-fold more papillae mm^{-2} after treatment with 1 µM flg22 than before. Untreated *cam2* plants produce ~8 papillae mm^{-2}, with no significant change after flg22 treatment. Untreated *cam7* and *cam2 cam7* plants were not different from Col-0 but deposited significantly less callose after flg22 treatment. Images are representative of the phenotypes for each plant line; n ≥ 12, per line.

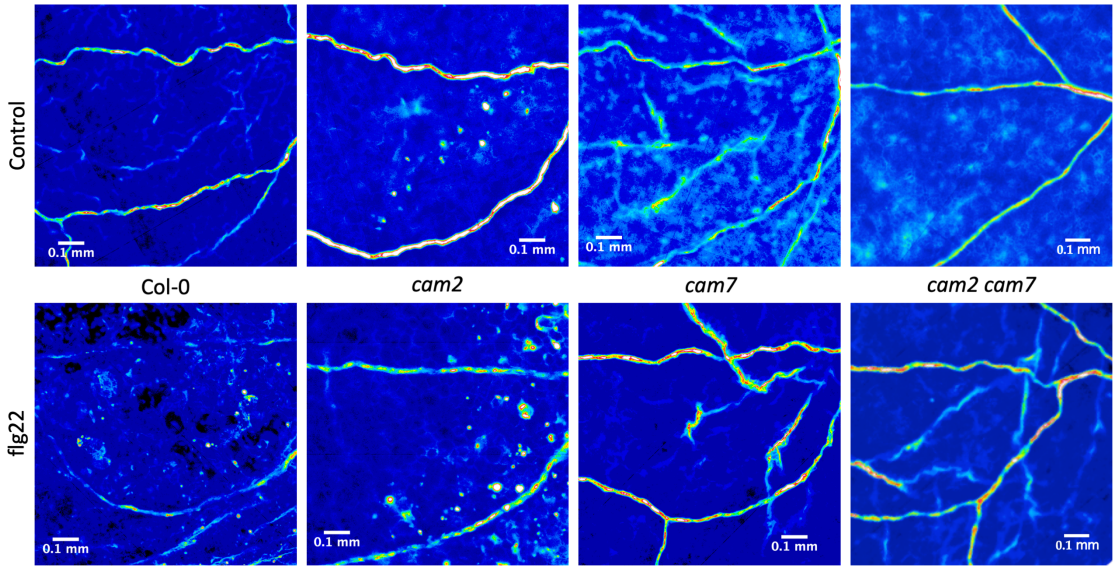

Supplementary Figure S3.3 *cam2*, *cam7*, and *cam2 cam7* mutations alter the deposition of callose in response to flg22. Col-0 deposits ~15-fold more papillae mm^{-2} after treatment with 1 µM flg22 than before. Untreated *cam2* plants produce ~8 papillae mm^{-2}, with no significant change after flg22 treatment. Untreated *cam7* and *cam2 cam7* plants were not different from Col-0 but deposited significantly less callose after flg22 treatment. Images are representative of the phenotypes for each plant line; n ≥ 12, per line.

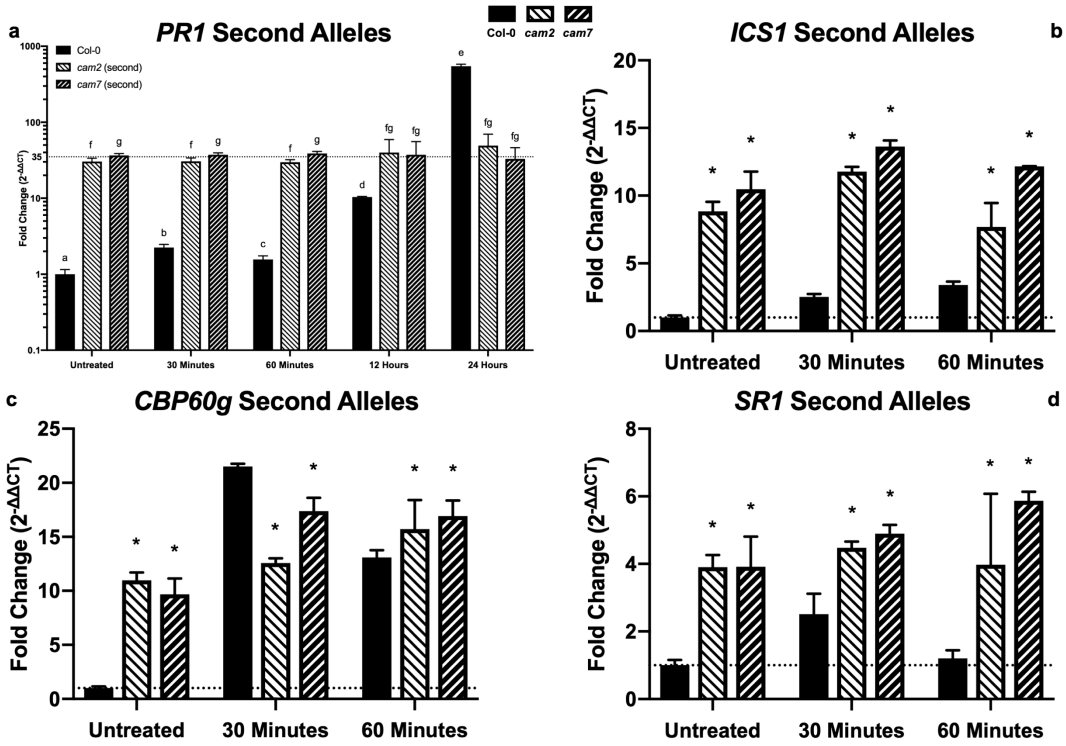

Supplementary Figure S3.4 *cam2* and *cam7* plants exhibit altered defense-related gene expression. Transcript levels of 10-day-old seedlings treated with 1 µM flg22 for 0 (untreated), 30, and 60 minutes. (**a**) Transcript level of *PR1*. (**b**) Transcript level of *ICS1*. (**c**) Transcript level of *CBP60g*. (**d**) Transcript level of *SR1*. Relative fold-change ($2^{-\Delta\Delta Ct}$) values were obtained by normalizing to untreated Col-0. Results represent mean ± s.d.; n = 3 biological replicates with 4 technical replicates from 3 independent experiments. Columns with asterisks (*) are statistically different from Col-0 at the given time point (2-way ANOVA; Dunnett's Test; $p < 0.05$).

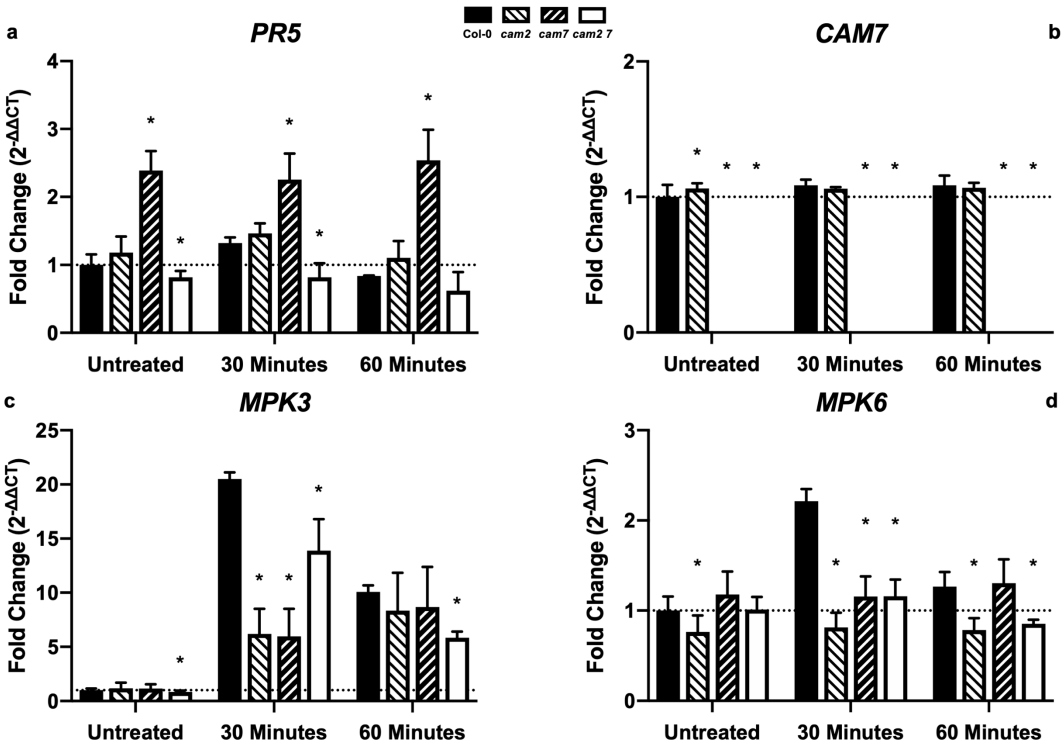

Supplementary Figure S3.5 *cam2*, *cam7*, and *cam2 cam7* plants exhibit altered *PR5*, *CAM7*, *MPK3*, and *MPK6* gene expression. Transcript levels of 10-day-old seedlings treated with 1 µM flg22 for 0 (untreated), 30, and 60 minutes. (**a**) Transcript level of *PR5*. (**b**) Transcript level of *CAM7*. (**c**) Transcript level of *MPK3*. (**d**) Transcript level of *MPK6*. Fold-change ($2^{-\Delta\Delta Ct}$) values are relative to untreated Col-0. Results represent mean ± s.d.; n = 3 biological replicates with 4 technical replicates from 3 independent experiments. Columns with asterisks (*) are statistically different from Col-0 at the given time point (2-way ANOVA; Dunnett's Test; $p < 0.05$).

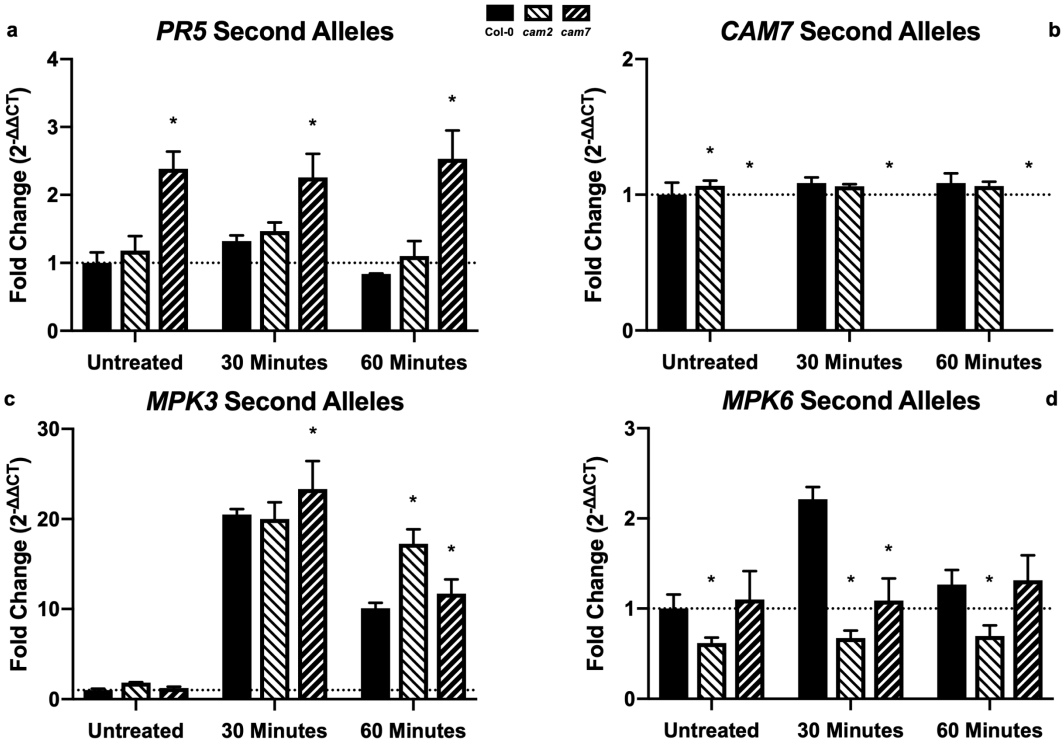

Supplementary Figure S3.6 *cam2* and *cam7* plants exhibit altered *PR5*, *MPK3*, *TCH2*, and *TCH3* gene expression. Transcript levels of 10-day-old seedlings treated with 1 µM flg22 for 0 (untreated), 30, and 60 minutes. (**a**) Transcript level of *PR5*. (**b**) Transcript level of *CAM7*. (**c**) Transcript level of *MPK3*. (**d**) Transcript level of *MPK6*. Relative fold-change ($2^{-\Delta\Delta Ct}$) values were obtained by normalizing to untreated Col-0. Results represent mean ± s.d.; n = 3 biological replicates with 4 technical replicates from 3 independent experiments. Columns with asterisks (*) are statistically different from Col-0 at the given time point (2-way ANOVA; Dunnett's Test; $p < 0.05$).

Chapter 4:

Significance and Future Perspectives

INTRODUCTION

The work contained in this dissertation provides evidence for the involvement of CaMs and CMLs in the responses to pathogens and touch stimuli. I began by describing the numerous response networks and pathways in which CaMs and CMLs are involved. The genetic regulation of CaM and CML expression, their involvement in other regulatory pathways, and their impact on plant responses to diverse stimuli are areas of intense research, and, as such, the resources to mine data describing their involvement in these systems are rich. Using these bioinformatics tools, I tested the characterization of certain *CAM* and *CML* transcripts – by Lee *et al.*, (2005) – as belonging to a highly-connected touch-responsive gene network. My evidence suggests that, on the whole, this characterization is correct. Further, I desired to test whether or not these genes, and the CaM and CML proteins they encode, were, at least in parallel, also involved in plant immunity. Indeed, my evidence suggests that some of the members of the touch-responsive network are involved in pathogen responses. These findings represent new insights into the intersection of stress-response pathways and, as with all steps forward, they have opened up many questions to answer and research avenues to go down. For example, CaM2, CaM7, and CML24 – three of the more intriguing members of this putative touch- and pathogen-responsive network due to their significantly-altered transcriptional and physiological responses to touch and pathogen treatments – merit significant further study. In the following sections I will highlight areas where I think my research has contributed to these new insights and introduce examples of the directions that my work may suggest for future investigations.

The Involvement of CaM2 and CaM7 in Plant Immunity

I have quantified the relative expression of a number of pathogen-response marker genes and found that mutations in *CAM2* and *CAM7* lead to altered expression patterns. Specifically, I found that the combination of near-constitutive induction of *CBP60g* and *SR1*, relative to Col-0, in these mutant backgrounds was accompanied by apparent constitutive expression of *ICS1*, irrespective of MAMP (flg22) treatment. ICS1 is an enzyme in a key intermediate step in SA production and its levels are usually taken as indications of modulation of SA production. Surprisingly, this increased level of *ICS1* induction did not lead to an expected increase in SA production (Wildermuth *et al.*, 2001), perhaps due to a lack of precursor (chorismate). However, *PR1* expression, which is frequently induced by SA production during plant immune responses (Tsuda *et al.*, 2013) was significantly elevated in these backgrounds, again, irrespective of flg22 treatment.

So, one clear direction for future study would be to investigate the relationship between mutations in *CAM2* and/or *CAM7* and the regulation of *PR1* expression. First, I think that the disconnect between *ICS1* induction and SA production is an important finding, worthy of follow up. CaM has been shown to be required for the *ICS1*-regulating activity of both *CBP60g* and *SR1*, as mutating residues in the CaM binding domains of each led to reduced and increased SA production, respectively (Wang *et al.*, 2009; Du *et al.*, 2009). Perhaps, CaM2 and CaM7 are the particular CaMs involved in regulating the expression of *ICS1* via *CBP60g* and *SR1*. This seems a reasonable idea, as my results indicate that CaM2 and CaM7 act downstream of MPK3/6 function but upstream of *PR1* expression.

The next step would be to determine the cause of the missing link between constitutive *ICS1* expression in these mutants and SA production. One important consideration is that *ICS1* expression may not reflect ICS1 protein levels (although this is the expectation in many papers on

SA and immunity). In addition, upregulation of *ICS1* expression would not *immediately* lead to increased SA levels. Quantification of chorismate and isochorismate, precursors of SA, after treating these mutants and wild type with flg22 could provide some needed elucidation. Another consideration is that the ICS1-dependent SA production pathway is not the only system responsible for SA production. Indeed, ICS2 (an ISC1 homolog) and phenylalanine ammonia lyase (PAL) also operate in parallel with ICS1 to produce SA to bolster plant defenses (Shine *et al.*, 2016), although the bulk of SA production appears to occur through ICS1 or ICS2 (Chen *et al.*, 2009). Therefore, I think it is now important to determine whether transcript abundance of *ICS1* in the *cam2*, *cam7*, and *cam2 cam7* mutants correlates with increased ICS1 protein enrichment, relative to Col-0. This would be a first step towards asking where the key regulatory steps in SA production could be.

The Possible Regulation of *CAM2* Expression by CaM7

One unexpected observation about the plant lines harboring the two *CAM7* mutant alleles that I experimented on is that *CAM2* expression is abolished. I think this is another key observation worthy of more investigation. This observation is not a relative expression problem, as we performed qPCR for the typical 40 cycles and saw no Ct curves for *CAM2* in *cam7* samples, a rather good indication that no transcript exists in the mRNA pool. Indeed, we measured *CAM2* levels in Col-0 and every other genotype we assayed, indicating that priming of oligonucleotides was also not an issue. Additionally, the oligonucleotides for transcriptional analyses via qPCR were designed to lie in the 3' UTR, just past the transcriptional stop site, a region devoid of homology between *CAM* genes encoding CaM isoforms.

It would seem that *cam7* plants should also be *bona fide cam2* RNA-null plants and behave as such. Generally speaking, my results indicate this is the case, as, especially at the level of gene

expression, it can be hard to distinguish a *cam7* mutant from a *cam2* mutant (e.g. in **Figure 3.2** and **Supplementary Figures S3.4, S3.5, and S3.6**), except with regard to *CAM7* expression. However, I did observe some pretty stark phenotypic differences with regard to both touch- and pathogen-responses (**Figure 2.3** and **3.4**, respectively) between the *CAM2* and *CAM7* nulls. What causes, then, the contrast between similar molecular phenotypes in *cam2* and *cam7* mutants but rather dissimilar physiological responses to these two stress stimuli?

Answers to this question could come from further research into the potential regulation of *CAM2* expression by CaM7; while I have found that there are two regulatory domains that could be bound by CaM7 in the promoter of *CAM2*, further biochemical analysis would be necessary to determine if this binding is likely, *in vivo* (as in Abbas *et al.*, 2014) and whether it leads to CAM7-dependent regulation of the *CAM2* promoter. This could be accomplished via various binding assays, such as DNA electrophoretic mobility shift; chromatin immunoprecipitation; DNA pulldown; microplate capture and detection; and reporter assays. Further characterization of the *cam2 cam7* double mutant could also provide insight into the unexpected disconnect between gene expression and phenotype, in these mutants, and the differences between the single and double mutants.

What Does it Mean that Two CaM Mutants in *Arabidopsis* Exhibit 10-Fold Increases in Resistance to One Particular Bacterial Pathogen?

The field as a whole now has a fairly well-characterized molecular network to describe the response to *Pto* DC3000. A lot of effort has been expended in cataloging the ins-and-outs of the plant response to the *Pseudomonads* (with extensive analyses of PTI, ETI, SAR, HR, etc.) and other plant pathogens. This effort has led to the development of numerous tools for analyzing the

defensive capabilities of plants (especially *Arabidopsis thaliana* and *Solanum lycopersicum*). Although my work highlights defense-related functions of the CaMs and CMLs (particularly the TCH proteins) against *Pto* DC3000, the functions of these proteins in response to other pathogens should be further elucidated. Therefore, while I have used the existing models to guide my analysis of CaM/CML action in defense - I have jumped into the stream and let it carry me along, with my peers – there is plenty of room for future plant pathological study.

Ah, but the Socratic question posed above is less about 'why have we done what we've done?' and more about 'what are the implications?' Often, the results of pathogenicity assays using *Pto* DC3000 are preliminary screens that lead to experiments using elicitors from other bacterial (or fungal, or insect) pests. Indeed, there is evidence of homology and parallel/shared responses in these systems, especially as they relate to Ca^{2+} signatures (Kwaaitaal *et al.*, 2011) – as intriguing plant genotypes are frequently challenged with other flagellin epitopes, EF-Tu-derived peptides, and fungal and insect chitin – and the more we explore the signaling cascade precipitated by one elicitor of plant defenses, the more we potentially learn about others.

Not only do my results suggest the potential for improvement in responses to various pests of *Arabidopsis* through manipulation of CaM2 and CaM7, there is also the real possibility that the discoveries I have made using this system could be translated to crop species. Importantly, I think that translational research into the activity of CaM and CML homologs in plant defense could yield insights into methods of improving crop species and minimizing the economic or food-safety impacts of bacterial, fungal, and insect pests. The key observation here is that *CAM2* and *CAM7* knockouts enhance defense without an obvious tradeoff in vegetative growth. One important consideration is that we do not know whether the enhanced response to *Pto* DC3000 would carry over to other pathogens. This would be an important observation to follow up on in both

Arabidopsis and in mutants of orthologous genes in crops. Therefore, investigating avenues for *Arabidopsis*-based and translational research into the CaM/CML-mediated pathogen-response network in crop species would be a natural outcome of this research.

Other Interesting Findings in the Network Analysis

Certainly, I have not explored every avenue for analysis of the touch- (and, putative pathogen-) responsive genes identified by Lee *et al.* (2005). Foremost in my mind is the role that *CML24* (*TCH2*) plays in these responses. TCH2 may be a true hub of activity, integrating and decoding Ca^{2+} signatures produced in response to diverse stimuli and interacting with numerous systems (Delk *et al.*, 2005; Tsai *et al.*, 2007; Ma *et al.*, 2008; Wang *et al.*, 2011; Tsai *et al.*, 2013; Yang *et al.*, 2014). Additionally, I think *CML12* (*TCH3*) is an incredibly interesting member of this network, being both a canonical touch-responsive gene and having a previously identified role in defense against insect feeding (Vadassery *et al.*, 2012; Aldon *et al.*, 2018). Finally, *CML5* and *CML9* are two potentially important members of the network, especially in the context of defense responses. CML5 sticks out not just because of our analyses, but as it is one of only two (the other being CML4) CaM/CML proteins that is membrane-bound and targeted to the endomembrane system (Ruge *et al.*, 2016). CML9, on the other hand, has been found to be involved in flagellin-dependent signaling, negatively regulating *PR1* expression and callose deposition (Leba *et al.*, 2012). Therefore, *CML5* and *CML9* could also be sources of fruitful follow-up studies.

Oh! Come and See the *Fallacy* Inherent in the System!

With an eye toward the future of technology used in molecular biology, I see relative fold-change as an Achilles heel of qPCR. Therefore, while it has always been clear that to compare fold-

induction between genes is fraught with potential problems, perhaps we need to take the lesson to heart and abandon relative gene expression measures altogether. I would invest in RNAseq-based transcription profiling of the mutants in this study. Uncoupling the inferred expression of these defense marker genes from reference genes – that may vary in expression depending on growth conditions and treatments – would add credibility to the kinds of analyses I, and my peers, have performed and the resultant widespread survey of molecular responses is almost certain to open up new molecular pathways to be explored. Lastly, I would propose to attempt to correlate the expression of critical defense marker genes with the enrichment of the proteins they encode, as this is induction in its truest form.

LITERATURE CITED

Abbas, N., Maurya, J.P., Senapati, D., Gangappa, S.N. and Chattopadhyay, S. (2014) Arabidopsis CAM7 and HY5 physically interact and directly bind to the HY5 promoter to regulate its expression and thereby promote photomorphogenesis. *Plant Cell*, **26**, 1036–52.

Aldon, D., Mbengue, M., Mazars, C. and Galaud, J.-P. (2018) Calcium Signalling in Plant Biotic Interactions. *Int. J. Mol. Sci.*, **19**, 665.

Chen, Z., Zheng, Z., Huang, J., Lai, Z. and Fan, B. (2009) Biosynthesis of salicylic acid in plants. *Plant Signal. Behav.*, **4**, 493–6.

Delk, N.A., Johnson, K.A., Chowdhury, N.I. and Braam, J. (2005) CML24, regulated in expression by diverse stimuli, encodes a potential Ca^{2+} sensor that functions in responses to abscisic acid, daylength, and ion stress. *Plant Physiol.*, **139**, 240–53.

Du, L., Ali, G.S., Simons, K.A., Hou, J., Yang, T., Reddy, A.S.N. and Poovaiah, B.W. (2009) Ca2+/calmodulin regulates salicylic-acid-mediated plant immunity. *Nature*, **457**, 1154–1158.

Kwaaitaal, M., Huisman, R., Maintz, J., Reinstädler, A. and Panstruga, R. (2011) Ionotropic glutamate receptor (iGluR)-like channels mediate MAMP-induced calcium influx in *Arabidopsis thaliana*. *Biochem. J.*, **440**, 355–373.

Leba, L.-J., Cheval, C., Ortiz-Martín, I., Ranty, B., Beuzón, C.R., Galaud, J.-P. and Aldon, D. (2012) CML9, an Arabidopsis calmodulin-like protein, contributes to plant innate immunity through a flagellin-dependent signalling pathway. *Plant J.*, **71**, 976–89.

Lee, D., Polisensky, D.H. and Braam, J. (2005) Genome-wide identification of touch- and darkness-regulated Arabidopsis genes: a focus on calmodulin-like and XTH genes. *New Phytol.*, **165**, 429–44.

Ma, W., Smigel, A., Tsai, Y.-C., Braam, J. and Berkowitz, G.A. (2008) Innate immunity signaling: cytosolic Ca2+ elevation is linked to downstream nitric oxide generation through the action of calmodulin or a calmodulin-like proteins. *Plant Physiol.*, **148**, 818–28.

Ruge, H., Flosdorff, S., Ebersberger, I., Chigri, F. and Vothknecht, U.C. (2016) The calmodulin-like proteins AtCML4 and AtCML5 are single-pass membrane proteins targeted to the endomembrane system by an N-terminal signal anchor sequence. *J. Exp. Bot.*, **67**, 3985–96.

Shine, M.B., Yang, J.-W., El-Habbak, M., Nagyabhyru, P., Fu, D.-Q., Navarre, D., Ghabrial, S., Kachroo, P. and Kachroo, A. (2016) Cooperative functioning between phenylalanine ammonia lyase and isochorismate synthase activities contributes to salicylic acid biosynthesis in soybean. *New Phytol.*, **212**, 627–636.

Tsai, Y.-C., Delk, N.A., Chowdhury, N.I. and Braam, J. (2007) Arabidopsis potential calcium sensors regulate nitric oxide levels and the transition to flowering. *Plant Signal. Behav.*, **2**, 446–54.

Tsai, Y.-C., Koo, Y., Delk, N.A., Gehl, B. and Braam, J. (2013) Calmodulin-related CML24 interacts with ATG4b and affects autophagy progression in Arabidopsis. *Plant J.*, **73**, 325–35.

Tsuda, K., Mine, A., Bethke, G., Igarashi, D., Botanga, C.J., Tsuda, Y., Glazebrook, J., Sato, M. and Katagiri, F. (2013) Dual Regulation of Gene Expression Mediated by Extended MAPK Activation and Salicylic Acid Contributes to Robust Innate Immunity in Arabidopsis thaliana H. Hirt, ed. *PLoS Genet.*, **9**, e1004015.

Vadassery, J., Scholz, S.S. and Mithöfer, A. (2012) Multiple calmodulin-like proteins in Arabidopsis are induced by insect-derived (Spodoptera littoralis) oral secretion. *Plant Signal. Behav.*, **7**, 1277–80.

Wang, L., Tsuda, K., Sato, M., Cohen, J.D., Katagiri, F. and Glazebrook, J. (2009) Arabidopsis CaM binding protein CBP60g contributes to MAMP-induced SA accumulation and is involved in disease resistance against Pseudomonas syringae. *PLoS Pathog.*, **5**, e1000301.

Wang, Y., Wang, B., Gilroy, S., Wassim Chehab, E. and Braam, J. (2011) CML24 is Involved in Root Mechanoresponses and Cortical Microtubule Orientation in Arabidopsis. *J. Plant Growth Regul.*, **30**, 467–479.

Wildermuth, M.C., Dewdney, J., Wu, G. and Ausubel, F.M. (2001) Isochorismate synthase is required to synthesize salicylic acid for plant defence. *Nature*, **414**, 562–565.

Yang, X., Wang, S.-S., Wang, M., Qiao, Z., Bao, C.-C. and Zhang, W. (2014) Arabidopsis thaliana calmodulin-like protein CML24 regulates pollen tube growth by modulating the actin cytoskeleton and controlling the cytosolic Ca(2+) concentration. *Plant Mol. Biol.*, **86**, 225–36.

Appendix I:

The Automated Botanical Contact Device: Conception and Application

This chapter has been formatted for submission to *Plant Methods*.

I would like to acknowledge the following people for contributing to the results for this chapter: Caleb P. Fitzgerald, Nathan Miller, Jerry Miao, Johnathan Lombardino, and Simon Gilroy.

Caleb P. Fitzgerald designed and constructed the apparatus and programmed the software that operates it. I was responsible for assisting with the expansion of the apparatus and generating all of the results. Nathan Miller developed the image-analysis software used herein. Jerry Miao developed the software for operating the imaging components. Johnathan Lombardino nurtured the plants in this study. Simon Gilroy and I wrote all parts of the manuscript.

INTRODUCTION

Under current methods of greenhouse and growth chamber cultivation, plants do not receive the frequent, ambient mechanical (e.g. touch) stimuli they would experience when growing outdoors. There are no changing winds, no rain, and – ideally – no other organisms brushing against them. This lack of touch stimulus can lead to plant morphology that deviates wildly from that of field-grown plants. For example, plants grown in growth chambers have enlarged leaves and elongated petioles [1]. They are also naïve with regard to many stresses, as they lack the priming stimuli provided by natural biotic and abiotic interactions [2]. Indeed, greenhouse-grown plants are prone to a range of related issues such as increased susceptibility to pathogen attack and reduced stress tolerance.

Touch stimulation is known to improve agronomically/horticulturally important plant features such as pathogen resistance and time of flowering. Using fans to simulate wind and employing people to brush plants with canes are common attempts at a solution to this issue. However, the plants remain weak and frail compared to field-grown plants. In addition, the mechanical stimulation is highly heterogeneous and poorly controlled, when using these approaches. This results in reduced agronomic output and increased use of exogenous chemical and energy inputs. Importantly, for research purposes, these kinds of “artificial” mechanical stimuli are very hard to reproducibly apply over long periods of time

Creating a device that could systematically provide touch stimuli to plants, such as the model plant *Arabidopsis thaliana*, and track morphometric and physiological changes would enable researchers to approach both fundamental and applied questions about the touch-induced regulation of plant growth. In fact, while automated systems that analyze phenotypic differences using various imaging techniques are common [3], a high-throughput device for applying repeat

mechanical stimulus while also measuring its effect has yet to be published. An additional benefit, the commercial use of a scalable, configurable, and tightly regulated touch stimulus device would provide less-costly approach to manipulate plants and alleviate the symptoms of indoor growth.

Accordingly, we have developed a device that provides controlled, intermittent touch stimulation to plants, on a row-by-row basis. The device is called the Automatic Botanical Contact Device (ABCD). The equipment design breaks down into four major components: (1) the frame and lighting apparatus, designed to provide structure to the device and allow for sustained growth during extended experiments; (2) a linear motion assembly to allow for a stimulation arm to move back and forth; (3) wiring and electronics for control of the linear motion assembly; and (4) camera mounts, cameras, and independent computer control, to allow for continuous, highly configurable image capture.

Frame and Lighting

In order to provide necessary rigidity for the stimulation bar's movement without transmitting vibration throughout the structure, plus the need to support multiple flats of plants with the associated weight of soil and water, the equipment was constructed of extruded 6105-T5 aluminum (80/20 Inc., Columbia City, IN, USA). Building from the ground up, construction began with the truss system and then the rectangle platform on which the plants grew (**Figure i.1a**). A platform rack with an adjustable frame was designed to accommodate flats of different sizes (**Figure i.2a**). To increase throughput, the unit employed stackable Tier N platforms (**Figure i.1b**), allowing multiple independent experiments to be conducted. In its most recent iteration, the ABCD was configured with two tiers: Tier 1 (including the truss system) and Tier 2.

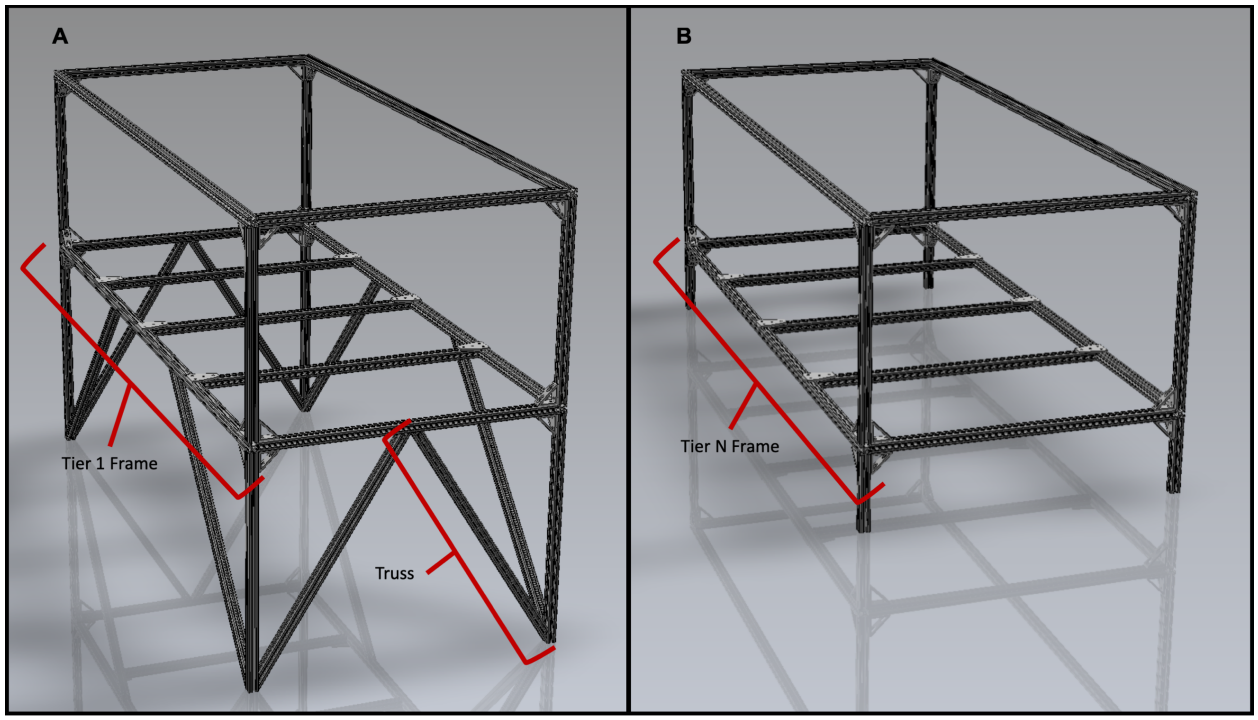

Figure i.1 Design of Automated Botanical Contact Device Frame and Support Structure. (**A**) Computer model of the structural design of the Tier 1 frame and support trusses. (**B**) Computer model of the structural design of the Tier N frame. The final outside dimensions of both structures are 10' x 4', with a combined height of 8'. Both Structures are made from 1.00" x 1.00" T-slotted extruded aluminum bars that are reinforced by tall gusseted inside corner brackets at the angles. Support cross bars are joined to the frame by tee flat plates. 45 degree support bars provide structural integrity to the trusses on the Tier 1 frame. All components are from 80/20 Inc. (Columbia City, IN, USA).

The lighting apparatus was constructed of the same extruded aluminum as the frame. Five two-foot LED fixtures, connected in series and controlled by a plug timer, were mounted, spanning the width of the plant growth area (**Figure i.2b**). One lighting apparatus was installed atop the Tier 1 frame and the other was installed above the Tier 2 frame. These two lighting apparatuses are wired independently to allow for separate day-night light cycles. Affixing a breathable black fabric mesh around the outside of the Tier 1 and Tier 2 frames completes the configuration of the independent lighting zones.

Linear Motion Assembly

The linear motion assembly consisted of an X-Carve linear motion gantry and a MakerSlide (**Figure i.2c** and **i.2d**, respectively; both components from Inventables, Chicago, IL, USA). An extruded aluminum bar (touch bar; **Figure i.4c**) was connected between two gantry side plates (**Figure i.2c**; Inventables). To the outside of the gantry side plates, stepper motors (**Figure i.2c**; Inventables) that run in-series on the MakerSlide rails, were installed. These stepper motors allowed the bar to be moved backward and forward under user control. Dual bearing V-wheels (**Figure i.2c**; Inventables) mounted to the gantry plates provided tension against the frame and smooth idler wheels (**Figure i.2c**; Inventables) were installed to reduce friction as the drivetrain rolls along the MakerSlide rails. The stepper motors that drove the touch bar were guided by GT2

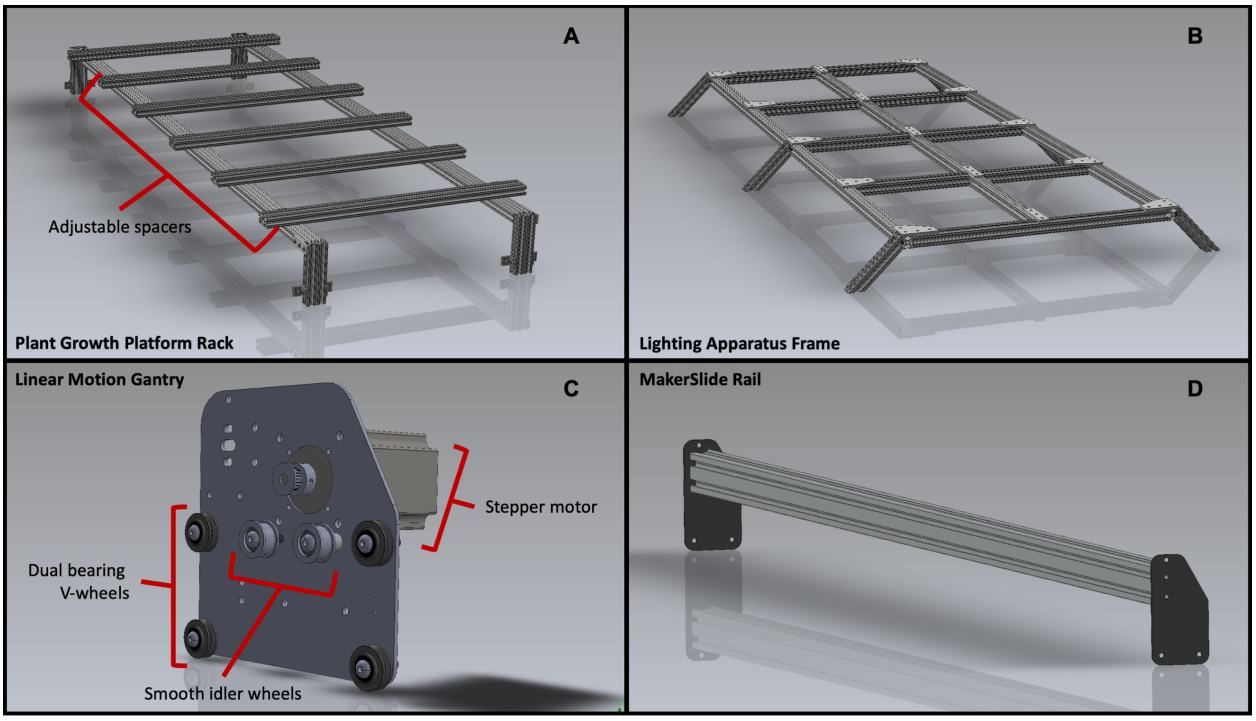

Figure i.2 Design of Plant Growth Platform, Lighting Apparatus, and Linear Motion Assembly. (**A**) Computer model of the structural design of the Plant Growth Platform Rack. Flats of plants fit between the adjustable spacers. (**B**) Computer model of the structural design of the Lighting Apparatus frame. In the assembled apparatus, LED ballasts are affixed to the underside. (**C**) Computer model of the Linear Motion Gantry, as assembled. (**D**) Computer model of the MakerSlide Rail. The dual bearing V-wheels on the Linear Motion Gantry in **C** slide on the MakerSlide Rail in **D.** Components in **A** and **B** are from 80/20 Inc. (Columbia City, IN, USA). Components of **C** and **D** are from Inventables (Chicago, IL, USA).

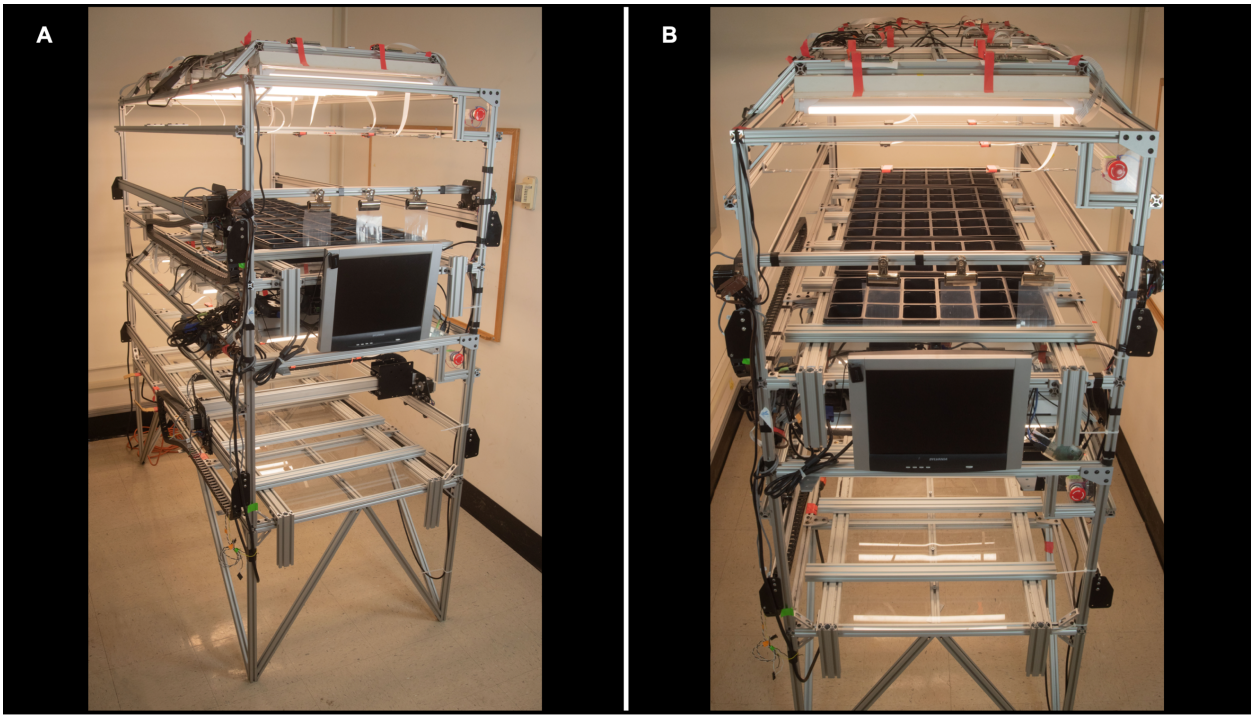

Figure i.3 Automated Botanical Contact Device, Assembled. (**A**) Angle view of the ABCD, upon assembly. (**B**) Front view of the ABCD, upon assembly. This self-contained unit can hold 10 flats with 18 traditional inserts, each. The plant growth platform rack (**Figure i.2a**) can be moved vertically to adjust light intensity. 20 Raspberry Pi computers, each outfitted with one Pi camera, can be configured to image plants at any pre-assigned interval, via the interface at the front. Affixed to the Touch Bar are three bulldog clips that can hold various materials for touch stimulus. The Touch Bar can also be configured to apply touch stimulus to rows of plants at any pre-assigned interval.

belting (**Figure i.5d**; Inventables) connected at both ends of the MakerSlide rails. Outside of the gantry, a drag chain (**Figure i.3a**; Inventables) protected power and communication cables from the drivetrain mechanisms. Additionally, the material used to contact the plants was fixed to this bar by X-ACTO bulldog clips (**Figure i.5a**; Elmer's Products, Inc., Westerville, OH, USA) using adjustable slide-in T-nuts (80/20, Inc., Columbia City, IN, USA). Although multiple materials could be used, clear polyethylene plastic sheets were found to provide stiff but flexible touch stimuli that were highly reproducible. Cutting thin strips in the polyethylene sheets, like fingers, reduced drag, preventing injury to, or uprooting of, the plants (**Figure i.5a**).

Electronics and Wiring for Linear Motion Assembly

To drive the Linear Motion Assembly, the combination of an Arduino Uno (Arduino, Somerville, MA, USA) and an Arduino gShield (Inventables) was employed (**Figure i.5c**). The Arduino gShield controlled the stepper motors driving each linear motion gantry along the GT2 belting. A 30353-07 enclosed power supply (**Figure i.5c**) provided power to the Arduino, Arduino gShield, and cooling fan. A Raspberry Pi sent commands to the Arduino gShield via a master interface at the front of the ABCD (**Figure i.4c**). Providing the commands from the Raspberry Pi to the Arduino gShield was a software interface called Universal Gcode Sender. Universal Gcode Sender delivered Gcode commands to the Arduino, which used GRBL command language to execute the commands via the connection between the Arduino gShield and the stepper

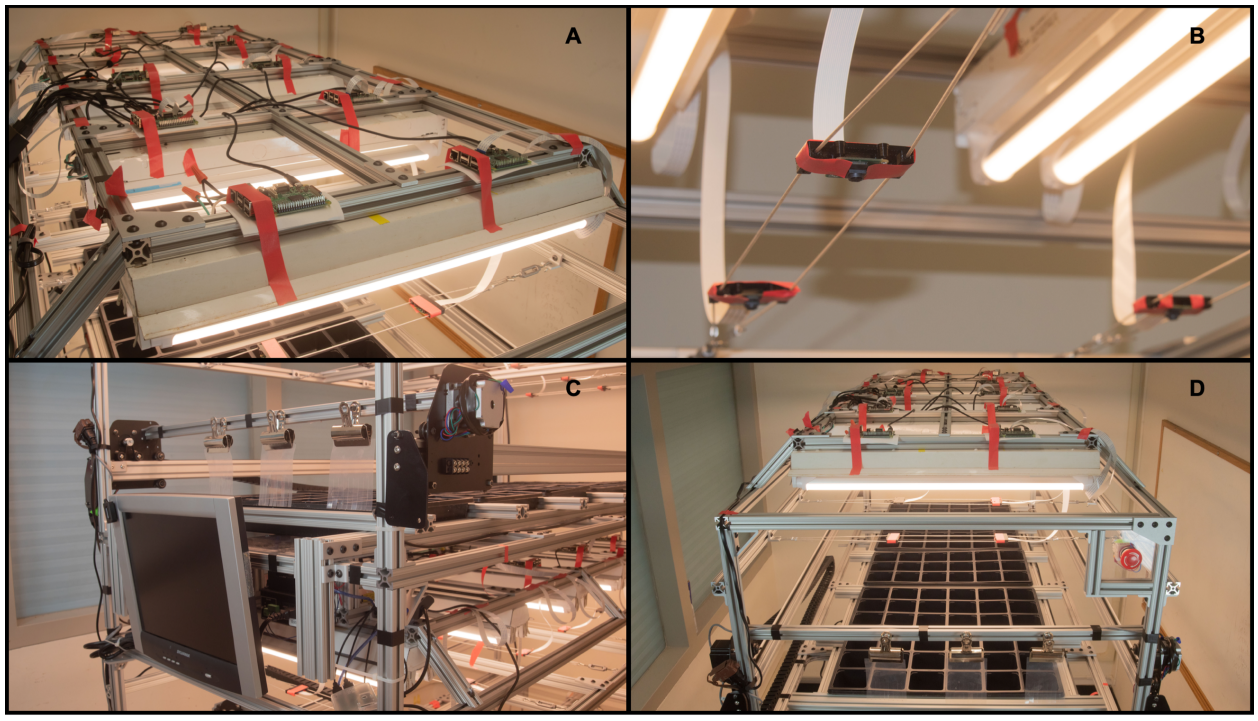

Figure i.4 Automated Botanical Contact Device, Detail Views. (**A**) 10 Raspberry Pi computers are affixed to the top of each Lighting Apparatus frame. Each computer can be configured individually or as slaves to the master interface. (**B**) The Raspberry Pi cameras are mounted to steel cables. The steel cables are attached at either end to inside corner brackets attached to T-slotted bars, and can be adjusted using slide-in T-nuts. (**C**) The master interface, Touch Bar, and Linear Motion Gantry. (**D**) View of the Tier N structure. An emergency stop button is affixed to the Tier N frame to allow instantaneous shut down of the Linear Motion Gantry and Touch Bar.

motors. Commands for movement along the x-axis were decoded, driving the Linear Motion Assembly from one end of the ABCD to the other, and back. Additionally, GRBL commands could encode movement along three axes, enabling future expansion of the hardware.

Imaging Components

The final pieces required for plant imaging-ready assembly of the ABCD were the cameras and the systems to control them. To this end, a scalable, inexpensive option was employed: Raspberry Pi computers and cameras (**Figure i.4a** and **i.4b**; Raspberry Pi Foundation, Cambridge, UK). In the most recent iteration, 20 Raspberry Pi computers controlled 20 Raspberry Pi cameras. The computers were networked wirelessly and controlled by a master Raspberry Pi via a software

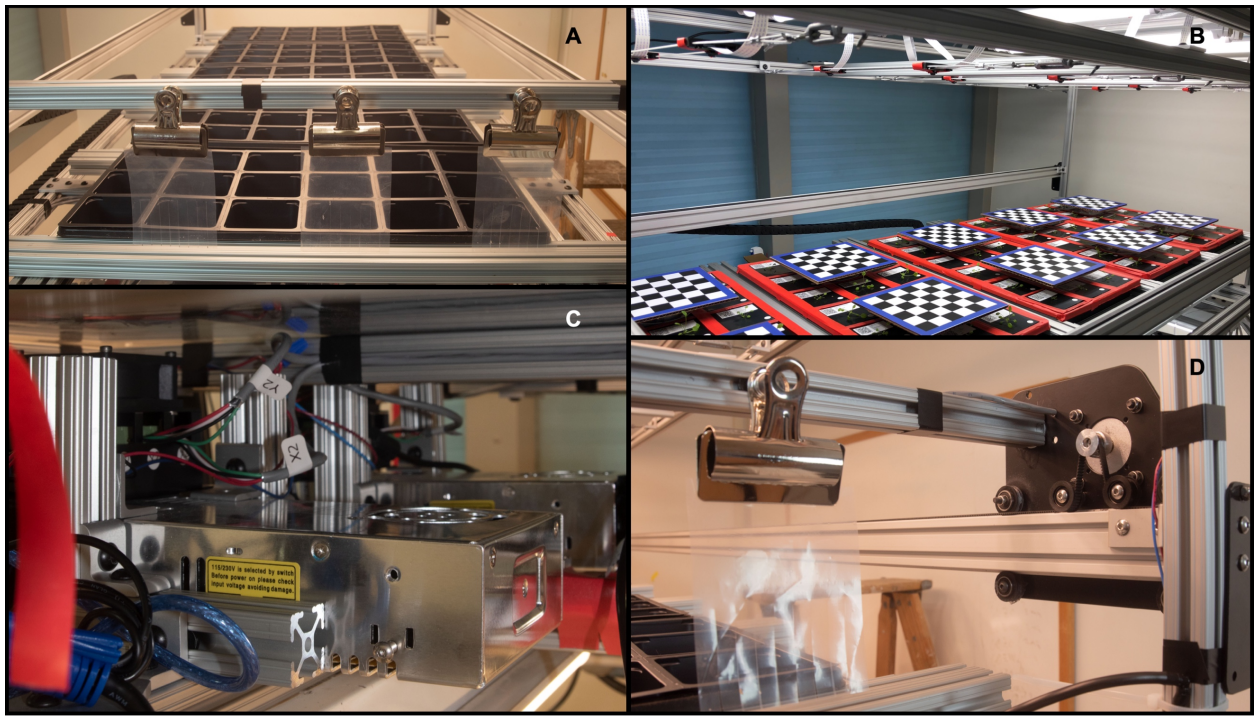

Figure i.5 Automated Botanical Contact Device, Detail Views (continued). (**A**) The touch bar configured with three polyethylene sheets, for staggered row touching. (**B**) Flats with checkerboards that allow for off-angle adjustments after image acquisition. (**C**) An Arduino Uno, gShield controller, power supply and fan control the stepper motors driving the Linear Motion Gantry. (**D**) The Linear Motion Gantry is mounted on the MakerSlide rail. The gantry is driven along by the stepper motor and GT2 belting, which is affixed to the MakerSlide rail. The bulldog clip holding the polyethylene sheet is attached to the Touch Bar by a slide-in T-nut. Adjustments to the bulldog clip are made by loosening the screw in the slide-in T-nut.

interface called Flashlapse ABCD, developed by Jerry Miao (undergraduate engineering student, UW-Madison, Madison, WI, USA). The Flashlapse ABCD interface ran on Python (Python Software Foundation, Wilmington, DE, USA) and allowed users to schedule image acquisition at any interval and automatically upload to a cloud storage service or a user's CyVerse.org (CyVerse, University of Arizona Bioscience Research Laboratories, Tucson, AZ, USA) data store.

CyVerse, an NSF-funded data infrastructure provider, allows registered users to import, share, and store data; analyze data via their Discovery Environment platform; use fully-configurable virtual machines for high-power computation; and interact with experts to devise new methods of data analysis. Using CyVerse's Discovery Environment for implementation, Dr. Nathan Miller developed the phytoMorph Image Phenomics Tool Kit, which contains the Overhead Plant Tracker App.

RESULTS

To test the morphometric and physiological changes in plants responding to repeated touch stimuli, we employed the ABCD. We chose to assay *Arabidopsis thaliana* wild type Col-0 and RBOH mutants *rbohc*, *rbohd*, *rbohf*, and *rbohd*/*f*. Plants were touched every 5 mins for 8 days (192 hours). Col-0 exhibited significant reduction in growth percentage after repeated touch stimuli (**Figure i.6** and **Supplementary Figures Si.2-Si.5**). The *rbohc* and *rbohd* mutants exhibited wild type untouched growth but, when touched, grew significantly larger than touched Col-0. The *rbohf* and *rbohd*/*f* mutants exhibited reduced untouched growth but only *rbohf* was significantly larger than Col-0 after repeated touching. These results indicate that *rbohc* and *rbohd*

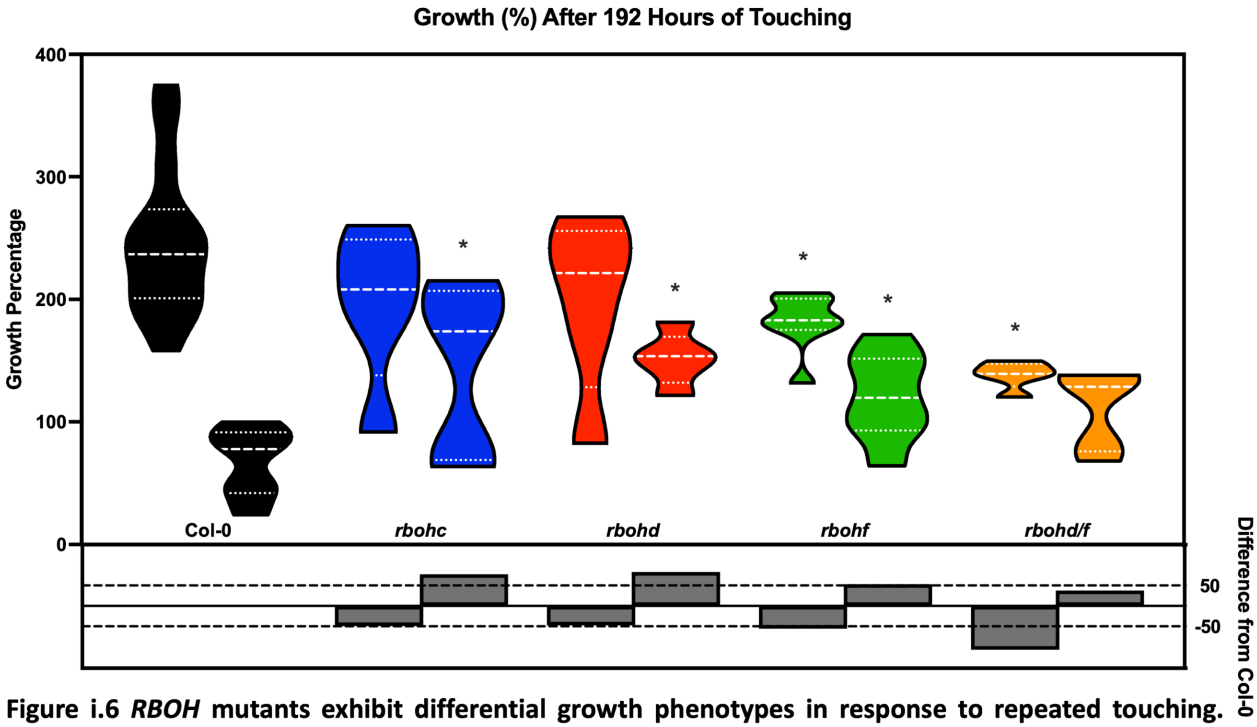

Figure i.6 *RBOH* mutants exhibit differential growth phenotypes in response to repeated touching. Plants were touched at 5 minute intervals over 8 days using the Automated Botanical Contact Device. Increased growth over the 8 days is reported as growth percentage (x100). The difference between untouched (left bar) and touched (right bar) from Col-0 for each genotype is reported as percentage change (x100) and indicated by the white brick bars. Each mutant exhibited a significant difference in percentage change, compared to Col-0 ($n \geq 5$; 2-way ANOVA; Dunnett's Test; $p < 0.05$).

are significantly less responsive to repeated touching. The *rbohf* mutant is also less responsive to repeated touching, as it exhibits significantly less untouched growth than Col-0 but touched *rbohf* plants are significantly larger than Col-0. Finally, the *rbohd/f* mutants exhibit severe impairment in both general growth and touch-responsiveness. The *rbohd/f* mutants exhibit significantly reduced untouched growth, relative to Col-0, and touched *rbohd/f* plants are neither significantly different from touched Col-0 plants nor untouched *rbohd/f* plants. Results of this method of direct stimulation and measurement are discussed in more detail in **Chapter 2**.

DISCUSSION

Previous studies have applied mechanical stimulus – especially touch – in many ways that have not been standardized. In various cases, researchers have sprayed water [4], bent leaves and

stems [5], gyrated whole plants via orbital shaker [6], grown seedlings on hard agar surfaces [7], and stimulated mature plants via carriage-driven polyethylene sheets [8]. Comparing the results of studies such as these is a cumbersome task, as the mechanical load and measurement technique are not consistent throughout. Thus, we have engineered a robot that can routinely and repeatably stimulate plants of variable ages and stages of development, while making consistent measurements of their growth.

By incorporating imaging and the ability to change the zones of touch stimulation, the system adds flexibility to growth chamber and greenhouse systems where, e.g., plants flowering in different zones could be optimized to provide successive cropping from a single growth space through the ability of touch stimulation to delay flowering. Similarly, pest resistance could be tuned to prevailing or expected conditions through touch stimulation-triggered defense responses in an entirely pesticide-free approach. The device also provides critical data via customizable imaging and adjustable touch stimulation to evaluate plant responses and optimize algorithms to help researchers and growers mechanically "tune" the health and productivity of their plants. As a side benefit, this device could readily be installed in commercial greenhouses and the control algorithms adjusted to regulate plant growth, development and physiology, for example, to allow growers to control which plants come into flower in accordance with market demands.

MATERIALS AND METHODS

Plant Material and Growth Conditions

Seeds from each plant line were imbibed for 20 min in sterile H_2O and sown into a single hole cut into the center of a black acrylic square (75 mm L x 75 mm W x 4.5 mm H) resting on standard #1801 pot inserts containing Fafard Germination Mix (Sun Gro Horticulture). The acrylic

squares were labeled with QR codes encoding the genotype and position (in the machine) information. The pots were randomized in pairs (one mechanically stimulated row next to one unstimulated row) in flats with space for 18 pots. Seeds were stratified in a 4˚C cold-room for 2 days and grew for 21 days post-germination in the ABCD platform rack in 16 hours light/8 hours dark (long-day) photoperiod under 30,000 to 45,000 lux (**Supplementary Figure Si.6**) at 22˚C, before starting touch. On day 20 after germination, imaging began of rosettes from above by Raspberry Pi camera. Each square image captured 9 seedlings in a 3 x 3 arrangement. Touch stimulation by 1 cm fingers cut into polyethylene sheets began at 21 days after germination, via programming of the master interface. The touch interval was 5 minutes. Touching and imaging continued for >8 days. These images were uploaded to CyVerse (https://de.cyverse.org) for image analysis. Development (i.e. percent growth) of each rosette every hour was then evaluated via Overhead Plant Tracker application software.

Image Construction and Analysis

To prepare for image acquisition and analysis by the Overhead Plant Tracker App, the image scene was constructed with 4 colors to make a relatively straightforward machine vision problem. Red tape was used as a boundary to segment the pot regions, blue was used as the identifying color for the checkerboard, black was used as the background to obscure the color complexities of the soil medium, and white labeled the container for the QR code and its associated metadata. For the black background of each pot in the images, a black acrylic square was laid over the soil. This simple color scheme combined with the following pseudo-code was used to label regions and extract digital biomass:

1. Find Pots (**Supplementary Figure Si.1a**) – Red
   a. Transform RGB image to Lab color space
   b. Find red pixels via thresholding the a-channel.
   c. Label red tape border as the largest 8-connected object.
   d. ID pot regions as 9 holes in the red tape border.

2. Find Checkerboard (**Supplementary Figure Si.1b**) – Blue
   a. Transform RGB image to Lab color space.
   b. Find blue pixels via thresholding the b-channel.
   c. ID checkerboard region as object > 500,000 pixels.

3. Read QR (**Supplementary Figure Si.1c**) – White
   a. Identify white pixels via dithering map.
   b. Find the largest 8-connected component.
   c. Read the QR text using java package.

4. Measure Biomass (**Supplementary Figure Si.1d**) – Green
   a. ID green pixels by clustering via Gaussian Mixture Model.
   b. Remove 8-connected components with area < 300 pixels.
   c. Count biomass as number of remaining green pixels.

Statistical Tests and Data Analysis

Multiple *t*-tests were performed to compare the mean percentage growth at each time point in Col-0 to the mean percentage growth at each timepoint in the mutant plants, in untouched and touched samples. The results of the *t*-test were considered significant if the p-value was < 0.05. For those timepoints where the difference between the means of untouched and/or touched Col-0 and mutant plant growth percentage were significant, the mean was calculated for the difference between (mean) untouched Col-0 and (mean) untouched mutant and the difference between (mean) touched Col-0 and (mean) touched mutant, at each timepoint. This can be written as $((U_{WT} - U_{mutant} + T_{WT} - T_{mutant}) / 2)$, where "U" means untouched, "T" means touched, and "WT" means wild type. This measure denotes divergence of mean growth of the mutants from Col-0 for both untouched and touched plants, i.e., overall "Sensitivity" to stresses (e.g. touch) or other forces. Negative "Sensitivity" values indicate mutants that are less sensitive to this force than Col-0. Positive

"Sensitivity" values indicate mutants that are more sensitive to this force than Col-0. These values can be an indication of the extent to which each mutant diverges from Col-0 with regard to growth.

LITERATURE CITED

1. Mishra Y, Johansson Jänkänpää H, Kiss AZ, Funk C, Schröder WP, Jansson S. Arabidopsis plants grown in the field and climate chambers significantly differ in leaf morphology and photosystem components. BMC Plant Biol. 2012;12:6.

2. Conrath U, Beckers GJM, Flors V, García-Agustín P, Jakab G, Mauch F, et al. Priming: getting ready for battle. Mol Plant Microbe Interact. The American Phytopathological Society; 2006;19:1062–71.

3. Humplík JF, Lazár D, Husičková A, Spíchal L. Automated phenotyping of plant shoots using imaging methods for analysis of plant stress responses – a review. Plant Methods. BioMed Central; 2015;11:29.

4. Braam J, Davis RW. Rain-, wind-, and touch-induced expression of calmodulin and calmodulin-related genes in Arabidopsis. Cell. 1990;60:357–64.

5. Lee D, Polisensky DH, Braam J. Genome-wide identification of touch- and darkness-regulated Arabidopsis genes: a focus on calmodulin-like and XTH genes. New Phytol. 2005;165:429–44.

6. Der Loughian C, Tadrist L, Allain J-M, Diener J, Moulia B, de Langre E. Measuring local and global vibration modes in model plants. Comptes Rendus Mécanique. 2014;342:1–7.

7. Zha G, Wang B, Liu J, Yan J, Zhu L, Yang X. Mechanical touch responses of Arabidopsis TCH1-3 mutant roots on inclined hard-agar surface**. Int Agrophysics. De Gruyter Open; 2016;30:105–11.

8. Paul-Victor C, Rowe N. Effect of mechanical perturbation on the biomechanics, primary growth and secondary tissue development of inflorescence stems of Arabidopsis thaliana. Ann Bot. Oxford University Press; 2011;107:209–18.

SUPPLEMENTARY FIGURES

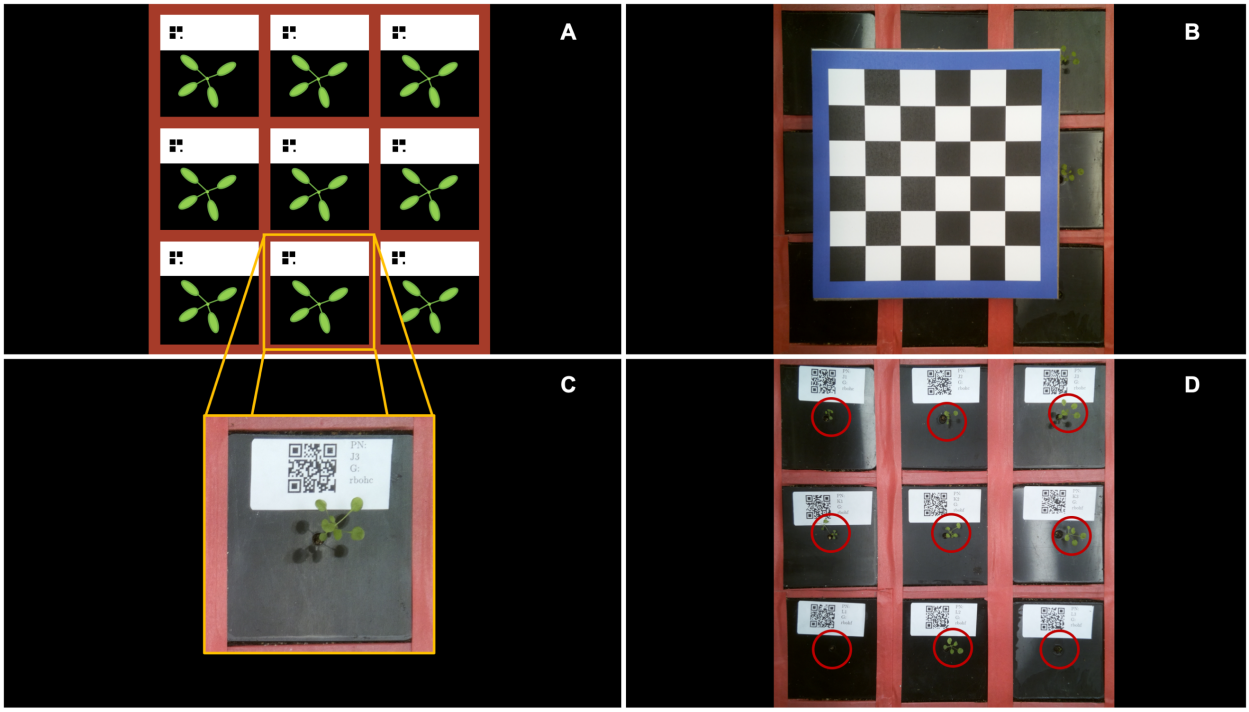

Supplementary Figure Si.1 Workflow for Extracting Growth Data from Digital Images via Overhead Plant Tracker Software. (**A**) Idealized 9 x 9 stratum of plants for image analysis. RGB values for this and subsequent images are transformed to Lab color. Red pixels are identified as boundaries for pots. (**B**) Checkerboard is placed over plants during initial image acquisition to allow for off-angle adjustments. (**C**) Pots with individual plants identified during **A** are identified via QR metadata. (**D**) Green pixels in each individual pot classified during **A** are identified by clustering via Gaussian Mixture Model. Plant biomass is reported as green pixels in each pot after removal of background and QR placard.

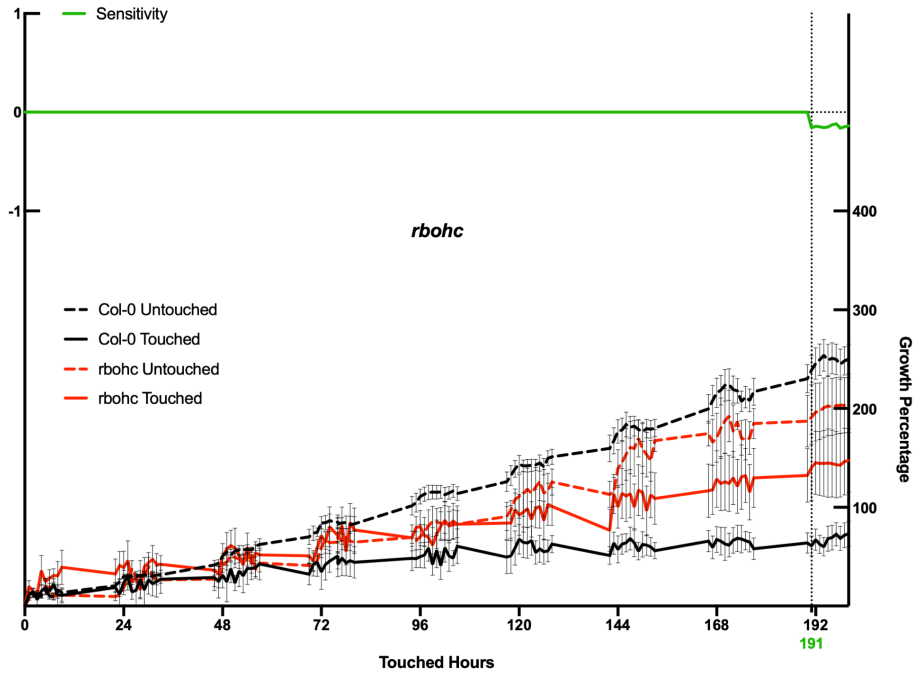

Supplementary Figure Si.2 *rbohc* is significantly less sensitive to repeated touch stimulus than Col-0. Plants were touched every 5 minutes for >8 days and imaged every hour. Percent growth was extracted from images at each time point ($\Delta A/A_0$). Sensitivity (green trace) is a measure of divergence of the mean growth at each time point from Col-0 for both untouched and touched measures, denoting sensitivity to some stress or force (e.g. touch). *rbohc* plants exhibit no significant difference in growth of untouched plants, but exhibit decreased growth inhibition due to touch, relative to Col-0.

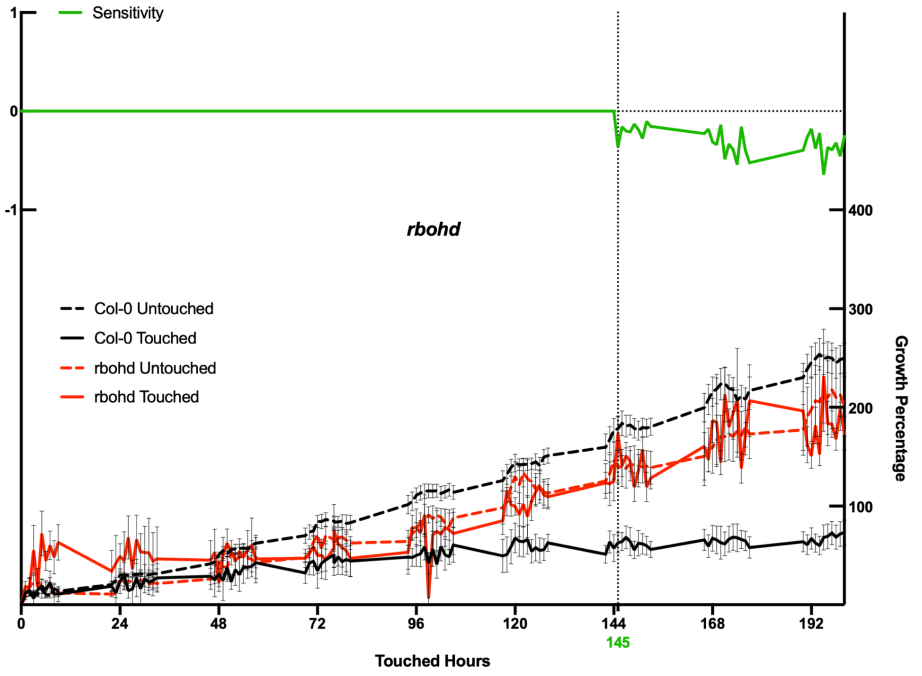

Supplementary Figure Si.3 *rbohd* is significantly less sensitive to repeated touch stimulus than Col-0. Plants were touched every 5 minutes for >8 days and imaged every hour. Percent growth was extracted from images at each time point ($\Delta A/A_0$). Sensitivity (green trace) is a measure of divergence of the mean growth at each time point from Col-0 for both untouched and touched measures, denoting sensitivity to some stress or force (e.g. touch). *rbohd* plants exhibit no significant difference in growth of untouched plants, but exhibit decreased growth inhibition due to touch, relative to Col-0.

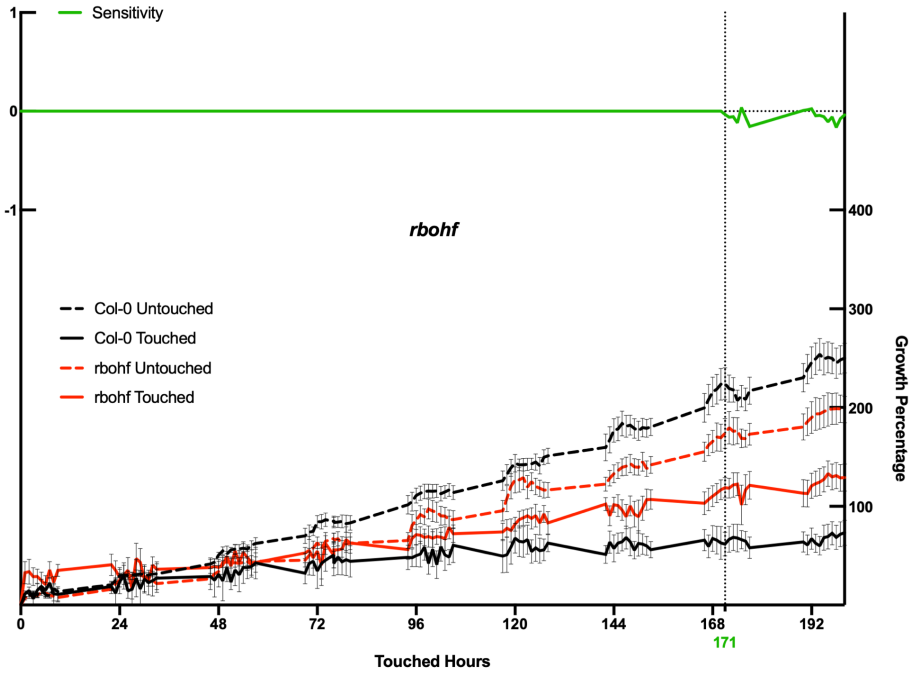

Supplementary Figure Si.4 *rbohf* is significantly less sensitive to repeated touch stimulus than Col-0. Plants were touched every 5 minutes for >8 days and imaged every hour. Percent growth was extracted from images at each time point ($\Delta A/A_0$). Sensitivity (green trace) is a measure of divergence of the mean growth at each time point from Col-0 for both untouched and touched measures, denoting sensitivity to some stress or force (e.g. touch). *rbohf* plants exhibit significant difference in growth of untouched plants, and exhibit decreased growth inhibition due to touch, relative to Col-0.

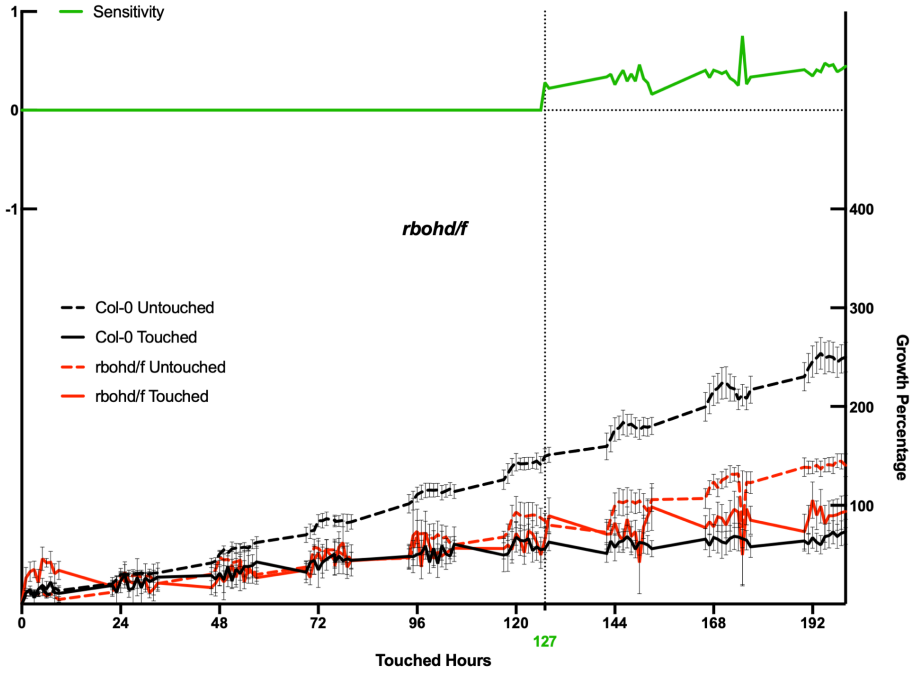

Supplementary Figure Si.5 *rbohd/f* is significantly less sensitive to repeated touch stimulus than Col-0. Plants were touched every 5 minutes for >8 days and imaged every hour. Percent growth was extracted from images at each time point ($\Delta A/A_0$). Sensitivity (green trace) is a measure of divergence of the mean growth at each time point from Col-0 for both untouched and touched measures, denoting sensitivity to some stress or force (e.g. touch). *rbohd/f* plants exhibit a significant difference in growth of untouched plants and exhibit decreased growth inhibition due to touch, relative to Col-0.

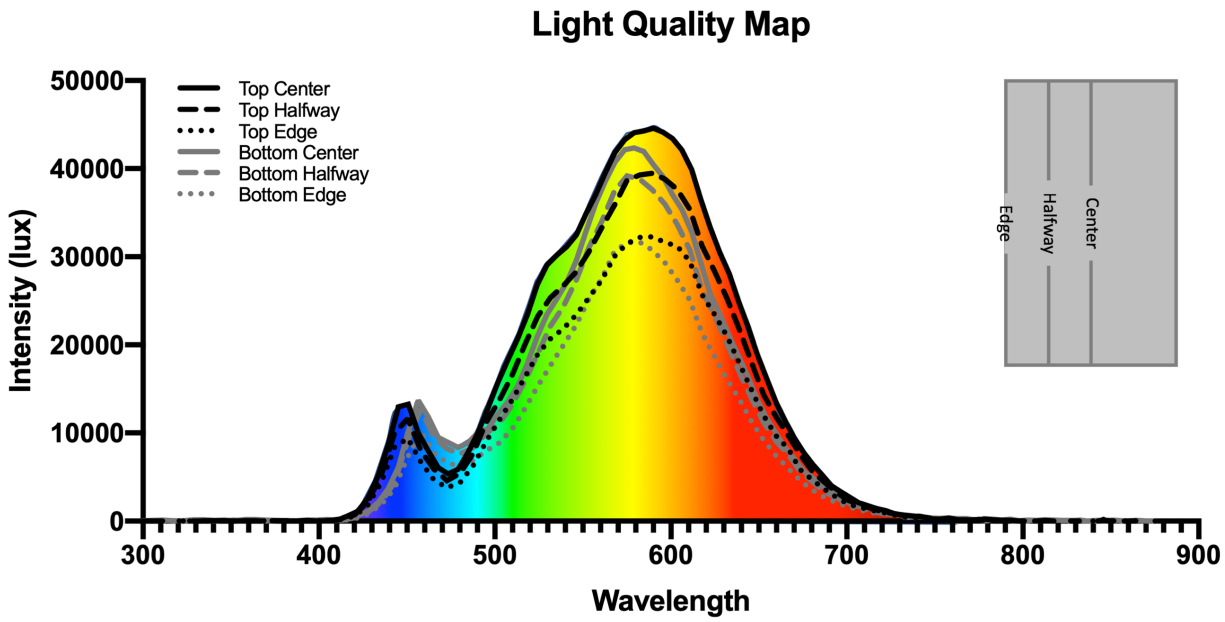

Supplementary Figure Si.6 Light quality map of ABCD. Light quality measurements from three points on each level of the ABCD. The inset diagrams the locations of the measurements.

Appendix II:

CaM2 and CaM7 Contribute to Intracellular Ca^{2+} Signaling

INTRODUCTION

Calcium, is an important second messenger in eukaryotic systems, and is required for adaptive responses to many stimuli (Berridge *et al.*, 2000; Clapham, 2007; Poovaiah and Du, 2018). The mechanism by which these stimuli elicit the requisite response involves exquisitely sensitive cellular influx and efflux machinery that evolved to maintain cytosolic calcium concentration ($[Ca^{2+}]_{cyt}$) much lower than the environment of early life provided (Sanders *et al.*, 1999). The low $[Ca^{2+}]_{cyt}$ needed to prevent, for example, phosphate precipitation from early plant cells was approximately 10^{-7} M (Gilroy *et al.*, 1986; Bush, 1995; Sanders *et al.*, 1999). Therefore, influx of only a small number of Ca^{2+} ions could amount to a significantly large increase in $[Ca^{2+}]_{cyt}$. Thus, organisms with cells harboring molecules capable of detecting and/or scavenging Ca^{2+} ions (particularly at low molar concentrations) and instructing the cell to reduce the $[Ca^{2+}]_{cyt}$ would have had an adaptive advantage.

During the interaction between pathogenic bacteria and plants, particular microbe-associated molecular patterns (MAMPs) act as elicitors of plant defense responses. For example, bacterial flagella are composed of flagellin monomers and within flagellin lies a 22-amino acid epitope (flg22), which has been well-characterized for triggering plant immune responses (Jones and Dangl, 2006; Veluchamy *et al.*, 2014; Suarez-Rodriguez *et al.*, 2007; Ranf *et al.*, 2011). The flg22 molecule is recognized by the pattern-recognition receptor (PRR) flagellin-sensitive 2 (FLS2) via its extracellular leucine-rich repeat domain (Chinchilla *et al.*, 2006). Treatment with purified flg22 triggers defense responses in both root and shoot tissues of *Arabidopsis thaliana*. This kind of defense response is called pattern-triggered immunity (PTI). PTI triggers local defense responses and can lead to plant-wide increases in immunity, i.e. systemic acquired resistance (SAR).

One hallmark of early PTI responses is the rapid increase in $[Ca^{2+}]_{cyt}$ immediately after bacterial (or MAMP) elicitation (Knight *et al.*, 1991; Blume *et al.*, 2000; Ranf *et al.*, 2011). However, the pumps and channels responsible for producing the appropriate calcium signature needed for initiating PTI are, as yet, mostly uncharacterized. Although we do know that the tonoplast autoinhibited Ca^{2+} ATPases ACA4 and ACA11 are linked somehow to defense signaling (Boursiac *et al.*, 2010), as are the plasma membrane ACAs, ACA8 and ACA10 (Frei dit Frey *et al.*, 2012), with ACA8 being found in a complex with FLS2, their roles are not well characterized. For example, knockouts in *ACA8* and *ACA10* abolish flg22-triggered Ca^{2+} increases, yet these pumps are expected to normally attenuate Ca^{2+} increases, and so their knockouts should, in theory at least, lead to increased signal amplitudes. Similarly, cyclic nucleotide gated channels have also been linked to defense responses (Ma *et al.*, 2012) but are not modulated by the flg22 perception machinery.

The kinetics of the differential elevations in $[Ca^{2+}]_{cyt}$ generated by the signal-responsive Ca^{2+} flux machinery (i.e. their frequency, amplitude, duration, and localization) define their stimulus-specificity and constitute their 'calcium signature' (McAinsh and Pittman, 2009; Dodd *et al.*, 2010). Furthermore, it is known that Ca^{2+}-binding proteins (CaBPs), like calmodulin (CaM), are required for connecting elevations in $[Ca^{2+}]_{cyt}$ to enzymatic activity, protein-protein interactions, and transcriptional regulation (Hashimoto and Kudla, 2011). Consistent with these ideas, pathogen attack has been demonstrated by many researchers to both increase $[Ca^{2+}]_{cyt}$ and rely on the activity of a range of CaBPs to initiate plant immunity (e.g., (Kim *et al.*, 2002; Dodd *et al.*, 2010; Galon *et al.*, 2010; Kudla *et al.*, 2010; Seybold *et al.*, 2014; Tsuda and Somssich, 2015). Intriguingly, the ACAs and CNGC channels are regulated by interactions with CaM,

suggesting that this CaBP might play a role in both interpreting Ca^{2+} signatures and in controlling the machinery that generates them.

As part of my studies on the role(s) of CaM2 and CaM7 in pathogen responses, I generated mutant lines expressing the Ca^{2+} reporter YC-Nano65 to begin to characterize how these proteins may affect the flg22-triggered Ca^{2+} signals, themselves. Here, I report a preliminary characterization of these *CAM2* and *CAM7* mutants that indicates that they generate attenuated Ca^{2+} influxes into the cytosol in response to flg22. This observation highlights potential novel interactions between CaBPs and the generation of the signals they would conventionally interpret. This behavior may provide a possible mechanism for the altered defense status of *CAM2* and *CAM7* mutants that I previously reported in **Chapter 3**.

RESULTS

flg22-Dependent Ca^{2+} Influx is Reduced in *cam2* and *cam7* Cotyledons

As CaM could be involved in regulating the passage of cations – such as Ca^{2+} – into the cytosol, we observed the flux of $[Ca^{2+}]_{cyt}$ via the ratiometric, genetically-encoded, fluorescent protein-based Ca^{2+} sensor YC-Nano65 (Horikawa *et al.*, 2010) before and after treatment with 1µM flg22. This sensor is expressed throughout plant tissues via the promoter of UBQ10 and, as Ca^{2+} levels increase, emission from cyan fluorescent protein (CFP) decreases slightly and the Förster Resonance Energy Transfer (FRET) signal from the yellow fluorescent protein partner within YC-Nano65 increases. An increase in the ratio of FRET:CFP (ΔR) thus is reflective of the increase in $[Ca^{2+}]_{cyt}$. We found that 1 µM flg22 elicited a significantly smaller increase in $[Ca^{2+}]_{cyt}$ in cotyledons from *cam2* and *cam7* plants, compared to Col-0 (**Figure ii.1**). In all cases, peak Ca^{2+}-influx occurred at ~4 minutes post-elicitation with flg22. Even after normalization via baseline

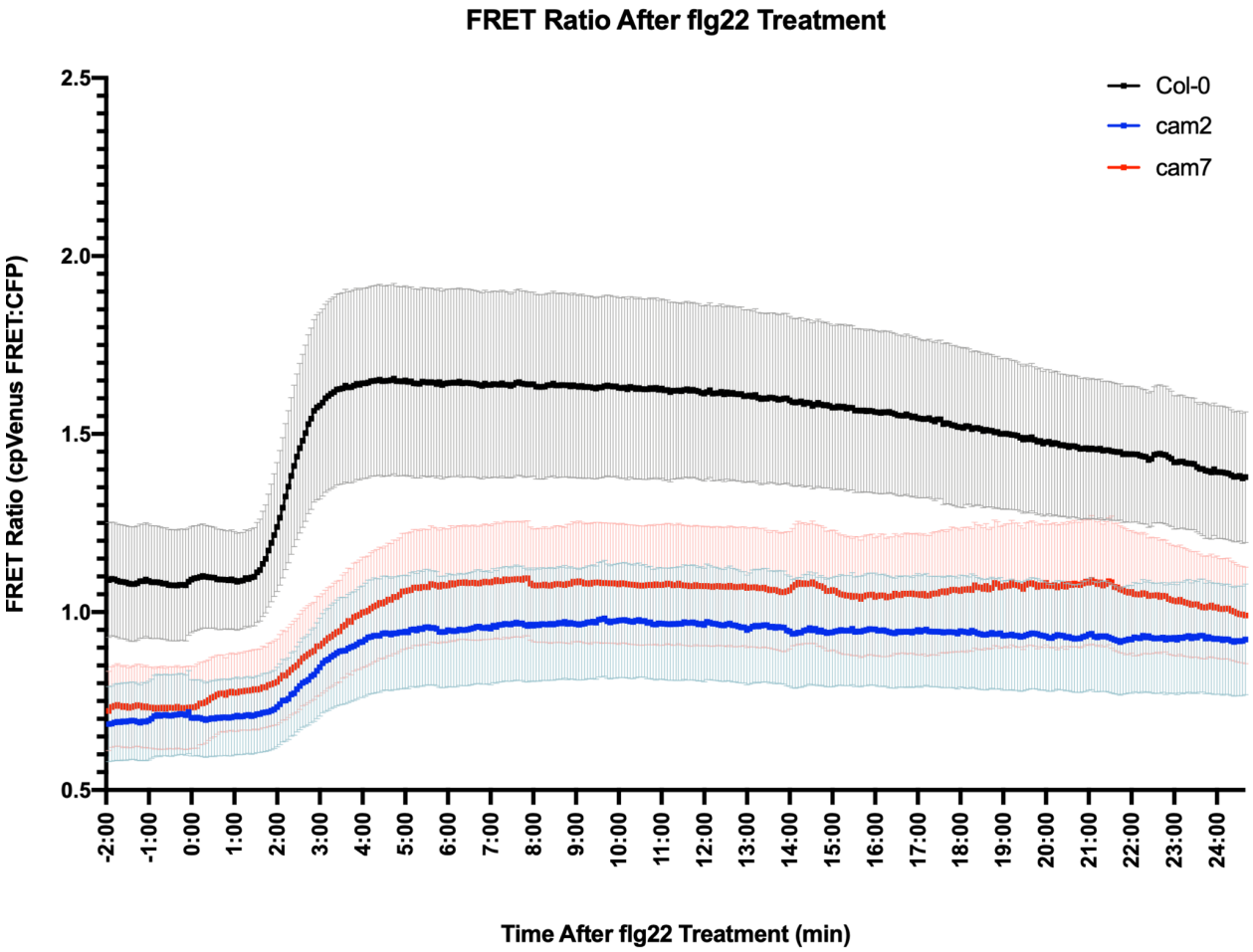

Figure ii.1 *cam2* and *cam7* plants exhibit reduced flg22-induced Ca^{2+} elevation. FRET ratios (cpVenus FRET:CFP) indicating that *cam2* and *cam7* plants exhibit attenuated Ca^{2+} influx in cotyledons, in response to 1 µM flg22 elicitation. Data represent mean ± SEM; n = 8, per treatment.

FRET subtraction, this trend continued (**Figure ii.2**). flg22-triggered Ca^{2+}-influx in *cam2* deviated from Col-0 from 2 minutes 16 seconds post-elicitation to 18 minutes 12 seconds post-elicitation, well after [Ca^{2+}] began to return to baseline, in Col-0. This Ca^{2+}-influx, in *cam7*, deviated from Col-0 from 2 minutes 16 seconds post-elicitation to 10 minutes 28 seconds post-elicitation. These finding suggests that CaM2 and CaM7 may be important for proper influx of Ca^{2+} during MAMP perception in aerial parts.

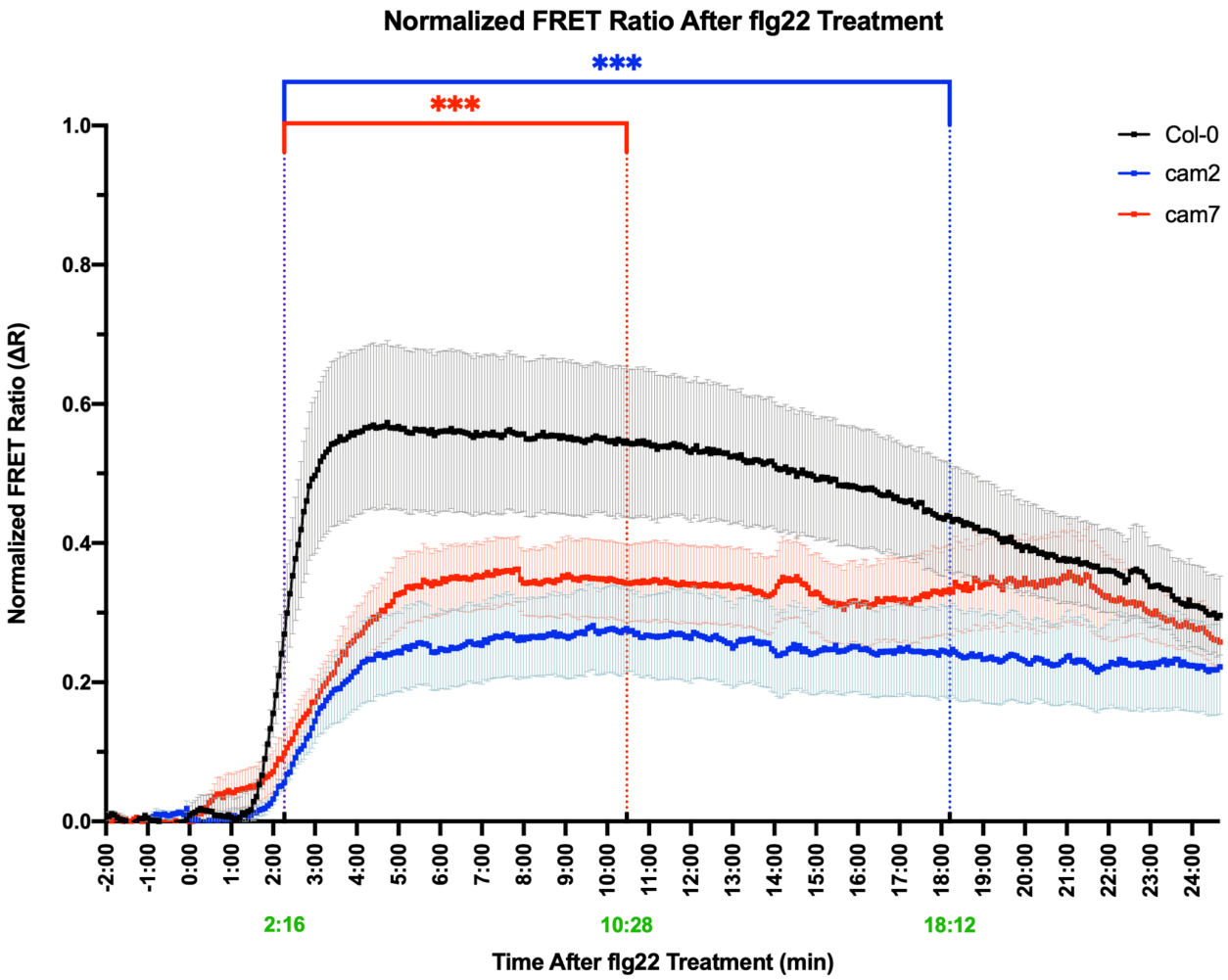

Figure ii.2 *cam2* and *cam7* plants exhibit reduced flg22-induced Ca^{2+} elevation. Baseline-normalized FRET ratios (ΔR) indicating that *cam2* and *cam7* plants exhibit attenuated Ca^{2+} influx in cotyledons, in response to 1 µM flg22 elicitation Data represent mean ± SEM; n = 8, per treatment.

DISCUSSION

Ca^{2+} signals elicited by various stimuli are critical to initiating adaptive responses that enable plants to defend themselves (Lecourieux *et al.*, 2006). Here I demonstrate that mutations in *CAM2* and *CAM7* lead to attenuated increases in $[Ca^{2+}]_{cyt}$ in response to the bacterial elicitor flg22. These alterations in Ca^{2+} signal in *cam2* and *cam7* mutants appear to not only be reductions in total $[Ca^{2+}]_{cyt}$ increase, but also a delay in peak FRET fluorescence, corresponding to a delay in the

influx of Ca^{2+} into the cytosol. The delayed signals are on the order of seconds but could potentially alter the ability of plants to adequately respond to bacterial infection.

Mutations in *CAM2* and *CAM7* do not lead to any obvious growth phenotypes but, as described in **Chapter 3**, lead to improved resistance to the hemibiotrophic bacterial pathogen *Pseudomonas syringae* pv. *tomato* DC3000, relative to Col-0. Furthermore, I described in **Chapter 3** that *cam2* and *cam7* mutants exhibit approximately constitutive expression of some defense transcripts related to the production of defense-related hormone, salicylic acid. Additionally, these expression levels are not significantly changed after flg22 treatment. It is possible that these defense transcripts are already at saturation and are, therefore, insensitive to additional stimulus inputs (i.e. Ca^{2+} signals). It is also possible that, as **Figure ii.1** indicates, basal $[Ca^{2+}]_{cyt}$ is reduced in *cam2* and *cam7* mutants and the increases in $[Ca^{2+}]_{cyt}$ elicited by flg22 are not large enough to meet some threshold level to further activate defense.

If these $[Ca^{2+}]_{cyt}$ increases are not enough to precipitate a defense response, and baseline $[Ca^{2+}]_{cyt}$ is reduced, relative to wild type, then the basal activation of defense exhibited by these mutants is likely the result of the alteration of some downstream component of the pathway and not the result of elevated $[Ca^{2+}]_{cyt}$. If the increases in $[Ca^{2+}]_{cyt}$ are enough to precipitate a defense response, but the defense related transcripts are already at saturation, then the reduced basal $[Ca^{2+}]_{cyt}$ and attenuated increase after flg22 treatment could be the result of feedback inhibition of the activity of the Ca^{2+} influx machinery.

This work on *CAM2* and *CAM7* is the first to report that *CAM* mutants exhibit attenuated Ca^{2+} signals in response to flg22 treatment. CaMs have previously been shown to bind to cyclic nucleotide gated channels (CNGCs) at the plasma membrane to inhibit binding of cyclic nucleotides (e.g. cAMP), thus preventing activation of the channel and reducing Ca^{2+} influx (Hua

et al., 2003; Abdel-Hamid *et al.*, 2010). There is the possibility, therefore, that CaM2 and/or CaM7 interacts directly with some component of the Ca^{2+} influx machinery at the plasma membrane or tonoplast, which could place their activity in plant defense responses upstream of Ca^{2+} signaling or as part of the downstream feedback inhibition, perhaps through the activity of CNGCs.

MATERIALS AND METHODS

Plant Material and Growth Conditions

Arabidopsis thaliana lines, each harboring one of two loss-of-function alleles in *CAM2* (*cam2-1* and SALK_066990) and *CAM7* (*cam7-1* and SALK_074336) were acquired from the *Arabidopsis* Biological Resource Center at Ohio State University and confirmed to be homozygous for their respective insertions.

For the following experiments, seeds were imbibed with sterile H_2O (20 mins), sterilized with 70% (v/v) ethanol (1 min), 20% (v/v) bleach (2 mins), and washed three times with sterile H_2O. Sterile seeds were sown onto 12-well cell culture plates plates containing ½-strength Linsmaier and Skoog (LS) Modified Basal Medium (PhytoTechnology Laboratories), 1.0% (w/v) Phytagel (Sigma Life Science) and 1.0% (w/v) sucrose (growth medium, hereafter). Seedlings were grown for 10 to 14 days after germination in 16 hours light/8 hours dark (long-day) photoperiod under 100 μE m^{-2} sec^{-1} at 22˚C in a plant-growth chamber.

Ratiometric Ca^{2+} Imaging

Cotyledons were detached from seedlings and placed between a thin layer of growth medium and a coverslip, adaxial side down, 2 hours prior to imaging. A 5mm x 5mm well was cut into the gel near the leaf's cut-end prior to imaging, for the application of 1 μM flg22 suspended in liquid

growth medium (no Phytagel). 1 μM was the chosen [flg22] as it elicited a large FRET signal without reaching saturation (**Supplementary Figure Sii.1**). Imaging was performed on a Zeiss LSM 710 inverted confocal microscope equipped with a 5x/0.16 M27 EC Plan-Neofluar objective. Excitation of the YC-Nano65 sensor was performed with the 458nm laser line and emission for cpVenus and CFP were obtained at 525-540nm and 460-505nm, respectively. Time series FRET data was normalized via the following equation: $\Delta R = (R - R_0)$, where R is the ratio of cpVenus emission (FRET):CFP emission (FRET ratio) and R_0 is the average baseline value of this FRET ratio prior to flg22 treatment. FRET ratio data was analyzed using the image calculator tool in ImageJ (Schindelin *et al.*, 2015).

LITERATURE CITED

Abdel-Hamid, H., Chin, K., Shahinas, D., Moeder, W. and Yoshioka, K. (2010) Calmodulin binding to Arabidopsis cyclic nucleotide gated ion channels. *Plant Signal. Behav.*, **5**, 1147–1149.

Berridge, M.J., Lipp, P. and Bootman, M.D. (2000) The versatility and universality of calcium signalling. *Nat. Rev. Mol. Cell Biol.*, **1**, 11–21.

Blume, B., Nurnberger, T., Nass, N. and Scheel, D. (2000) Receptor-Mediated Increase in Cytoplasmic Free Calcium Required for Activation of Pathogen Defense in Parsley. *Plant Cell*, **12**, 1425.

Boursiac, Y., Lee, S.M., Romanowsky, S., Blank, R., Sladek, C., Chung, W.S. and Harper, J.F. (2010) Disruption of the Vacuolar Calcium-ATPases in Arabidopsis Results in the Activation of a Salicylic Acid-Dependent Programmed Cell Death Pathway. *Plant Physiol.*, **154**, 1158–1171.

Bush, D.S. (1995) Calcium Regulation in Plant Cells and its Role in Signaling. *Annu. Rev. Plant Physiol. Plant Mol. Biol.*, **46**, 95–122.

Chinchilla, D., Bauer, Z., Regenass, M., Boller, T. and Felix, G. (2006) The Arabidopsis Receptor Kinase FLS2 Binds flg22 and Determines the Specificity of Flagellin Perception. *Plant Cell*, **18**, 465 LP – 476.

Clapham, D.E. (2007) Calcium Signaling. *Cell*, **131**, 1047–1058.

Dodd, A.N., Kudla, J. and Sanders, D. (2010) The Language of Calcium Signaling. *Annu. Rev. Plant Biol.*, **61**, 593–620.

Frei dit Frey, N., Mbengue, M., Kwaaitaal, M., et al. (2012) Plasma Membrane Calcium ATPases Are Important Components of Receptor-Mediated Signaling in Plant Immune Responses and Development. *Plant Physiol.*, **159**, 798–809.

Galon, Y., Aloni, R., Nachmias, D., et al. (2010) Calmodulin-binding transcription activator 1 mediates auxin signaling and responds to stresses in Arabidopsis. *Planta*, **232**, 165–178.

Gilroy, S., Hughes, W.A. and Trewavas, A.J. (1986) The measurement of intracellular calcium levels in protoplasts from higher plant cells. *FEBS Lett.*, **199**, 217–221.

Hashimoto, K. and Kudla, J. (2011) Calcium decoding mechanisms in plants. *Biochimie*, **93**, 2054–2059.

Horikawa, K., Yamada, Y., Matsuda, T., et al. (2010) Spontaneous network activity visualized by ultrasensitive Ca2+ indicators, yellow Cameleon-Nano. *Nat. Methods*, **7**, 729–732.

Hua, B.-G., Mercier, R.W., Zielinski, R.E. and Berkowitz, G.A. (2003) Functional interaction of calmodulin with a plant cyclic nucleotide gated cation channel. *Plant Physiol. Biochem.*, **41**, 945–954.

Jones, J.D.G. and Dangl, J.L. (2006) The plant immune system. *Nature*, **444**, 323–9.

Kim, M.C., Panstruga, R., Elliott, C., Müller, J., Devoto, A., Yoon, H.W., Park, H.C., Cho, M.J. and Schulze-Lefert, P. (2002) Calmodulin interacts with MLO protein to regulate defence against mildew in barley.

Nature, **416**, 447–451.
Knight, M.R., Campbell, A.K., Smith, S.M. and Trewavas, A.J. (1991) Transgenic plant aequorin reports the effects of touch and cold-shock and elicitors on cytoplasmic calcium. *Nature*, **352**, 524–526.
Kudla, J., Batistic, O. and Hashimoto, K. (2010) Calcium signals: the lead currency of plant information processing. *Plant Cell*, **22**, 541–63.
Lecourieux, D., Ranjeva, R. and Pugin, A. (2006) Calcium in plant defence-signalling pathways. *New Phytol.*, **171**, 249–269.
Ma, Y., Walker, R.K., Zhao, Y. and Berkowitz, G.A. (2012) Linking ligand perception by PEPR pattern recognition receptors to cytosolic Ca2+ elevation and downstream immune signaling in plants. *Proc. Natl. Acad. Sci.*, **109**, 19852–7.
McAinsh, M.R. and Pittman, J.K. (2009) Shaping the calcium signature. *New Phytol.*, **181**, 275–294.
Poovaiah, B.W. and Du, L. (2018) Calcium signaling: decoding mechanism of calcium signatures. *New Phytol.*, **217**, 1394–1396.
Ranf, S., Eschen-Lippold, L., Pecher, P., Lee, J. and Scheel, D. (2011) Interplay between calcium signalling and early signalling elements during defence responses to microbe- or damage-associated molecular patterns. *Plant J.*, **68**, 100–13.
Sanders, D., Brownlee, C. and Harper, J.F. (1999) Communicating with calcium. *Plant Cell*, **11**, 691–706.
Schindelin, J., Rueden, C.T., Hiner, M.C. and Eliceiri, K.W. (2015) The ImageJ ecosystem: An open platform for biomedical image analysis. *Mol. Reprod. Dev.*, **82**, 518–529.
Seybold, H., Trempel, F., Ranf, S., Scheel, D., Romeis, T. and Lee, J. (2014) Ca2+ signalling in plant immune response: from pattern recognition receptors to Ca2+ decoding mechanisms. *New Phytol.*, **204**, 782–790.
Suarez-Rodriguez, M.C., Adams-Phillips, L., Liu, Y., Wang, H., Su, S.-H., Jester, P.J., Zhang, S., Bent, A.F. and Krysan, P.J. (2007) MEKK1 is required for flg22-induced MPK4 activation in Arabidopsis plants. *Plant Physiol.*, **143**, 661–9.
Tsuda, K. and Somssich, I.E. (2015) Transcriptional networks in plant immunity. *New Phytol.*, **206**, 932–947.
Veluchamy, S., Hind, S.R., Dunham, D.M., Martin, G.B. and Panthee, D.R. (2014) Natural variation for responsiveness to flg22, flgII-28, and csp22 and Pseudomonas syringae pv. tomato in heirloom tomatoes. *PLoS One*, **9**, e106119.

SUPPLEMENTARY FIGURE

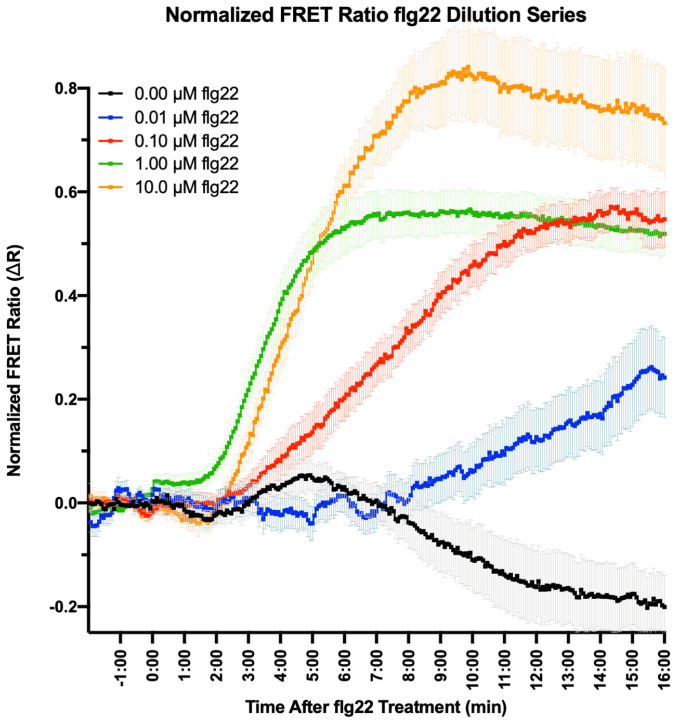

Figure Sii.1 Ca^{2+} signaling in response to flg22 dilution series in Col-0 cotyledons. A dilution series of 0 – 10 µM flg22 in growth medium was used to treat cotyledons from Col-0 to determine the concentration that elicited a clear flg22-response without reaching a saturating FRET ratio (ΔR). Data represent mean ± SEM; n ≥ 6, for each concentration.

Thank you all. Don’t forget to tip your kitchen staff, on the way out.